Factors affecting Keratocyte Colonisation of Novel Keratoprosthetic Biomaterials

Susan Sandeman

A thesis submitted in partial fulfilment of the requirements of the University of Brighton for the degree of Doctor of Philosophy

December 1998

University of Brighton

Contents

Abstract

A Keratoprosthesis (KPro) which incorporates all of the features required for long-term retention within the cornea has yet to be developed. Integration is dependent on the induction of an adequate response to corneal injury with limited inflammation and a return to relative quiescence. The keratocyte repair response is central to corneal remodelling and may be disrupted by corneal ageing and the accumulation of senescent keratocytes. Since senescence associated disruption of keratocyte activity has the potential to inhibit KPro biointegration within the cornea, the following study sought to investigate aspects of the EK1.BR keratocyte repair response and changes occurring with senescence of cells in culture. The limitations of using cultured senescent EK1.BRs to make inferences about changes in keratocyte responsiveness in the ageing cornea were assessed by comparing migratory responsiveness with that of keratocytes derived from an elderly donor. A preliminary investigation of suitable KPro skirt materials, capable of enhancing keratocyte adhesion, was also carried out since keratocyte adhesion to the KPro periphery enhances integration within the cornea and may limit cellular downgrowth.

It was found that senescence inhibits aspects of the keratocyte repair response and may be detrimental to KPro integration. A significant decline in keratocyte migration and in migratory responsiveness to EGF was observed. Keratocyte ability to contract a collagen matrix was unaffected while a significant increase in gelatinase MMP-2 activity occurred. Comparison of elderly donor keratocyte proliferative and migratory capacity with that of EK1.BR keratocytes aged in culture suggests that this model may be used to make general inferences about the effects of corneal ageing on keratocyte behaviour. The study also identified a suitable KPro skirt material on the basis of its ability to enhance keratocyte adhesion and spreading. The potential impact of keratocyte senescence on corneal wound healing and KPro retention within the cornea requires further investigation into the mechanisms of keratocyte senescence and methods to accommodate changes in the senescent keratocyte repair response.

List of Tables

List of Figures

Acknowledgements

I would like to thank my supervisors Dr. Andrew Lloyd, Dr. Richard Faragher, Dr. Marcus Allen and Mr. Christopher Liu for their assistance in the completion of this Ph.D.

This thesis is dedicated to my family and especially to Michael.

Abreviations

Activator protein-1	AP-1
Amino peptidase M	APM
Azo-iso-butyronitrile	AIBN
Bovine corneal endothelial cell	BCE
Bovine serum albumin	BSA
Calcein-acetoxymethyl ester	Calcein-AM
Cumulative population doublings	CPDs
Cyclin dependent kinases	cdks
Cyclin kinase inhibitors	CKIs
4,6-Diamidino-2-phenylindole	DAPI
2-(dimethylamino)ethyl methacrylate	DEM
Dimethyl formamide	DMF
Dimethyl sulfoxide	DMSO
Dipeptidyl peptidase II	DPPII
Epidermal growth factor	EGF
Ethidium homodimer-1	EthD-1
Ethylene dimethacrylate	EDMA
Extracellular matrix	ECM
Fibroblast growth factor	FGF
Fibronectin	FN
Foetal calf serum	FCS
Gelatin binding fragment	GBD
Glycosaminoglycan	GAG
Hyaluronic acid	HA
Interferon	IFN
Interleukin	IL
Keratoprosthesis	KPro
MAP kinase kinase	MEK
Matrix metalloproteinase	MMP
Methacrylic acid	MA
Mitogen-activator protein kinase	MAP kinase
Modified eagles medium	MEM
Osteo-odonto-keratoprosthesis	OOKP
Penicillin/streptomycin	P/S

Phenoxyethyl methacrylate	PEM
Plasminogen activator inhibitor	PAI-1
Platelet derived growth factor	PDGF
Poly(hydroxyethyl methacrylate)	p(HEMA)
Polymethyl methacrylate	PMMA
Polytetrafluoroethylene	PTFE
Polyvinyl alcohol	PVA
Phosphate buffered saline	PBS
Proliferating cell nuclear antigen	PCNA
Proteoglycan	PG
Retinoblastoma protein	Rb
Senescence associated β-galactosidase	SA-β-Gal
Serum response factor	SRF
Sodium dodecyl sulphate	SDS
Sodium dodecyl sulphate polyacrylamide gel electrophoresis	SDS-PAGE
Tissue inhibitors of matrix metalloproteinases	TIMP
Tissue-type plasminogen activator	t-PA
Transforming growth factor	TGF
Tumor necrosis factor	TNF
Urokinase-type plasminogen activator	u-PA

Chapter 1

Introduction

1.1Rationale

Corneal misfunction is the second major cause of blindness and has been estimated to result in loss of vision for more than ten million people worldwide (Chirila, 1994). Artificial corneae (keratoprostheses) (KPros) made of various polymer materials have been developed in order to treat corneal blindness which fails to respond to standard keratoplasty (corneal transplant). A number of designs and materials have been investigated. However, all KPros currently available produce serious complications often leading to implant extrusion (Hicks et al, 1997[a]). Recent studies have focused on the development of materials which encourage peripheral colonisation of the prosthesis. Long-term success of keratoprosthetic designs appears to be primarily determined by the induction of a normal wound healing response to keratoprosthetic implantation followed by general integration of the KPro within the host tissue.

Age related changes in ocular function are important since most of the estimated forty million people affected by blindness are above the age of forty five (Hyman, 1987). A number of structural and functional changes have been observed in the ageing cornea and an age dependent decline in corneal wound healing has been noted (Dutt et al, 1994). However, the underlying mechanisms by which these changes occur has yet to be elucidated. In dividing tissues the accumulation of permanently non-dividing, senescent fibroblasts appears to occur in an age dependent manner. This may contribute to a decline in repair capacity since senescent fibroblasts exhibit structural and functional changes detrimental to wound repair (Eleftheriou et al, 1991; Albini et al, 1988; Takeda et al, 1992; Millis et al, 1992). If senescent keratocytes with similar structural and functional changes accumulate with age in the cornea a decline in the repair response and in the success of KPro devices would be expected. An awareness of the changes in senescent keratocyte activity may help to elucidate the mechanisms promoting disruption of normal corneal function with age. Since KPro biointegration is dependent in part on the host keratocyte response to wounding the development of methods to correct or accommodate alterations in senescent keratocyte

function may assist in the long-term success of keratoprosthetic implantation within the aged population.

The following review first outlines corneal structure and the role of keratocytes in structural maintenance and corneal wound repair. Secondly, cell senescence and its potential effects on corneal wound repair are considered. Thirdly, polymer plastics currently used in the development of KPros are described, including current complications limiting long-term implant success. The study then considers aspects of the keratocyte repair response potentially altered by senescence and factors which may then be incorporated into keratoprosthetic design to promote the host repair response and counteract any repair deficiencies. Finally, the adhesion characteristics of keratocytes onto various potential KPro skirt materials are investigated.

1.2 The Cornea

The cornea is a transparent, avascular structure continuous anteriorly with the scleral layer of the eye (Nishida, 1997). Centrally the cornea has a diameter of 0.5 mm which thickens peripherally to a diameter of 0.7 mm. It coats the anterior chamber, covering the pupil and iris and has a protective and light refractory function (Rawe et al, 1994). The absence of vascular tissue within the cornea necessitates the diffusion of oxygen and nutrients from the tear fluid which bathes the anterior cornea and protects it from dehydration. The aqueous humor provides an additional source of nutrients and other factors required for corneal function.

The cornea is formed by the epithelium, Bowman's membrane, stroma, Descemet's membrane and endothelium (Figure 1.1). The nonkeratinised, stratified squamous epithelial layer is approximately 50 to 52 μm thick and is made up of three, morphologically distinct cell types. Anteriorly two to three layers of superficial cells rest on two to three central layers of wing cells followed posteriorly by a single layer of basal cells. Only the basal layer possesses mitotic activity and produces daughter cells which differentiate anteriorly and desquamate into the

Figure 1.1
The Structural Organisation of the Cornea (after Gray & Paterson, 1994).

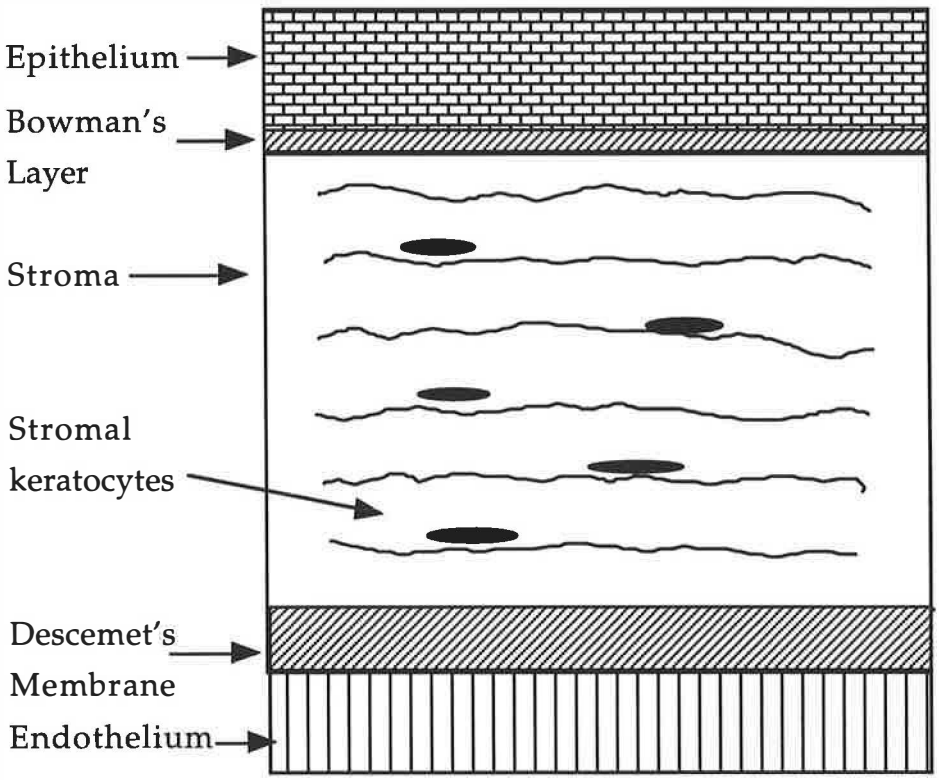

tear film. Cell turnover is rapid, occurring every seven to fourteen days (Hanna et al, 1961). The basal cells also synthesise a basement membrane which mediates adhesion to the underlying Bowman's layer and stroma. Basal cells adhere to the basement membrane via hemidesmosome attachments and type VII anchoring fibrils which pass through the basement membrane and form anchoring plaques with type I collagen in the stroma (Gipson et al, 1987; Kenyon, 1979). Bowman's membrane is a layer of closely packed collagen fibrils and proteoglycans (PGs) and appears as a less ordered anterior portion of the stroma under electron microscope. Synthesis appears to be coordinated by both epithelial and stromal cell activity (Albert & Jakobiec, 1994). The stroma makes up 90% of the cornea and consists primarily of parallel collagen bundles interspersed with keratocytes and surrounded by glycoprotein rich in keratin sulphate and chondroitin sulphate (Nishida, 1992). Collagen fibrils are assembled into fibres which form approximately three hundred lamellae within the stroma (Svoboda et al, 1998; Worthington, 1984). Between the collagen lamellae flattened keratocytes spread out spindle shaped processes and interconnect via gap junctions (Maurice, 1987). Descemet's membrane separates the stroma from the inner, simple squamous layer of cells forming the endothelium. The 7 μm thick membrane is synthesised by cells of the endothelium and consists of an anterior banded and posterior non-banded zone (Levy et al, 1996). The anterior zone has a hexagonal lattice structure with nodes at each lattice vortex attached by fibrillar rods made primarily of type VIII collagen (Sawada et al, 1990). The posterior zone has a more amorphous structure made up primarily of collagen type IV and laminin (Fitch et al, 1990). Fibronectin, heparin sulphate and dermatin sulphate proteoglycans are also contained within the membrane. The endothelium is a monolayer of 5 μm thick, hexagonal, flattened cells whose primary function is to regulate stromal hydration (Green, 1991). Ion transport systems maintain an osmotic gradient and thus the relative detergescence and transparency of the cornea. The endothelium also allows passage of nutrients from the aqueous humor to the non-vascularised corneal tissue.

Maintenance of corneal structural integrity is important for vision since over two thirds of light refraction occurs in the cornea (Nishida, 1997). Corneal transparency is primarily determined by collagen fibril alignment and associated proteoglycan binding (Svoboda et al, 1998). Fibres are densely packed within each lamella with a small mean fibril diameter of 25 nm and uniform interfibrillar spacing (Komai & Ushiki, 1991). The co-polymerisation of collagen types I and V within collagen fibrils may help to maintain the small mean collagen fibril diameter necessary for transparency (Birk et al, 1990). Fibrillar size and differences in the refractive index of collagen and glycosaminoglycans should produce light scattering and opacity. However, uniformity of fibrillar diameter and parallel fibril arrangement produce destructive interference of diffracted light so that only undiffracted rays pass through the cornea intact (Davison, 1991). Transparency is also dependent on endothelial regulation of stromal hydration. Loss of the endothelial barrier results in free flow of fluid from the anterior chamber. Corneal swelling and the subsequent disruption of collagen fibrillar arrangements may lead to corneal opacity.

1.3 The Keratocyte and Corneal Structure

The organisation of the stromal extracellular matrix (ECM) is dictated by keratocyte activity. Approximately 2.4 million keratoyctes are present within the stroma where they fill only 2 to 3% of the total stromal volume (Moller-Pedersen et al, 1994; Otori, 1967). They are quiescent in the resting cornea and turnover is estimated at approximately two to three years (Nishida, 1997). However, keratocytes may be quickly activated in response to stromal injury for involvement in the wound healing response. Activated keratocytes migrate into the wound and are adapted to produce the various structural proteins, enzymes, enzyme inhibitors and growth factors required to remodel the stroma and re-establish corneal transparency. Keratocytes act in conjunction with signals from the ECM so that cell maintenance of ECM integrity is in turn important for cell growth and growth factor responsiveness (Nakagawa et al, 1989). Adhesion to the ECM is mediated primarily by the integrin family of cell surface receptors (Rouslahti, 1991). Each

receptor is a heterodimer of an α and β subunit. Eleven α subunits and six β subunits have been identified and variation in subunit combinations produces integrin receptor specificity for the various structural proteins found within the corneal ECM (Nishida, 1997; Watt, 1994).

1.3.1 Structural Proteins

1.3.1.1 Collagen

The protective and light refractory structure of the cornea is formed primarily by collagen which makes up 70% of the dry weight of the cornea (Svoboda et al, 1998). Eighteen different collagen types have currently been identified and are divided into five structural and functional categories including the most common fibrillar collagens (types I, II, III, V and XI), the sheet or network forming collagens (types IV, VI and VII), the fibril associated collagens with interrupted triple helices (FACIT) (types IX, XII, XIV, XVI and IXVI), the short chain collagens (types VIII and X), the membrane associated collagens with interrupted triple helices (MACIT) (types XIII and XVII) and the multiplexins which have multiple triple helix domains interrupted by non-collagenous domains (types XVIII and XV) (Svoboda et al, 1998). A number of collagen types appear transiently during corneal development. In the adult stroma, as in other connective tissues the primary structural protein is type I collagen (Marshall et al, 1991[a]). Collagen types III, V and VI have also been identified (Zimmermann et al, 1986; Marshall et al, 1991[b]). Detection of labelling for collagen types I, III and V within individual collagen fibrils suggests that these three collagen types co-assemble within the same fibril while type VI collagen is found in the interfibrillar spaces (Newsome et al, 1982; Marshall et al, 1991[a,b]; Marshall et al, 1993). Collagen types I, III, V and VI are also found in Bowman's layer (Marshall et al, 1991[a,b]). The corneal epithelial basement membrane contains collagen types III, IV, VII and XVII; secreted by basal epithelial cells rather than keratocytes. Type VII collagen forms anchoring fibrils which attach the basement membrane to Bowman's layer possibly by adhesion to type VI collagen (Marshall et

al, 1991[b]). Type IV collagen is sparser in the corneal epithelial membrane than in other basement membranes and is found in higher proportion in Descemet's membrane with type VIII collagen (Fini & Girard, 1990[a]). Collagen types V, VI and possibly type XII have also been identified in Descemet's membrane; secreted by the underlying endothelium.

1.3.1.2 Fibronectin

Fibronectin (FN) is a multifunctional matrix glycoprotein and is widely distributed in connective tissues. In the unwounded cornea FN has been identified surrounding keratocytes and at the stromal and endothelial edges of Descemet's membrane (Gibson et al, 1993). It is synthesised by keratocytes within the stromal matrix where it binds to the cell membrane and to other matrix components, promoting ECM stability. Other sources of FN to the cornea include tear fluid, aqueous humor, limbal blood vessels, epithelial and endothelial cells (Ding & Burstein, 1988). Two forms of FN, resulting from variations in postranslational modification have been isolated. One has a lower molecular weight, is synthesised in the liver and found in plasma (pFN). The other is isolated from cellular sources (cFN). Carbohydrate groups make up 4 to 9% of the FN molecule and contribute to FN heterogeneity (Gibson et al, 1993).

FN consists of two polypeptide chains joined by disulfide bonds (Hynes & Yamada, 1982). Each consists of three types of homologous, repeating amino acid sequences, types I, II and III, and contains various splicing sites whose sections are spliced to form pFN but left unspliced to form cFN (Gibson et al, 1993). Repeat sequences form various domains within the FN molecule, creating multiple binding sites for the cell membrane and other ECM components including fibrin, collagen, PGs and heparin (Hynes & Yamada, 1982). Fibronectin is involved in numerous processes including cell/matrix adhesion (Wojciak-Stothard et al, 1997; Ejim et al, 1993), cytoskeletal structure (Hynes, 1981) and chemotactic cell migration (Shimizu et al, 1997; Postlethwaite et al, 1981).

1.3.1.3 Proteoglycans

The PGs are a structurally diverse family of molecules consisting of a core protein attached to one or more glycosaminoglycans (GAGs). The GAG sidechains are made up of repeating disaccharide units and mediate many of the interactions of the PGs with other matrix components (Rouslahti, 1989). During embryogenesis hyaluronic acid (HA) is the primary GAG found within the developing cornea. Synthesis gradually declines so that no HA is found in the resting adult cornea. However, synthesis does reoccur following injury (Nishida, 1997). The primary PGs found within the adult cornea are lumican, containing keratin sulphate GAG sidechains and decorin, containing chondroitin and dermatan sulfate sidechains (Hassell et al, 1992; Svoboda et al, 1998). Keratin sulfate GAGs tend to be concentrated in the posterior cornea possibly because oxygen is not required for synthesis (Svoboda et al, 1998). Both collagen associated and non-associated PGs are found within the cornea. The collagen associated PGs form links between stromal collagen fibrils to regulate fibrillar structure for the maintenance of corneal transparency (Hassell et al, 1983). GAGs have a high water binding capacity and also contribute to the regulation of stromal hydration (Tuft et al, 1993). PGs form multiple interactions, mediating cell adhesion to the ECM and the adhesion of matrix components to each other. Within the stroma type VI collagen adhesion to striated fibrillar collagen is mediated by decorin (Nakamura et al, 1994[a]). PGs may also concentrate soluble factors such as growth factors at sites of cell interaction for enhanced activity (Rouslahti, 1989).

1.3.1.4 Laminin

Laminin is found in the sub-epithelial layer of the cornea and in Descemet's membrane where its primary function is to mediate cell adhesion to the underlying basement membrane (Marshall et al, 1991[a]). In organ culture, it is also synthesised by keratocytes into the stroma where it forms basement membrane-like plaques (Hassell et al, 1992). Laminin is the major glycoprotein of basement membranes and tends to stimulate basement membrane associated cell migration and proliferation in a similar way to the FN mediated activity of

mesenchymal cells (Ocalan et al, 1988).

1.3.2 Secreted Enzymes

1.3.2.1 Matrix Metalloproteinases

The matrix metalloproteinases (MMPs) are a family of structurally related, zinc dependent endopeptidases which function at neutral pH and are primarily involved in degradation of the ECM (Murphy, 1995). They are secreted by some haematopoietic cells and by mesenchymal cells including keratocytes. Structural features common to most MMPs include a 'cysteine switch' containing propeptide domain lost on activation, a catalytic calcium and zinc-binding domain containing a conserved HEXXH sequence motif, a variable, proline rich hinge region and a C-terminal domain (Birkedal-Hansen, 1995).

At least eighteen MMPs have currently been characterised (Yong et al, 1998). They tend to have closely related specificities and are broadly organised on the basis of domain structure and substrate preference into four sub-families; the collagenases (1,8,13 and a 4th collagenase without numerical designation), gelatinases (2,9), stromelysins (3,7,10,11) and membrane type (MT)-MMPs (14,15,16,17). Four other members have been identified but have yet to be assigned a grouping (Yong et al, 1998). In general, collagenases degrade fibrillar collagens, the gelatinases degrade basement membrane collagens, denatured collagens and FN while stromelysins have a broader substrate specificity, acting on PGs, FN and laminin as well as collagens (Matrisian, 1990; Murphy, 1995). The membrane type MMPs remain bound to the cell membrane and cleave pro-MMP-2, the collagens and gelatin (Yong et al, 1998). Although all of the MMP subfamilies are involved in collagen degradation the initial breakdown of collagen types I, II and III requires collagenase activity.

Regulation of MMP activity is important to prevent uncontrolled breakdown of the ECM. Enzyme activity is tightly maintained at the level of gene transcription and enzyme activation. MMPs are synthesised as required in response to various growth factor and cytokine signals. In general, the cytokines interferon (IFN)-α, β, γ,

interleukin (IL)-1 α,β, tumour necrosis factor (TNF)-α and the growth factors fibroblast growth factor (FGF), epidermal growth factor (EGF) and platelet derived growth factor (PDGF) induce MMP transcription while transforming growth factor (TGF)-β and IL-4 repress it (Woessner, 1991; Birkedal-Hansen, 1995). Activator protein-1 (AP-1) binding sites have been found in the promoter regions of the gelatinase MMP-9, the stromelysins and the collagenases indicating that stimuli induce the formation of AP-1, the leucine zipper bound heterodimer of proto-oncogene products c-fos and c-jun, in order to induce the expression of these MMPs (Matrisian, 1990; Woessner, 1991). Inhibition of stromelysin activity by TGF may also be mediated by c-fos which forms part of a protein complex that binds to the TGF inhibitory element (TIE) in the promoter region of the stromelysin gene (Matrisian, 1990). The MMPs are secreted in zymogen form for activation extracellularly and are inhibited by tissue inhibitors of matrix metalloproteinases (TIMPs) (Birkedal-Hansen, 1995). Enzyme latency is maintained by a 'cysteine switch' mechanism where by a cysteine thiol group found in the highly conserved PRCGVPDV sequence of the propeptide domain remains coordinately bound to a zinc ion in the active site of the catalytic domain. Activation involves disruption of the disulfide bond linking cysteine and zinc so that an open form of the pro-enzyme, susceptible to autocatalytic cleavage, is produced.

The inactive pro-enzyme may be cleaved by physiological activators such as plasmin (Murphy & Docherty, 1992). Plasmin is a broad spectrum protease involved in the degradation of proteins involved in cell to cell and cell to matrix interactions and in the activation of other degradative enzymes including the MMPs (Birkedal-Hansen et al, 1993). The synthesised protease is inactive and requires the secretion of tissue-type plasminogen activator (t-PA) or urokinase-type plasminogen activator (u-PA) for activation. t-PA is primarily involved in fibrinolysis while u-PA mediates cell migration and tissue remodelling. Both cleave arg-val bonds to produce the active plasmin from plasminogen and are regulated by plasminogen activator inhibitor (PAI-1) activity. Plasmin is localised to cell adhesion plaques where u-PA is bound to specific cell

receptors in order to localise activity (Murphy, 1995). Stromelysin is rapidly activated by plasmin and appears to additionally potentiate activation of collagenase and the gelatinase MMP-9 (Murphy & Docherty, 1992). In contrast MMP-2 is not succeptable to plasmin or other protease activity and appears to be activated by a fibroblast membrane mediated process (Murphy et al, 1992). Plasmin may also mediate MMP-1 secretion by disrupting FN interactions with integrin receptors localised at cell membrane focal adhesion sites to produce alterations in F-actin mediated intracellular signalling pathways (Berman, 1994).

The normal cornea undergoes limited structural remodelling and only MMP-2 is constitutively secreted by keratocytes (Fini & Girard, 1990[a]; Girard et al, 1991). Keratocytes passaged in culture also secrete collagenase and stromelysin (Girard et al, 1991). In addition collagenase and the gelatinase MMP-9 are secreted within the cornea following injury (Azar et al, 1996). MMP-9 is secreted primarily by corneal epithelial cells while keratocytes secrete primarily MMP-2 (Fini & Girard, 1990[a]; Ye & Azar, 1998). Both epithelial cells and keratocytes have been identified as sources of collagenase (Brown & Weller, 1970; Gordon et al, 1980).

1.3.2.2 Tissue Inhibitors of Matrix Metalloproteinases

Specific regulation of both active and inactive MMPs occurs by the formation of non-covalent complexes with TIMPs (Matrisian, 1994; Birkedal-Hansen, 1995). Four different TIMPs, consisting of two distinct domains, have currently been identified and bind to the MMPs with varying affinity (Yong et al, 1998). The TIMP N-terminal domain is sufficient for MMP inhibition and binds to the MMP catalytic domain. The C-terminal domain also contains enzyme binding sites and appears to enhance TIMP inhibitory activity on MMP binding (Wojtowicz-Praga et al, 1997). All of the TIMPs are characterised by twelve conserved cysteine residues which form six disulfide bonds and produce a six loop structure (Murphy & Docherty, 1992). Each contains a consensus sequence, VIRAK, in the N-terminal domain and a leader sequence which is cleaved prior to mature enzyme formation (Gomez et al, 1997).

Both TIMP-1 and TIMP-2 are secreted by keratocytes within the corneal stroma (Brown et al, 1991). They share a similar distribution although TIMP-1 tends to be present in greater quantities (Murphy, 1995). TIMP-1 is an inducible, 28 kDa glycoprotein with greatest affinity for the pro-gelatinase MMP-9. Expression is controlled by a number of cytokines and growth factors. The enzyme contains an AP-1 binding site within its promoter region allowing coordinated MMP and TIMP expression (Yong et al, 1998). TIMP-2 is a 21 kDa, unglycosylated protein which appears to be constitutively expressed and has a preferential affinity for the pro-gelatinase MMP-2 (Gomez et al, 1997; Murphy & Docherty, 1992). Less is known about the regulation of TIMP-2 activity. TIMP-1 and TIMP-2 are both multifunctional proteins and have an additional role in the inhibition of angiogenesis. TIMP-1 is also involved in the promotion of gonadal steroidogenesis (Gomez et al, 1997). TIMP-3 and TIMP-4 are less well characterised. TIMP-3 is a 20kDa protein widely distributed in connective tissue. TIMP-4 was most recently isolated by molecular cloning and occurs predominantly in cardiac tissue (Gomez et al, 1997).

Within the resting cornea limited remodelling occurs. Following wounding the activated keratocyte is stimulated to move into the wound and begin synthesis of products involved in corneal tissue repair (Tuft et al, 1993). A controlled balance in the synthesis of ECM degrading proteases such as the MMPs with TIMPS and structural proteins is important for rebuilding corneal structural integrity. Failure to control the balance of products secreted by the keratocyte during the remodelling process results in disruption of normal ECM structure and subsequently the functional properties of the cornea.

1.4 The Keratocyte and Corneal Wound Healing

1.4.1 The Wound Healing Process

Corneal wound repair involves a carefully regulated sequence of events designed to restructure the cornea so that a return to visual acuity may be achieved. An initial inflammatory response is followed by matrix remodelling and further long-term resolution of the resulting scar tissue. A FN and fibrin plug derived from the tear film fills the wound

and provides a provisional matrix for cell migration (Tuft et al, 1993; Greiling & Clark, 1997). Damaged cells produce chemotactic signals which initiate the inflammatory response. Neutrophils followed by macrophages migrate into the wound where they phagocytose debris and infectious pathogens (Mutsaers et al, 1997). They also release cytokines which contribute to the activation of resident corneal cells. Peripheral epithelial cells initially migrate towards the area of tissue damage by sliding across the FN mesh and basement membrane. Hemidesmosomal attachments to the basement membrane are released and temporary attachments to basement membrane type IV collagen are formed via cell membrane integrin receptor mediated FN, laminin and glycoprotein binding. These links are associated with cytoskeletal actin and are broken and reformed by plasmin activity (Tuft et al, 1993). New epithelial cells are formed to replace those migrating into the wound. Epithelial cells cover the wound and eventually differentiate to form the original stratified squamous corneal surface (Schultz et al, 1992). The wound is initially covered by a thickened epithelium which is gradually pushed upwards during stromal remodelling (Davison & Galbavy, 1986; Tuft et al, 1993).

Activated keratocytes are primarily responsible for remodelling the damaged stroma. Apoptosis of anterior stromal keratocytes occurs immediately following epithelial disruption (Wilson, 1997; Szerenyi et al, 1994). Once re-epithelialisation has occurred the remaining keratocytes proliferate and migrate into the wound (Wilson et al, 1996; Moller-Pedersen et al, 1998; Helena et al, 1998). Plasmin mediated removal of the fibrin plug occurs (Kao et al, 1998). Activated keratocytes round up and lose their attachments to surrounding cells (Maurice, 1987). They contain α-smooth muscle actin in their cytoplasm and peripheral cells appear to line up along the margin of tissue damage to contract the wound (Jester et al, 1995). Keratocytes begin to remodel the granulation tissue by the secretion of collagen, MMPs and cytokines with both autocrine and paracrine mediated activity (Schaffer & Nanney, 1996). Wounding appears to initiate an IL-1α mediated autocrine feedback loop within the keratocyte which is responsible for induction of

the keratocyte repair phenotype (West-Mays et al, 1997). Initial collagen deposition within the scar occurs in an irregular pattern. Later, progressive remodelling involves the interweaving of old and new collagen fibrils to produce a more regular fibrillar arrangement and promote the return of corneal transparency (Davison & Galbavy, 1986; Fini et al, 1992[a]). Bowman's membrane is not repaired following damage. In wounds transecting the cornea endothelial cells tend to spread across the gap and may eventually re-secrete Descemet's membrane (Cameron, 1997).

1.4.2 Collagen and Corneal Wound Healing

A chemotactic response to collagen and collagen peptides has been observed in dermal fibroblasts (Postlethwaite et al, 1978). Following corneal injury damaged collagen fibrils, in addition to other stimuli, may attract keratocytes into the area of tissue damage to initiate ECM remodelling. Alkali burn models of wound healing in the rabbit cornea indicate that collagen types III and V are initially synthesised by activated keratocytes followed later by the synthesis of type I collagen (Saika et al, 1996). The production of collagen based scar tissue with variable interfibrillar spacing in the stroma initially results in corneal opacity (Rawe et al, 1994). Gradual remodelling generally produces resolution of the scar and a return to transparency (Rawe et al, 1992). However, mechanical strength at the scar site is permanently reduced and collagen lamellar structure and fibril size distribution are altered (Cintron et al, 1978). Collagen fibrils are initially randomly distributed with a large range of interfibrillar spacing but gradually form more ordered collagen bundles running parallel to the epithelial surface (Rawe et al, 1992). Transparency is dependent on restoration of ordered collagen fibrillar structure which is in part dependent on PG distribution within the remodelling stroma.

1.4.3 Proteoglycans and Corneal Wound Healing

Following corneal wounding a decrease in PG synthesis occurs, possibly indicating an increase in PG turnover, and synthesis is of PGs with a larger molecular size (Funderburgh & Chandler, 1989). An increase in

heparin sulfate and decrease in dermatan sulfate occurs. Sulfation of these GAGs is increased while that of keratan sulfate declines (Funderburgh & Chandler, 1989). Larger PGs fill less ordered interfibrillar spaces in early scars and result in increased stromal swelling. Increased hydration appears to facilitate remodelling by providing a more fluid environment but also contributes to opacity by fibrillar disruption (Rawe et al, 1992). Over time the number of interfibrillar spaces and abnormal PGs within the stroma is reduced (Hassell et al, 1983).

Synthesis of HA by both epithelial cells and keratocytes is observed following corneal injury (Fitzsimmons et al, 1992). The exact function of HA in corneal wound repair is unknown. It may function additionally in tissue hydration or in stimulating cell proliferation and migration (Nakamura et al, 1992).

1.4.4 Fibronectin and Corneal Wound Healing

FN appears rapidly on the wound surface following corneal injury. It provides a temporary scaffold across the bare wound for cell adhesion, migration and reformation of the ECM and acts as a chemoattractant for additional cell migration (Gibson et al, 1993; Mensing et al, 1983; Kondo & Yonezawa, 1992; Saika et al, 1993). Sources of FN may vary depending on the severity and type of corneal wound (Ding & Burstein, 1988). Both pFN and cFN are found on the wound surface. pFN may be present in tears or gain access via the conjunctival vasculature. Activated epithelial cells and keratocytes synthesise additional cFN (Gibson et al, 1993; Ohashi et al, 1983).

FN mediated cell adhesion to the matrix occurs by the interaction of specific FN domains with a number of integrin receptors on the cell membrane. The primary site of interaction for the $\alpha 5\beta 1$ integrin receptor is with an arginine-glycine-aspartic acid (RGD) sequence located in the cell-binding domain of FN (Gibson et al, 1993). Corneal epithelial cell adhesion to FN is additionally mediated by fragments within the heparin binding domain (Mooradian et al, 1992). FN also adheres to the

cell membrane at focal adhesion sites which interact intracellularly with the cytoskeleton (Peters & Mosher, 1987). A coordinated increase in cell membrane integrin receptor expression and focal clustering occurs in conjunction with FNs appearance for mediation of cell attachment and migration (Nishida, 1992; Watt, 1994). Cell migration appears to occur by protease degradation and reformation of the cell-FN focal contacts. Corneal epithelial cell migration was observed in response to FN mediated rearrangement of intracellular actin filaments (Nakagawa et al, 1985). Fibronectin may also induce cytoskeletal changes conducive to keratocyte migration and the synthesis of other factors involved in the cell's response to wounding (Berman, 1994). Other potential roles for FN include debris opsonisation for cellular phagocytosis and chemotaxis of other inflammatory cells (Gibson et al, 1993).

1.4.5 Growth Factors and Corneal Wound Healing

The corneal repair response is driven predominantly by growth factors and cytokines secreted initially by inflammatory cells and then by corneal epithelial cells and activated keratocytes. These host cells act in association with each other by paracrine and autocrine feedback mechanisms to coordinate the remodelling process (Ellis et al, 1992; Pancholi et al, 1998). The exact mechanisms by which specific growth factors mediate wound repair is unknown. However their role in stimulating cell proliferation, migration and the synthesis of ECM structural proteins and proteases is well established.

EGF and TGF-α have both been identified in tear fluid and may be involved in initial exocrine stimulation of corneal epithelial migration (Schultz et al, 1992). Proliferation, migration and adhesion of epithelial cells to the FN matrix all appear to be mediated by EGF activity which is in turn modulated by TGF-β (Nishida, 1992). PDGF-β receptors have also been identified on the corneal epithelial membrane and PDGF addition appears to increase cytosolic calcium levels (Nishida, 1992). EGF, TGF-α, TGF-β and IL-1α have been detected in all three corneal layers (Wilson et al, 1994[a]). EGF, EGF receptors and mRNA for IL-1α, keratinocyte growth

factor (KGF) and FGF have been identified in epithelial cells and keratocytes (Wilson et al, 1992; Wilson et al, 1993). KGF, secreted by keratocytes, is a member of the FGF family and appears to act at corneal epithelial cell KGF receptors as a paracrine mediator of epithelial cell proliferation (Sotozono et al, 1994). IL-1α is thought to initiate a positive feedback loop which activates the keratocyte repair phenotype. The cytokines IL-1α and β are secreted by corneal epithelial cells and also appear to have a paracrine effect on keratocyte activity, inducing apoptotic death. They may mediate the observed apoptotic death of anterior stromal keratocytes following epithelial debridement and help to modulate corneal restructuring following wounding (Wilson et al, 1996). An increase in collagenase secretion in response to bFGF stimulation has been observed in dermal fibroblasts and may occur similarly in keratocytes (Buckley-Sturrock et al, 1989). PDGF, EGF and bFGF were all found to stimulate keratocyte migration while migration was inhibited by TGF-β (Andresen et al, 1997). Proliferation of both keratocytes and epithelial cells was also stimulated by EGF and bFGF but was inhibited by TGF-β (Pancholi et al, 1998). TGF-β was also found to stimulate collagen production by keratocytes but had a chemotactic rather than an inhibitory effect on keratocyte and epithelial cell migration (Schultz et al, 1992). Discrepancy in the observed effects of TGF-β on keratocyte migration may reflect the dependence of cell response on the experimental system used. Cell response to cytokine activity may also depend on the moderating influence of particular extracellular environments indicating that the balanced activity of a number of cytokines is an important aspect of wound healing (Ellis et al, 1992).

1.4.6 MMPs and Corneal Wound Healing

Following corneal wounding synthesis of the constitutively expressed gelatinase MMP-2 is upregulated. Synthesis of collagenase and the gelatinase MMP-9 is also initiated (Gordon et al, 1980; Azar et al, 1996). MMP-9 has been localised within the epithelium and is secreted primarily by corneal epithelial cells (Fini et al, 1992[a]; Ye & Azar, 1998).

Activity tends to peak early in the repair process and decline rapidly suggesting a role in the initial inflammatory response and in epithelial basement membrane reassembly (Fini et al, 1992[a]). MMP-2 is secreted primarily by keratocytes and activity tends to decline slowly (Fini & Girard, 1990[a]; Fini et al, 1992[a]) suggesting involvement in the more long-term remodelling of the primary matrix (Paul et al, 1997).

Intrastromal epithelial cell migration occurs during the process of corneal wound repair and is delayed by MMP inhibitors suggesting the involvement of MMP activity (Azar et al, 1996). The production of collagenase first requires corneal epithelial cell interaction with the stroma indicating that the interaction of stromal and epithelial cells modulates the keratocyte repair response (Brown & Weller, 1970; Johnson-Muller & Gross, 1978). Mediators involved in regulating MMP secretion by keratocytes include IL-1 and TGF-β. IL-1 induces primary cultures of keratocytes to express MMP-9, collagenase and stromelysin and increases MMP-2 expression. TGF-β modulates this effect. It represses collagenase and stromelysin expression but increases MMP-2 expression (Girard et al, 1991). As in other tissues the coordinated secretion of specific MMP inhibitors also regulates MMP activity. TIMP-1 has been localised at the epithelial basement membrane with MMP-9 during early corneal wound healing where it appears to regulate MMP-9 involvement in early remodelling processes (Ye & Azar, 1998).

1.4.7 Age Related Changes in Corneal Structure and Response to Wounding

The cornea undergoes a number of changes with age which may alter corneal function and response to wounding. Since the keratocyte is primarily responsible for maintenance of corneal stromal structure some of these changes may be related to age specific alterations in the keratocyte phenotype.

A general decline in collagen turnover has been observed with age as well as a decline in elasticity, solubility and susceptibility to enzyme and

thermal degradation (Sell & Monnier, 1989). An increase in corneal collagen fibril diameter and a reduction in interfibrillar spacing occurs which may contribute to the increase in light scattering observed with age and ultimately to loss of visual acuity (Daxer et al, 1998; Malik et al, 1992; Olsen, 1982). Fibril diameter is primarily altered by the age related addition of more collagen molecules (Daxer et al, 1998). Increased non-enzymic crosslinking between collagen molecules also occurs and may contribute to the increase in fibril diameter by increasing intermolecular spacing (Malik et al, 1992). More crosslinking within each collagen fibril will additionally result in loss of elasticity (Bailey, 1987). In the sclera a decline in dermatin sulfate has been observed with age. Changes in the ratio of interfibrillar PG to collagen have been observed in the corneal stroma which may also contribute to the reduction in collagen interfibrillar spacing by an increase in fibrillar swelling (Scott et al, 1981).

The corneal epithelium thickens with age, in some cases as a result of reduplication. General deterioration of the epithelial basement membrane and a decline in epithelial cell adhesion to Bowman's membrane by anchoring fibrils and hemidesmosomes also occurs (Alvarado et al, 1983). Changes in α_6 and β_4 integrin subunit distribution have been found along the basal epithelial cell surface and may contribute to loss of epithelial adhesion to the basement membrane (Trinkaus-Randall et al, 1993). Following injury the reduplicated basement membrane tends to be lost with the epithelium, slowing epithelial cell migration and re-epithelialisation (Kenyon, 1979). A decline in type IV collagen may also occur with additional effects on epithelial adhesion to the underlying matrix (Marshall et al, 1993). One of the prerequisites for the long-term success of a KPro design is the maintenance of an intact epithelium to prevent infection, dehydration and downgrowth into the underlying tissue. Loss of epithelial adhesion with age may therefore increase the difficulty with which this goal is achieved. Also, epithelial-stromal interactions contribute to keratocyte remodelling activity following wounding and may be altered by a decline in epithelial migration across the wound surface.

The corneal endothelium exhibits a decline in cell density, a decline in it's ability to maintain an ionic gradient and an increase in cell size with age (Doughty, 1994; Wigham & Hodson, 1987; Sherrard et al, 1987). Descemet's membrane, on which the endothelium rests also thickens. Endothelial cell division occurs slowly in humans and injury is accommodated primarily by cell spreading (Hoppenreijs et al, 1996). However, endothelial cell proliferation and the contribution which cell division makes to endothelial wound closure appear to decline with donor age (Hoppenreijs et al, 1994). Loss of cell density with age may result in an inability to deal sufficiently with endothelial damage and subsequently in loss of functional integrity. A reduction in the ability of the endothelium to maintain an ionic gradient may also lead to corneal oedema and visual disruption although evidence indicates that compensation occurs and that no reduction in endothelial permeability takes place (Wigham & Hodson, 1987). Since collagen-PG association and collagen fibrillar structure are already altered by age additional changes in endothelial maintenance of hydration coupled with disruption of epithelial activity may be sufficient to slow or even prevent a return to corneal transparency following injury.

In dermal tissue a decline in wound healing with age has been observed and has been tentatively related to changes in fibroblast activity (Holt et al, 1992; Grove, 1982; Barker & Blair, 1968; Ashcroft et al, 1995). Within the cornea age related effects on the outcome of refractive surgery have been attributed to a decline in corneal wound healing (Dutt et al, 1994). However, little is known about the effect of age on keratocyte function. A decline in keratocyte density has been observed with age and would be expected to reduce the repair response (Moller-Pedersen, 1997). Embryonic keratocyte division has been detected within organ cultured corneae over a twenty four hour time period suggesting a level of cell division which may result in the accumulation of senescent keratocytes over time (Hyldahl, 1986). A similar accumulation of senescent keratocytes within the cornea would be expected with age and may contribute to some of the age related changes in corneal structure, function and wound repair previously observed.

1.5 Senescence

Normally dividing cells, with the exception of germline and possibly some stem cells, possess a finite replicative capacity and reach a permanently non-dividing state called senescence (Hayflick & Moorhead, 1961; Hayflick, 1965). Following initial explantation a period of rapid cell division occurs followed by a decline in replicative capacity until all cells within the culture become senescent. However, cultures do not grow as a homogeneous population of dividing cells which simultaneously enter senescence (Smith & Hayflick, 1974). Rather, senescence may occur at each round of the cell cycle, with increasing probability as the number of cell divisions rises, until senescence is certain (Kipling & Faragher, 1997). Senescent cells remain metabolically active and can respond to mitogens by increased transcriptional activity. However, in contrast to quiescent cells, senescent cells cannot be stimulated to synthesise DNA and divide. In addition, cells exhibit alterations in morphology, in cell to cell and cell to substratum contact characteristics and in the expression of intracellular and secretory proteins (Cristofalo & Pignolo, 1993; Sherwood et al, 1988; Maciera-Coelho, 1983). Since senescent cells arrest in a distinct growth state, show irreversible changes in genetic expression and exhibit functional changes unrelated to inhibition of DNA synthesis it has been suggested that senescence is a form of terminal differentiation (Seshadri & Campisi, 1990; Peacocke & Campisi, 1991). However, investigation of differentiation and apoptosis in relation to keratinocyte senescence suggests that senescence and differentiation are two distinct processes (Norsgaard et al, 1996).

Replicative senescence has primarily been studied in human diploid fibroblasts since fibroblasts can be easily cultured and analysed for alterations in growth characteristics (Koli & Keski-Oja, 1992; Littlefield, 1996). Since the finite lifespan of these cells was first recorded a number of observations have been made which suggest that senescence contributes to and can be studied as an *in vitro* model of the ageing process. Fibroblasts senesce after a species and tissue specific number of division cycles at a rate which is related to the lifespan of the donor

species. Cells from species exhibiting longevity undergo a greater number of cell divisions in culture than those with a shorter lifespan (Vojta & Barret, 1995). The number of cell divisions a cell culture undergoes is also inversely related to the age of the tissue donor with fibroblast cultures from elderly donors senescing after fewer cell divisions than cultures from young donors (Peacocke & Campisi, 1991; Bruce & Desmond, 1991). Fibroblast cell strains from donors with ageing disorders such as Werner's syndrome also exhibit an attenuated lifespan prior to senescence on comparison with cells from unaffected individuals suggesting that the accumulation of senescent fibroblasts is linked to the ageing process (Faragher et al, 1993).

1.5.1 The Genetic Basis for Senescence

1.5.1.1 Random Error Versus Genetic Control

Theories to explain replicative senescence may be grouped into two general categories (Campisi, 1997; Monti et al, 1992). The random error theory suggests that senescence is the result of cumulative random errors over time produced by mutational genetic damage, the accumulation of defective proteins and destruction by free radicals (Cristofalo & Pignolo, 1993). In contrast, the genetic control theory explains senescence as an intrinsic genetic programme that, once triggered, switches off the replicative capability of the cell. Evidence from cell fusion and microcell mediated experiments indicate that senescence is primarily a genetically controlled process with a possible contribution from cumulative genetic damage (Cristofalo & Pignolo, 1993; Smith & Lincoln, 1984).

Initial heterokaryon studies fusing senescent with young proliferating fibroblasts revealed inhibition of proliferation in the young cell nuclei. Fusion of enucleated senescent fibroblasts with proliferating cells also inhibited DNA synthesis suggesting that the pathway to senescence involves expression of an inhibitory protein into the cytoplasm (Dreschler-Lincoln & Smith, 1983). Gene fusion studies between senescent and immortal cells produce a majority of senescent hybrids indicating a dominant senescent phenotype and suggesting that

immortal cells contain a recessive genetic defect in genes related to production of the senescent state (McCormick & Campisi, 1991; Smith & Pereira-Smith, 1996). Studies involving fusion of different immortal cell lines indicate that multiple genes are involved in senescence (Dice, 1993) and have established four complementation groups based on the production of immortal or senescent hybrids (Pereira-Smith & Smith, 1988). Those fusions producing an immortal hybrid cell line were placed in the same complementation group indicating loss of both copies of the same senescence related genes. Those that produced a hybrid cell line with limited growth potential were placed in different complementation groups and were considered to have different genetic defects so that the normal, dominant, senescent related gene was expressed in such cases to induce senescence. Hybrids of a number of different immortal cell lines and differentiated cell types revealed similar results indicating a common, genetically controlled mechanism for induction of replicative senescence in different cell types (Hensler & Pereira-Smith, 1995).

1.5.1.2 Senescence Related Genes

Senescence related genes have been mapped to chromosomes 1, 4, 7, 11, 18, and X using microcell mediated chromosome transfer experiments of a single normal chromosome into immortal human cells. Only chromosomes 1, 4 and 7 were tested more stringently to show an effect on one complementation group with no effect on others and have been found to cause senescence in cell lines assigned to complementation groups C, B and D respectively (Hensler et al, 1994; Ning et al, 1991; Ogata et al, 1993). Sasaki et al (1994) showed that transfer of either chromosome 1 or chromosome 18 into the same cell line produced cells with finite lifespan supporting the model of multiple pathways to senescence and suggesting that immortal cells contain defective genes in each of these pathways to overcome senescence (Vojta & Barrett, 1995). The existence of multiple pathways to senescence may explain why spontaneous immortalisation of human cell cultures almost never occurs. It is also difficult to induce immortalisation by ultraviolet, chemical or viral agents. Immortalisation occurs more frequently in rodent species indicating that the stringency with which senescence

occurs is species specific (Peacocke & Campisi, 1991).

1.5.2 Mechanisms for the Induction of Senescence

1.5.2.1 The Cell Cycle

The induction of senescence appears to involve a genetic switch which is able to count the number of divisions a cell has undergone and activate changes in cell cycle regulation to inhibit further cell division. Mammalian cell division occurs in response to external mitogenic stimulation and involves progression of cells through the four stages of the cell cycle known as Gap 1 (G_1), DNA synthesis (S), Gap 2 (G_2) and mitosis (M). DNA replication occurs in S phase. Cell growth and the synthesis of non-DNA components occurs in G_1 prior to S phase while further growth occurs in G_2 prior to cell division during mitosis. A restriction point (R) is found towards the end of the G_1 phase after which the cell is committed to complete the division cycle. Cells may temporarily exit the cell cycle and enter a state of quiescence called $G0_Q$ but may be stimulated to re-enter the cell cycle in contrast to senescent cells.

Mitogenic stimulation of cell division begins with receptor activation of sequential phosphorylation pathways such as the mitogen-activated protein kinase (MAP kinase) cascade. The MAP kinases may be stimulated by a number of signalling pathways including that involving the GTP-binding proto-oncogene product ras (Bowen et al, 1998). Ras is a membrane bound G-protein which can be activated by membrane receptor tyrosine kinase phosphorylation. Activation of a second proto-oncogene product raf by ras αGTP binding is followed by phosphorylation of MAP kinase kinase (MEK). MEK in turn phosphorylates and activates MAP kinase. MAP kinase enters the cell nucleus and interacts with transcription factors involved in activation of genes required for cell cycle progression and repression of those genes whose products have inhibitory cell cycle activity.

Progression of cells through the G_1, S and G_2 phases of interphase into

mitosis is controlled by the cyclins and cyclin dependent kinases (cdks). Five classes of cyclin have currently been identified and are referred to as cyclins A to E. Cyclins are temporally expressed throughout the cell cycle and bind to cdks to form complexes capable of activating proteins required at each stage of the cell cycle (Grana & Reddy, 1995). cdk phosphorylation is required for the formation of an active cyclin-cdk complex and activity is further regulated by the presence of cyclin kinase inhibitors (CKIs) such as p21 and p27 which bind directed to the cdk-cyclin complexes (Morgan, 1995). All cyclins with the exception of cyclin D peak at specific points within the cell cycle with maximum activity at these points. Cyclin A is associated with cdk2 and is found in late G_1 and the S phase of the cell cycle. Cyclin B is associated with cdc (cdk1) and is present from late S phase into mitosis. Cyclin D associates with both cdk4 and cdk6 and appears to control progression of the cell through G_1. Cyclin E peaks at the end of G_1 and associates with cdk2. Potential targets for cdk phosphorylation include the lamin B receptors, which may be involved in nuclear membrane dissociation (Courvalin et al, 1992), the histone H1 during chromosome condensation and various transcription factors and DNA binding proteins (Bowen et al, 1998). Changes in the balance of cdk inhibitors, cdks, cyclins, cdk activators and factors involved in cyclin degradation produce the temporal rise and fall in specific cyclin-cdk activity which drives the cell cycle.

The molecular basis for induction of replicative senescence has yet to be fully elucidated although a number of contributory factors have been identified. The DNA content of senescent cells indicates that they are arrested in G_1 phase of the cell cycle (Campisi, 1997). Serum stimulated senescent fibroblasts express early and middle G_1 genes but not late G_1 genes suggesting senescent cells are arrested in late G_1 (Stein & Dulic, 1995). Nucleolar association and chromatin condensation patterns of senescent W1.38 cells also suggest that cells arrest at the late G_1-S boundary (Pignolo et al, 1998[a]). Changes in the balance and control of molecular processes regulating the cell cycle appear to prevent cells from genetic expression of factors required to initiate DNA synthesis.

Permanent upregulation of factors which normally temporally inhibit the passage of pre-senescent cells through the G_1S restriction point until appropriate mitogen stimulation has been observed in senescent cells. The normal cascade of events leading to cell cycle progression is prevented leaving senescent cells permanently fixed in a post-mitotic state. Factors permanently upregulated in senescent fibroblasts include the tumour suppressor protein p53 and the cdk-inhibitors p21 and p16. The tumour suppressor retinoblastoma protein Rb is also permanently activated by hypophosporylation (Figure 1.2).

One mechanism proposed for induction of senescence suggests that progressive telomere shortening, observed with continued cell division of most somatic cells, leads to eventual DNA disruption or the activation of some other mechanism by which senescence suppressing genes are repressed and senescence associated genes activated. Induction of p53 expression occurs. cdk inhibition by a p53 dependent or independent pathway then leads to loss of cyclin-cdk activity and expression of genes required for progression of the cell cycle, ultimately resulting in senescence (Vazori & Benchimol, 1996; Wynford-Thomas, 1996).

1.5.2.2 Rb and p53 Tumour Suppressor Proteins

The p53 tumour suppressor protein is a transcription factor which is activated following DNA damage to halt cell division prior to DNA repair or, where damage is severe, to induce cell apoptosis. p53 acts as a transcription factor for a number of genes including the cdk inhibitor p21 which binds to proliferating cell nuclear antigen (PCNA)-DNA polymerase delta to inhibit DNA replication and, among others, the cdk portion of the cyclin D-cdk complex to prevent cell entry into S phase (El-Deiry et al, 1993).

The tumour suppressor retinoblastoma protein, Rb, is constitutively expressed and is active in unphosphorylated form during G_1 of the cell cycle. It binds to the E2F transcription factor to inhibit activation of genes involved in cell cycle progression such as cyclin A, cdc-2, DNA

Figure 1.2

Changes in the expression and activity of factors regulating G_1 of the cell cycle following senescence (for review see Stein & Dulic, 1995; Smith & Pereira-Smith, 1996). ↑ indicates that expression is increased in senescent fibroblasts. ↓ indicates that expression is decreased in senescent fibroblasts. X indicates that expression is inhibited in senescent fibroblasts.

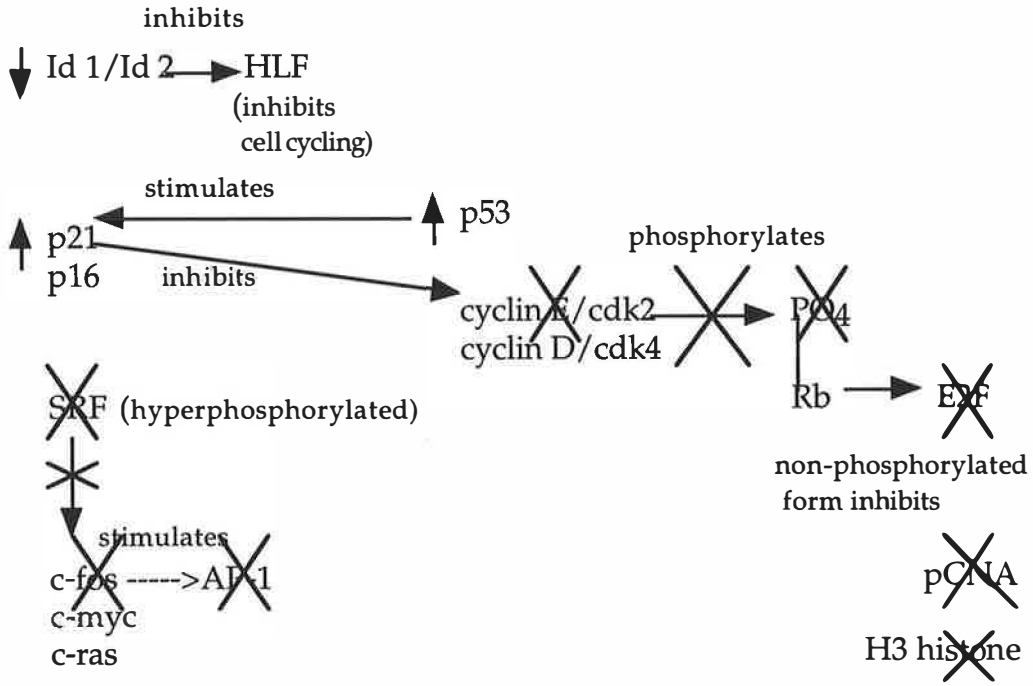

polymerase-α and thymidine kinase (Weinberg, 1995; Chellappan et al, 1991). Rb is phophorylated and inactivated by cyclin D/cdk activity towards the end of G_1 allowing E2F transcriptional activity to continue and remains in hyperphosphorylated, inactive form through S, G_2 and M.

Both p53 and Rb are important for induction and maintenance of the senescent state since they control cell cycle progression beyond the G_1/S restriction point. The simian virus SV40 proto-oncogene T antigen is able to prolong the proliferative lifespan of human diploid fibroblasts and can induce already senescent cells to undergo a single round of DNA synthesis by binding to and inactivating Rb and p53 (McCormick & Campisi, 1991). However, T-antigen studies suggest that pathways independent of p53 and Rb prevent cell immortalisation. Senescent cells not expressing large T-antigen are in mortality 1 (M1). Fibroblasts that express the antigen inhibit p53 and Rb activity and undergo further rounds of cell division but still eventually enter a decline and crisis state called mortality 2 (M2) (Stein & Dulic, 1995; Cristofalo & Pignolo, 1993). M2 is a process distinct from M1 senescence during which apoptotic-like cell death occurs and suggests that factors independent of p53 and Rb activity also mediate pathways leading to permanent growth arrest (Garkavtsev et al, 1998). In senescent cells Rb is present only in an unphosphorylated state and therefore continues to inhibit cell cycle progression into S phase (Voijta & Barrett, 1995). Inhibition of p53 activity using monoclonal antibodies induced senescent cells to enter the cell cycle and greatly reduced p21 expression (Gire & Wynford-Thomas, 1998). Also, Rb protein reexpression in Rb/p53 deficient tumour cells was found to induce cell senescence (Xu et al, 1997). Vazori & Benchimol (1996) demonstrated an increase in p53 levels in senescent fibroblast cultures. Evidence using the clone LacZ21 containing a β-galactosidase (β-gal) reporter construct to reflect p53 transactivation activity also supports a direct role for p53 in cell senescence. Dominant negative p53 mutants showed an extended lifespan and lacked β-gal activity (Bond et al, 1996).

1.5.2.3 The Cyclins

Since cdk phosphorylation in complex with cyclin D and Cyclin E is involved in cell progression beyond the G1S boundary the induction of senescence is likely to involve a reduction in the activity of these cyclin complexes. In senescent fibroblasts a reduction in cyclin A and cyclin B expression was observed while an increase in the expression of cyclin D and cyclin E occurred (Lucibello et al, 1993; Dulic et al, 1993). Although levels of cyclin D and E were enhanced in senescent cells a reduction in cdk activating kinase suggests that overall cyclin/cdk complex activity is diminished (Wong & Riabowol, 1996; Fukami et al, 1995; Dulic et al, 1993). Growth factor induced cyclin D production and cdk2 activity were found to decline in aged rat hepatocytes when compared with young cells also indicating a loss of cyclin D activity with senescence (Liu et al, 1998). Although cyclin E associated kinase activity is lacking in senescent fibroblasts overexpression is still insufficient to overcome the senescent state (Stein & Dulic, 1995).

1.5.2.4 c-fos

The proto-oncogenes c-myc, c-ras and c-fos are all immediate early genes expressed in early G_1 and are vital to the control of the pre-replicative transition phase leading to DNA synthesis (McCormick & Campisi, 1991). Both c-fos and c-myc mRNA synthesis can be induced by PDGF and EDF in human fibroblasts (Paulsson et al, 1987). Expression of c-myc and c-ras are unchanged in senescent cells. However, transcriptional repression of the proto-oncogene product c-fos in response to serum and growth factor stimulation is observed (Peacocke & Campisi, 1991). Since c-fos is essential to DNA synthesis and cell proliferation it has been suggested that c-fos repression may be important for maintenance of the senescent state (Seshadri & Campisi, 1990). Expression normally occurs in early G_1 phase. c-fos forms a heterodimer with c-jun to make up the transcription factor AP-1 which is an important activator of a number of genes involved in cell cycle progression. However, induction of c-fos in senescent cells fails to stimulate DNA synthesis suggesting that other blocking agents are also required (Rose et al, 1992).

Hyperphosphorylation of the nuclear phosphoprotein serum response factor (SRF) in senescent fibroblasts may be responsible for c-fos repression since SRF binds to the serum response element in the promoter region of c-fos and exhibits limited binding capability in hyperphosphorylated form (Stein & Dulic, 1995; Dimri et al, 1996). Further inhibition of c-fos activity may involve deficient activation of the protein kinase C pathway possibly by increased ceramide levels (Venable et al, 1994) or alternatively by inactivation of the MAP kinase signal transduction pathway (Stein & Dulic, 1995). Both pathways are capable of c-fos induction. Cristofalo & Tresini (1998) found that, in contrast to serum and growth factor induced c-fos expression, c-fos induction by ultraviolet irradiation and antioxidant treatment was unaffected by senescence. Senescence was found to affect the extracellular regulated kinase (ERK) pathways to c-fos activation but not alternative pathways involved.

1.5.2.5 E2F

The transcription factor E2F is a heterodimeric complex of a number of related gene products including E2F-1 and is required for the expression of a number of late G_1 genes involved in cell proliferation (Dimri et al, 1996). Two potential E2F binding sites are present on the promoter region of the c-fos gene (Chellappan et al, 1991). Continued inhibition of E2F activity by Rb binding could therefore contribute to the repression of c-fos in senescent cells. The downregulation of E2F-1 in senescent cells (Dimri et al, 1994) and inhibition of active E2F suggests that E2F may be important in the maintenance of replicative senescence. However, restoration of E2F expression failed to induce DNA synthesis (Voijta & Barrett, 1995).

1.5.2.6 Id1 and Id2

Transcription of early immediate Id1 and Id2 helix-loop-helix (HLH) genes is also repressed in senescent cells (Dimri et al, 1996). These proteins inhibit the activity of at present unidentified HLH transcription factors by forming non-active dimers with HLH transcription factors preventing the dimerization of these factors to form an active DNA

binding domain. Dimri et al (1996) suggest the existence of a specific bHLH transcription factor that acts in conjunction with Rb and is repressed by Id1.

1.5.2.7 Cyclin Dependent Kinase Inhibitors

Early studies suggested that the increased expression of one or more inhibitory proteins may form the end point of a pathway producing induction of the senescent state (Smith & Lincoln, 1984; Dice, 1993). Cdk-inhibitors are important regulators of the cell cycle and overexpression of G_1 associated cdk inhibitors would be expected to limit cell cycle capacity. p21 (SDI1, CIP1, WAF1) and p16 (INK 4a) are members of two different cdk-inhibitor families and are both constitutively overexpressed in senescent fibroblasts (Wong & Riabowol, 1996; Robetorye et al, 1996). Upregulation of p21 expression occurs in response to enhanced p53 activity although continued p21 expression in p53 mutant fibroblasts suggests that p21 is also activated by p53 independent mechanisms (Bond et al, 1995). p21 inhibits a broad range of kinases including cdk2, cdk4 and cdk 6 activity (Robetorye et al, 1996) while p16 binds only to cdk4 and cdk 6 (Serrano, 1997). Both inhibitors may prevent cyclin D associated cdk activity in G_1 and Rb inactivation by phosphorylation so that a stop on cell cycle progression is permanently in place. Fibroblasts in which the p21 gene was inactive exhibited an extended lifespan (Brown et al, 1997). Also expression of p21 and p16 in young human diploid fibroblasts induced some of the changes occurring in senescence including decreased rates of proliferation, accumulation of unphosphorylated Rb, senescence associated β-galactosidase (SA-β-Gal) activity and changes in cell morphology (McConnell et al, 1998). In Rb negative cells p16 levels were found to increase while re-introduction of Rb reduced p16 levels suggesting a negative feedback mechanism limiting p16 expression (Serrano et al, 1997). Alcorta et al (1996) found a rise in fibroblast p21 expression just prior to senescence followed by a decline and subsequent rise in p16 activity suggesting that p16 rather than p21 is primarily active in the final stages of senescence. Brenner et al (1998) found that p16 levels rose dramatically with the onset of senescence in human mammary epithelial cells (HMEC) while p21

levels did not change indicating that in these cells p16 is primarily involved in senescence. Mutations in members of the p16 family but not the p21 family of cdk inhibitors are common in a number of different cancer cell types also indicating a predominant role for p16 in senescence (Okamoto et al, 1994).

1.5.2.8 Telomeric Loss

Telomeric loss has been suggested as the source of a negative signal limiting cell replication. Telomeres consist of non-transcribed, short repeat, T-G rich sequences which cap the ends of all eukaryotic chromosomes (Greider, 1990). They are well conserved between different species and protect chromosome ends from damaging fusion with other chromosomes. Incomplete replication of DNA due to the need for an upstream RNA primer produces a shortening of telomeric ends on progression through an increasing number of cell divisions (Marx, 1994). The enzyme telomerase, consisting of a telomerase RNA component (hTR), a telomerase associated protein 1 (TP1) and a telomerase catalytic component, is capable of re-synthesising telomeric sequences which are lost at replication in a number of lower organisms (Stein & Dulic, 1993). However, in humans most normal cells other than stem cells lack this enzyme and exhibit progressive telomeric loss on replication. In contrast, most tumours and immortal cells express telomerase supporting the implication that the timed induction of senescence by progressive telomere shortening acts as a protective mechanism against uncontrolled cell proliferation (Oshimura & Barrett, 1997).

Evidence supports a role for telomeric shortening in the onset of senescence. Comparison of terminal restriction fragment (TRF) length (incorporating telomere and some subtelomeric sequences) and signal intensity in young and old cultured human fibroblasts revealed a direct proportionality between replicative capacity and mean TRF length (Allsopp & Harley, 1995). The amount of telomeric shortening has also been correlated with tissue donor age (Martin et al, 1993). The expression of telomerase by most immortal cells (Chiu & Harley, 1997) and the

expression of telomerase by 90 to 95% of late stage malignant tumours (Finkel, 1996) also suggest that the lack of telomerase expression and subsequent telomere shortening which occur in normal cells is fundamental to senescence. Recent experiments using the cloned telomerase catalytic sequence directly implicate telomere shortening as a causal factor in cell senescence. Transfection of the telomerase catalytic subunit into telomerase negative, normal human cell types increased telomere length and cell replicative lifespan while telomere shortening and cell senescence occurred in all negative controls (Bodnar et al, 1998). Horikawa et al (1998) found that the introduction of normal chromosome 3 into a human renal cell carcinoma cell line produced progressive telomere loss by repression of the catalytic subunit component of telomerase, resulting in cell senescence.

The mechanisms by which telomere length controls the induction of senescence are unknown. It was originally suggested that telomere shortening eventually deleted essential replicative genes. However, the almost immediate reversal of cell immortalisation by the removal of T antigen repression of p53 and Rb suggests that essential replicative genes are not deleted but inhibited. Wright & Shay (1992) suggested a reversible, positional repression by which, as telomeres shorten, genes restricting senescence are incorporated into the heterochromatic region and come under telomere repressional effects.

The re-expression of telomerase and subsequent halt on telomere erosion is thought to be a potential mechanism by which tumour cells bypass senescence. Rb/p53 inhibited cells which have progressed beyond the M1 stage of senescence are still telomerase negative and it is thought that telomerase induction allows cells to progress beyond the M2 final crisis stage of senescence and become immortal (Wright & Shay, 1992). However, not all tumour cells are telomerase positive and some telomerase negative, immortalised cell lines were still found to maintain telomere length (Finkel, 1996). Also, telomerase negative knockout mice show no decrease in susceptibility to tumorigenesis suggesting that an alternative mechanism by which senescence is

bypassed exists (Wynford-Thomas & Kipling, 1997). Such evidence also suggests that other factors may act in addition to telomere shortening to regulate the induction of senescence.

1.5.3 The Senescent Phenotype

The senescent fibroblast is phenotypically distinct from its non-senescent counterpart. Cells tend to be larger and more variable in shape (Koli & Keski-Oja, 1992). Chromosomal aberrations occur more frequently (Sherwood et al, 1988). Increases in nuclear, nucleolar, lysosomal and mitochodrial size are observed as well as an increase in actin and a more rigid cytoskeletal structure (Maciera-Coelho, 1983). An increase in membrane permeability and changes in membrane lipid content occur. The net negative charge of the cell membrane decreases, possibly as a result of a decline in membrane bound sialic acid (Bosmann et al, 1976; Milo & Hart, 1976). Changes in membrane charge and the secretion of substances mediating adhesion may also influence the decrease in saturation density and cell adhesion which occurs (Maciera-Coelho, 1983).

The induction of senescence appears to alter the interaction of individual fibroblasts with the surrounding environment and to induce metabolic and secretory changes which remove protein expression from the matrix signalling pathways regulating non-senescent fibroblast activity in relation to growth conditions (Sottile et al, 1987). Young cultured cells enter a quiescent state on serum deprivation but can be reactivated by increasing serum concentration. In contrast, senescent cells do not respond to serum deprivation by decreased product secretion. Cells exhibit a decreased responsiveness to growth factors (Eleftheriou et al, 1991) and an overexpression of matrix degrading proteins irrespective of growth conditions (West et al, 1989).

A fall in protein synthesis occurs, possibly as a result of the decreased expression of the ribosomal protein PHE-7 (Peacocke & Campisi, 1991). However, a decline in degradation processes produces an overall increase in cellular protein (Koli & Keski-Oja, 1992). There is an increase

in the expression of novel and defective proteins (Cristofalo & Pignolo, 1993; Sottile et al, 1987). A PCR-based, differential display technique has identified at least twenty three genes that are differentially expressed in senescent human fibroblasts (Linskens et al, 1995). Screening of subtracted cDNA libraries has also identified at least fifteen cDNA clones that are overexpressed in senescent human fibroblasts including a wide range of enzymes, structural and binding proteins (Lecka-Czernik et al, 1996). EPC-1, a protein involved in the density dependent growth arrest of young cells, is not expressed in senescent fibroblasts and may explain the observed decrease in saturation density (Pignolo et al, 1994; Takeda et al, 1992). Overexpression of a putative transmembrane shock protein, LPC-1, also occurs and may contribute to the morphological changes and decline in stress response observed in senescent cells (Pignolo et al, 1998[b]). The WS3-10 gene expressing a putative calcium binding protein is overexpressed in senescent human fibroblasts and suppresses calcium dependent membrane currents on induction (Liu et al, 1994; Grigoriev et al, 1996). Inhibition of calcium dependent processes may produce further changes in gene expression and secretion. The protein terminin exists in young and quiescent cells but is expressed in a unique 60/57 kDa form in senescent cells, allowing the potential identification of these cells in culture (Wang et al, 1991).

Senescent fibroblasts exhibit changes in the synthesis and secretion of structural proteins and remodelling proteases. Expression of the collagenase MMP-1 is upregulated while TIMP-1 expression is decreased (Sottile et al, 1988; Millis et al, 1989; Millis et al, 1992; West et al; 1989). Overexpression of t-PA and PAI-2 also occurs independent of growth conditions (West et al, 1996). An increase in the gelatinase MMP-2 and in TIMP-2 mRNA levels has also been observed (Zeng & Millis, 1994). Changes in the secretion of growth factors and cytokines regulating MMP secretion also occur. Levels of IL-1α and β, which are known to increase MMP-1 expression, are raised in senescent fibroblasts while levels of TGF-β, which is known to inhibit MMP-1 expression, decline (Zeng & Millis, 1994, Zeng et al, 1996). The enhanced expression of the collagenase MMP-1 in senescent fibroblasts and the apparent AP-1

mediated mechanism of induction in response to IL-1 and PMA suggest that induction can also occur by a c-fos independent mechanism or that c-fos repression is not complete in senescent cells.

Secretion of FN, collagen and the proteoglycans is also altered in senescent fibroblasts. Fibronectin derived from senescent fibroblast cultures has a larger molecular weight and is deficient in its ability to bind collagen (Chandrasekhar et al, 1983). Although FN secretion is enhanced in senescent cells (Kumazaki et al, 1991), its ability to mediate adhesion of cells to the ECM is decreased (Eleftheriou et al, 1991). A decline in collagen and proteoglycan synthesis occurs in senescent dermal fibroblasts and fibroblasts derived from older donors (Takeda et al, 1992). Changes in ECM structure may limit growth factor exposure to cell membrane receptors explaining in part the decreased responsiveness of senescent cells to FGF, EGF and PDGF (Eleftheriou et al, 1991).

1.5.4 Senescence and Corneal Wound Healing

The contribution which senescence makes to the ageing process is unknown. However, senescent cells are known to accumulate with age in culture at a rate which reflects the age of the donor and have also been found to accumulate with age *in vivo*, in the dermis and epidermis, using a SA-β-Gal marker (Dimri et al, 1995). The effect which fibroblast senescence has on the wound healing process is also unknown. Rates of dermal wound healing have been correlated with the proliferative capacity of dermal fibroblasts in culture and were inversely related to donor age suggesting that an increase in senescence within the dermal fibroblast population slows wound healing (Bruce & Deamond, 1991).

Evidence suggests that senescence contributes to some of the changes in tissue function which occur with age and to the decline in tissue response to wounding. Senescent fibroblasts fail to proliferate in response to mitogenic stimuli and exhibit a decline in migration rates. In addition, changes in fibroblast morphology, response to cytokine stimulation and in the secretion of structural proteins and remodelling proteases may limit the ability of senescent fibroblasts to remodel the

matrix following wounding. In the cornea restoration of vision following wounding depends on regulating the keratocyte repair response, a process which is disrupted in the senescent fibroblast.

The presence of senescent keratocytes in the cornea in numbers great enough to affect corneal functioning has yet to be directly established. However, keratocyte turnover within the cornea occurs approximately every two to three years and keratocyte division within the embryonic cornea has been detected indicating that senescent keratocytes accumulate in the cornea as a result of cell division over time (Nishida, 1997; Hyldahl, 1986). Keratocyte senescence may also occur following corneal injury where proliferation follows anterior keratocyte apoptosis in order to repopulate the damaged stroma (Wilson et al, 1996). In addition, senescence may follow corneal exposure to potential mutagens such as ultraviolet light (Faragher et al, 1997). Since avenues exist by which senescent keratocytes may accumulate within the cornea the potentially debilitating effects of senescence on ocular function and on the success of keratoprosthetic implants require further investigation.

1.6 Keratoprostheses

Artificial corneal implants or KPros, consisting of a central, clear optic surrounded by an anchoring skirt, have been designed to treat corneal blindness by replacing opaque corneal tissue with a clear visual window (Figure 1.3). KPros were considered as early as the eighteenth century (Cardona, 1962). However, with the success of donor corneal transplants (keratoplasty), KPros were not developed further until it was observed that standard keratoplasty was not successful in all cases. Patients who are unable to sustain corneal transplants include those with severe chemical burns or chronic inflammation and patients with oculo-cutaneous diseases such as Stevens-Johnson syndrome and ocular cicatricial pemphigoid. These diseases commonly produce conjunctival and corneal epithelial inflammation leading to vascularization and opacity (Dohlman & Terada, 1998; Chiou et al, 1998). For such patients the development of a successful KPro is the only means by which sight may be restored. A number of materials and designs have been

Figure 1.3
An example of a Cardona, mushroom style Keratoprosthesis.

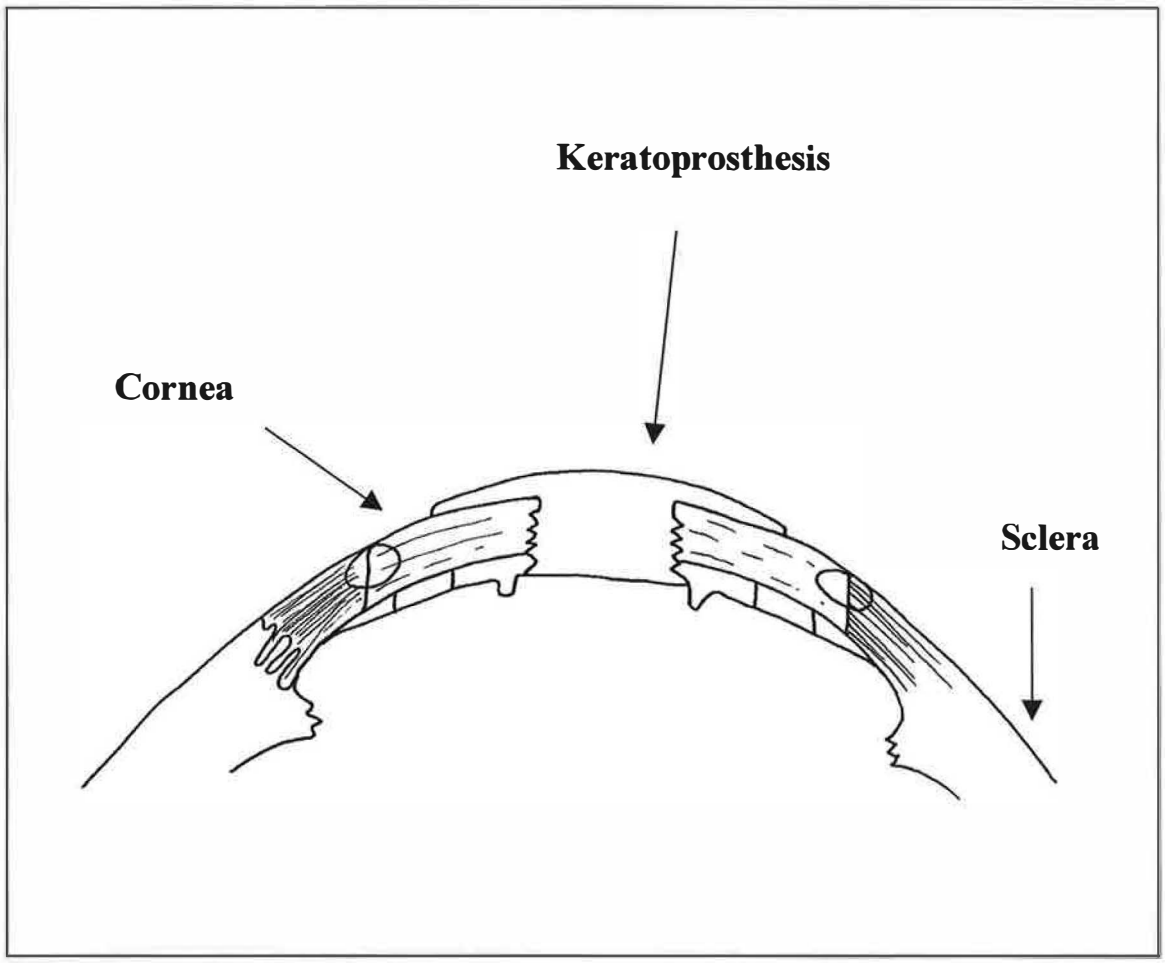

investigated. However, long-term success with purely plastic KPros has yet to be achieved. All KPros currently available produce serious complications such as implant extrusion, retroprosthetic membrane formation, infection, inflammation and glaucoma (Hicks et al, 1997[a]). Complications have commonly arisen because integration of the KPro materials within the host corneal tissue has failed to occur. Non integrative materials which induce an excessive inflammatory response characterised by MMP overactivity may contribute to tissue melting and KPro extrusion, particularly in patient groups requiring KPros where corneal inflammation may already be an underlying condition (Fitton et al, 1998). Friction at the tissue KPro interface caused by the hardness of the material and lack of nutrient flow to the tissue anterior to the implant tends to produce tissue necrosis and implant extrusion. Recent KPro designs have attempted to limit complications such as chronic inflammation and tissue necrosis by the use of biocompatible materials with mechanical properties that limit friction at the tissue-prosthesis interface. Materials have been developed to encourage peripheral colonisation and firm adhesion of the central optic to the skirt material in order to limit epithelial downgrowth, retroprosthetic membrane formation and the potential for infection. Designs have also attempted to incorporate materials which allow epithelialisation anterior to the prosthesis, providing a protective barrier against infection and cell downgrowth. The posterior surface should ideally limit cell growth and the potential for membrane formation. The incorporation of an ultraviolet blocking agent within the KPro is also desirable.

KPros currently in clinical use tend to be polymethyl methacrylate (PMMA) based (Table 1.1). However, the success of these KPros is constrained by a number of the complications previously described. Osteo-odonto-keratoprostheses (OOKPs), peripherally anchored by material taken from the patient's own tooth, have shown some success (Ricci et al, 1992). Few alternative KPro designs have been successfully developed to the point of clinical trial. Those currently under consideration include a poly(hydroxyethyl methacrylate) (p(HEMA)) based KPro, a KPro consisting of a polyvinylalcohol (PVA) core and

Name of Group	KPro Design
Cardona (1991)*	PMMA optic, teflon skirt covered by a dacron mesh.
Dohlman & Doane (1994)*	'Collar button' design. PMMA front plate and stem with a second PMMA plate screwed into the back.
Ricci et al (1994)*	Strampelli design. Acrylic optic attached to a skirt made of tooth.
Hicks et al (1998)	p(HEMA) optic, 80wt% water p(HEMA) hydrogel skirt.
Legeais et al (1995) (1998)	PMMA or polyvinylpyrrolidone coated polydimethylsiloxane optic, PTFE IMPRA skirt.
Trinkaus-Randall et al (1997)	Polyvinyl alcohol optic, polybutylene-polypropylene fibrous melt-blown web skirt.
Jacob-LeBarre & Caldwell (1990)	Polyurethane optic, gore-tex annular ring skirt.
Leon et al (1997)	PMMA optic, coralline hydroxyapatite skirt.
Pintucci et al (1995)	PMMA optic, dacron skirt.

Table 1.1 Existing KPro designs. * Denotes designs which are currently in clinical use.

polybutylene/polypropylene skirt and a KPro consisting of a PMMA core attached to an expanded polytetrafluroethylene (PTFE) skirt made by IMPRA (Chirila, 1997; Tsuk et al, 1997; Legeais et al, 1995).

1.6.1 PMMA

PMMA was first considered as a KPro material after it was observed that corneae could tolerate PMMA splinters (Stone & Herbert, 1953). Original Cardona implants consisted of a PMMA optical cylinder and an interlamellar supporting plate (Cardona, 1962; Castroviejo et al, 1969). Design and surgical technique modifications reduced extrusion rates from 32% to 21.3% (Cardona, 1969). However problems commonly stemmed from inadequate hydration of corneal layers overlying the support plate (Castroviejo et al, 1969). A bolt and nut design was introduced to reduce corneal dehydration and cover the cylinder/host tissue junction in order to limit extrusion (Cardona, 1969). The KPro consisted of a PMMA coated contact lens and a PMMA cylinder which screwed into the contact lens and into a PMMA nut placed against the corneal endothelium. Complications included growth of tissue over the optical element of the keratoprosthesis, erosion and aseptic necrosis of surrounding corneal tissue leading to implant extrusion (Cardona, 1969). In a study reviewing the success of forty nine penetrating PMMA keratoprostheses an extrusion rate of 32.7% was observed and maintenance of visual acuity for more than one year occurred in only 48.6% of cases (Barnham & Roper-Hall, 1983).

Stone & Herbert (1953) initially developed the idea of a peripheral KPro skirt containing holes or pores to allow better host tissue ingrowth. Girard (1983) later modified the Cardona design using a supporting skirt made of Dacron or Proplast to stabilise the implant by encouraging fibroblast ingrowth. 58% of patients initially obtained good visual acuity dropping to 20% at the end of a follow-up period of twelve years. Complications occurred in all cases. Conjunctival overgrowth was most common. Conjunctival retraction or scleral erosion occurred in 48% of all cases. Other complications included glaucoma, implant extrusion, retinal detachment, leakage, endopthalmitis and epithelial invasion of

the keratoprosthesis shaft (Girard, 1983). A later report indicated a decline in the rate and number of early complications following improvements in surgical technique and implant design. However, uncontrolled glaucoma and retinal detachment were still common (Girard, 1983). The current Cardona model consists of a PMMA optic cylinder, Teflon skirt and Dacron mesh. A review of the model's success revealed little sustained visual improvement for cases with poor tear fluid production although some success was found in cases without such complications (Cardona, 1991). Further improvements have included coating PMMA with type 1 collagen to enhance implant biocompatability (Kirkham & Dangel, 1991).

Another PMMA KPro in clinical use is the Dohlman-Doane collar-button design consisting of a front plate and shortened stem with a second plate screwed into the back (type I). The design has been modified for use in dry eyes with poor or no tear production (type II). The front plate of the type II KPro has a cylinder attached which protrudes through a permanently closed eyelid. A study of eleven patients over three years revealed visual improvement in six of the patients. Complications included retroprosthetic membrane formation, glaucoma, retinal detachment, uveitus and unscrewing of the prosthesis (Dohlman & Doane, 1994). Initial coverage of the type I KPro with a conjunctival flap and anti-collagenase treatment were considered to be important in the success of the prostheses.

1.6.2 Hydrogels

Hydrogels possess a number of properties which make them suitable for use as KPro materials. Glycolmethacrylates were initially selected for use on the basis of biological inertness, ability to modify water content and mechanical properties, and good gel transparency (Wichterle & Lim, 1960). Unlike the initial PMMA KPros their ability to absorb water allows nutrient diffusion to tissues anterior to the KPro, maintaining anterior corneal tissue integrity. The use of p(HEMA) hydrogels has also overcome difficulties in adhesion of the two KPro components since p(HEMA) may be modified for use as both the non-porous optic and the

porous skirt (Hicks et al, 1997[a]). Pores may be introduced into the skirt material by the incorporation of increasing amounts of water prior to polymerisation. Since HEMA but not p(HEMA) is soluble in water the use of more than 45 wt% water during polymerisation results in phase separation of the p(HEMA) and the production of pores within the resulting polymer. Water content, crosslinker and initiator concentration can each be varied in order to alter pore size (Kremer et al, 1994; Walther et al, 1994). A KPro design consisting of a central, non-porous p(HEMA) optic attached to a peripheral, porous p(HEMA) skirt by an interpenetrating meshwork may then be constructed by polymerisation of one component in the presence of the second previously polymerised component (Hicks et al, 1997[b]). Initial subcutaneous implantation of p(HEMA) showed that the material was non-toxic and well tolerated (Jeyanthi & Rao, 1990). On examination of suitable KPro skirt materials Chirila et al (1993) found that an 80 wt% water, collagen containing p(HEMA) sponge allowed maximal fibroblast invasion. p(HEMA) sponges with 10 to 30 μm diameter pores implanted into rabbit corneae were well tolerated and showed fibrovascular invasion of the material (Crawford et al, 1993). Collagen type III was identified in sponges implanted into rabbit corneae for twenty eight days indicating cell invasion and a normal wound healing response (Chirila et al, 1996). Crawford et al (1996) implanted the p(HEMA) KPro designs into five rabbit corneae. Anterior stromal erosion and epithelial downgrowth occurred in two cases. However, no extrusion or capsule formation occurred and fibrovascular ingrowth was observed. A later study inserting a penetrating KPro into eight rabbit corneae revealed mechanical weakness and subsequent tearing of the skirt material in four cases (Hicks et al, 1996). Attempts to improve mechanical strength have included the use of the crosslinker divinyl glycol (DVG) instead of ethylene dimethacrylate (EDMA), the incorporation of the comonomer 4-t-butyl-2-hydroxycyclohexyl methacrylate (TBCM) and pre-colonisation of the polymer by initial subcutaneous implantation. Contrary to expectation TBCM reduced or had no effect on polymer tensile strength while subcutaneous implantation strengthened the polymer (Chirila et al, 1995). While an increase in mechanical strength was observed in

designs using the crosslinker DVG initial polymers exhibited inhomogeneities such as swelling and stratification, thought to be due to the reduced free radical activity of DVG compared to EDMA (Clayton et al, 1997[a,b]). The use of a more reactive accelerator system eliminated problems with stratification and subsequent KPros have incorporated DVG as the crosslinker. A dry eye model with an optic protrusion through the eyelid has also been developed for use (Hicks et al, 1997[b]). Attempts to improve cell adhesion to the KPro by incorporating the comonomer methyl methacrylate reduced mechanical strength and produced no improvement in cell adhesion (Vijayasekaran et al, 1997). The latest report of twenty KPros followed for twenty one months showed an 80% retention rate and no indication of common KPro complications such as retroprosthetic membrane formation and glaucoma. However, poor mechanical strength and calcium deposition were still observed (Hicks et al, 1998). Various anti-collagenase treatments have been investigated in an attempt to inhibit excessive inflammation and tissue melting following KPro implantation. While a number of the drugs showed no *in vivo* activity, medroxyprogesterone was found to reduce gelatinolytic activity both *in vitro* and *in vivo* (Fitton et al, 1998).

Lee et al (1996) have designed a homobifunctional membrane of p(HEMA) grafted onto silicone rubber as a KPro material which allows surface epithelialisation but prevents downgrowth. Corneal epithelial cells attached and grew onto 55 and 75 $\mu g\ cm^{-2}$ p(HEMA) grafted materials. However, epithelial downgrowth was observed on implantation of the membrane leading to the development of a heterobifunctional membrane with an upper surface grafted with material supporting cell adhesion and a lower surface grafted with material inhibitory to cell adhesion. Silicone rubber coated with HEMA or collagen on the upper surface and with 2-methacryloyloxyethyl phosphorylcholine (MPC) on the lower surface successfully prevented epithelial downgrowth by inhibiting cell attachment onto the lower surface (Chang et al, 1998). The concentration of p(HEMA) grafted onto

silicone rubber was found to be important since large amounts inhibited implant transparency.

1.6.3 Optic Support Materials

Various porous skirt materials have been developed to encourage KPro integration by allowing peripheral host cell invasion of the KPro. A number of non-porous PTFE based materials incorporating micropores have been investigated. Of the three PTFEs IMPRA, Proplast and Gore-Tex only IMPRA showed successful invasion and collagen deposition. 100% extrusion occurred using Proplast while Gore-Tex produced influx of inflammatory and necrotic cells with some extrusion of the material (Legeais, et al, 1992). Keratocyte ingrowth was greater when pores of 50 μm rather than 20 μm diameter were used (Legeais et al, 1994). Additionally, the type and arrangement of collagen deposition using the expanded PTFE made by IMPRA was similar to that seen in normal wound healing (Drubaix et al, 1996). Surprisingly, the opaque PTFE polymers became transparent following implantation and collagen fibril deposition. The pattern of HA synthesis within the implants was similar to that observed in normal wound healing and may also be involved in the production of polymer transparency along with collagen deposition (Drubaix et al, 1998). IMPRA discs implanted into the anterior chamber and sutured to the posterior corneae of twenty rabbits were also well tolerated, producing keratocyte invasion and collagen deposition within the implant. These results suggest the potential for a through and through design, passing into the anterior chamber, using this material (Renard et al, 1996). A preliminary clinical trial using a four piece KPro consisting of a fluorocarbon skirt and a PMMA optic, fixation clip and sealing ring inserted into the corneae of twenty four patients resulted in improved visual acuity in 70% of the patients. Complications included three cases of implant extrusion, five cases of retroprosthetic membrane formation and five cases of buccal mucosa tissue necrosis. Ulceration and necrosis tended to occur at the PMMA-fluorocarbon and PMMA-cornea interface and the authors recommended against the use of PMMA as an optic material (Legeais et al, 1995). A second, modified KPro design was made using

polyvinylpyrrolidone coated polydimethylsiloxane as the central optic melted to the PTFE skirt. A clinical trial involving thirteen patients over a follow-up period of three to nine months resulted in improved visual acuity for nine of the patients. Epithelialisation across the surface of the KPro did not occur and five out of the thirteen KPros failed (Legeais & Renard, 1998).

Trinkaus-Randall et al (1991) have developed a novel moulding procedure linking an 80:20% polybutylene-polypropylene fibrous melt-blown web skirt material to a central PVA hydrogel optic made from poly(vinyl-trifluoroacetate) (Tsuk et al, 1997). Results following insertion of discs of the skirt material into rabbit corneae indicated successful invasion of stromal keratocytes with settling of inflammation, protein synthesis and collagen deposition by invading cells. The discs became firmly adherent to the surrounding host tissue and had a low extrusion rate (Trinkaus-Randall et al, 1991). Pretreatment of the implanted discs with fibroblasts increased the amount of collagen synthesis observed (Trinkaus-Randall et al, 1994). Successful fibroblast invasion required a fiber diameter of 2 to 12 μm and a void volume of 88% (Trinkaus-Randall et al, 1991). On comparison of a polybutylene/polypropylene web, Dacron and IMPRA, the polybutylene/polypropylene web produced 50% less corneal oedema and neovascularisation during weeks two to six and quicker subsidence of inflammation than the other porous materials. Extensive fibroplasia and evidence of a normal wound healing response were also indicated (Wu et al, 1996).

Methods to enhance epithelial growth across the PVA/polybutylene-polypropylene KPro surface have been investigated since maintenance of a continuous corneal epithelial sheet across the implant provides a barrier to infection and epithelial downgrowth between the optic/skirt and KPro/tissue interface. Trinkaus-Randall et al (1988) initially observed PVA maintenance of epithelial growth. Latkany et al (1997) modified the surface of the PVA hydrogels using argon radio frequency plasma treatment. Corneal epithelial cell proliferation and ECM

production were observed including the detection of the adhesion proteins laminin and integrin subunits. Epithelial cells migrated across organ cultured corneae containing argon plasma treated PVA to form a continuous sheet after three weeks. Implantation of the complete KPro, preseeded with stromal fibroblasts and argon plasma treated on the anterior PVA surface, into twenty five rabbit corneae over a maximum of 188 days revealed extensive fibroplasia, FN deposition and epithelial migration across the surface of the KPro (Trinkaus-Randall et al, 1997). However, only partial epithelialisation occurred three weeks after implantation in comparison with the complete epithelialisation observed in organ culture (Trinkaus-Randall et al, 1997). Argon plasma treated materials also produced less oedema and neovascularisation following implantation (Wu et al, 1998). Trinkaus-Randall & Nugent (1998) found that GAG deposition within the KPros occurred in a pattern similar to that observed in the normal injured cornea with an increase in dermatin sulfate and a decline in keratin sulfate. Within the same study controlled release systems incorporating bFGF and TGF-β into an alginate gel or a poly(lactic/glycolic) acid microsphere system were investigated in an attempt to enhance fibroplasia and wound repair. The successful incorporation of a ultraviolet absorbing monomer into the PVA optic material has also been demonstrated and will allow the KPro to take on the usual role of the cornea in protecting the retina from excessive exposure to ultraviolet light (Tsuk et al, 1997).

Linnola et al (1996) tested titanium and bioactive glass-ceramic coated titanium as suitable skirt materials surrounding a central PMMA optic cylinder in an attempt to limit epithelial downgrowth. On histological examination 83% of bioactive glass-ceramic coated keratoprostheses and 73% of the titanium prostheses showed no significant epithelial ingrowth. Inflammation was limited and the implant was well tolerated by the corneal tissue suggesting that glass-ceramic coated titanium may be a suitable material for use in construction of keratoprostheses (Linnola et al, 1996). Coralline hydroxyapatite has also been considered as a skirt material based on its high biocompatability and invasiveness, again using PMMA as the central optic material (Leon et al, 1997).

Fibrovascular ingrowth was observed in all of the implants over a twelve month follow-up period. However, tissue erosion occurred in eight out of the twelve corneae. Pintucci et al (1995) have developed a KPro consisting of a Dacron skirt and a central PMMA optic. The KPro was first pre-colonised with connective tissue by implantation under the lower eyelid and was coated with oral mucosa following insertion. Clinical trials following the progress of twenty patients over four years found that improved visual acuity was maintained in 65% of all cases. Oral mucosal necrosis occurred in 50% of cases and was corrected by mucosal regrafting. Other complications included retroprosthetic membrane formation, epithelial overgrowth, endopthalmitis, retinal detachment and two spontaneous extrusions (Pintucci et al, 1995).

1.6.4 Polyurethanes

Bruin et al (1993) developed a polyurethane material for KPro use incorporating Coumarin 102 as an ultraviolet light absorber. Three discs of the material implanted into rabbit corneae were well tolerated and were retained over the one year follow-up period. Jacob-LeBarre and Caldwell (1990) have designed a KPro using a polyurethane material as the central optic attached to a six pronged annular ring skirt made of 60 μm porous Gore-Tex. Gore-Tex was selected on comparison with other materials including Dacron, Teflon, ceramic and Proplast based on the high rate of cellular invasion and lack of extrusion observed following implantation. A polyurethane optic was selected because no cellular invasion occurred and the material was retained within the cornea. Some extrusion of the final KPro design occurred but was attributed to problems in surgical technique.

1.6.5 Osteo-Odonto-Keratoprostheses

OOKP surgery was initially developed by Strampelli. The patient's tooth, including the alveolar dental ligament, is used for the skirt material to assist biointegration and surrounds an acrylic optic. A study of eighty five OOKPs carried out over a twenty five year period indicated long-term retention of the implants within the eye (Marchi et al, 1994). Secondary glaucoma was the major complication found following

surgery. Two extrusions occurred and were attributed to loss of the alveolar dental ligament through inflammation. Three retinal detachments and three retroprosthetic membrane formations were also observed (Ricci et al, 1992). While the technique offers good long-term success the length and complexity of the procedures involved are disadvantages.

1.6.6 Summary

A number of polymers exhibit properties conducive to the success of KPro implants. While PMMA based KPros appear to lack the properties conducive to corneal integration the p(HEMA) KPro and the polybutylene-polypropylene/PVA KPro designs have produced some promising results. However, incorporation of all the attributes necessary to eliminate complications leading to implant extrusion in one model has yet to be achieved. Current research has sought to reduce optic rigidity, improve the core-skirt junction and decrease the invasiveness of surgical techniques used (Hicks et al, 1997[a]). Further investigation into the factors influencing cell migration and colonisation of implants will assist in the selection of polymers most suitable for use in the future production of KPros. More specifically, elucidation of factors related to senescent fibroblast migration and colonisation of implants will take into account age related difficulties in the success of keratoprosthetic designs.

1.7 Aims and Objectives

An adequate keratocyte repair response is central to the successful incorporation of KPro materials within the cornea. Evidence suggests that senescent fibroblasts accumulate with age in dividing tissues and that phenotypic changes occurring with senescence are detrimental to the repair response. It was hypothesised that the accumulation of senescent keratocytes occurs with age in culture and has detrimental effects on aspects of the keratocyte repair response. These may limit KPro integration within the cornea. In addition, a porous material which may be adapted to enhance peripheral keratocyte adhesion and colonisation of the implant is required. The aims of the current study

were therefore:

1. To establish an *in vitro* model of keratocyte ageing in culture by the serial passage of the embryonic keratocyte cell strain EK1.BR.
2. To use the model to assess whether senescence alters aspects of the keratocyte repair response including keratocyte migration, migration in response to EGF, FN and HA, keratocyte contractile ability and keratocyte secretion of the gelatinase MMPs.
3. To test the validity of the EK1.BR model of corneal ageing by comparing late passage EK1.BR keratocyte migratory activity with that of an elderly donor keratocyte cell strain.
4. To modify p(HEMA) based hydrogels in order to develop a potential KPro skirt material characterised by the enhancement of cell adhesion and spreading.
5. To further modify the material by the incorporation of pores in order to promote keratocyte colonisation of the polymer.

Chapter 2

Characterisation of the Human Embryonic Keratocyte Cell Strain EK1.BR

2.1 Characterisation of EK1.BR keratocyte proliferative lifespan using the monoclonal antibody Ki67

2.1.1 Introduction

The proliferative lifespan of dividing cell cultures may be assessed using specific markers which identify dividing cells. Cell cycle associated marker proteins against which monoclonal antibodies have been developed include PCNA and pKi67. The incorporation of bromodeoxyuridine (BrdU) or tritiated thymidine may also be used as a measure of DNA synthesis to indicate cell division (Iatropoulos & Williams, 1996).

Few markers exist which specifically identify senescent cells within a culture. Dimri et al (1995) have developed a histochemical assay which detects SA-β-Gal activity at pH 6 in senescent fibroblasts. However, the assay was not found to provide a universal marker for senescence (Dimri et al, 1995). Antibodies against a second senescence specific 57 KDa terminin protein have also been used to distinguish between senescent and non-senescent fibroblasts (Wang & Tomaszewski, 1991).

In the absence of a specific marker for the senescent state the presence of an increasing number of non-cycling cells with increasing serial passage can be measured using proliferation associated markers such as Ki67 (Kill et al, 1994). The Ki67 monoclonal antibody has been used as a prognostic indicator of tumour growth and to measure cell growth fractions in culture. The antibody recognises a non histone associated nuclear antigen found in dividing cells at all stages of the cell cycle (Gerdes et al, 1983). pKi67 appears to associate with the chromosomes during mitosis and accumulates in the dense fibrillar area of the nucleolus during interphase (Heidebrecht et al, 1996; Verheijen et al, 1989; Kill, 1996). Its role is unknown but may include enhancement of ribosomal synthesis in the nucleolus and assistance in the maintenance of chromosomal structure during mitosis (Chatterjee et al, 1987; Sawhney & Hall, 1992).

While no distinction can be made between senescent, quiescent and

terminally differentiated cells utilising Ki67 a decline in Ki67 positivity is observed on increasing serial passage and a percentage of less than 5% positivity correlates sufficiently with the senescence of a cell culture. The current study sought to characterise the proliferative lifespan of the keratocyte cell strain EK1.BR using Ki67 as a marker of proliferation.

2.1.2 Materials & Equipment

Modified eagles medium (MEM), foetal calf serum (FCS), penicillin/streptomycin (P/S), trypsin-EDTA solution (1x) and tissue culture plastics were supplied by Life Technologies Ltd., 3 Fountain Drive, Inchinnan Business Park, Paisley, PA4 9RF, UK.

Phosphate buffered saline (PBS) was supplied by OXOID Ltd., Basingstoke, Hampshire, UK.

The Ki67 mouse anti-human primary antibody and the FITC-conjugated rabbit anti-mouse IgG secondary antibody were supplied by DAKO, Denmark House, Angel Drove, Ely, Cambridge, CB7 4ET, UK.

The 4,6-Diamidino-2-phenylindole (DAPI) containing commercial mountant was supplied by Vector Laboratories Inc., 16 Wulfric Square, Peterborough, PE3 8RF. UK.

Sodium azide was supplied by Sigma-Aldrich Company Ltd, Fancy Rd, Poole, Dorset, BH12 4QH, UK.

The EK1.BR keratocyte cell strain derived from an embryonic donor had previously been initiated within the department (Dropcova et al, 1999).

Nuaire IR autoflow water jacketed CO_2 incubator supplied by Jencons (Scientific) Ltd., Cherry Court Way Industrial Estate, Stanbridge Rd, Leighton, Bussard, LU7 8UA, UK.

Denley BS 400 centrifuge supplied by Denley Instruments, Daux Rd, Billingshurst, W. Sussex, RH14 7SJ, UK.

Leitz fluorescent microscope supplied by Leica Microsystems (UK) Ltd., Davy Avenue, Knowhill, Milton Keynes, MK5 8LB, UK.

2.1.3 Methods

2.1.3.1 Cell Culture

Cultures of the human keratocyte cell strain EK1.BR were grown in 15 ml of MEM supplemented with 10% (v/v) FCS and 1% (v/v) P/S in 75 cm^2 tissue culture flasks. Cells were incubated at 37°C in a humidified 5% CO_2/air incubator and were replated on reaching confluency using a 1x trypsin-EDTA solution. Media was removed and keratocytes were washed with 6 ml of PBS for thirty seconds. On aspiration of PBS 4.5 ml of 1x trypsin-EDTA solution was added to each flask. Cells were incubated at 37°C for approximately ten minutes until cells detached from the flask base. 6 ml of media was added to each flask in order to dilute the trypsin. The cell suspension was then transferred to a universal tube and centrifuged at 400g for five minutes, forming a pellet of cells at the base of the tube. Cells were resuspended in 6 ml of media and the number of viable cells was counted using a haemocytometer. At each passage the number of population doublings (pds) the cell culture had undergone was calculated using the formula given below.

$$PD = \frac{\log_{10} \text{cell number harvested} - \log_{10} \text{cell number previously seeded}}{\log_{10} 2}$$

Flasks were reseeded at 6000 cells cm^{-2} and reincubated at 37°C.

2.1.3.2 Immunocytochemical Detection of Ki67 Activity

Cells were seeded onto 13 mm circular coverslips placed in 35 mm tissue culture dishes at a density of 3000 cells per cm^2. Late passage cells with a slow proliferative capacity were seeded at a density of 6000 cells per cm^2. Keratocytes were incubated in a humidified 5% CO_2/air incubator at 37°C for seventy two hours. Growth media was removed and the coverslips were washed three times in PBS. Cells were fixed in a 1:1 solution of

methanol:acetone for four to five minutes at room temperature. Coverslips were again washed three times with PBS and placed with cell surface facing upwards in a humidifying chamber. The primary mouse anti-human Ki67 antibody was diluted 1:20 with PBS buffer containing 1% (v/v) FCS and 0.3% (w/v) sodium azide. 50 µl of diluted antibody was pipetted onto the cell surface of each coverslip. Cells were incubated overnight at 4°C and primary antibody was removed by washing the coverslips ten times in each of three universal tubes containing PBS. The coverslips were replaced in the humidifying chamber and coated with 50 µl of a 1:20 dilution of secondary rabbit anti-mouse IgG antibody. Cells were incubated for four hours at room temperature or overnight at 4°C. Secondary antibody was removed by again washing cells in PBS followed by ten washes in distilled water. Coverslips were mounted on a slide using mountant with DAPI and viewed under fluorescent microscope. DAPI positive cells, indicating total cell number, and Ki67 positive cells were counted at a wavelength of 420 nm and 525 nm respectively in each of a number of fields across each coverslip until 1000 DAPI positive or 200 Ki67 positive cells were recorded.

2.1.4 Results & Discussion

Morphological changes were observed on increasing serial passage of keratocyte cultures. Cells at late passage tended to be larger, flattened, vacuolated and showed contact inhibition at a lower cell density so that fewer cells were present across the culture (Figure 2.1). Figure 2.2 indicates the proliferative lifespan of the EK1.BR cell strain. As expected, a general decline in Ki67 positivity was observed on increasing serial passage (Figure 2.3). 58% of early passage cultures at 6 cpds were estimated to be Ki67 positive while in late passage cultures at 41 cpds the Ki67 positive fraction declined to 5%. The percentage of dividing cells remained fairly high until late in the proliferative lifespan of the keratocyte cultures. Ki67 positive counts indicated a cycling cell fraction of more than 38% until 39 cpds at which point the number of Ki67 positive cells dropped more rapidly until, at 41 cpds, the majority of keratocytes were non-dividing. Some fluctuation in the percentage of Ki67 positive cells was found particularly at intermediate cpds. This may

Figure 2.1
Comparison of EK1.BR keratocyte cultures at (a) 35 and (b) 50 cumulative population doublings (x400 magnification).

(a)

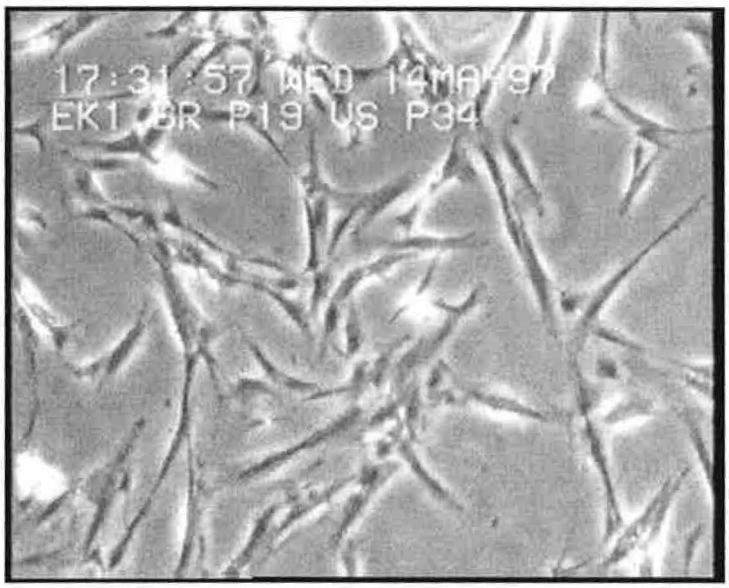

(b)

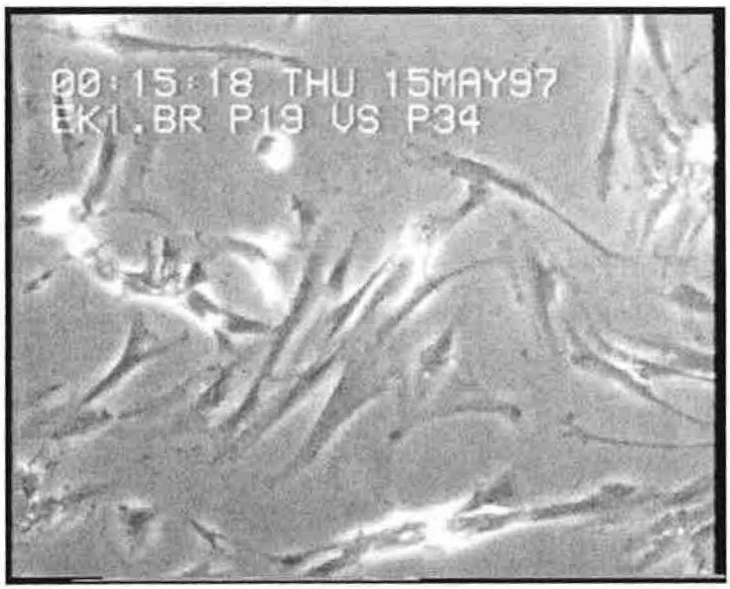

Figure 2.2
Cumulative growth curve for the embryonic keratocyte cell strain EK1.BR.

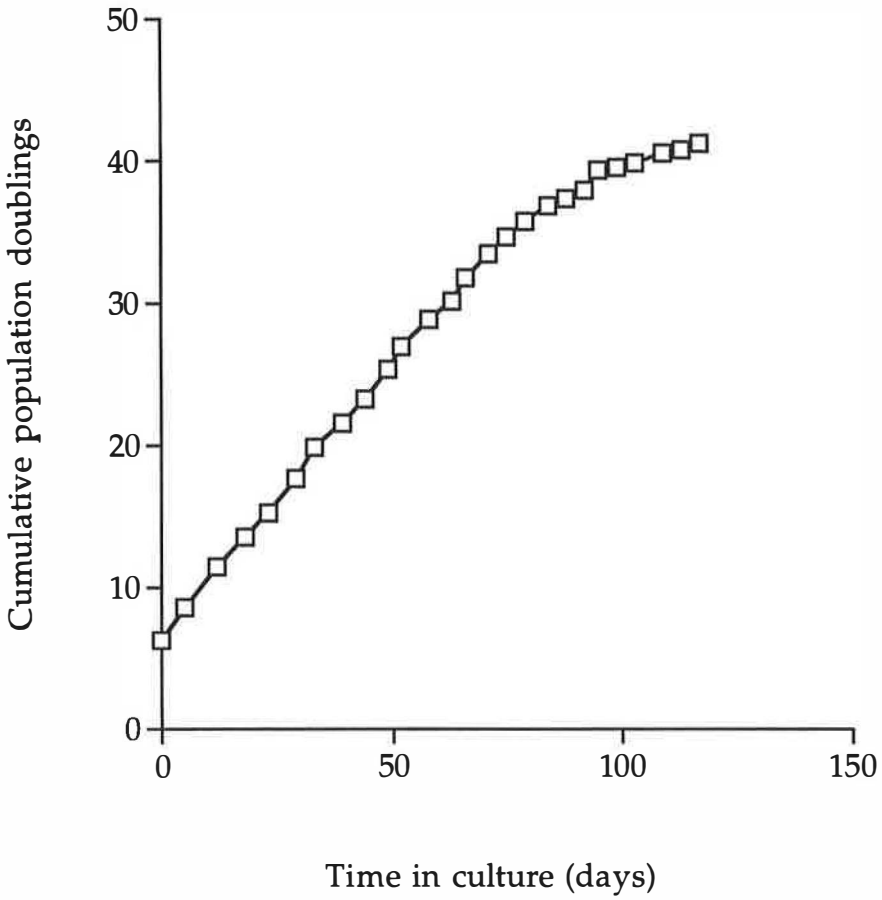

Figure 2.3
Changes in % Ki67 positive EK1.BR keratocytes on increasing serial passage.

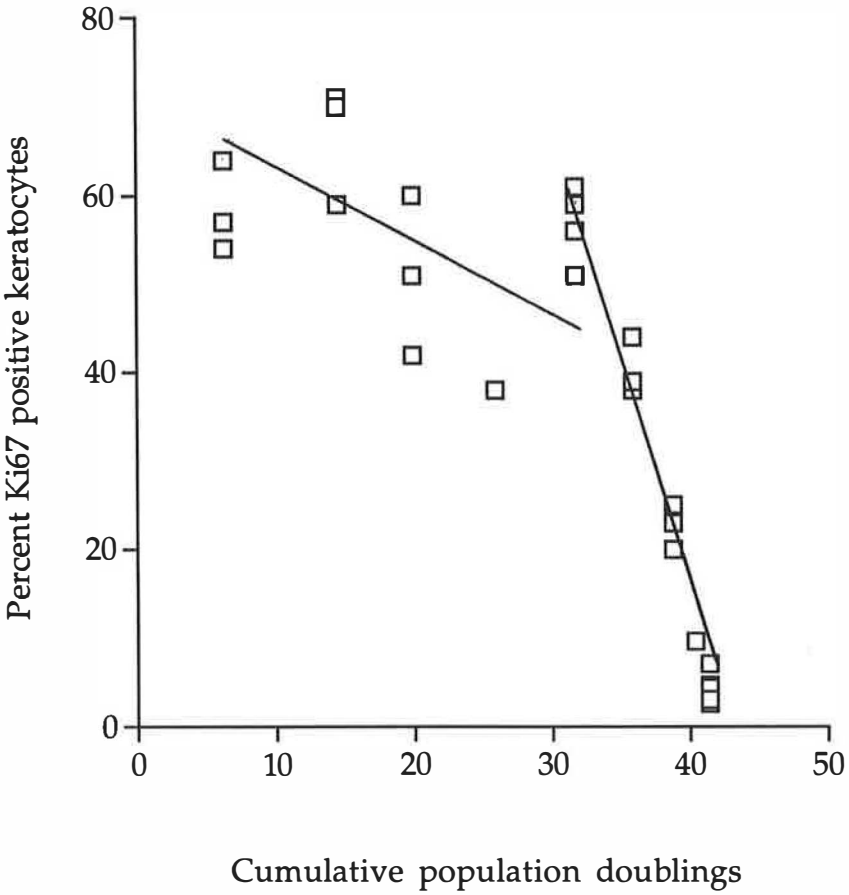

represent variability in the proliferative capacity of subclones of a specific keratocyte population. Regression analysis of the Ki67 results given in figure 2.3 indicated that the data is better described by two regression lines. The sum of the residuals after fitting one regression line to the data was 87.95 while the sum of the residuals after fitting two regression lines was 41.33 for the first line and 3.04 for the second line with a slope of -0.6 and -6.6 respectively. The results indicate that a slower initial decline in the percentage of proliferating cells occurs and is followed by a more rapid reduction in proliferative capacity after approximately 32 cpds.

A higher seeding density was selected for late passage keratocytes following the sparcity of cells observed in late passage assays. Early passage cultures were not seeded at this density because cell growth over three days would have been too rapid, leading to confluency across the coverslips. However, it may have been better to select an intermediate seeding density for both early and late passage assays since seeding density can affect cell growth characteristics and may have introduced an additional variable into the assays.

A number of cell samples at different cpds were used to measure Ki67 positivity rather than subculture of one initial sample so that results reflected any variability within the cell population. At 41 cpds less than 5% of keratocytes stained positive for the proliferation associated antigen Ki67. Cultures of these cells also failed to reach confluency over a three week period and were therefore considered senescent at a cpd of 41.

2.2 Histochemical Analysis of the Foetal Keratocyte Cell Strain EK1.BR

2.2.1 Introduction

The distribution of hydrolase activity in the human cornea has been investigated in detail in order to understand how these proteases may contribute to inflammation, wound healing and the process of graft rejection following keratoplasty (Coupland et al, 1994[a]; Coupland et al, 1993). The membrane bound hydrolase amino peptidase M (APM) and the lysosomal hydrolase dipeptidyl peptidase II (DPPII) are both active in human stromal keratocytes. While APM is only found in the human corneal stroma DPPII is detected in all three human corneal layers. Histochemical analysis indicates moderate to strong APM activity in the corneal stroma, mild DPPII activity in stromal and endothelial layers and moderate DPPII activity in the epithelium (Coupland et al, 1993).

The peptidases DPPII and APM are found in various tissues throughout the body. APM is a membrane bound N terminal exopeptidase and is active in a pH range of 6 to 9. It is a metalloenzyme bound to two zinc atoms and is present in large amounts in the brush border of intestinal enterocytes and in the cells of the renal proximal tubule. The large increase in activity during the remodelling stage of corneal wound repair suggest that APM may be involved in collagen matrix turnover (Pahlitzsch & Sinha, 1985). DPPII is a lysosomal exopeptidase with optimal activity at pH 4.5 to 5.5. The enzyme is involved in intralysosomal and extracellular proteolysis, cleaving N-terminal dipeptides from tripeptides with lysine, phenylalanine or leucine as the N-terminal amino acid and alanine or proline as the penultimate amino acid. DPPII may also be involved in PG and protein turnover within the cornea, particularly during development (Coupland et al, 1993).

Since both peptidases are detectable in stromal keratocytes in varying amounts and APM is found only in the stromal layer of the cornea the EK1.BR keratocyte cell strain may be characterised by the histochemical detection of APM and DPPII activity (Dropcova et al, 1999). Enzyme activity is detected by an azo-coupling reaction in which a substituted naphthol substrate is first cleaved by the enzyme. The resulting primary

reaction product reacts with a coupling reagent to from an insoluble azo dye which is visible under light microscope. Appropriate 4-methoxy-2-naphthylamide derivatives were used as substrates with Fast Blue B as the coupling reagent for detection of enzyme activity. For each assay a negative control was set up by excluding substrate from the incubation solution. The assays were also repeated using bovine corneal endothelial (BCE) cells to show a distinction in histochemical response between the two cell types.

2.2.2 Materials

L-alanine-4-methoxy-2-naphthylamide, Fast Blue B, dimethyl formamide (DMF), paraformaldehyde and glutaraldehyde were supplied by Sigma-Aldrich Company Ltd, Fancy Rd, Poole, Dorset, BH12 4QH, UK.

Lysine-pro-4-methoxy-2-naphthylamide was supplied by Bachem (UK) Ltd, 69 High Street, Saffron, Walden, Essex, CB10 1AA, UK.

Sodium cacodylate, mono- and di-basic sodium phosphate and Aquamount were supplied by MERCK Ltd, Hunter Boulevard, Magna Park, Lutterworth, Leics, LE17 4XN, UK.

Bovine corneal endothelial cells were supplied by the American Type Culture Collection (ATCC), catalogue number 1248.

2.2.3 Methods

2.2.3.1 Cell Preparation

Keratocytes over a range of cpds were plated onto 13 mm coverslips in 35 mm tissue culture dishes and incubated in a humidified 5% CO_2/air incubator at 37°C for seventy two hours until cells reached a semi-confluent state. Following incubation, media was aspirated from the tissue culture dishes and cells were washed three times in phosphate buffered saline (PBS). Cells were fixed for two minutes in 2% (w/v) paraformaldehyde containing 0.2% (v/v) glutaraldehyde in phosphate buffer at pH 7.4 for detection of DPPII and APM activity. Fixative was aspirated and coverslips were washed three times in PBS prior to

addition of incubation media.

2.2.3.2 Detection of APM Activity

3.5 mg of Fast Blue B dissolved in a few drops of DMF was mixed with 10 ml of 0.1M phosphate buffer at pH 7.4 (see Appendix 1 for buffer recipes). 3 mg of the substrate L-alanine-4-methoxy-2-naphthylamide was dissolved in a few drops of DMF. The Fast Blue B solution was then added to the substrate and filtered. Coverslips were incubated in the filtered solution either overnight at 4°C or at 37°C for three to four hours. Following incubation coverslips were washed three times in PBS, once in distilled water and were mounted in Apathy's syrup for viewing under the light microscope. Cells that were positive for APM activity stained red.

2.2.3.3 Detection of DPPII Activity

3.5 mg of Fast Blue B dissolved in a few drops of DMF was added to 10 ml of 0.1M cacodylate buffer at pH 5.5 and mixed with 3.5 mg of the substrate lysine-pro-4-methoxy-2-naphthylamide dissolved in a few drops of DMF. Coverslips were incubated in the filtered solution and were treated as for the detection of APM activity. Cells with positive DPPII activity stained red.

2.2.4 Results & Discussion

Cultures of the EK1.BR keratocytes stained positive for both APM and DPPII activity (Figure 2.4). Cultures incubated in solution excluding substrate showed no dye precipitation indicating that the red colouration was a result of keratocyte APM and DPPII activity. Results are in agreement with other studies showing moderate APM and DPPII activity in the human foetal corneal stroma. Mild DPPII activity and strong APM activity were also previously detected in the adult corneal stroma indicating variations in the intensity of hydrolase activity between foetal and adult eyes (Coupland et al, 1993).

APM and DPPII activity were not detected in the BCE cells (Figure 2.5). Previous histochemical studies found no APM activity and mild DPPII

Figure 2.4
Characterisation of EK1.BR keratocytes by cytochemical detection of APM (a) and DPPII (b) activity. (c) and (d) are respective negative controls.

(a)

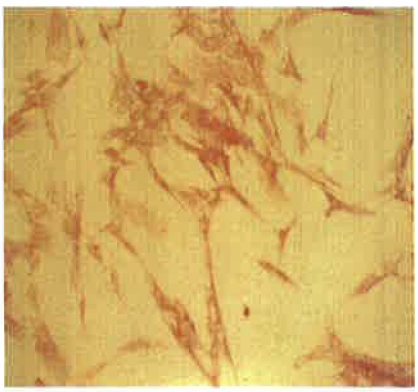

(c)

(b)

(d)

Figure 2.5
APM (a) and DPPII (b) activity in bovine corneal endothelial cells. (c) and (d) are respective negative controls.

(a)

(c)

(b)

(d)

activity in the bovine corneal endothelial layer (Coupland et al, 1994[b]). Some variation in the detection of hydrolase activity may be produced by the use of cultured cells rather than corneal tissue for cytochemical analysis. Since APM activity is only found in the stromal layer of the cornea the results of the present study confirm the identity of the EK1.BRs as stromal keratocytes.

Chapter 3

EK1.BR Keratocyte Migration into a Collagen Gel Matrix

3.1 Introduction

3.1.1 Keratocyte Migration

Keratocyte migration is a vital part of corneal wound healing and mediates the speed with which KPro integration within the cornea can occur (Lauffenburger & Horwitz, 1996). Activated keratocytes migrate into the area of tissue damage along a FN mesh and secrete proteases and structural proteins for ECM remodelling (Tuft et al, 1993). Migration is initiated by the ECM, mediated by signals from growth factors and structural proteins such as FN and collagen (Shimizu et al, 1997).

The process of cell migration is controlled primarily by the actin cytoskeleton which associates indirectly with the ECM via attachments to integrin membrane receptors. Other membrane receptors may also influence cytoskeletal activity following ligand binding to allow a coordinated response to ECM signalling (Schor, 1994). Actin is found within the cell in both monomeric and polymeric form and undergoes rapid polymerisation on ligand-receptor binding to form microfilament bundles. In addition to it's role in migration actin also coordinates the activation of a number of metabolic and nuclear transcription pathways (Rao & Cohen, 1990). The process of migration occurs by forward protrusion of the cell and attachment to the matrix followed by cell traction, rearward detachment and retraction (Mitchison & Cramer, 1996). Prior to migration cells become morphologically polarised by molecular rearrangement so that integrin receptors with cytoskeletal links are concentrated at the leading edges of the cell. Actin filaments, which are randomly distributed under the cell membrane in resting cells, form parallel filament bundles at the leading edge and within the cell processes of migrating cells (Gibson & Anderson, 1977). Flattened lamellipodal ruffles and thinner filopodial extensions protrude from the cell front in association with actin polymerisation and form integrin mediated attachments to the matrix. These attachments remain while contractile forces project the cell forward. Matrix attachments are released at the rear of the cell followed by cell retraction. Integrins are primarily left on the substratum but may also be recycled by membrane surface dispersal or internalisation (Lauffenburger & Horwitz, 1996).

Other cell membrane receptors such as galactosyltransferase also mediate lamellipodal formation and spreading by attachment to oligosaccharide specific substrates within the matrix (Begovac et al, 1994). Thus, cell migration requires the coordinated activity of numerous intracellular molecular components, the cytoskeleton and membrane receptors in association with the ECM.

Senescent fibroblasts exhibit a number of changes in structure and protein synthesis which may reduce the coordinated response of the cell and contribute to a reduction in cell migration. A number of studies, comparing both young and old donor fibroblasts and early and late passage fibroblasts, have indicated that dermal fibroblast migration declines with age and with fibroblast senescence (Schneider & Mitsui, 1976; Kondo & Yonezawa, 1992). Time-lapse cinematographic studies also showed a decline in fibroblast motility with increasing serial passage (Wang, 1985). al-Khateeb et al (1997) used a collagen lattice based wound repopulation model to show that child donor derived dermal fibroblasts migrate into the wound significantly faster than fibroblasts from adult donors. Age and senescence appear to have a similar effect on dermal fibroblast migration suggesting that the accumulation of senescent fibroblasts may be a causative factor in the age related changes which occur. However, the role of senescence in the ageing cornea and changes in senescent keratocyte migration are less well established.

The environment used to investigate keratocyte migration is important since keratocyte activity occurs in conjunction with interrelated signalling mechanisms from the ECM (Nakagawa et al, 1989; Schor, 1994). Measurement of normal keratocyte migration is therefore more likely to occur by recreating an environment similar to that in which the cell interacts *in vivo.* Previous studies have shown that cell adhesion and migration vary depending on the substrate (Schor, 1980; Saltzman et al, 1991; Elsdale & Bard, 1972). Collagen matrices appear to most closely approximate the physiological environment of the fibroblast. Cells exhibit fibroblast morphology similar to that seen *in vivo* and, in contrast to cells plated on plastic surfaces, also appear to exhibit

proliferative constraints similar to those found *in vivo* (Sarber et al, 1981). A collagen matrix was therefore considered the most suitable environment in which to study keratocyte migratory behaviour.

3.1.2 Keratocyte Migration in Response to EGF

The process of keratocyte migration is regulated by various growth factors and cytokines. Along with other ECM components such as fibronectin (Kondo et al, 1992) and collagen type I (Gibson et al, 1993) they produce chemotactic and mitogenic signals that mediate keratocyte restructuring of the wound matrix. Fibroblast migration specifically requires growth factor stimulation and is inhibited by surumin induced inhibition of growth factor activity (Kondo & Yonezawa, 1992). Schreier et al (1993) found that the growth factors bFGF, TGF-β and PDGF still enhanced fibroblast migration following mitomycin C inhibition of proliferation indicating that cytokine enhanced cell migration is not simply a by-product of mitogenic stimulation. Growth factors bind to specific membrane receptors and may directly affect the cytoskeletal systems involved in migration or act indirectly by nuclear transcription factor activation and the subsequent secretion of additional cytokines, receptors, matrix proteins and proteases (Schor, 1994).

The growth factor EGF is an important mediator of corneal wound repair (Woost et al, 1985). It is found in the tear film and in all three layers of the cornea where it appears to stimulate the proliferation and migration of epithelial cells and keratocytes (Wilson et al, 1994; Pancholi et al, 1998; Andresen et al, 1997; Maldonado & Furcht, 1995, Schultz et al, 1992). Exogenous addition of EGF was also found to expediate corneal epithelial wound closure and to increase the tensile strength of healed stromal tissue (Schultz et al, 1994; Woost et al, 1985). EGF is a fifty three amino acid polypeptide and binds to a transmembrane receptor possessing an intracellular tyrosine kinase domain. On binding EGF the receptor dimerizes, activating tyrosine kinase and associated phosphorylation cascades (Nimni, 1997; Schultz et al, 1994). The effects of EGF on corneal epithelial wound closure appear to be mediated by phosphatidylinositol 3-kinase related signal transduction pathways (Zhang & Akhtar, 1997).

Initiation of DNA synthesis occurs in association with increased c-fos and c-myc mRNA levels (Paulsson et al, 1987). EGF mediated corneal epithelial cell adhesion and migration appears to occur by the synthesis of FN and an increase in FN receptors on the cell membrane (Nishida et al, 1992). FN accumulates in the matrix around the epithelial cells and bound FN causes actin filament reorganisation and initiates cell migration (Nakagawa et al, 1985). EGF, secreted by keratocytes, has autocrine and paracrine effects on epithelial cell and keratocyte activity and acts in association with other growth factors such as TGF-β in order to moderate cellular responses and prevent excessive activation (Pancholi et al, 1998). TGF-β is secreted by keratocytes and epithelial cells and tends to antagonise the effects of EGF. It shares the same membrane receptor as EGF but in contrast to EGF it inhibits keratocyte migration and MMP-1 secretion and stimulates collagen synthesis. The levels of each secreted growth factor dictate whether migration or collagen synthesis primarily occurs.

Senescence induces changes in the fibroblast's response to growth factor stimulation. Growth factor signals fail to induce cell division in senescent cells as a result of inhibitory blocks on cell cycle progression (Zeng & Millis, 1996). DNA synthesis in response to EGF addition has been shown to significantly decline as fibroblasts age in culture. The number of EGF receptors remained constant until cultures were effectively senescent suggesting that changes in intracellular pathways mediating EGF's effect rather than changes in the number of membrane receptors were responsible (Tang et al, 1994). In dermal fibroblasts the cell's migratory response to growth factor stimulation is also reduced. On exposure of human dermal fibroblasts to growth factor containing conditioned media in a Boyden chamber assay late passage cell cultures, elderly donor cell cultures and cell cultures from donors with progeroid syndromes showed a significant decline in migratory response to chemotactic stimulation (Albini et al, 1988). In contrast, no change in TGFβ-1 stimulated type I collagen synthesis or collagen gel contraction was observed on comparison of young and old donor dermal fibroblasts. Such results indicate that cytokines have multiple effects on fibroblast

activity which appear to be differentially effected by cell ageing (Reed et al, 1994). EGF has previously been shown to enhance keratocyte migration into a collagen gel matrix (Andresen et al, 1997). However, the effects of senescence on the keratocyte's migratory response to growth factor stimulation have not been considered.

3.1.3 Keratocyte Migration in Response to FN

FN has a multifunctional role in cell-matrix interactions and mediates the cell's migratory response through interaction with $\alpha 5\beta 1$ integrin receptors clustered at focal adhesion points on the cell membrane (Maldonado & Furcht, 1995). Results showing that exogenous application of FN enhances rates of corneal epithelial wound closure indicate that FN is central to the process of corneal wound healing (Nishida et al, 1984). Following wounding FN is chemotactic and provides a scaffold over which cells can migrate (Shimizu et al, 1997; Mensing et al, 1983). A coordinated increase in integrin receptor expression and focal clustering occurs in conjunction with FNs appearance (Watt, 1994). Cytoskeletal actin filaments contact the cell membrane at these points and undergo rearrangement following increased FN binding to initiate the process of migration (Nakagawa et al, 1985; Hynes, 1981). Continuous disruption and reformation of fibronectin-integrin bonds by activated proteases allows cell migration to progress (Gibson et al, 1993).

The domains responsible for initiating cell migration are still under investigation. The RGDS motif, found in the cell binding domain of FN, was initially identified as a vital sequence for cell adhesion and migration (Nishida, 1992). Other sequences on the heparin binding domain may also regulate cell adhesion (Gibson et al, 1993; Mooradian et al, 1992). Transmembrane experiments initially appeared to show that only the non-gelatin binding domains of FN were involved in dermal fibroblast chemotaxis at concentrations ranging from 2.5 to 50 $\mu g\ ml^{-1}$ (Postlethwaite et al, 1981). However, later studies using a collagen gel assay more analogous to ECM conditions showed a significant migratory response to the gelatin binding domain (GBD) at concentrations from 0.1

pg ml^{-1} but no response to FN and other fragments of the FN molecule (Schor et al, 1996). Results suggest that cell responsiveness to FN domains depend on the experimental environment.

The chemotactic effect of FN on dermal fibroblast migration declines with increasing age of donor, increasing serial passage and for fibroblasts derived from donors with progeroid syndromes (Albini et al, 1988). The structure of FN derived from senescent fibroblasts is altered. Although secretion is enhanced FN has a larger molecular weight and is less able to mediate cell adhesion to the ECM (Kumazaki et al, 1991; Chandrasekhar et al, 1983). FN is vital to keratocyte migration so that changes in keratocyte responsiveness to exogenous FN or in the structure of secreted FN may have an inhibitory effect on the migratory response.

3.1.4 Keratocyte Migration in Response to HA

Hyaluronic acid (HA) is found in the cornea after wounding and appears to act as an additional mediator of the repair process, including the migratory response. The molecule is a negatively charged, linear glycosaminoglycan consisting of the repeated disaccharide unit of glucuronic acid and N-acetylglucosamine and remains unbound to a central protein (Fitzsimmons et al, 1992). It is a highly viscous and elastic component of the extracellular matrix (ECM) and is most commonly found in soft connective tissue where it acts as a lubricant and shock absorber. Other physiological roles include maintenance of tissue structure and hydration, regulation of cell proliferation, migration and plasma protein distribution (Laurent & Fraser, 1992). HA is used clinically in ophthalmic surgery to protect the corneal endothelium from surgical trauma and to maintain the shape of the anterior chamber (Goa & Benfield, 1994). It is also used in ophthalmic drug delivery systems and as a tear substitute for dry eye conditions (Sintzel et al, 1996). Preliminary investigation suggests that HA has potential use in the treatment of corneal epithelial disruption produced by dry eye conditions (Yokoi et al, 1997), in the treatment of joint diseases and as a diagnostic marker (Laurent & Fraser, 1992).

HA production rapidly increases following wounding (Molander et al, 1993; Drubaix et al, 1997) suggesting a role in wound repair and the potential for use in acceleration of the healing process. Exogenous application of HA was found to increase rates of wound closure following punch biopsy of the hampster cheek pouch (King et al, 1991) and was also found to increase the healing rate of tympanic membrane perforations and of cutaneous ulcers (Goa & Benfield, 1994). HA was found to stimulate rabbit corneal epithelial cell migration and proliferation suggesting that these effects contribute to wound closure (Nakamura et al, 1992; Inoue & Katakami, 1993). HA interacts with specific cell surface receptors such as the CD44 receptor to produce cell detachment from the matrix and stimulation of migration. Glioma cells were found to detach, cluster and round up when seeded onto HA coated surfaces. This effect was reversed in part by inhibition of CD44 receptor functioning (Koochekpour et al, 1995). A novel Receptor for HA Mediated Motility (RHAMM) has also been identified (Turley, 1992). HA was found to produce protein phosphorylation and stimulate locomotion of H-ras transformed cells by interaction with RHAMM. Receptor inhibition prevented smooth muscle cell migration into cell monolayer wounds supporting a role for HA in cell migration during wound repair. Co-localisation of RHAMM and cytoskeletal actin beneath sites of cell membrane ruffling suggest that HA receptor interaction induces transduction pathways regulating cytoskeletal rearrangement to enable cell mobility (Turley, 1992). HA may also enhance cell mobility by binding to the GAG binding sites on collagen and fibronectin, preventing cell surface proteoglycan binding and inhibiting cell attachment to collagen (Rouslahti, 1989).

HA is not normally found in the corneal stroma but is quickly synthesised and secreted by epithelial and stromal cells following wounding (Fitzsimmons et al, 1992; Fagerholm et al, 1992). CD44 receptors for HA have been located on epithelial, stromal and endothelial cell membranes suggesting HA interacts with these cells (Asari et al, 1992). EGF and bFGF are both involved in the corneal response to wounding and were found to stimulate HA synthesis in

chick corneal stromal cells (Nakazawa, et al, 1996). It is therefore likely that HA plays a role in the corneal repair mechanism in part by stimulation of cell migration into the wounded area. The following study investigated the effect of HA on EK1.BR keratocyte migration into a collagen gel matrix in order to consider the *in vitro* effect of HA on this part of the repair response.

Migration is a vital aspect of the keratocyte response to wounding and any changes in migration would be detrimental to corneal tissue repair. The following study sought to investigate the effect of *in vitro* senescence on keratocyte migration into a collagen gel matrix. Since EGF, FN and HA are mediators of the corneal response to wounding their effect on keratocyte migration into a collagen gel matrix and changes occurring following cellular senescence were also investigated. The potential effect of FN/HA incorporation within the collagen gel matrix was compared with that on addition to the cell suspension. The two variations in the assay were carried out in order to assess whether direct or indirect exposure of the cells to FN/HA by addition to the cell suspension or gel matrix respectively made a selective difference to keratocyte migration.

3.2 Materials & Equipment

Vitrogen 100 purified, pepsin solubilised, bovine, dermal collagen dissolved in 0.012N HCl (2.9mg/ml) was supplied by Imperial Laboratories, Portway Industrial Estate, Andover, Hampshire, UK.

Calcein-acetoxymethyl ester (Calcein-AM) in dimethyl sulphoxide (DMSO) (1mg/ml) was supplied by Molecular Probes, distributed by Cambridge Bio Science, 25 Signet Court, Newmarket Road, Cambridge, CB5 8LA, UK.

4,6-Diamidino-2-phenylindole (DAPI), hyaluronic acid isolated from rooster comb, tissue culture grade EGF from mouse submaxillary glands, fibronectin derived from human plasma and the 45kDa gelatin binding fragment were supplied by Sigma-Aldrich Company Ltd., Fancy Rd,

Poole, Dorset, BH12 4QH, UK.

LSM 410 invert laser scan microscope supplied by Zeiss, PO Box 78, Welwyn Garden City, Herts., AL7 1LU, UK.

3.3 Methods

3.3.1 Collagen Gel Preparation

A 3.0 mg ml^{-1}, vitrogen 100 collagen stock solution was diluted to a concentration of 1.75 mg ml^{-1} using a vitrogen diluter solution of MEM, 10% (v/v) PBS, 0.6% (w/v) HEPES and 0.225% (w/v) $NaHCO_3$ (see Table 3.1). Six gels were prepared for each experiment using two four well tissue culture plates. 0.5 ml of collagen solution was placed in each well and incubated at 37°C for one hour. Cultures from cpd 8 to 42 were used for the invasion assays. Keratocytes were passaged during the gel incubation as described in section 2.1.3. Cells were resuspended in media so that 0.6 ml of media containing $1x10^5$ cells could be added to each gel. Cells were subsequently seeded onto the gels and incubated for seventy two hours at 37°C in a humidified 5% CO_2/air incubator.

Reagent	Volume
MEM	90ml
PBS	10ml
NaHCO3	0.225g
HEPES	0.6g

Table 3.1 Vitrogen diluter recipe

3.3.2 Evaluation of Keratocyte Migration

Keratocyte migration was examined by fluorescent microscopy using the fluorochrome calcein AM. Surface media was removed and gels were washed three times with PBS. 0.4 ml of calcein AM in PBS (0.05 mg ml^{-1}) was added to each well and gels were incubated for ten minutes. A laser scanning confocal microscope was used to assess depth of migration. Cell migration was recorded in each field by setting the surface of the gel to zero and increasing the focus depth in 50 µm increments. The number of cells present within each interval was recorded and totalled for thirty fields in each gel. These totals were used to calculate the mean cell count found at each 50 µm interval migration depth for six gels in each experiment. A chi-square test for statistical significance was used to analyse the data, comparing three separate experiments using early passage keratocyte cultures with three separate experiments using late passage keratocyte cultures.

The fluorochrome DAPI was used to confirm that the cell density across the surface of each gel was similar. Following each migration assay calcein AM was removed, gels were washed three times with PBS and fixed with a 1:1 solution of methanol:acetone for four minutes. Gels were again washed with PBS following removal of fixative. 0.4 ml of DAPI in PBS (0.05 mg ml^{-1}) was added to each gel. Gels were incubated for ten minutes and viewed under fluorescent microscope. A surface count of cell nuclei in three fields for each gel was recorded (Appendix 2).

3.3.3 Keratocyte Migration in Response to EGF

Keratocytes were preincubated in MEM supplemented with 0.5% (v/v) FCS and 1% (v/v) P/S for twenty four hours prior to the preparation of the collagen gels. Low serum conditions were used in order to minimise the amount of EGF present in addition to that added to the experimental gels. Six collagen gels (1.7 mg ml^{-1}) were prepared as described in section 3.3.1. Keratocytes were passaged as described in section 2.1.3. $8x10^5$ cells were spun down by centrifugation at 400g and were resuspended in 4.8

ml of media. For each experiment a 25 µl aliquot of EGF (stock concentration of 0.1 mg ml^{-1} dissolved in sterile water) was diluted to 5 µg ml^{-1} by the addition of 0.475 ml of PBS. 2.4 ml of cell suspension was transferred to a separate universal tube and 10 µl EGF (5 µg ml^{-1}) was added to give a final concentration of 20 ng ml^{-1} EGF. 0.6 ml of cell suspension containing EGF and $1x10^5$ cells was seeded onto each of three collagen gels. Three control gels were also set up by adding 0.6 ml of cell suspension without EGF to each gel. Gels were incubated for seventy two hours at 37°C, stained with calcein AM and viewed under fluorescent microscope for analysis of cell migration as described in section 3.3.2.

Mean keratocyte migration into the three EGF gels and three control gels was calculated for each assay. A chi-square test of statistical significance was used to analyse the data, comparing results from four separate assays using early passage keratocytes (cpd=10-12) with those from four separate assays using late passage keratocytes (cpd=38-41). Cell density on the surface of each gel was verified using a DAPI stain for cell nuclei as previously described in section 3.3.2. Six fields were counted across each gel and a mean value for these counts was obtained (Appendix 2). Ratios of the mean total number of keratocytes migrating in response to EGF to the mean total number of keratocytes migrating into the control gels for each assay were calculated from eight separate experiments using early passage keratocytes and seven separate experiments using late passage keratocytes. Results were used from assays with more widely varying DAPI counts since only similar cell densities across the control and EGF gels within each assay were required to calculate ratios with accuracy.

3.3.4 Keratocyte Migration in Response to FN

3.3.4.1 FN or GBD Added to the Cell Suspension

Three sets of migration assays were set up for each of the FN types. Eight collagen gels were prepared for each experiment as described in section 3.3.1. Prior to setting up each assay keratocytes were incubated in 0.5% (v/v) serum containing media for twenty four hours. Low serum

conditions were used to minimise the additional effect of FN, present in the serum in unknown quantities, on keratocyte migratory activity. Serial dilutions of FN or GBD were prepared and cells were passaged as described in section 2.1.3 during the hour incubation required to set the collagen gels. $1.8x10^6$ keratocytes were spun down and resuspended in 10.8 ml of 0.5% (v/v) serum containing media. 1.8 ml of cell suspension was added to each of four universal tubes for the preparation of two gels for each of the three concentrations used and two control gels. FN or GBD concentrations of 1 $\mu g\ ml^{-1}$, 0.01 $\mu g\ ml^{-1}$ and 0.00001 $\mu g\ ml^{-1}$ were used. 100, 1, 0.1 and 0.001 $\mu l\ ml^{-1}$ stock concentrations were prepared from an initial stock of 1 mg ml^{-1} in each case. 0.018 ml of a 100x concentrated solution was added to each of three universal tubes to produce the range of concentrations given above (eg 0.018 ml of 100 $\mu g\ ml^{-1}$ stock was added to 1.8 ml of cell suspension to give a final, approximate concentration of 1 $\mu g\ ml^{-1}$ in the first universal tube). 0.6 ml of cell suspension containing $1x10^5$ cells was added to each gel.

Gels were incubated at 37°C in a humidified 5% CO_2/air incubator for seventy two hours. Keratocyte migration into the collagen gels was analysed as described in section 3.3.2.

3.3.4.2 FN or GBD Added to the Gel Solution

Three sets of migration assays were set up for each FN type. Eight gels were used for each experiment including two control gels and two gels for each of the 1, 0.01 and 0.00001 $\mu g\ ml^{-1}$ concentrations of FN or GBD. Stock solutions were prepared at concentrations of 100, 1, 0.1 and 0.001 $\mu g\ ml^{-1}$ from an initial stock of 1 mg ml^{-1} FN or GBD. 8 ml of vitrogen gel solution was prepared as described in section 3.3.1. 1485 μl of the gel solution was transferred to each of three universal tubes. 1500 μl was added to a fourth universal tube for the two control gels. 15 μl of a 100x concentrated FN or GBD stock was added to each universal to produce

the three concentrations given above (eg. a 1 μg ml^{-1} concentrated gel solution was made by adding 15 μl of the 100 μg ml^{-1} stock to 1485 μl gel solution in the first universal tube). 0.5 ml of gel solution was added to each well and gels were set at 37°C for one hour. Keratocytes were passaged as described in section 2.1.3. $1x10^5$ cells suspended in 0.6 ml of 0.5% (v/v) serum containing media were seeded onto each gel.

Gels were incubated at 37°C in a humidified 5%CO_2/air incubator for seventy two hours. Keratocyte migration into the collagen gels was analysed as described in section 3.3.2. Keratocyte cultures from 15 to 27 cpds were used for the migration assays involving FN and GBD. The Friedman test for statistical significance was used to analyse the data, comparing keratocyte migration into the control gels with that into the FN/GBD containing gels at the three different concentrations used.

3.3.5 Keratocyte Migration in Response to HA

3.3.5.1 Preparation of HA

HA was supplied as a solid and was dissolved in PBS by dialysis. Dialysis tubing was separated in boiling water. A knot was tied in one end of the tubing. HA was inserted and the tubing was sealed by tying a second knot. The tubing was weighted and suspended in a beaker of PBS for two to three days. HA in solution was removed and the concentration was calculated by measuring the volume held within the tubing the HA was dissolved in. The final concentration may be varied by altering the length of dialysis tubing used. The solution was filter sterilised prior to use in the migration assays.

3.3.5.2 HA Added to the Gel Solution

EK1.BR keratocytes were cultured as described in section 2.1.3. Cells were incubated in 0.5% (v/v) serum containing media twenty four hours prior to setting up each assay. 8 ml of collagen gel solution (1.75 mg ml^{-1}) was made up as described in section 3.3.1. 1.5 ml of gel solution was added to each of four universal tubes (one control and one for each of

the three HA concentrations used). A stock concentration of 10 mg ml^{-1} HA was used to prepare concentrations of HA in the gel solutions of 1 mg ml^{-1}, 0.5 mg ml^{-1} and 0.1 mg ml^{-1} (see Table 3.2). Two four well plates were used to set up eight gels. Two control gels were set up by the addition of 0.5 ml of gel solution to two of the wells. Two gels at each HA concentration were also set up. Gel solutions were incubated for one hour at 37°C to set. 0.6 ml of cell suspension containing $1x10^5$ cells was seeded onto each gel and gels were incubated for seventy two hours at 37°C in a humidified 5% CO_2/air incubator. Cell migration was assayed described in section 3.3.2. Keratocyte cultures from 18 to 26 cpds were used for all migration assays involving HA.

3.3.5.3 HA Added to the Cell Suspension

Eight collagen gels were set up as described in section 3.3.1 and incubated for one hour at 37°C to set. Cells were passaged and 1.8 ml of cell suspension containing $3x10^5$ cells was added to each of four universal tubes. HA was added to three of the universal tubes to give HA solutions of 1 mg ml^{-1}, 0.5 mg ml^{-1} and 0.1 mg ml^{-1} (see Table 3.3). 0.6 ml of cell suspension containing $1x10^5$ cells was added to each gel to produce two control gels and two gels at each HA concentration. Gels were again incubated at 37°C in a humidified 5% CO_2/air incubator for seventy two hours. Cell migration was assayed as described in section 3.3.2. The Friedman test for statistical significance was used to analyse the migration data for three separate experiments comparing keratocyte migration into the control gels with that into the HA containing gels at the three different concentrations used.

	Amount of gel solution added (ml)	Amount of 10 mg/ml stock solution of HA added (ml)
Control	1.5	-
1 mg/ml Solution	1.35	0.15
0.5 mg/ml Solution	1.43	0.07
0.1 mg/ml Solution	1.49	0.01

Table 3.2 Amount of hyaluronic acid (HA) added to each gel solution.

	Amount of cell suspension (ml)	Amount of 10 mg/ml stock solution of HA added (ml)
Control	1.8	-
1 mg/ml Solution	1.8	0.18
0.5 mg/ml Solution	1.8	0.09
0.1 mg/ml Solution	1.8	0.018

Table 3.3 Amount of hyaluronic acid (HA) added to each cell suspension

3.4 Results

3.4.1 Keratocyte Migration

Some keratocyte migration into the collagen gels occurred at all cpds. In each case the majority of migrating cells penetrated the collagen matrix to a depth of 50-100 μm as shown in Figure 3.1a. The number of cells gradually diminished further into the gels and few cells were found at depths greater than 400 μm. Comparison of Figures 3.1a, 3.1b, 3.1c and 3.1d indicates that at each cpd cell number declines as gel depth increases.

Early passage keratocyte cultures migrated into the gels to a greater extent than late passage keratocyte cultures. Figure 3.1 indicates that, as the

Figure 3.1
Scatter graphs (a), (b), (c), and (d) indicate changes in the mean number of keratocytes migrating to depths of 50-100 μm, 100-150 μm, 150-200 μm and 200-250 μm respectively with increasing serial passage of cells.

(a).

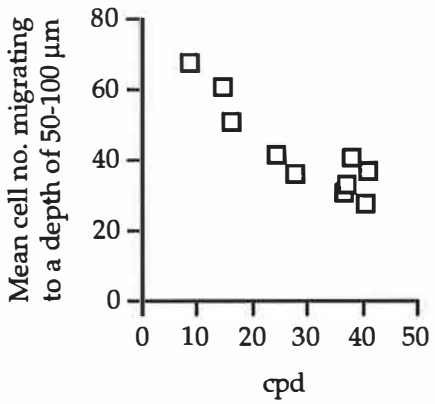

(b).

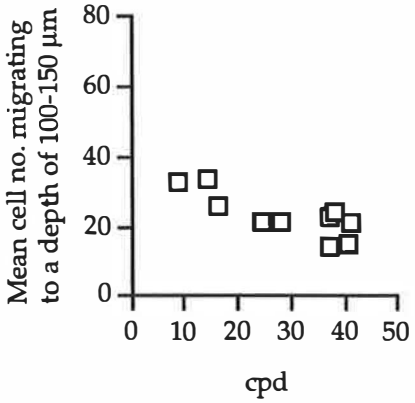

(c).

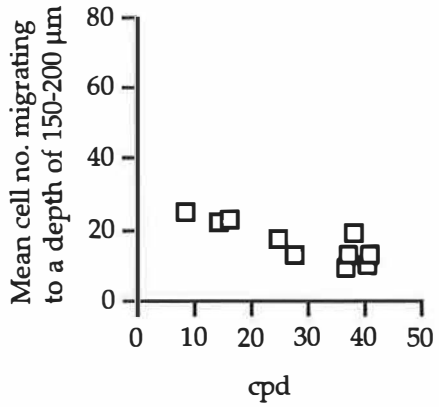

(d).

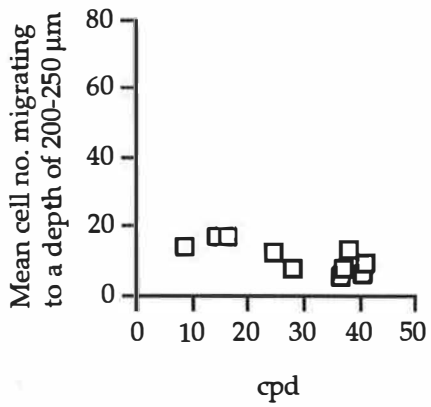

number of cpds increased, a general decline in the number of cells migrating to each migratory depth occurred. Comparison of the mean number of keratocytes migrating to each segmental depth for six gels in each of three separate experiments using early passage kera tocytes and three separate experiments using late passage keratocytes revealed a significant decrease in the number of late passage keratocytes invading the gels ($p< 0.001$, 6 d.f.) (Figure 3.2). Table 3.4 suggests that this is the general trend for each migration depth at which the presence of cells was recorded. Although keratocyte migration declined with increasing serial passage, the depth to which keratocytes migrated did not appear to alter substantially. Keratocytes at 40 cpd did not penetrate the gels to a depth greater than 350 μm. However for cells at all other cpds there does not appear to be noticeable variation in the maximum depth of gel penetration recorded.

migration depth (μ)	mean cell no. (cpd=15)	mean cell no. (cpd=16)	mean cell no. (cpd=37)	mean cell no. (cpd=41)
50-99.9	61	51	33	28
100-149.9	34	26	23	15
150-199.9	22	23	13	10
200-249.9	17	17	8	6
250-299.9	9	14	7	4
300-349.9	5	9	3	1
350-399.9	4	4	1	1
400-449.9	2	2	1	
450-499.9	0.3	1	0	
500-549.9	0.2	1	1	
550-599.9		0.2		
600-649.9		0.3		

Table 3. 4 Comparison of mean cell numbers migrating to each gel depth across 30 fields in each of 6 gels for keratocytes at cpd 15, 16, 37 and 41.

Figure 3.2
Comparison of early passage EK1.BR keratocyte migration with that of late passage EK1.BR keratocytes. Results are expressed as the mean+/- SEM (n=3)

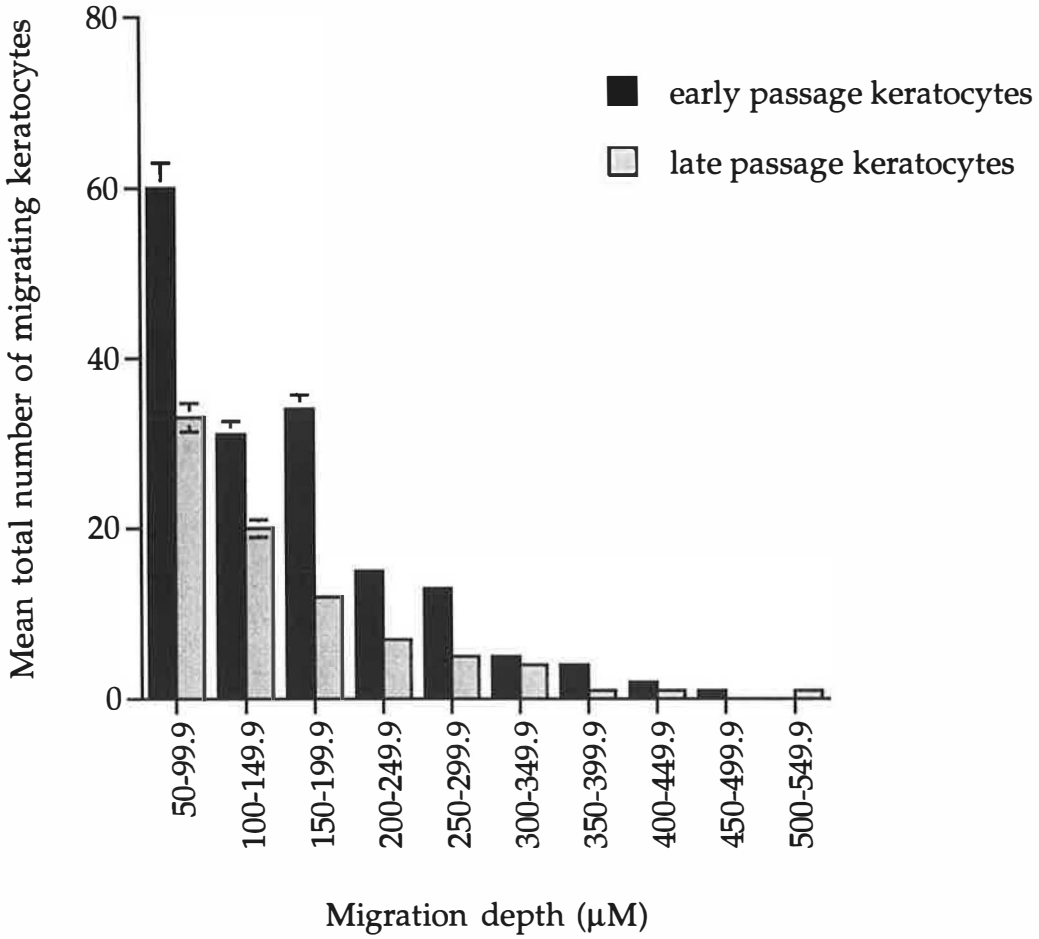

3.4.2 Keratocyte Migration in Response to EGF

Keratocytes responded to EGF stimulation by a significant increase in the number of cells migrating into the collagen gels ($p < 0.001$, 4 d.f.) and an increase in depth of gel penetration at all cpds (Figures 3.3, 3.4 & 3.5). The ratio of mean total number of keratocytes migrating into the collagen gels in the presence of EGF to those migrating into the control gels was greater than one in all cases (Figure 3.6).

A significant difference in the migratory response of early and late passage keratocytes to EGF stimulation was observed. The total numberof early passage keratocytes migrating into the collagen gels in response to EGF was significantly greater than the number of late passage cells migrating into the gels under the same conditions by a factor of approximately two to three ($p < 0.001$, 7d.f.) (Figure 3.5). Figure 3.6 indicates that the ratio of total keratocyte migration in the presence of EGF to total control gel keratocyte migration is generally higher for keratocytes at low cpds. Two sets of migration assays using late passage keratocytes yielded ratios equivalent to those found for early passage keratocytes. However, this does not reflect a greater response to EGF by these late passage keratocytes (see section 3.5.2). In general response to EGF declined on increasing serial passage producing lower migration ratios. Little change in the number of keratocytes migrating into control gels, in the presence of 0.5% (v/v) serum containing media, was observed on increasing serial passage (Figure 3.5).

DAPI counts were used to verify that seeding densities on the EGF and control gels were approximately equal since differences here would have a marked effect on the resulting ratios of EGF to control gel migration. Some counts indicated that, although original seeding densities were theoretically constant at 1×10^5 cells per gel, some sets of gels had a sparser cell distribution than others. Comparison of data was only made using gels with similar surface densities.

Figure 3.3
Comparison of early passage EK1.BR keratocyte migration in the presence of EGF with migration in the absence of EGF. Results are expressed as the mean +/- SEM (n=4) (cpd=10-12).

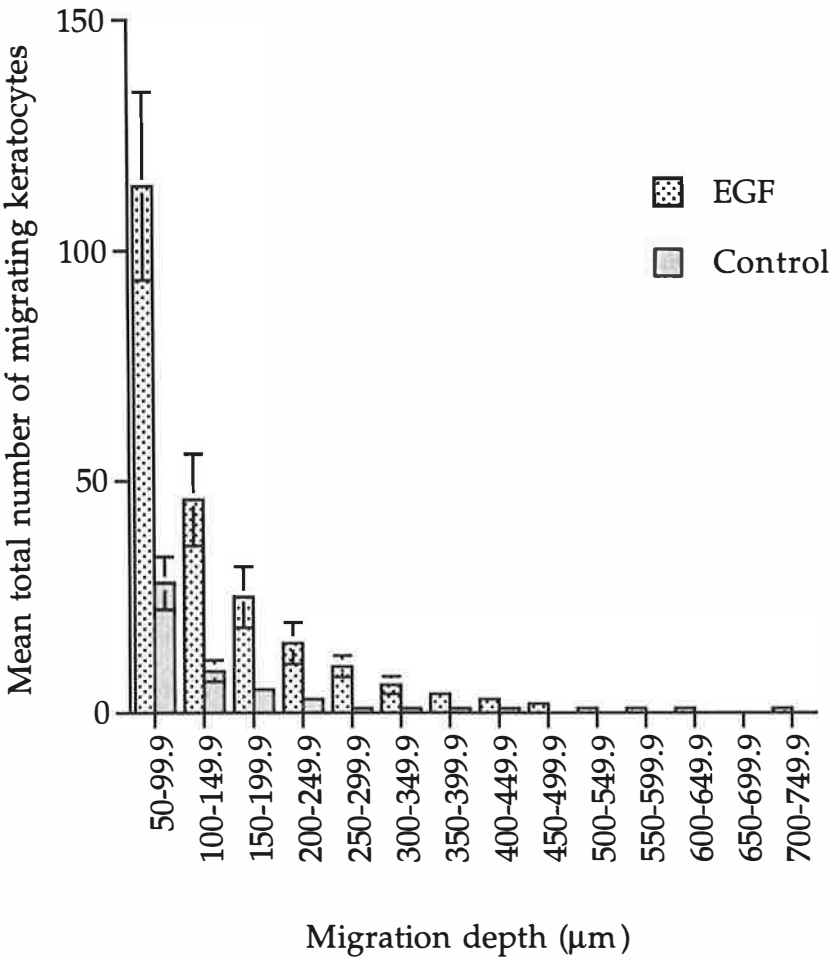

Figure 3.4
Comparison of late passage keratocyte migration in the presence of EGF with migration in the absence of EGF. Results are expressed as the mean +/- SEM (n=4)
(CPD= 38-41.)

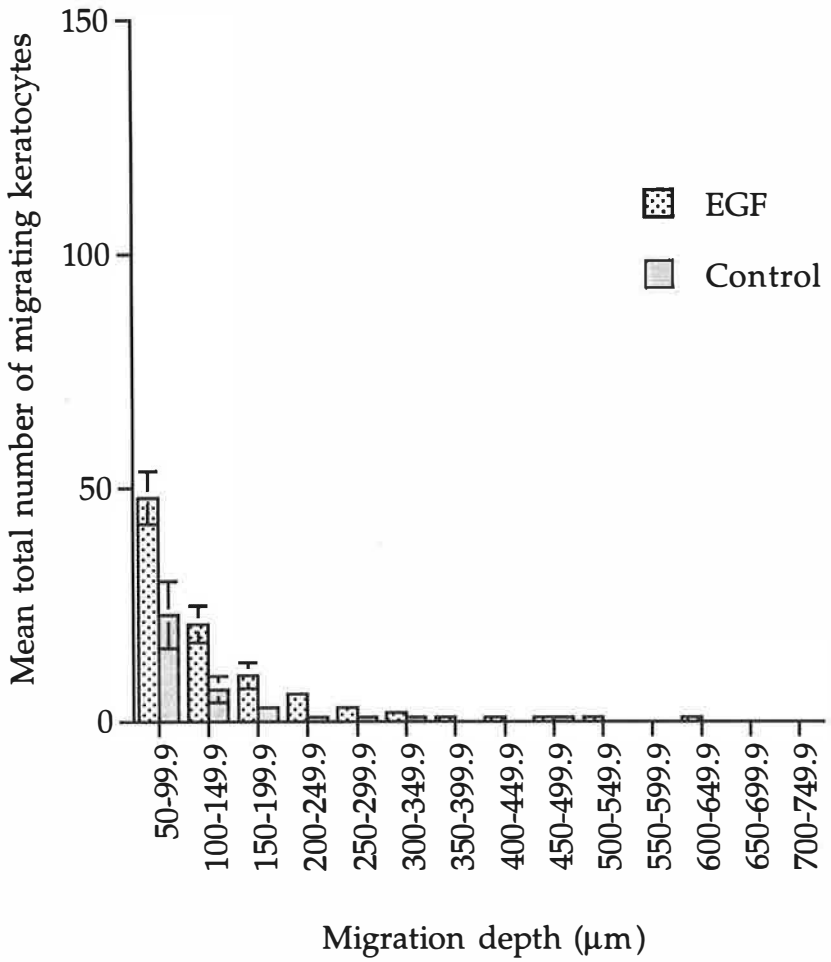

Figure 3.5
Comparison of total keratocyte migration into early and late passage EGF gels with that into control gels. Results are expressed as the mean +/- SEM.

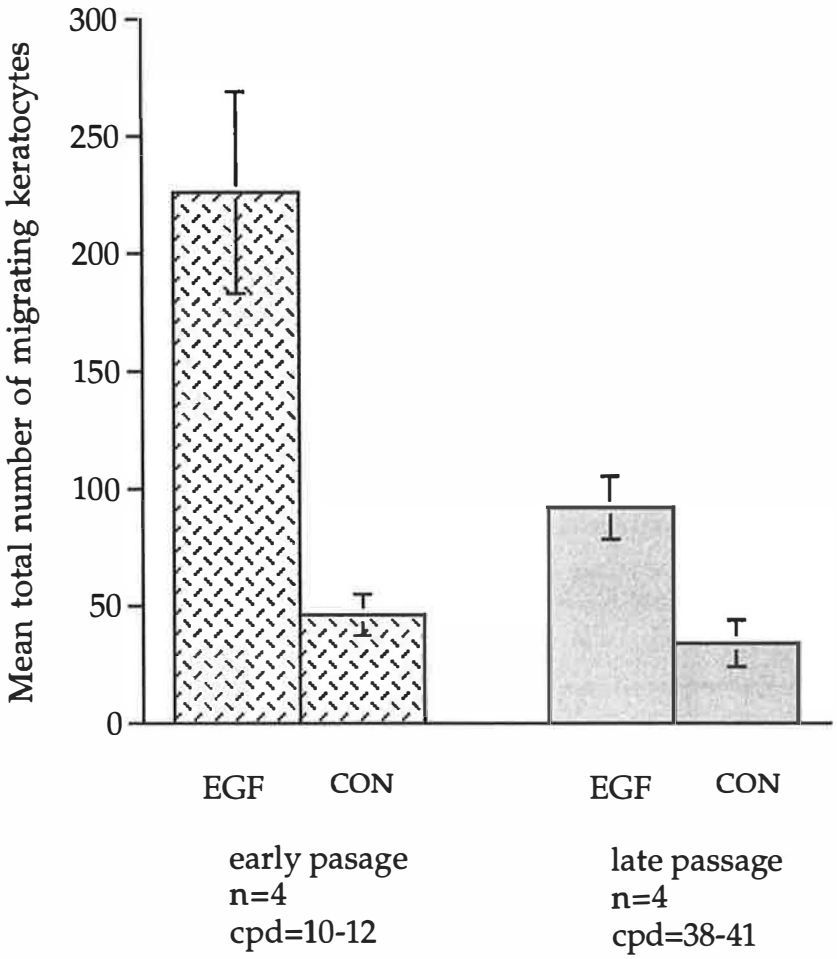

Figure 3.6
Comparison of the ratios of total keratocyte migration in response to EGF to total keratocyte migration in the absence of EGF at early and late passage. n=8 for assays using early passage keratocytes (cpd=8-15). n=7 for assays using late passage keratocytes (cpd=38-41).

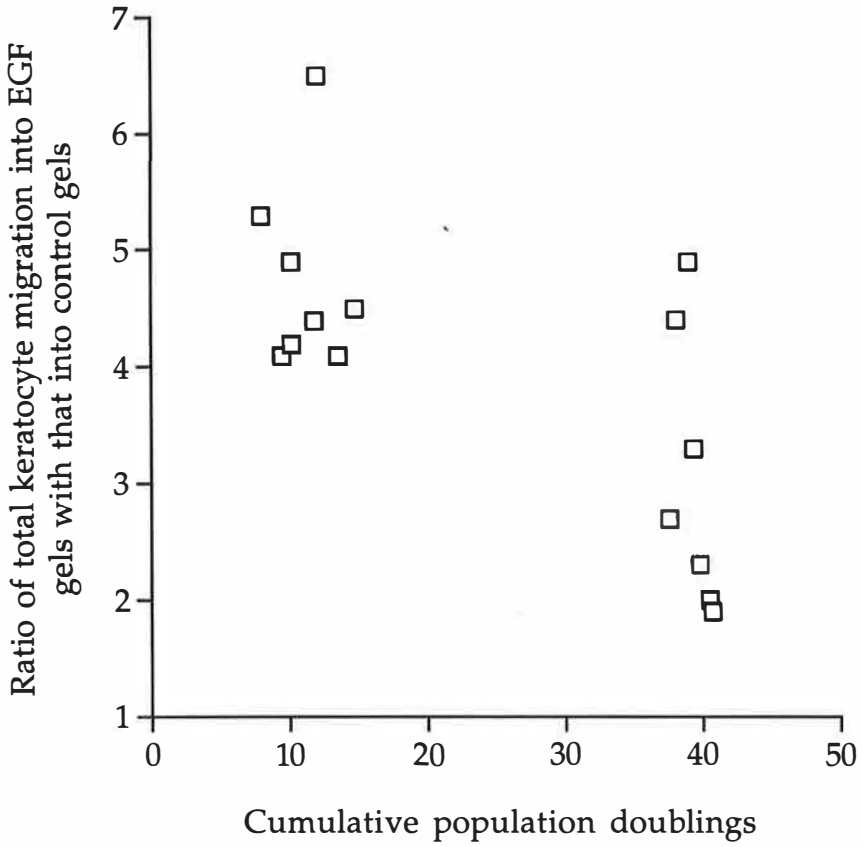

3.4.3 Keratocyte Migration in Response to FN

Addition of FN or GBD to the gel solution or to the cell suspension at concentrations ranging from 1 to 10^{-5} μg ml^{-1} had no significant effect on EK1.BR keratocyte migration into the collagen gels ($p>0.01$). The ratio of cell migration into experimental versus control gels was near to one in each case (Figure 3.7). The number of cells migrating into the gels was low in control and experimental gels with a maximum of eleven cells counted across thirty fields. Although Figure 3.7 suggests some inhibition of cell migration by FN and GBD this is probably a result of the small total cell number migrating into the gels rather than a real effect (Figure 3.8 and Figure 3.9).

3.4.4 Keratocyte Migration in Response to HA

Following HA addition to the cell suspension or the gel solution no significant difference in keratocyte migration into the collagen gels was observed ($p>0.01$). Cell migration into the gels when HA was added to the cell suspension was similar to that observed when HA was added to the gel solution. Keratocyte migration into the gels was limited in both control and HA gels. A slight increase in the total number of cells migrating into the gels was observed when HA was added to the gel solution and when HA was added to the cell suspension at a concentration of 1mg ml^{-1}. However, little real effect on cell migration was apparent in the presence of HA since keratocyte migration was only increased by a maximum of five cells (Figure 3.10).

3.5 Discussion

3.5.1 Keratocyte Migration

The results of this study show for the first time that keratocyte migration is inversely related to the age of the cells in culture. A significant decline in the number of keratocytes invading the collagen gels was found in assays using late passage cultures. However, the maximum depth to which keratocytes invaded the gels did not appear to decrease with increasing cpd. Early and late passage keratocytes migrated to a similar maximum depth. The results suggest that the majority of cells migrating into the collagen gels are non-senescent since senescent keratocytes with

Figure 3.7
Addition of fibronectin or GBD to the gel solution or cell suspension has no effect on EK1.BR keratocyte migration (n=3).

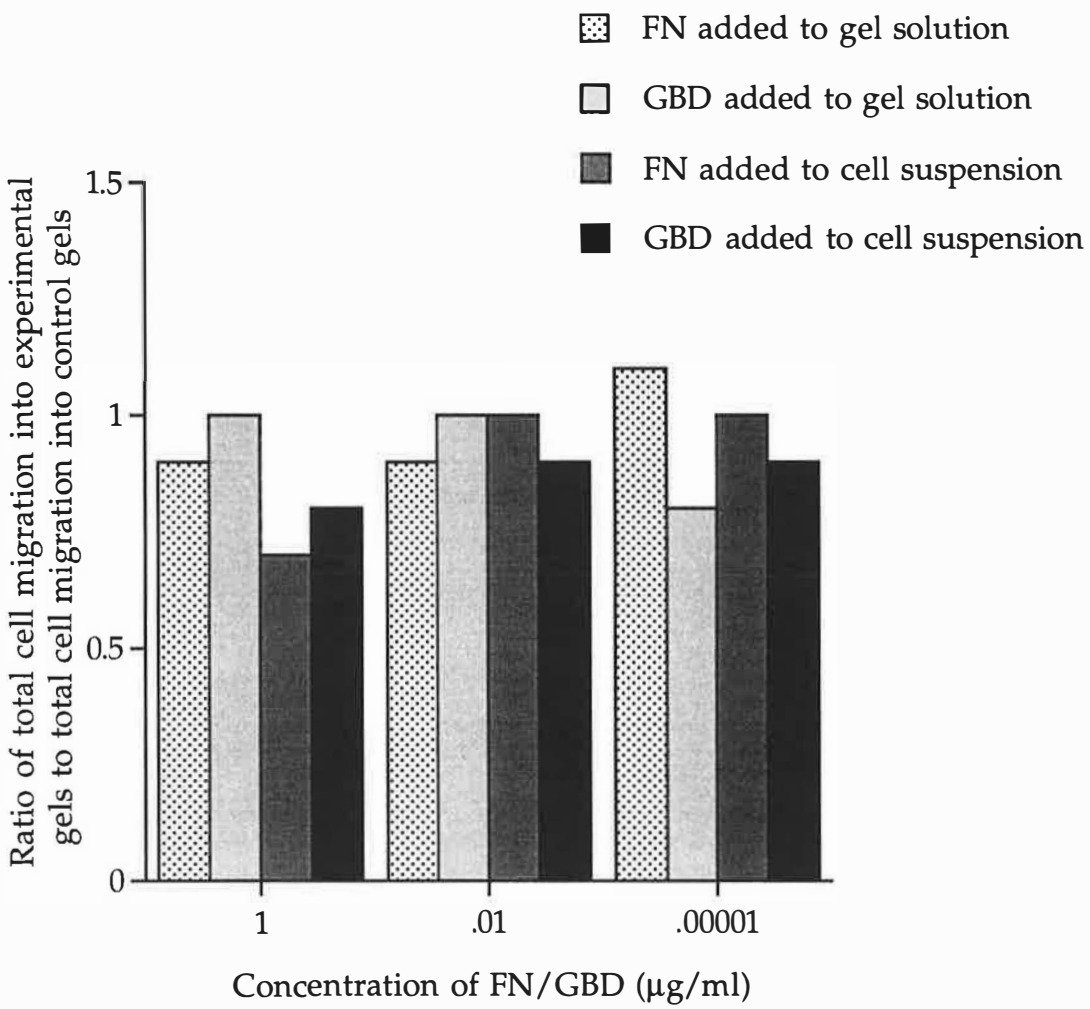

Figure 3.8
Addition of GBD to the gel solution or to the cell suspension has no effect on EK1.BR keratocyte migration into a collagen gel. Results are expressed as the mean +/- SEM (n=3).

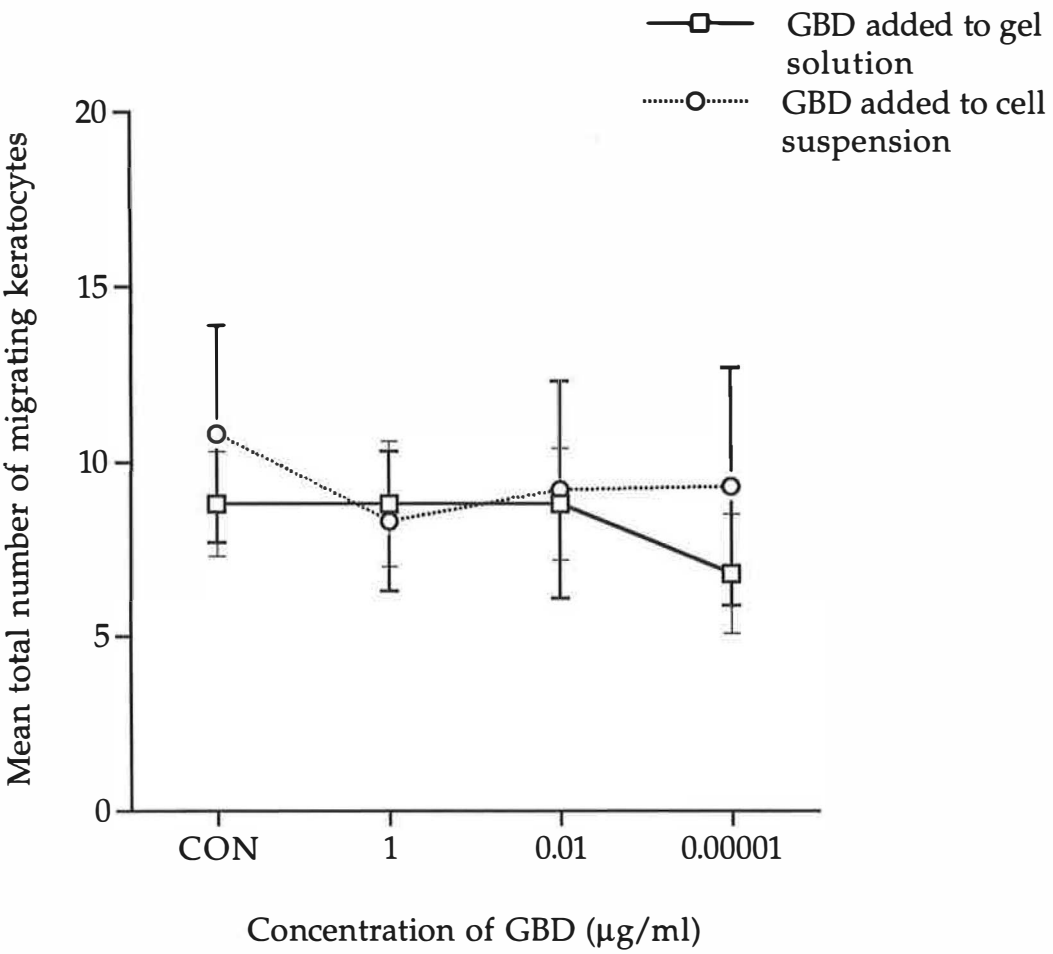

Figure 3.9
Addition of FN to the gel solution or to the cell suspension has no effect on EK1.BR keratocyte migration into a collagen gel. Results are expressed as the mean +/- SEM (n=3).

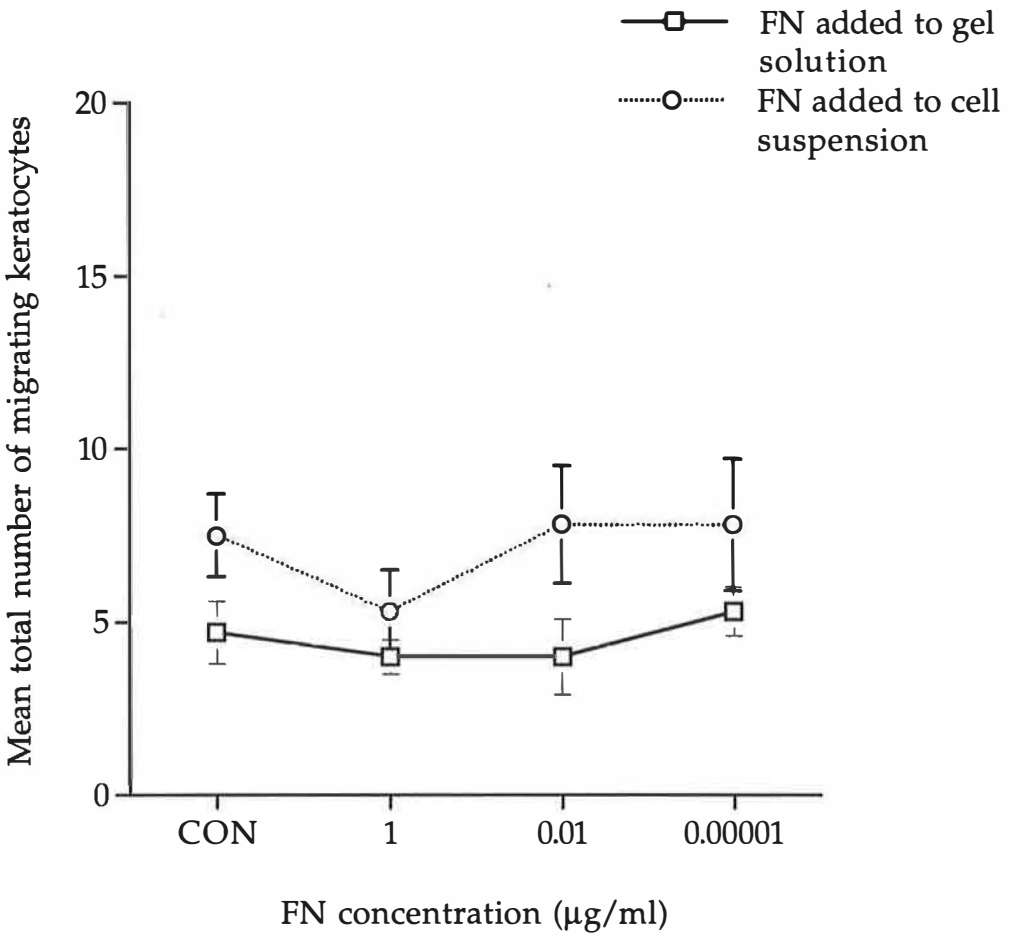

Figure 3.10
Addition of hyaluronic acid to the cell suspension or gel solution has no effect on EK1.BR keratocyte migration into a collagen gel. Results are expressed as the mean +/- SEM (n=3).

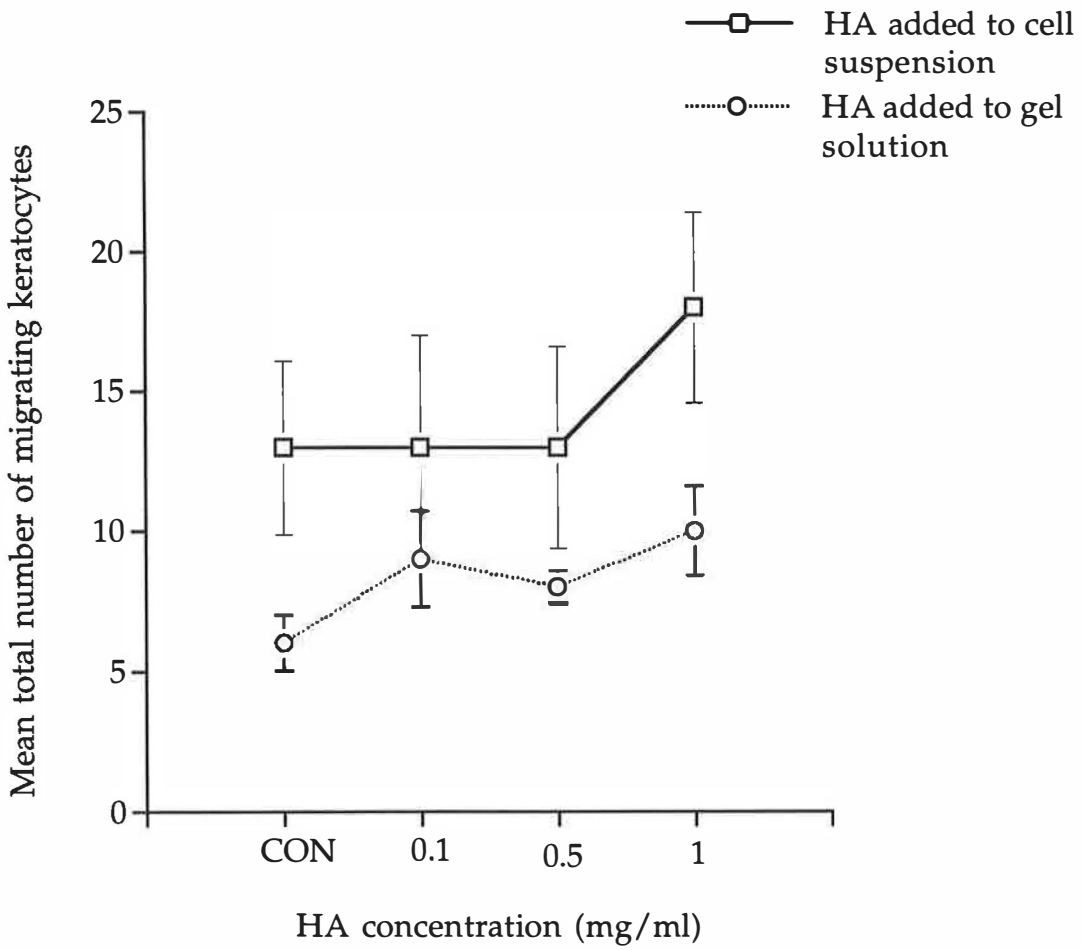

a diminished migratory capacity would produce a lower maximum depth of migration. At late passages the majority of the keratocytes are senescent so that the number of cells migrating into the gels is significantly less.

It is unlikely that the observed decline in migration was merely a result of the reduced proliferative response of keratocyte cultures to EGF on increasing cpd. It has previously been shown that EGF induces fibroblast migration independently of its effect on cell proliferation (Schreier et al, 1993) and that fibroblast proliferation within collagen gels is low (Sarber et al, 1981). In addition, the seeding density of keratocytes onto the collagen gels was very high so that contact inhibition of proliferation was probable. However, further assays in the presence of an inhibitor of cell division such as mitomycin C are necessary in order to completely exclude the possibility that changes in the proliferative capacity of late passage keratocytes may have influenced the observed decline in migratory capacity.

A number of changes in the structure of senescent keratocytes and in the coordination of mechanisms regulating cell activity may alter the migratory capacity of the cell. The actin cytoskeleton, which is central to the process of migration, appears to take on a more rigid structure in senescent fibroblasts (Wang & Gundersen, 1984). An increase in crosslinking between intermediate filaments may also contribute to cytoplasmic rigidity causing the rate at which migratory signals are converted to actual motion by the cell to be reduced (Wang, 1985). Senescent cells are larger and flattened and reduction in the formation of microfilament bundles may occur because changes in cell shape hinder normal microfilament assembly (Macieira-Coelho, 1983). Migration is dependent on cell adhesion to the matrix which is also reduced in senescent cells. The altered ability of FN, collagen and the PGs to mediate the process of adhesion may contribute to this decline. At all levels of cell functioning the factors involved in mediating migration are changed with senescence so that efficient coordination of the process is limited. The results of this study suggest that in the keratocyte, as in

fibroblasts from other dividing tissues, structural and functional changes also occur with senescence which alter the motility of the cell.

3.5.2 Keratocyte Migration in Response to EGF

Results indicate that the growth factor EGF specifically upregulates the process of keratocyte migration and that the mechanisms by which migration is enhanced become less efficient with age so that a decline in migratory response to EGF occurs. The addition of EGF caused the keratocytes to migrate further into the gels and to a maximum depth which was similar at all cpds. Results again suggest that the majority of late passage keratocytes migrating into the gels are non-senescent. Senescent cells, with a diminished migratory response to EGF stimulation, would not be expected to migrate into the gels to the same depth as non-senescent keratocytes.

While migration in response to EGF decreased on increasing serial passage the number of keratocytes migrating into the control gels, in 0.5% (v/v) serum containing media, remained fairly constant. Two exceptions were observed for two sets of late passage migration assays, coincident with the only two high migration ratios observed for late passage keratocytes. In both cases keratocyte invasion into the control gels was reduced while migration into the EGF gels was comparable to the other late passage assays producing the two unexpectedly high ratios observed in Figure 3.6.

The ability of the keratocytes to migrate in very low levels of serum suggests that they may secrete factors which autonomously mediate migration. In addition, the steady levels of migration into the control gels at both early and late passage indicate that no change in the secretion of these factors or in cell responsiveness occurs with increasing serial passage. The secretion of autonomous migration stimulating factors by foetal fibroblasts has been suggested in other studies (Kondo et al, 1993). One factor involved in autonomous foetal skin fibroblast migration has been identified as the heparin binding protein, migration stimulating factor (MSF) (Schor et al, 1988; Grey et al, 1989). MSF is autonomously

produced by foetal skin fibroblasts in confluent cultures and by tumour cells but not by adult skin fibroblasts and may mediate foetal fibroblast migration by stimulating hyaluronic acid synthesis (Schor et al, 1988; Ellis et al, 1992). Schor et al (1985) compared the density dependence of adult and foetal fibroblast migration using cell density migration index values and observed an abrupt transition in the migratory characteristics of foetal skin fibroblasts to those of the adult phenotype at late passage, prior to senescence. While the secretion of autonomous factors may explain keratocyte migration into the control gels in this study no decline in migration into the control gels was observed at late passage. The ability to autonomously secrete migration stimulating factors may have been retained. Alternatively this method of measuring cell migration may not be sensitive enough to detect a transition phase from autonomous secretion by foetal keratocytes. Comparison of foetal and adult keratocyte migration in the absence of EGF or serum supplementation would indicate whether such factors influence foetal keratocyte migration. A similar, constant level of migration by adult keratocytes at both early and late passage would suggest a baseline endogenous migratory capacity, unchanged by *in vitro* ageing, rather than autonomous migration factor synthesis by the EK1.BR keratocytes.

The cellular changes which alter the senescent keratocyte's migratory response to EGF stimulation are unknown. A decline in the number of cell surface EGF receptors and a subsequent decrease in stimulus strength may occur. However, a study using lung derived WI-38 fibroblasts suggests that, while changes in receptor associated kinase activity occur following senescence, the number and ligand binding affinity of fibroblast EGF receptors remain the same (Phillips et al, 1983). A further possibility is that changes occur in the transduction mechanisms initiated by EGF stimulation which reduce the cell's response. Translocation of the second messenger protein kinase C (PKC) to the cell membrane following stimulation is reduced in senescent fibroblasts limiting its capacity to activate intracellular pathways such as those resulting in formation of the transcription factor AP-1 (DeTata et al, 1993). Enhanced ceramide levels appear to inhibit phospholipase D

(PLD) and subsequent diacylglycerol (DAG) formation so that PKC cannot be activated (Venable et al, 1994). Evidence suggests that the fibroblast's impaired response to growth factor stimulation is a result of disrupted intracellular signalling mechanisms rather than a large reduction in receptor activity (Macieira-Coelho, 1983; Cristofalo & Pignolo, 1996). In addition, senescence related changes in cell structure and in the expression of and structure of secreted ECM components mediating the process of migration may contribute to the decline in EGF induced cell motility. These include the changes in actin cytoskeleton, FN, collagen and the PGs previously mentioned as potential inhibitors of keratocyte migration (Wang & Gundersen, 1984; Wang, 1985; Chandrasekhar et al, 1983; Takeda et al, 1992).

The present study confirms previous results showing that EGF stimulates human keratocyte migration (Schultz et al, 1992; Andresen et al, 1997). In addition, results indicate for the first time that the age related decline observed in keratocyte migration results, in part, from a fall in responsiveness to EGF stimulation.

3.5.3 Keratocyte Migration in Response to FN

FN is involved in cell locomotion and the GBD fragment has been shown to stimulate dermal fibroblast migration into a collagen gel matrix system. It was therefore expected that some effect on keratocyte migration would be seen. However, at the concentrations used (10^{-5} to 1 $\mu g\ ml^{-1}$), FN and GBD showed no effect on keratocyte migration into the collagen gel matrix. Chemotactic response to FN varies with cell type (Mensing et al, 1983) so that the failure of keratocytes to respond to FN or GBD in this system may represent changes in the response of fibroblasts derived from different tissues. Keratocytes may be less affected by the addition of exogenous fibronectin or may be selectively responsive to FN specifically derived from corneal sources. Rabbit corneal epithelial wound closure is enhanced by the addition of plasma FN (Nishida et al, 1984). It is thought that FN is initially derived from plasma following corneal wounding but is subsequently derived from cellular sources. Since epithelial migration occurs initially to close the wound these cells may be more responsive to plasma FN while keratocyte migration occurs

later and may be more responsive to endogenously secreted cellular FN. Additionally, the chemotactic effect of collagen on keratocyte migration may dominate within the collagen matrix assay so that again exogenous FN has little additional effect on migration into the gels. Use of FN derived from corneal cells will indicate whether the source of FN used to stimulate keratocyte migration is important. Application of FN directly to a non-collagenous surface may reveal any enhancement of keratocyte migration more clearly; isolating fibronectin's effect from that of collagen.

3.5.4 Keratocyte Migration in Response to HA

For both the FN and HA collagen gel invasion assays keratocyte migration was lower than that observed in the other migration assays. Total cell migration counts were also low for the control gels indicating that the reduction did not result from inhibition of cell adhesion by FN, GBD or HA. Control cell migration counts were approximately half those seen for the EGF control gels. The reason for this general reduction in cell migration is unknown. However, for both sets of assays a regular coverslip was substituted for the haemocytometer coverslip and may have changed the volume of the chamber. Overestimation of cell numbers would have resulted in the seeding of fewer cells onto the collagen gels and may have resulted in the observed reduction in total cell number. The use of averages from a number of haemocytometer counts in future may help to more accurately estimate total cell number and better regulate gel seeding densities.

Evidence suggests that HA is involved in the process of keratocyte migration. High levels of HA synthesis appear to be involved in the enhanced migration of foetal dermal fibroblasts and high molecular weight HA was found to enhance the migration of confluent adult dermal fibroblasts in a collagen gel assay (Chen et al, 1989, Ellis et al, 1992). However, under the conditions used in this assay system, HA had very little effect on EK1,BR keratocyte migration into the collagen gels. Previously HA was found to stimulate migration of various glioma cell lines across polycarbonate filters in a chemotactic assay. The effect was

dose dependent using concentrations from 0 to 1 mg ml^{-1} HA and migration was increased by 36 to 135% in the various cell lines used (Koochekpour et al, 1995). Turley (1992) also found that exogenous HA transiently stimulated migration of H-ras transformed cells up to forty eight hours after initial mutant gene induction but only at concentrations of less than 0.1 $\mu g\ ml^{-1}$. The migration of uninduced fibroblasts was not dependent on HA stimulation suggesting that tumour cells possess altered regulation of and responsiveness to HA. Since HA is thought to be involved in tumour metastasis the heightened migratory response of these glioma and H-ras transformed cells to HA may be related in part to cell transformation. However, evidence for the involvemnet of HA in the enhancement of normal cell migration indicates that HA migratory responsiveness is not restricted to transformed cell types. Instead, it may also vary depending on the cell type, HA source and assay system used, as for FN.

Measurement of corneal epithelial cell migration down the sides of a cultured corneal block indicated significant ($p<0.01$) enhancement of cell migration following incubation with 0.5 to 1 mg ml^{-1} HA. Migration was enhanced by approximately 50% independently of differences in molecular weight over a range of $9x10^4$ to $280x10^4$ (Nakamura et al, 1992). HA was derived from rooster comb and it's effects were augmented by the addition of FN indicating that FN may mediate the migratory response of the corneal epithelium to HA (Nakamura et al, 1994[b]). The failure of EK1.BR keratocytes to respond to HA may indicate differences in the responsiveness of epithelial cells and keratocytes to exogenous HA as for FN. In addition it may indicate differences in foetal keratocyte responsiveness to HA. Foetal wound fluid has been found to contain much lower levels of hyaluronidase than adult wound fluid suggesting less degradation of HA secreted by embryonic cells (West et al, 1997). The effect of autonomously secreted HA by the embryonic EK1.BR keratocytes may therefore be augmented so that additional HA has no extra effect on migration. As for FN, it may be that in the collagen matrix assay system the chemotactic effect of collagen was maximal so

that HA had limited additional effect on cell migration. Further study using an alternative assay, adult keratocytes and different sources of HA may help to clarify these issues.

3.5.5 Summary

Keratocyte migration into a collagen gel matrix declines with senescence of cells in culture. EGF enhanced keratocyte migration while FN, GBD and HA had no effect on migration in this assay system. Keratocyte migration in response to EGF specifically declined with increasing keratocyte senescence suggesting that a reduction in migratory responsiveness to cytokine stimulation may occur with corneal ageing and may slow the keratocyte's response to wounding. The reduction in keratocyte migration also has implications for keratocyte colonisation of KPro skirt materials. EGF has been suggested as part of a combination therapy following corneal injury to stimulate the keratocyte repair response and offset the inhibitory side-effects of anti-inflammatory corticosteroid treatment (Woost et al, 1985). Since the migratory response to EGF declined but was not abolished in the senescent keratocyte cultures of this study EGF addition may also be a mechanism by which the inhibitory effects of senescence on keratocyte migration following corneal wounding may be reduced.

Chapter 4

Adult Keratocyte Migration into a Collagen Gel Matrix in Response to EGF

4.1 Introduction

The progression of fibroblast cultures through their replicative lifespan to senescence has been used as a model to study the effects of ageing on the fibroblast phenotype *in vivo* (Schneider & Mitsui, 1976). Such a model assumes that cell populations in dividing tissues progress through an increasing number of cell divisions with age resulting in the accumulation of senescent cells, as occurs on increasing serial passage in culture. Changes in tissue structure may then be explained in part by changes in the senescent fibroblast phenotype. If keratocytes within the corneal stroma behave as keratocytes in culture the migratory response of late passage embryonic keratocyte cultures should reflect that of adult keratocyte cultures.

Both monolayer and collagen gel assay systems have been used to show that adult dermal fibroblasts migrate more slowly than foetal dermal fibroblasts at seeding densities above $3x10^3$ cells cm^{-2} (Kondo & Yonezawa, 1992; Schor et al, 1988; Schor, 1994). Embryonic dermal fibroblast migration decreased with increasing serial passage and late passage embryonic fibroblast migration was similar to that of adult donor fibroblasts in the monolayer assay. Such results suggest that passage of embryonic dermal fibroblast cultures reflects the changes occurring in dermal fibroblast migratory capacity with age *in vivo* (Kondo & Yonezawa, 1992).

In chapter 3 serial passage of the EK1.BR embryonic keratocyte cell strain was used as a model of corneal ageing in order to measure changes in the migratory response to wounding. However, validation of the model is necessary since additional variables related to differences in adult and embryonic keratocyte phenotype may affect migration. Also, previous data comparing changes in the characteristics of young versus old donor fibroblasts and early passage versus late passage fibroblasts suggests that serial passage of fibroblasts may not be an exact measure of the effects of ageing on the fibroblast phenotype. Schneider & Mitsui (1976) compared parameters such as cell population doubling time, cell number at confluency and cell RNA and protein content. They found both

quantitative and qualitative differences in the results from skin fibroblast cultures of young and old donors when compared with those observed for early and late passage cultures of WI-38 foetal lung fibroblasts. No significant difference was observed in the cellular RNA or protein content of young and old donor dermal fibroblasts while in late passage WI-38 cultures cellular RNA and protein content were significantly increased on comparison with early passage cultures. While significant differences were observed for some parameters between young and old donor fibroblast cultures they were always much greater on comparison of early and late passage WI-38 cultures. Investigation of differences in the synthesis of collagen, FN and PGs by early versus late passage and young versus old donor dermal fibroblasts also suggest differences in some of the changes which occur in cell activity with age in culture and in dividing tissues (Takeda et al, 1992). PG and collagen synthesis declined with increasing serial passage and on comparison of young and old donor fibroblast cultures. In contrast, while detection of FN mRNA declined rapidly on serial passage of cells, levels remained high in elderly donor fibroblast cultures. These differences may be explained by the expectation that senescent fibroblasts will accumulate to a greater extent in culture than within dividing tissues with age and will exaggerate the detection of senescent associated changes in the fibroblast phenotype. However, they suggest that the interpretation of results from studies comparing early and late passage cultures should be moderated by those comparing young and old donor fibroblast activity.

Interpretation of results from wound repair studies using serially passaged embryonic cell strains as a model of ageing may also be complicated by differences in embryonic and adult fibroblast wound healing processes, unrelated to the ageing process. Foetal wounds tend to heal without leaving a scar and foetal fibroblasts secrete different levels of the proteases mediating wound remodelling (Cullen et al, 1997). Foetal dermal fibroblast migration also appears to be mediated by different regulatory factors to those involved in adult fibroblast migration (Kondo & Yonezawa, 1995). Thus, while studies using an

embryonic keratocyte cell strain at early and late passage may generally reflect the effects of ageing on keratocyte function within the cornea validation of the EK1.BR model of corneal ageing is necessary.

The longer lifespan of embryonic keratocytes and the shortage of donor corneal material available for laboratory work make the availability of the EK1.BR keratocytes an advantage to their use. Previous studies suggest that subtle changes exist in embryonic and adult dermal fibroblast characteristics and in the effects of ageing on fibroblasts in culture and within dividing tissues. In order to ascertain whether changes in the behaviour of early and late passage EK1.BRs adequately reflect those occurring in the cornea with age the following study compared adult keratocyte migration in response to EGF stimulation with that previously found for the embryonic keratocyte cell strain EK1.BR.

4.2 Materials

A time expired donor cornea was supplied by the Bristol Eye Bank.

Materials for the collagen gel assays were supplied as indicated in section 3.2. Materials cell culture and for the Ki67 assay were supplied as indicated in section 2.1.2.

Mouse anti-human anti-vimentin and mouse anti-human anti-pan cytokeratin primary monoclonal antibodies were supplied by Sigma-Aldrich Company Ltd, Fancy Rd, Poole, Dorset, BH12 4QH, UK.

4.3 Methods

4.3.1 Establishment of an Adult Keratocyte Cell Strain

The cell strain 13769(A) was initiated from the cornea of an 88 year old donor. The cornea was placed in a tissue culture dish containing media and the surrounding sclera was cut away. The cornea was cut into small fragments of tissue. The base of a 25 cm^2 tissue culture flask was moistened with 5 ml of media (MEM supplemented with 10% (v/v) FCS and 1% (v/v) P/S). The flask was inclined at an angle and tissue

fragments were placed at the top of the flask using tweezers. The flask was incubated for forty eight hours at 37°C in a humidified 5% CO_2/air incubator and was positioned at an angle to allow adherence of the tissue to the flask base. The flask was repositioned horizontally and incubation was continued for two to four weeks until an outgrowth of keratocytes was observed from the primary explant with a width of approximately 2 cm. The primary culture was passaged by trypsination as described in section 2.1.3. Trypsin was left covering the cells for twenty five minutes. Cell number was counted using a haemocytometer and cells were transferred to a 12.5 cm^2 flask and incubated at 37°C. On the second passage the number of cells present in the flask was counted and the cpd was calculated from zero. Once established the adult keratocyte cell strain was cultured in the same way as the embryonic cell strain EK1.BR. The cells were identified as keratocytes by the detection of the intermediary filament vimentin and the absence of keratin (section 4.3.3.2) (Andresen et al, 1997).

4.3.2 The Effect of EGF on Adult Keratocyte Migration into Collagen Gels

The collagen gel experiments were set up as described previously for the EK1.BR keratocytes in section 3.2. DAPI counts were made for six fields across the surface of each gel to verify an even cell distribution between control and EGF gels and between assays (Appendix 2). Mean keratocyte migration across thirty fields in each of three control and three EGF gels was compared in three separate assays using cells at early passage (cpd 4-7) and four separate assays using cells at late passage (cpd 12-15). Results were analysed using a chi-square test for statistical significance.

4.3.3 Immunocytochemistry

4.3.3.1 Immunocytochemical Detection of Ki67 Activity

The percentage of proliferating keratocytes present throughout the lifespan of the adult cell population was analysed using a Ki67 immunocytochemical assay as described previously in section 2.1.3.

4.3.3.2 Immunocytochemical Detection of Vimentin/ Cytokeratin

Adult keratocytes at 7 cpds were passaged and seeded onto coverslips in

35 mm tissue culture dishes at a density of 3000 cells cm^{-2}. The keratocyte cultures were incubated for seventy two hours at 37°C in a humidified 5% CO_2/air incubator. Media was aspirated off and the coverslips were washed three times in PBS. Cells were incubated in a 1:1 methanol:acetone fixative for four minutes and again washed three times in PBS. Coverslips were placed in a humidifying chamber with the cell surface facing upwards. One chamber was set up for the vimentin assay, one for the cytokeratin assay and one as a negative control containing only the secondary antibody. Both primary antibodies were diluted 1:20 with PBS buffer containing 1% (v/v) FCS and 0.3% (w/v) azide. 40 µl of mouse anti-human anti-vimentin antibody was pipetted onto each of the coverslips in one chamber while 40 µl of mouse anti-human anti-cytokeratin antibody was added to the coverslips in the second chamber. 40 µl of the PBS buffer was pipetted onto the coverslips in the third chamber. The cells were incubated at 4°C overnight. Each coverslip was washed ten times in each of three universal tubes containing PBS to remove the primary antibody. 40 µl of FITC-conjugated rabbit anti-mouse IgG secondary antibody was pipetted onto each coverslip and cells were incubated at 4°C overnight. The secondary antibody was removed by again washing cells in PBS followed by ten washes in distilled water. Coverslips were mounted on slides in mountant containing DAPI and viewed under fluorescent microscope in order to detect the presence of vimentin or cytokeratin within the cells.

4.4 Results

4.4.1 The Effect of EGF on Adult Keratocyte Migration into Collagen Gels

Adult keratocyte migration in response to EGF was similar at both early and late passage ($p>0.1$, 10 d.f.) (Figure 4.1). However, EGF was calculated to have a significant effect on early passage adult keratocyte migration while at late passage no significant difference in keratocyte migration was observed ($p<0.001$, 9 d.f.; $p>0.1$, 9 d.f. respectively). Surprisingly, the number of adult keratocytes migrating into both the EGF and control gels was higher than that observed for the embryonic EK1.BR keratocytes, particularly migration into the control gels which was approximately

Figure 4.1
Comparison of adult and embryonic total keratocyte migration into late and early passage EGF gels with that into control gels. Results are expressed as the mean +/- SEM.

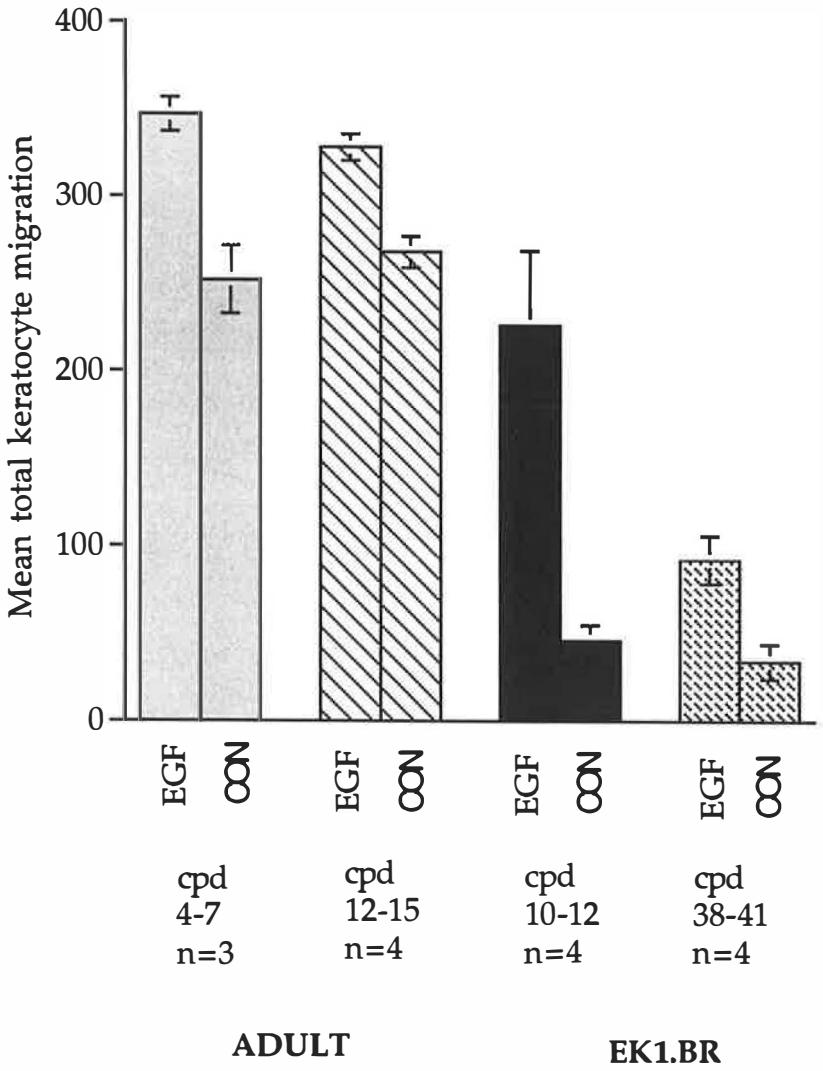

five times greater than that observed for the EK1.BRs. Early passage EK1.BR keratocyte migration in response to EGF was five times greater than that into the control gels while for adult keratocytes and late passage EK1.BRs the ratio of total keratocyte migration in the presence and absence of EGF was much smaller.

4.4.2 Immunocytochemistry

4.4.2.1 Ki67

The adult keratocyte cell strain 13769A had a much shorter proliferative lifespan than that of the EK1.BRs and senesced at 17 cpds (Figure 4.2). Senescence was indicated by the failure of cells in culture to grow to confluency and a Ki67 positive cell percentage of less than five. A general decline in adult keratocyte proliferative capacity was observed from early to late passage as for the EK1.BRs (Figure 4.3). However, the percentage of Ki67 positive cells dropped much more rapidly. The maximum Ki67 positive value obtained from early passage cultures was lower than that for the EK1.BR cultures at 56% rather than 71% suggesting a larger non-cycling fraction within the initial adult keratocyte cell culture. A regression line was fitted to the data in figure 4.3 and indicated a slope of -3.1.

4.4.2.1 Vimentin/Cytokeratin

Vimentin was strongly detected in the adult keratocyte cultures while no reaction with the antibody against cytokeratin was observed (Figure 4.4). Since cytokeratin is found in corneal epithelial cells but not in stromal keratocytes and vimentin is present in cells of mesenchymal origin the cell cultures were identified as uncontaminated adult keratocytes.

4.4 Discussion

The observed increase in adult keratocyte migration is in contrast to previous studies using dermal fibroblasts which found that adult fibroblast migration was less than that of foetal fibroblasts. Previous studies employed different experimental regimes to examine dermal fibroblast migration and were not specifically considering the effects of EGF on cell migration (Schor et al, 1988; Kondo & Yonezawa, 1992).

Figure 4.2
Cumulative growth curve for the adult keratocyte cell strain 13769A.

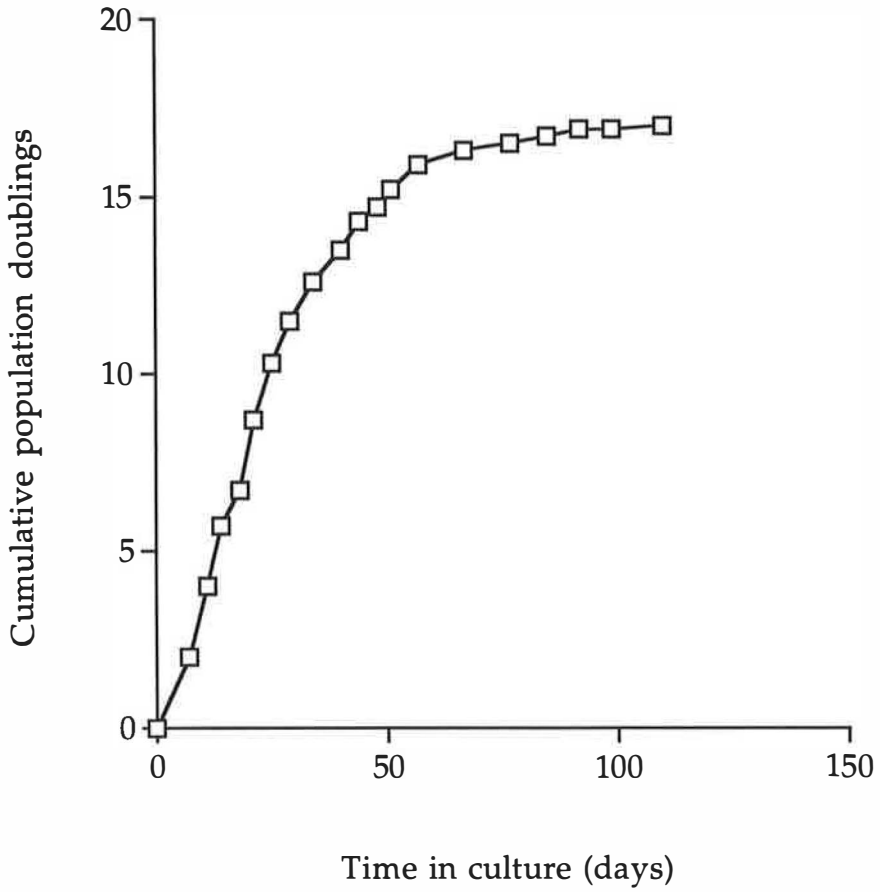

Figure 4.3
Changes in percent Ki67 positive adult keratocytes on increasing serial passage.

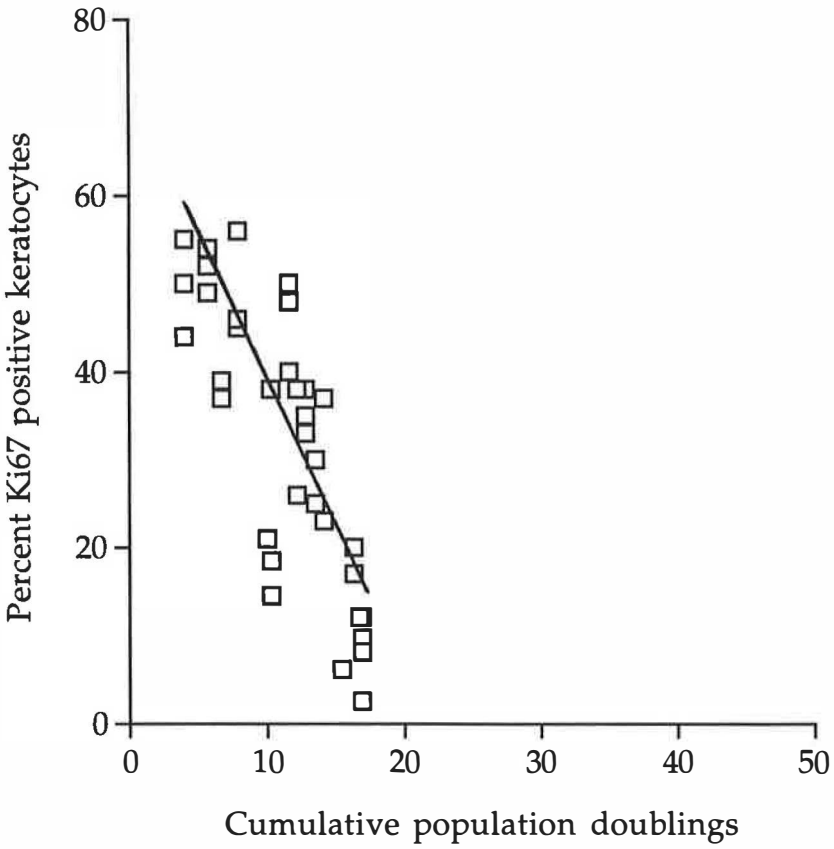

Figure 4.4
Characterisation of the adult keratocyte cell strain by the detection of the intermediary filament vimentin. Keratocyte cultures stained (a) positive for vimentin and (b) negative for cytokeratin.

(a)

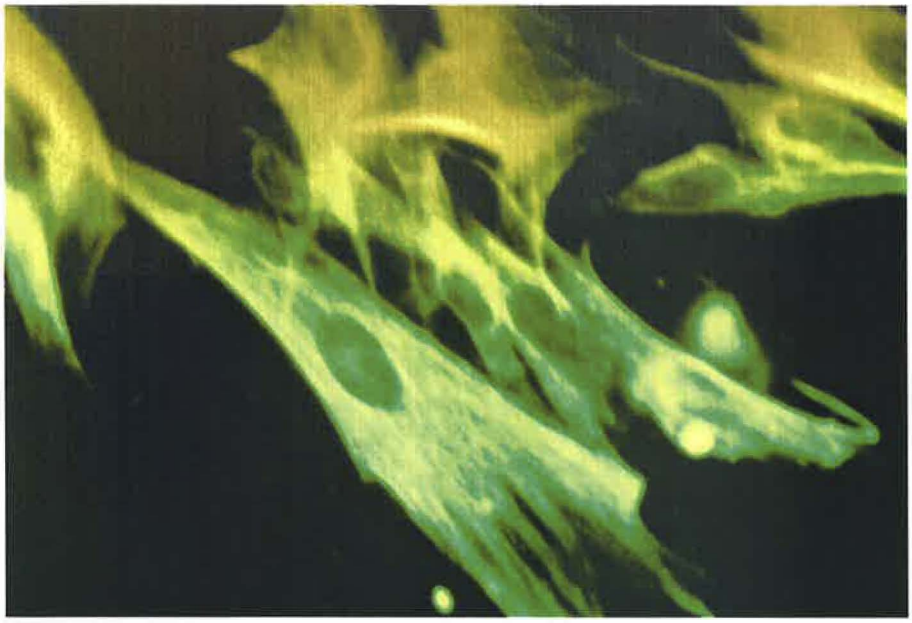

(b)

However, it is still surprising that the migratory capacity of adult keratocytes was greater than that of the embryonic keratocytes since conditions were the same for the two sets of experiments. Variability between keratocyte cell strains is unlikely to fully explain the observation since preliminary results for other adult keratocyte cell strains suggest a similar migratory pattern in these keratocytes also.

Results may be influenced by the time at which analysis takes place. al-Khateeb et al (1997) analysed dermal fibroblast migration into a collagen gel wound model over four to twelve days and found that child donor fibroblasts migrated significantly more rapidly than adult donor fibroblasts. The present study measured keratocyte migration after only three days in order to limit the potential effects of proliferation on cell numbers. A longer incubation period prior to analysis may have distinguished more accurately differences in long-term migratory capacity. However, it is unlikely to explain the marked increase in adult keratocyte migration into the control gels when compared with that of the EK1.BRs.

It has previously been shown that fibroblasts exhibit changes in growth factor dependency for migration as they progress from the embryonic to adult state (Kondo & Yonezawa, 1995). It may be that adult keratocytes have undergone a change in growth factor dependency from EGF to another factor, required in smaller amounts for enhancement of cell migration. The large number of adult keratocytes migrating into the control gels may then be explained by the presence of this factor in amounts sufficient to enhance keratocyte migration in the low serum media. In chapter 3 the possibility that EK1.BRs secrete an autonomous migration stimulating factor which maintains control cell migration in the absence of serum was discussed. Previous studies have indicated that foetal but not adult dermal fibroblasts produce an autonomous migration stimulating factor which enables them to migrate independently of serum stimulation (Schor et al, 1988). However, the high levels of adult keratocyte migration into the control gels in the present study suggest that adult rather than embryonic keratocytes are

more likely to secrete an autonomous factor which supports migration in minimal serum. The possibility may be tested by analysis of the effects of serum free media conditioned by adult keratocyte cultures on keratocyte migration.

It has also been observed that adult dermal fibroblast migration significantly increases in response to EGF with little change in foetal fibroblast migration (Ellis et al, 1997). These results are in marked contrast to those for the adult and embryonic keratocyte cultures. EK1.BR keratocyte migration was significantly increased in response to EGF while adult keratocyte migration in response to EGF was limited suggesting that results may additionally reflect differences in the responsiveness of dermal and corneal fibroblasts. Variability in the behaviour of fibroblasts from different tissue types has previously been established in studies comparing dermal and lung fibroblast activity (Kondo & Yonezawa, 1992).

While total adult keratocyte migration was greater than that for the EK1.BRs a decline in migratory response to EGF, similar to that seen for late passage EK1.BRs, was observed. Migration of adult keratoyctes into the control gels was approximately five times higher than that observed for embryonic keratocyte migration into control gels so that although the total number of adult keratocytes migrating into the gels was higher the ratio of EGF to control gel migration was low. No significant difference in the effect of EGF on adult keratocyte migration was observed from early to late passage suggesting that adult keratocytes already exhibit a reduction in migratory responsiveness to EGF at early passage and parallel the behaviour of late passage EK1.BRs in this respect so that no further reduction in migratory response to EGF is detected.

The Ki67 data suggests that adult keratocytes also parallel the proliferative capacity of late passage EK1.BRs. The rapid decline in Ki67 positivity found for adult keratocytes from 4 to 17 cpds appears to reflect that seen for late passage EK1.BRs from 30 to 40 cpds (Figure 2.1). The slope of the regression line for the adult Ki67 data was -3.1 which tends

towards that of the second regression line fitted in figure 2.3 for the late passage EK1.BRs rather than to the slope of the regression line fitted to the early passage data. Results support the premise that the serial passage of EK1.BR keratocytes may be used as a model to reflect the proliferative lifespan of keratocytes in the cornea.

Results indicate that the responses of keratocytes aged in culture reflect some but not all of the changes in keratocyte activity occurring in the cornea with age. Total adult keratocyte migration was greater not less than total EK1.BR keratocyte migration at early passage. However, a loss of migratory responsiveness to EGF, similar to that observed for late passage EK1.BRs, was found. The proliferative capacity of adult keratocytes also appeared to reflect that of late passage EK1.BR keratocytes. The increased levels of migration may be due in part to differences in growth factor regulation of the embryonic and adult keratocyte migratory response. The analysis of migration in the present study may also have been carried out too early to adequately detect changes in the migratory characteristics of adult keratocytes. The decline in migratory response to EGF previously observed for late passage embryonic keratocytes does appear to be emulated by adult keratocytes suggesting that changes in growth factor responsiveness on serial passage of embryonic keratocytes is representative of similar changes occurring with age in the cornea. The reduced proliferative lifespan of the adult keratocyte cultures on comparison with the EK1.BR cultures also suggests that keratocyte turnover and the potential accumulation of senescent keratocytes occurs within the cornea over time.

Chapter 5

EK1.BR Contraction of a Collagen Gel Matrix

5.1 Introduction

Wound contraction is an integral part of the corneal response to wounding. The initial inflammatory response is followed by cell migration, granulation tissue formation and contraction of the wound margins. The scar which forms then undergoes further remodelling leading to scar resolution (Mutsaers et al, 1997). Wound contraction is mediated by activated fibroblasts or myofibroblasts which can be identified by the presence of microfilament bundles and the development of α-smooth muscle actin in their cytoplasm (Desmouliere, 1995). In the cornea myofibroblasts differentiate from keratocytes adjacent to the wound and appear to line up parallel to the wound margin, linked by gap junctions, to contract the wound (Jester et al, 1995). Myofibroblast differentiation and corneal fibroblast contraction are promoted by TGF–β which is secreted by inflammatory mediators, corneal epithelial cells and stromal fibroblasts within the wound (Kurosaka et al, 1998; Moulin et al, 1998; Jester et al, 1997) while IFNγ inhibits contractile activity (Moulin et al, 1998; Pakkar et al, 1998). Contraction involves an increase in the expression of integrin receptors $\alpha_1\beta_1$ and $\alpha_2\beta_1$ on the myofibroblast cell surface (Carver et al, 1995; Riikonen et al, 1995) and may involve increased tyrosine mediated phosphorylation of focal adhesion kinase and MAPK (Zent et al, 1998; Broberg & Heino, 1996). Following wound closure myofibroblasts disappear from the scar. They may return to quiescence or disappear as a result of apoptosis as occurs during the formation of dermal scar tissue (Desmouliere, 1995).

Fibroblast contraction of the collagen matrix has been established as a model of fibroblast wound contraction (Bell et al, 1979). Fibroblasts within the collagen matrix appear to behave like wound fibroblasts *in vivo* and produce an increase in collagen fibril density by integrin mediated attachment of cells to the collagen matrix. Reorganisation appears to be serum dependent and involve changes in the structure of pre-existing collagen fibrils rather than degradation and synthesis of a new collagen matrix (Guidry & Grinnell, 1985; Yamato et al, 1995).

Contraction requires cell attachment and spreading and may be induced by the forces generated on intracellular F-actin/ αSM-actin interaction with matrix bound fibronectin via integrin receptors. Stephens et al (1997) provide evidence to suggest that peripheral myofibroblast alignment and the formation of continuous integrin linked actin cables within the lattice contribute to gel contraction. The exact mechanisms by which fibroblasts contract the matrix are unclear. Locomotion based theories suggest that contraction is primarily produced by the rearrangement of collagen fibrils as fibroblasts migrate through the matrix (Harris et al, 1981; Ehrlich & Rajaratnam, 1990). However Yamato et al (1995) found condensed collagen fibrils only in regions adjacent to but not distant from lattice fibroblasts. If fibril condensation was a result of cell migration regions of condensation would be expected in cell sparse areas previously populated by fibroblasts prior to migration. Instead collagen contraction through continuous cycles of pseudopodal protrusion, integrin mediated fibril attachment followed by pseudopodal withdrawal by relatively stationary fibroblasts was suggested. Roy et al (1997) found that the release of forces generated by pseudopodal extension and retraction, occurring as cells migrate, was inconsistent with the forces required to produce sustained contraction of a collagen matrix also suggesting that collagen gel contraction is not primarily a result of fibroblast locomotion.

Disruption of the cell to cell and cell to matrix interactions which mediate the repair response can lead to excessive tissue deposition, contractile activity and hypertrophic scar formation or to an inadequate response and ulceration (Krieg, 1995). Investigation of changes in myofibroblast remodelling and contractile activity in the cornea are particularly important since here excessive scarring or ulceration may lead to visual impairment. A number of changes in the senescent fibroblast response to matrix signalling have been reported which may affect the ability of senescent cells to contract the matrix. Conflicting results have previously been obtained using a collagen gel contraction assay which showed an increase, decrease and little difference in the contractile ability of late passage dermal and lung fibroblast cultures

when compared to early passage fibroblast cultures (Gibson et al, 1989; Yamato et al, 1992; Bell et al, 1979). Kono et al (1990) found that dermal fibroblasts from young donors (0 to 15 years old) contracted a collagen gel matrix to a greater extent than fibroblasts from donors of all other age groups (adolescent, middle aged and elderly) at early passage but not at late passage suggesting that an increase in senescent cells may hinder contractile ability. Since previous results have been inconsistent and the ability of corneal fibroblasts to produce appropriate levels of wound contraction is vital to the maintenance of good visual quality following corneal wounding the following study sought to compare the ability of early and late passage EK1.BR keratocytes to contract a collagen matrix.

5.2 Materials

Materials were the same as those used for the collagen gel assays in section 3.2.

5.3 Method

EK1.BR keratocytes were passaged as previously described in section 2.1.3. Three universal tubes containing $2x10^6$, $8x10^5$ and $2x10^5$ cells were centrifuged at 400g and the cells were resuspended in 1 ml of MEM containing 10% (v/v) FCS and 1% (v/v) P/S. 4 ml of a 1.75 mg ml^{-1} collagen gel solution was made up by mixing 2.33 ml vitrogen collagen gel solution with 1.67 ml of a vitrogen diluter solution. 700 µl of collagen gel solution was added to each of four universal tubes. 50 µl of appropriate cell suspension was added to each universal tube to give three collagen gel solutions containing $1x10^5$, $4x10^4$, and $1x10^4$ cells and one control solution without cells. Two 35 mm tissue culture dishes at each cell concentration and two control gels were set up for each assay. 100 µl of cell containing collagen gel solution was pipetted onto the centre of each 35 mm tissue culture dish and left in the warm room at 37°C for one hour to set. 2 ml of media was added to each dish and the height of each of the eight gels was measured using the depth scanning device of a confocal microscope. The depth scanning device was zeroed

on the base of each dish at the centre of each gel. The height was then measured by raising the focus of the microscope through the grainy matrix of the gel until the interface between the gel and media was apparent. The gels were incubated in a humidified 5% CO_2 / air incubator at 37°C and the gel heights were measured daily for six days. The assays compared the ability of early passage cells from 18 to 24 cpds and late passage cells from 42 to 46 cpds to contract a collagen gel matrix. Four separate contraction assays using early passage keratocytes and three contraction assays using late passage keratocytes were carried out. Each assay included two gels at each cell concentration and two control gels. Results were analysed using the student t-test for statistical significance.

5.4 Results

EK1.BR keratocytes produced a steady decline in the height of the collagen gels over the six day period. Gel contraction was greatest between day zero and day one and depended on the number of cells present in the gels. Gels containing $1x10^5$ cells produced a greater level of gel contraction at all points of measurement than gels containing $4x10^4$ cells and $1x10^4$ cells (Figure 5.1 and 5.2). On days zero and one keratocytes were rounded and were beginning to extend spindle like protrusions into the matrix. From day two onwards cells tended to elongate and flatten out, exhibiting the normal spindle shaped morphology of the fibroblast. No significant difference was observed between the ability of early and late passage cells to contract the collagen gels ($p=0.97$).

5.5 Discussion

The ability of EK1.BR keratocyte cultures to contract a collagen matrix appears to be unaltered at late passage suggesting that the mechanisms involved in matrix contraction are relatively unaffected by cell senescence. Results are in contrast to the results of Yamato et al (1992) using lung fibroblasts and in general agreement with the results of Bell et al (1979) using dermal fibroblasts. Bell et al (1979) found that late passage fibroblasts could contract a collagen gel matrix containing 0.57

Figure 5.1
Early passage EK1.BR keratocyte contraction of a collagen matrix. 4 gel contraction assays were carried out with 2 gels at each cell concentration. Results are expressed as the mean gel height +/- SEM (n=8).

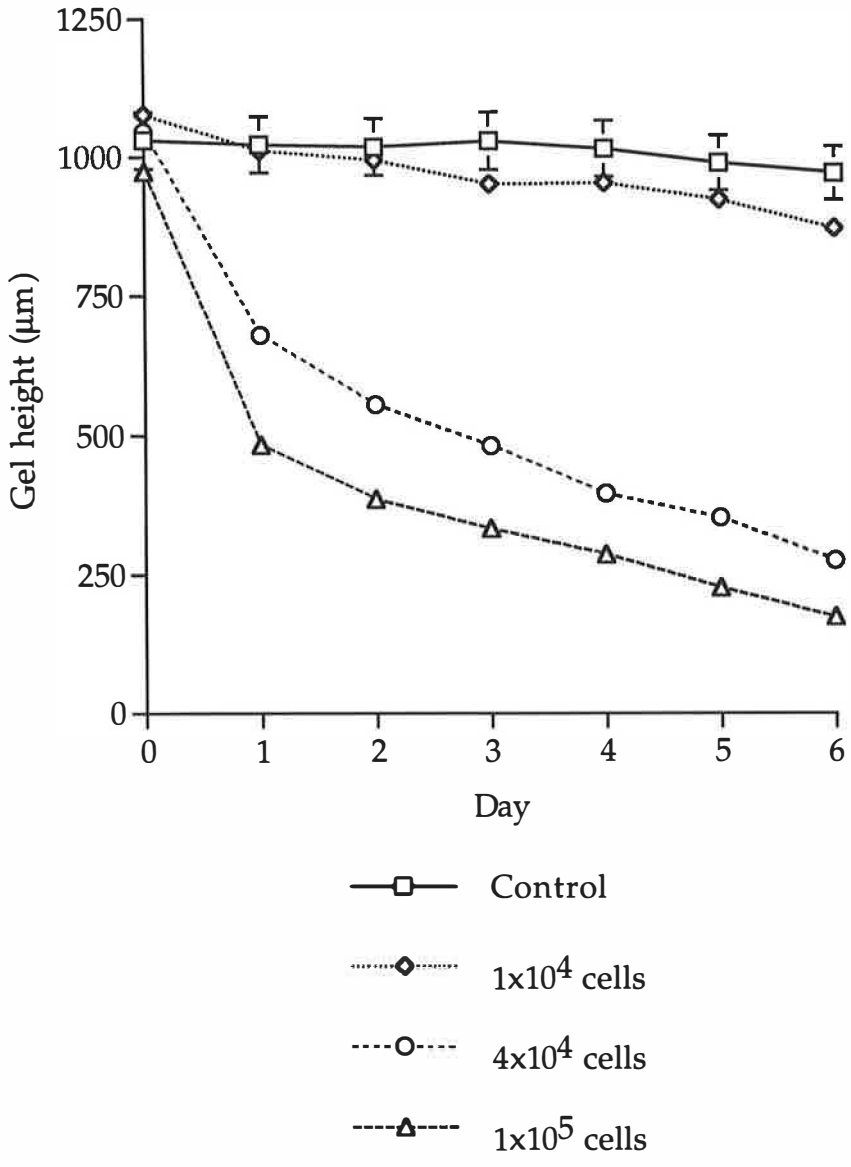

Figure 5.2
Late passage EK1.BR keratocyte contraction of a collagen matrix. 3 contraction assays with 2 gels at each cell concentration were set up. Results are expressed as the mean gel height +/- SEM (n=6).

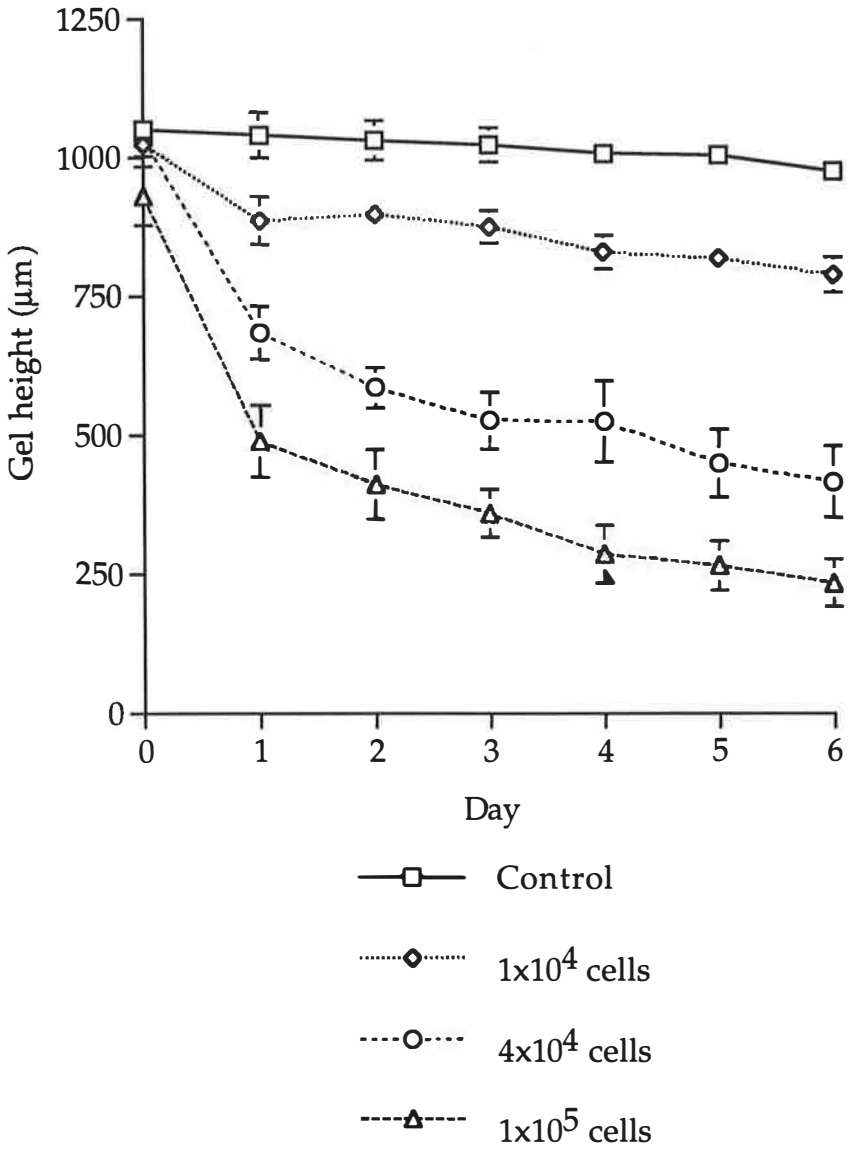

mg ml^{-1} protein to a similar, if not greater extent than early passage fibroblast cultures. The current study used a collagen gel concentration of 1.75 mg ml^{-1} while Yamato et al (1992) used a concentration of 3 mg ml^{-1}. Failure to identify differences in cell contractility in the present study may be due to the use of a lower collagen concentration since the lower concentration of collagen fibrils may require less force to produce a contractile response. Differences in contractile ability may be better observed using a denser collagen matrix since greater force is probably necessary to contract a denser collagen lattice to the same extent.

Contraction appears to require an integrated cellular response including increased $\alpha 1\beta 1$ and $\alpha 2\beta 1$ integrin receptor expression and fibronectin mediated cell attachment to the cell lattice. Attachment is via integrin receptors linked to α-actin microfilaments which undergo reorganisation for the generation of contractile force. Changes in actin structure, in FN synthesis and in FN's ability to mediate cell adhesion have been reported in senescent fibroblasts (Wang & Gundersen, 1984; Chandrasekhar et al, 1983). However, while these changes may affect fibroblast motility the processes involved in myofibroblast differentiation and generation of contractile force may be less affected so that no change in contractile ability is revealed by the collagen matrix contraction assay. Results also suggest that gel contraction can not fully be explained as a product of cell migration through the matrix since, in chapter 3 late passage keratocytes show a decline in migratory capacity within a collagen matrix (Sandeman et al, 1998). If contraction is a result of migration a subsequent decline in contractile ability would be expected.

It has been suggested that age related differences in healing following corneal surgical procedures occur as a result of a slower corneal response to wounding (Dutt et al, 1994). No difference in the contractile ability of early and late passage keratocyte cultures was observed in the present study suggesting that a decline in the ability of keratocytes to induce wound contraction does not contribute to this change.

Chapter 6

Ek1.BR Keratocyte Secretion of the Gelatinases

6.1 Introduction

The MMPs are central to the process of connective tissue matrix remodelling and are involved in a wide range of tissue degradation and resorption processes including wound healing, angiogenesis and bone growth (Matrisian, 1994; Woessner, 1994). Following injury damaged ECM fragments are catabolised by activated MMPs. MMP suppression follows so that a new collagen matrix can be rebuilt. Numerous interacting regulatory mechanisms ensure that MMP activity is appropriate to the requirements of a specific remodelling process. Cytokine mediated fibroblast secretion of specific MMP pro-enzymes and activating proteases is carefully balanced by secretion of TIMPs and inhibitory cytokines. The failure of these regulatory processes can result in elevated MMP activity and uncontrolled tissue breakdown. Such activity has been implicated in a number of disease processes including the degradation of articular and periarticular cartilage associated with rheumatoid arthritis and in the basement membrane dissolution associated with tumour metastasis (Matrisian, 1994; Drummond, 1996). MMP inhibitors are subsequently being developed as therapies in the treatment of these conditions (Zask et al, 1996).

In the cornea control of the remodelling process is particularly important since stromal collagen fibrillar structure must be restored in order to maintain corneal transparency and inadequate MMP remodelling can result in corneal haze and scarring. Excessive MMP activity has been implicated in the pathology of corneal ulceration and keratoconus (Smith & Easty, 1995; Fini et al, 1992[b]). The deposition of scar tissue and corneal thinning which occur in keratoconic corneae has been associated with increased MMP-2 activity in some studies (Smith et al, 1995). Other studies have shown no change in gelatinase levels or in the type of enzyme synthesised and suggest that altered protease inhibitor activity may explain the reported increase in gelatinase activity (Fini et al, 1992[b]). MMP inhibitors have been successfully used to limit corneal ulceration indicating that MMP overactivity is a contributing factor (Gray & Paterson, 1994). The process appears to involve enhanced MMP-9 secretion and basement membrane destruction (Matsubara et al, 1991).

Epithelial interaction with stromal cells stimulates collagenase expression suggesting that following basement membrane dissolution epithelial cell invasion of the stroma leads to further overexpression of collagenase and the progression of corneal ulceration (Johnson-Muller & Gross, 1971). In these cases MMP overactivity may result in structural disruption and prevent the cornea from functioning normally.

Changes occur in fibroblast MMP and TIMP expression with age which tend to shift the balance of processes involved in ECM remodelling towards tissue degradation. The synthesis and secretion of collagenase and stromelysin by late passage fibroblasts (Millis et al, 1992) and of collagenase by elderly donor fibroblasts (Sottile et al, 1988) were increased while levels of TIMP-1 mRNA were lower than those observed from early passage cultures and in cultures of young donor fibroblasts. A two fold increase in MMP-2 mRNA was observed in late passage fibroblast cultures while MMP-2 expression and activity remained similar to that of early passage cultures. In addition, an increase in TIMP-2 mRNA and protein expression was observed (Zeng & Millis, 1994). These changes appear to be produced by alterations in cell responsiveness to factors normally regulating MMP expression. Early passage fibroblast cultures respond to serum stimulation by increasing collagenase and TIMP expression while late passage fibroblast cultures constitutively express high levels of collagenase, lower levels of TIMP-1 and are unresponsive to serum stimulation (West et al, 1989).

Changes in the expression of MMPs by late passage fibroblast cultures may be due in part to a decline in TGF-β activity. Early passage fibroblast cultures respond to TGF-β by a reduction in collagenase and stromelysin expression, an increase in gelatinase MMP-2 expression and an increase in TIMP-1 (Girard et al, 1991). In late passage cultures a TGF-β neutralising antibody produced no effect on MMP expression while at early passage a significant increase in collagenase and stromelysin expression and a decrease in TIMP-1 expression had been observed. Results suggest that a decline in TGF-β activity may contribute to the increased levels of MMP secretion observed in late passage cultures

(Zeng et al, 1996). Edwards et al (1996) also found that TGF-β did not repress collagenase, stromelysin and gelatinase MMP-9 mRNA synthesis in late passage human fibroblasts but failed to show any change in the expression of these MMP transcripts. A decline in transcription factor AP1 and SRF DNA binding activity in late passage cells was also observed suggesting that changes in signalling pathways rather than TGF-β activity may be responsible for the diminished repression of MMP synthesis by TGF-β. Fini & Girard (1990)[b] observed that while PMA upregulated the expression of the gelatinase MMP-2 and stimulated the synthesis of collagenase, stromelysin and the gelatinase MMP-9 in primary corneal fibroblasts MMP-2 expression was selectively inhibited by PMA in passaged cells with continued upregulation of the other MMPs. Changes in specific MMP expression in response to PMA stimulation suggest that individual MMPs are independently regulated and that the interaction of pathways coordinating MMP expression in response to cell stimulation may be altered with passage of cells in culture.

MMP-2 (gelatinase A) is the only MMP secreted by quiescent stromal keratocytes and is upregulated with the induction of MMP-9 (gelatinase B) and collagenase following injury (Brown & Weller, 1970; Fini et al, 1992[a]; Azar et al, 1996). Any changes in MMP-2 expression following keratocyte senescence will therefore adversely affect corneal functioning and repair. While previous studies using human fibroblasts have associated upregulation of collagenase, stromelysin and the altered responsiveness of these MMPs to cytokine stimulation with senescence no change in MMP-2 activity was observed. The current study sought to investigate the activity of gelatinases secreted by the embryonic keratocyte cell strain EK1.BR and any changes in gelatinase activity occurring with senescence of these cells in culture.

The gelatinases secreted by the EK1.BR keratocytes were identified by zymographic detection of gelatinase activity. Zymography utilises sodium dodecyl sulphate polyacrylamide gel electrophoresis (SDS-PAGE)

so that protein samples are denatured and are separated on the basis of size. The gels also incorporate gelatin as a substrate for the gelatinases. Once the SDS is removed by washing the partially renatured enzymes digest the gelatin substrate. The position of the gelatinases is revealed as a clear band surrounded by a purple background following coomassie blue staining and destaining of the gels. Partial quantification is possible using a scanning densitometer to assess band intensity.

6.2 Materials and Equipment

Ammonium sulphate, HCl, $CaCl_2$, bovine serum albumin, Bromophenol Blue and glycerol were supplied by Sigma-Aldrich Company Ltd, Fancy Rd, Poole, Dorset, BH12 4QH, UK.

TRIS and Triton X-100 were supplied by MERK Ltd, Hunter Boulevard, Magna Park, Lutterworth, Leics, LE17 4XN, UK.

The dye reagent for the total protein assay, 40% Bis-acrylamide, gelatin, ammonium persulphate, TEMED, SDS, a high molecular weight SDS-PAGE marker, glycine and a coomassie brilliant blue staining and destaining kit were supplied by BIO-RAD Laboratories Ltd, Bio-Rad House, Maylands Avenue, Hemel Hempstead, Hertfordshire, HP2 7TD, UK.

Sorvall RC-5B refrigerated, superspeed centrifuge with an SS-34, 8 place rotor supplied by DuPont (UK) Ltd., Stevenage, Hertfordshire, UK.

Titertek multiscan plus MK11 plate reader (type 314) supplied by Flow Laboratories Ltd., PO Box 17, Second Avenue, Industrial Estate Irvine, Ayrshire, Scotland, UK.

ChemiImager™ 4000, low light imaging system supplied by Flowgen, Lynn Lane, Shenstone, Lichfield, Staffordshire, WS14 0EE, UK.

Mini-PROTEAN II electrophoresis cell supplied by BIO-RAD Laboratories Ltd, Bio-Rad House, Maylands Avenue, Hemel Hempstead,

Hertfordshire, HP2 7TD, UK.

6.3 Methods

6.3.1 Ammonium Sulphate Protein Precipitation

EK1.BR keratocytes were cultured as described in section 2.1.3. The proteins secreted by early and late passage cultures were isolated by ammonium sulphate protein precipitation. The small, highly charged ammonium and suphate ions bind to water and reduce the solubility of proteins when present in high concentrations, resulting in precipitation. Early passage cultures from 14 to 18 cpds and late passage cultures from 44 to 47 cpds were used. EK1.BR keratocytes were cultured in a humidified 5% CO_2/ air incubator at 37°C in 175 cm^2 tissue culture flasks containing MEM with glutamax supplemented with 10% (v/v) FCS and 1% (v/v) P/S. Once the keratocytes had grown to confluency the media was replaced with 25 ml of serum free media and the culture was incubated for a further four days. The conditioned media was then removed from the flasks and placed in a beaker on a magnetic stirrer. Saturated ammonium sulphate solution (761 g in 1 liter of distilled water) was added dropwise to the media to give a final concentration of 70% (w/v) (138 ml saturated ammonium sulphate solution added to 12 ml conditioned media). The solution was stored for a minimum of eighteen hours at 4°C and then centrifuged at 20 000g for sixty minutes at 4°C. A minimum of four 35 ml centrifuge tubes containing solution were spun down for each sample. Half of the resulting pellets were resuspended in TRIS-HCl sample buffer containing 10% (v/v) glycerol and 1% (v/v) SDS for zymography and half were resuspended in TRIS-HCl buffer at pH 6.8 for analysis of total protein content (see Appendix 1 for buffer recipes). Samples were stored at -20°C prior to analysis.

6.3.2 Total Protein Assay

The Bradford protein assay was used to calculate the protein concentration of each sample. The assay is based on a change in the absorbence maximum of the coomassie brilliant blue dye from 465 nm to 595 nm when protein binding occurs (Bradford, 1976). A standard curve of optical density against increasing protein concentration was

established for each protein sample using serial dilutions of bovine serum albumin (BSA). A stock solution of 500 μg ml^{-1} BSA (solution A) was prepared by adding 50 μl of 10 mg ml^{-1} initial stock BSA to 950 μl of TRIS buffer. 20, 40, 60, 80, and 100 μg ml^{-1} solutions of BSA were prepared by dilution of the 500 mg ml^{-1} stock with 1M TRIS buffer, pH 6.8 (Table 6.1). Samples underwent a 1 in 5 dilution with buffer to fit on to the standard curve. 50 μl of each standard solution and diluted sample was pipetted in triplicate into the wells of a ninety six well microtitre plate. The buffer solution was used as a negative control. A coomassie blue based BIORAD dye reagent concentrate underwent a 1 in 5 dilution with distilled water. 200 μl of the dye was added to each well. Dye absorbence was read at 595 nm. The mean absorbence of the negative control was subtracted from the mean absorbence for each standard/sample. Absorbence values for each standard dilution were used to plot a standard curve from which the sample protein concentrations were calculated (Appendix 3). The total protein secreted by eleven early passage keratocyte cultures (cpd=14-18) was compared with the total protein secreted by eleven late passage cultures (cpd=44-47) and analysed for statistical significance using the student t-test.

Stock solution μl	TRIS Buffer μl	Concentration μg/ml
100	400	100
80	420	80
60	440	60
40	460	40
20	480	20

Table 6.1: Dilutions of stock BSA for preparation of a standard protein concentration curve

6.3.3 Zymography

6.3.3.1 Gel Preparation

SDS-PAGE was carried out using a BIORAD Mini-PROTEAN II electrophoresis cell. Two large and two small glass gel casting plates and four spacers were cleaned using 70% (v/v) alcohol. Two glass plate sandwiches were assembled by placing a spacer along both short sides of a large glass plate overlaid by a small glass plate. Each was slotted into a clamp assembly, held in place by tightening the four clamp screws then transferred to the casting slots for gel pouring. A 40% bis-acrylamide solution was used to prepare an 8% running gel and a 4% stacking gel. The running gel was prepared by first adding 5.8 ml 1M TRIS-HCl at pH 8.8 and 5.6 ml sterile water to 3.2 ml 40% bis-acrylamide. The solution was mixed with 16 mg of gelatin, heated to dissolve the gelatin and degassed under vacuum for fifteen minutes. 150 µl of 10% (w/v) SDS, 400 µl of ammonium persulphate (10 mg ml^{-1}) and 20 µl of TEMED were then added to the solution. Fresh ammonium persulphate solution was made up just prior to each gel preparation. The gel solution was pipetted between the glass plates to a level marked 2 cm below the top of the large plate. The solution was overlaid with butanol and left to polymerise for forty five to sixty minutes. The stacking gel was prepared by mixing 600 µl of 1M TRIS-HCl at pH 6.8, 480 µl 40% bis-acrylamide, 3.6 ml sterile water with 48 µl of 10% (w/v) SDS. The solution was degassed for fifteen minutes. The butanol overlaying the running gel was removed and the surface of the gel was washed with sterile water. 200 µl of ammonium persulphate and 10 µl of TEMED were added to the stacking gel solution. A comb was placed between the glass plates and the stacking gel solution was pipetted between the comb teeth until no air bubbles remained and the solution covered the area beneath the comb. The stacking gel was allowed to polymerise for forty five minutes.

6.3.3.2 Sample Loading

500 ml of fresh running buffer was prepared by a 1 in 10 dilution of a stock solution of 72.1 g glycine and 15.1 g TRIS in 500 ml sterile water. 10% SDS was added to give a final SDS concentration of 0.1% (w/v). The

clamp assemblies containing the polymerised gels were transferred from the casting slots to the buffer chamber. The buffer chamber was filled with running buffer and the combs were removed from the gels. Markers and samples were loaded into the gel wells using a 10 µl syringe. A high range molecular weight standard was diluted 1 in 20 in bromophenol blue (0.0025% w/v) containing sample buffer and heated for two minutes at 95°C prior to loading. 1 µg and 0.5 µg samples from late passage and early passage cultures were run on the same gel. Gels were run at 80 V for two hours.

6.3.3.3 Detection of Gelatinase Activity

The gels were removed from the glass plates, washed with sterile water and incubated in 2.5% (w/v) Triton X-100 for thirty minutes at 37°C. The Triton X-100 solution was removed and the gels were incubated overnight in 0.05M TRIS-HCl at pH 7.4 containing 5mM $CaCl_2$ at 37°C. The buffer solution was removed, gels were overlaid with coomassie blue staining solution and left on a shaker set at 100 rpm for two to four hours at room temperature. The staining solution was removed and destaining solution was added (25 ml methanol, 10 ml glacial acetic acid and 65 ml distilled water). The gels were left on the shaker at 100 rpm and the destain solution was changed at regular intervals until white bands, indicating gelatinase activity and blue marker bands were apparent. Since MMP activity requires the presence of calcium and gelatinase activity is inhibited by thiol reagents, one assay was run in which one of the two gels was incubated overnight in buffer containing mercaptoacetic acid and a second assay was run in which one of the two gels was incubated overnight in calcium free buffer. Gelatinase activity was analysed by densitometry. Late passage and early passage 100 µg ml^{-1} protein samples were compared on each zymogram. The density of the white bands resulting from gelatinase activity in the two samples was expressed as a percentage of the total density of both bands (Appendix 4.1). The eight zymograms with paired data for late passage and early passage keratocyte gelatinase activity were analysed for statistical significance using Wilcoxon's signed rank test. IDV values, measured

from the zymograms as the sum of all pixel values after background correction, were used as a measure of gelatinase activity to express early passage gelatinase activity as a percentage of late passage gelatinase activity (Appendix 4.2). Units of gelatinase activity per 10^6 cells were calculated for the eleven protein samples obtained from early passage keratocyte cultures and were compared with those calculated from the eleven protein samples obtained from late passage keratocyte cultures using the Mann Whitney-U test for statistical significance (Appendix 4.3).

6.4 Results

6.4.1 Total Protein Concentration

The mean concentration of proteins secreted from early and late passage keratocyte cultures was similar. The mean protein concentration of conditioned media extracted from early passage cultures was 283.5 $\mu g\ ml^{-1}$ +/- 28.86 $\mu g\ ml^{-1}$(SEM, n=4) while that of conditioned media extracted from late passage cultures was 278.4 $\mu g\ ml^{-1}$ +/- 14.4 $\mu g\ ml^{-1}$ (SEM, n=5). However, when normalised to cell number using the haemocytometer counts obtained on passage of cell cultures the concentration of proteins secreted by late passage keratocyte cultures was significantly greater than that secreted by early passage cells ($p<0.01$, n=11) (Appendix 3). Late passage keratocytes secreted 179 $\mu g\ ml^{-1}$ +/- 15 $\mu g\ ml^{-1}$ total protein per 10^6 cells compared with the 85 $\mu g\ ml^{-1}$ +/- 8 mg ml^{-1} secreted by early passage cells (Figure 6.1). A decrease in saturation density was observed at late passage. Cell counts, made using a haemocytometer, indicated that a confluent 175 cm^2 flask of early passage keratocytes contained a mean of $3.5x10^6$ cells (n=4) while a confluent flask of late passage keratocytes contained a mean of $1.6x10^6$ cells (n=5) (Appendix 3).

6.4.2 Zymography

The distance migrated by the molecular weight markers was used to construct a calibration curve by which the molecular weights of the

Figure 6.1
Late passage EK1.BR keratocytes secrete more total protein per cell.

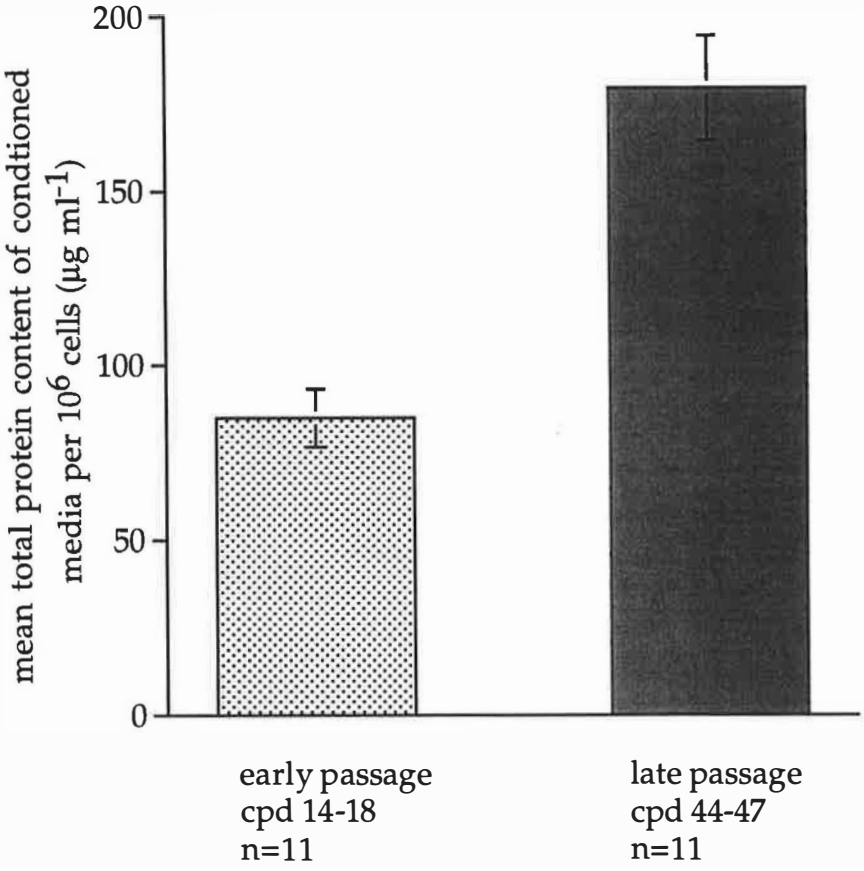

sample gelatinases could be calculated (Figure 6.2). Gelatinase activity was observed at a molecular weight of 70 KDa, approximating that previously found for the gelatinase MMP-2 (Azar et al, 1996; Fini & Girard, 1990[a], Smith et al, 1995). A second minor band at a slightly lower molecular weight was also present on some of the zymograms (Figure 6.3). Further gelatinase activity was observed at molecular weights of greater than 110 KDa. Addition of mercaptoacetic acid to the overnight zymogram incubation buffer or exclusion of calcium from the buffer inhibited enzyme activity so that no white bands on the zymograms were observed. Since MMPs are calcium dependent and gelatinase A but not collagenase or stromelysin is inactivated by thiol reagents (Smith et al, 1995) the MMP activity observed on the zymograms was identified as that of gelatinase A (MMP-2).

Densitometric analysis of gelatinase activity indicated that more gelatinase activity was present per mg of protein in media conditioned by early passage keratocytes than in media conditioned by late passage keratocytes (Figure 6.4) ($p=0.042$, $n=8$) (Appendix 4.1 and 4.2). However, when normalised to cell number using haemocytometer counts obtained on passage of cell cultures, gelatinase activity per cell was significantly greater in the protein samples extracted from late passage cultures than in those extracted from early passage cultures (Figure 6.5) ($p<0.05$, $n=11$) (Appendix 4.3). Protein samples loaded onto the zymograms at 100 $\mu g\ ml^{-1}$ resulted in early passage gelatinase activity which was 1.3 times that of late passage gelatinase activity (Figure 6.4) (Appendix 4.2). Calculation of the units of gelatinase activity (uA), based on the mean total protein concentrations for early and late passage cultures given in section 6.4.1 indicated 3.68 units of gelatinase activity for early passage cultures and 2.78 uA for late passage cultures. The units of activity were calculated as 283.5 $\mu g\ ml^{-1}$ total protein concentration multiplied by 1.3/100 $\mu g\ ml^{-1}$ loading concentration for early passage cultures and 278.4 $\mu g\ ml^{-1}$ total protein concentration multiplied by 1/100 $\mu g\ ml^{-1}$ loading concentration for late passage cultures. The mean number of keratocytes in early

Figure 6.2
Calibration curve of polypeptide molecular weight versus log distance of migration during SDS-PAGE zymography.

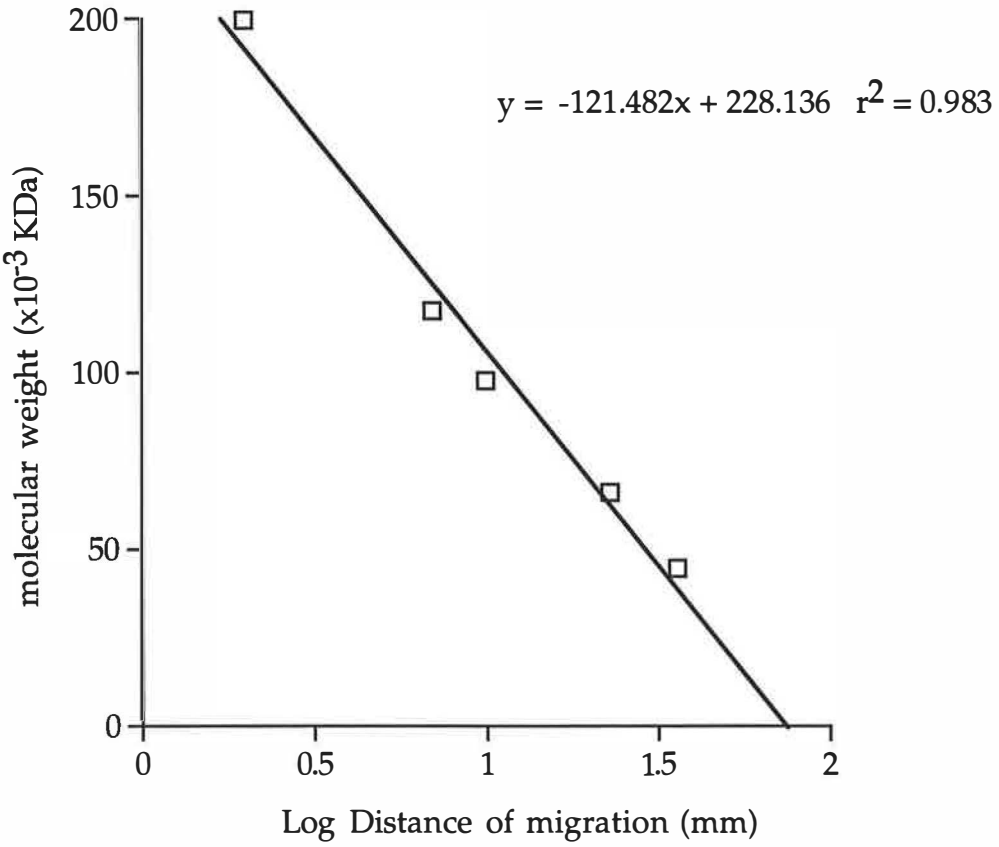

Figure 6.3
Sample zymogram showing MMP-2 activity. 1 μg of secreted protein from late and early passage keratocyte cultures was loaded into lanes 1 and 3 respectively. 0.5 μg of secreted protein from late and early passage keratocyte cultures was loaded into lanes 2 and 4 respectively.

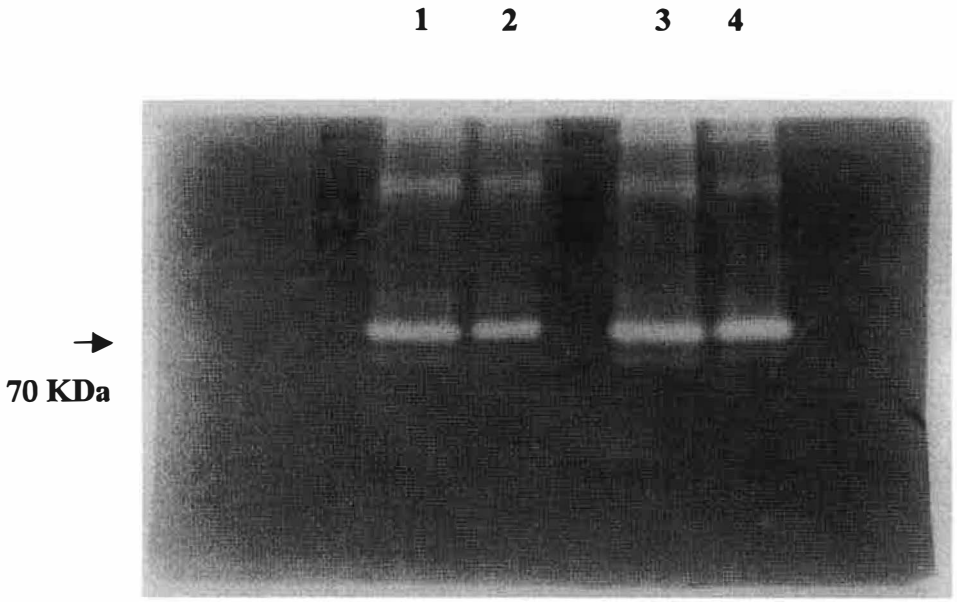

Figure 6.4
Early passage MMP-2 activity quantified as a percentage of late passage MMP-2 activity (n=8).

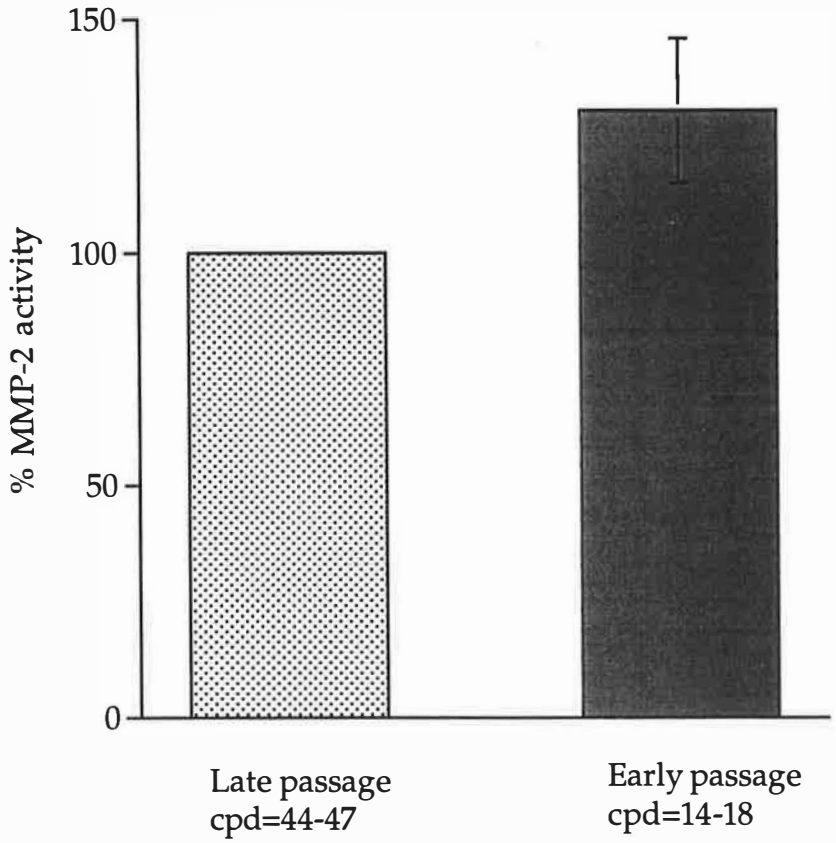

Figure 6.5
Units of gelatinase activity normalised to cell number for the protein samples extracted from early and late passage EK1.BR cultures. Results are expressed as the mean +/- SEM (n=11).

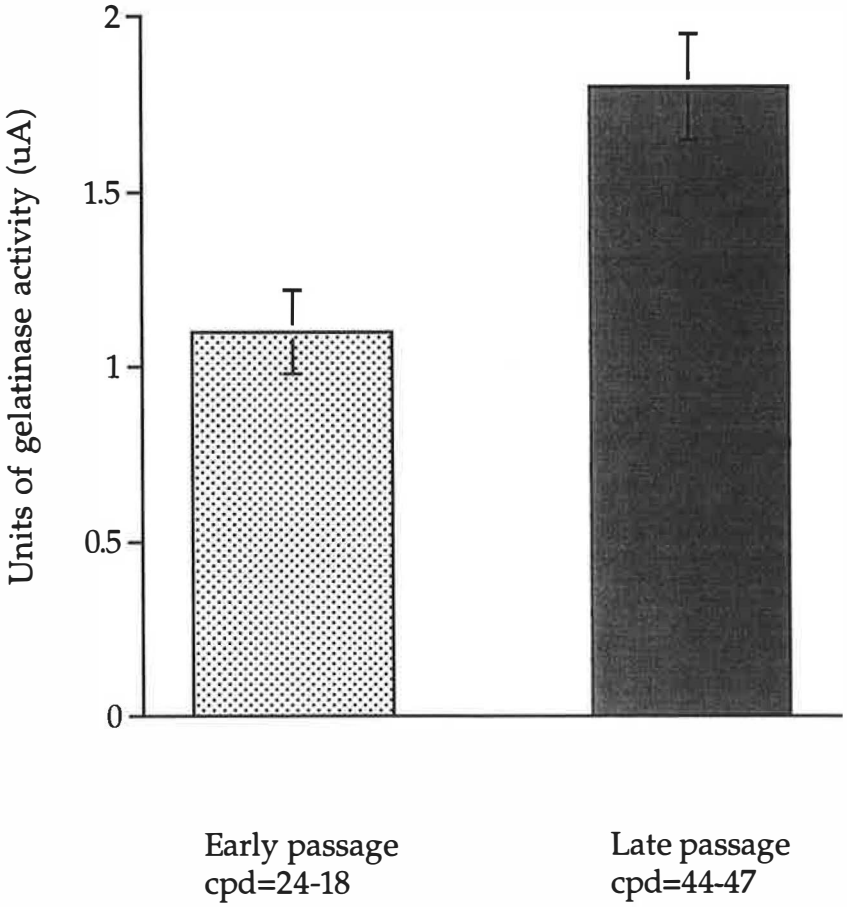

passage cultures was 3.5 x 10^6 cells while in late passage cultures it was 1.6 x 10^6 cells. Mean gelatinase activity per 10^6 cells was calculated by dividing activity by the number of keratocytes, given in Appendix 3, counted in each culture for the protein samples isolated from early and late passage cultures. Results indicated 1.1 +/-0.12 uA per 10^6 cells for early passage cultures and 1.8 +/- 0.15 uA per 10^6 cells for late passage cultures indicating an increase in gelatinase activity per cell in late passage keratocyte cultures (mean +/- SEM, n=11) (Appendix 4.3).

6.5 Discussion

Senescent EK1.BR keratocytes exhibited a decline in saturation density, as previously observed for cultures of senescent fibroblasts, and an increase in protein secretion per cell. Previous studies have identified differences in the type and amount of proteins synthesised by senescent fibroblasts. Protein synthesis was generally found to decrease while content within the cell increased suggesting a decline in protein degradation processes (Koli & Keski-Oja, 1992). However, an increase in the secretion of proteins such as FN and collagenase has been detected and may partly explain the increase in total protein secretion by senescent keratocyte cultures observed in the present study (Kumazaki et al, 1991; West et al, 1989).

The primary gelatinase secreted by EK1.BR keratocytes in culture was identified as the gelatinase MMP-2. Zymography allows visualisation of both active and pro-enzyme forms of the gelatinases since pro-enzymes are also renatured into an active form following removal of SDS. The second minor band observed on some of the zymograms may therefore represent the active form of MMP-2. Other studies have also identified a minor band of MMP-2 activity as that produced by the active form of the enzyme (Fini et al, 1992[a]; Zeng & Millis, 1994). Since most MMPs are secreted in pro-enzyme form, the minor band, representing the active form of the enzyme, will be present in smaller quantities and may not be visible on all zymograms, as was observed in this study. The 92KDa gelatinase MMP-9 was not detected in this study. MMP-9 is primarily

secreted by corneal epithelial cells but has been detected in the conditioned media of primary keratocyte cultures. However, on increasing serial passage levels declined until they were undetectable suggesting that detection may have been due to epithelial cell contamination (Fini & Girard, 1990[a]). MMP-9 may have been absent from the EK1.BR cultures or present at levels which were undetectable at the protein concentrations used.

The present study observed a decrease in gelatinase activity per mg of protein with increasing serial passage of keratocyte cultures. Densitometric analysis indicated that early passage gelatinase activity was 1.3 times that of late passage gelatinase activity. However, when normalised to cell number an increase in gelatinase activity per cell was indicated. 1.8 uA per 10^6 cells was detected in late passage cultures compared with the 1.1 uA per 10^6 cells detected in early passage cultures. Previously no change was found in gelatinase activity on passage of fibroblasts although an increase in mRNA was observed (Zeng & Millis, 1994). However, the previous study did not normalise gelatinase activity to cell number and it is not clear whether conditioned media containing 10% (v/v) FCS was used. Since FCS contains variable amounts of factors which may stimulate or suppress gelatinase expression and late passage cultures have been found to respond differently to cytokine stimulation the current study incubated confluent cultures in serum free media to collect samples for zymographic analysis. Inclusion of FCS introduces variables in addition to the number of cpds a fibroblast culture has undergone which may affect gelatinase expression. Girard et al (1991) found that TGF-β suppressed collagenase and stromelysin expression but enhanced the expression and activity of MMP-2 in early passage rabbit keratocytes. An increase in collagenase and stromelysin expression in late passage fibroblasts has been linked to a decline in TGF-β activity (Zeng et al, 1996). However, in the present study any reduction in the activity of endogenously secreted TGF-β had no apparent effect on MMP-2 secretion since a reduction rather than an increase in MMP-2 activity would then be expected.

The gelatinase MMP-2 is the only MMP found in the normal cornea where it is thought to have a surveillance role and may be involved in minor alterations to stromal fibrillar structure (Fini & Girard, 1990[a]). Any change in gelatinase activity with age will alter these processes and may ultimately affect corneal function. Minor changes in gelatinase activity are unlikely to have a large impact on the cornea. However, following corneal wounding collagenase and gelatinase MMP-9 expression also occurs. Additional changes to the activity of these enzymes make disruption of the repair process more probable. Previous studies have identified an increase in collagenase secretion by senescent fibroblasts (West et al, 1989). Further investigation of changes in the secretion of collagenase and the gelatinases as keratocyte senescence occurs will further highlight alterations in the ability of senescent keratocytes to adequately respond to corneal wounding.

Chapter 7

The Development of Polymers for Use in the Fabrication of a Novel Keratoprosthesis

7.1 Introduction

7.1.1 Suitable KPro Materials

The retention of KPro designs within the cornea requires the development and incorporation of materials which are conducive to integrative success. The peripheral skirt material, which anchors the central optical cylinder to surrounding tissue, is primarily responsible for the induction of a good integrative response to the implant. A malleable, compatible, porous material which limits friction and allows cell adhesion, spreading and growth will endeavour to limit inflammation and induce controlled matrix remodelling so that the implant becomes an integral component of the cornea.

Numerous studies have considered the ability of various biomaterials to encourage cell adhesion and growth. The process is complex and involves the interaction of a number of factors including surface charge, wettability (hydrophilicity/hydrophobicity), porosity and roughness. Cell adhesion and spreading tend to favour slightly hydrophilic materials which incorporate a positive charge and depend on initial serum protein absorption by the polymer (Lydon et al, 1985; Smetana et al, 1997; Lee et al, 1997). Pettit et al (1990) found that corneal epithelial outgrowth was greatest onto copolymers of p(HEMA)/ethylene methacrylate and p-hydroxystyrene/styrene with intermediate wettabilities. It was also found that serum proteins fibronectin and vitronectin were required for stromal cell attachment to methyl methacrylate (MMA) (Steele et al; 1997). Fibroblast proliferation was higher on a hydrophilic, glass surface when compared to that on an octadecyl, hydrophobic glass surface. Fibroblasts appeared to remodel fibronectin coated glass into an ECM type structure, providing a surface more conducive to fibroblast adhesion and growth (Altankov et al, 1994).

The elasticity, swellability and strength of p(HEMA) hydrogels have made them suitable for use in a number of biomedical applications including the manufacture of soft contact lenses. The material has also been used to develop a collagen coated, 80 wt%, water based p(HEMA) hydrogel. The design was well tolerated on implantation into rabbit

corneae and cell invasion into the pores of the material was observed (Crawford et al, 1993; Crawford et al, 1996). However, tensile strength was limited because of the high percent of water diluent required to achieve pores large enough for cell invasion (Hicks et al, 1998). Further modifications may be necessary before p(HEMA) based designs, suitable for corneal implantation, are obtained. Fibroblast adhesion to untreated p(HEMA) is limited and cells do not tend to spread or exhibit normal morphological features (Peluso et al, 1997; Bergethon et al, 1989). Cell adhesion characteristics have been improved by the incorporation of collagen (Civerchia-Perez et al, 1980) and by the addition of hydrophobic caprolactone (Peluso et al, 1997). Smetana et al (1997) found that monocyte adhesion was much greater onto co-polymers of p(HEMA) and positively charged 2-(dimethylamino)ethyl methacrylate (DEM) (10 Mol%) when compared with that onto p(HEMA) or a co-polymer of p(HEMA) and the negatively charged salt of methacrylic acid (MA) (3 Mol%). Bergethon et al (1989) had previously shown that the incorporation of either of the ionisable groups MA or DEM (0.1%vol) produced fibroblast spreading onto p(HEMA) hydrogels. Results indicate that the addition of charged monomers to p(HEMA) based hydrogels alters the cell adhesion and spreading characteristics of these polymers.

7.1.2 The Surface Charge Characteristics of p(HEMA) Based Hydrogels

The presence of a charged group within a p(HEMA) hydrogel can be demonstrated by the ability of the gel to bind to a charged dye and measured by the resulting change in light absorption characteristics of the hydrogel. Incorporation of MA introduces a pH dependent negative charge which increases polymer ability to bind to the positively charged dye methylene blue while absorption of the negatively charge dye amaranth remains low. MA has a low pKa of approximately 4.3 so that at pH 2 the polymer is completely protonated and methylene blue absorption is low. With increasing pH beyond the pKa of MA the polymer becomes completely unprotonated and negatively charged, producing an increase in methylene blue absorption. Methylene blue incorporation and light absorption will therefore increase with increasing MA content and with increasing pH beyond the pKa of MA

until complete protonation of the polymer. Incorporation of DEM, with a pKa of approximately 9.5, introduces a pH dependent positive charge into the polymer. An increase in amaranth binding occurs with increasing DEM concentration while methylene blue absorption remains low. Polymer absorption of methylene blue and amaranth may therefore be used as a semi-quantitative measure of MA or DEM content within a p(HEMA) hydrogel.

7.1.3 Polymer Cytotoxicity and Cell Adhesion Characteristics

Analysis of polymer suitability should include some measure of material cytotoxicity and cell adhesion characteristics since the successful incorporation of keratoprosthetic skirt materials within host corneal tissue is dependent on their ability to encourage cell adhesion and growth.

A viability/cytotoxicity assay may be carried out using the fluorescent markers calcein AM and the ethidium homodimer-1 (EthD-1). Calcein AM is cleaved by cellular esterases present within viable cells to form a fluorescent green product which is membrane impermeant. EthD-1 is a fluorescent red marker which only passes through the compromised membranes of non-viable cells. It binds with 1000 times more strength to nucleic acids than ethidium bromide and acts as a measure of polymer cytotoxicity. The assay quantifies the ability of different polymers to support cell adhesion and growth by comparing the number of calcein-AM positive (viable) and EthD-1 positive (non-viable) cells present on the surface of each material.

Since ATP levels increase with increasing cell number it is also possible to quantify cell adhesion to various polymers using a bioluminescent ATP assay. The light producing assay is a firefly luciferase catalysed reaction between ATP and luciferin. Prior to the assay cells are lysed to release the ATP.

$$\text{ATP} + \text{luciferin} + O_2 \xrightarrow{\text{luciferase}} \text{oxyluciferin} + \text{AMP} + \text{PPi} + CO_2 + \text{light}$$

The assay measures the amount of ATP present by the amount of light produced to give a second measure of the ability of different polymers to support cell adhesion and growth.

7.1.4 Free Radical Polymerisation

The polymers in the present study were formed using a free radical method of polymerisation. A moderate rise in temperature induces the homolytic decomposition of low energy nitrogen bonds within the azo-iso-butyronitrile (AIBN) initiator molecule to generate two high energy free radicals and a nitrogen molecule (Figure 7.1a). The radicals attack monomer molecules present in solution to form further radicals and initiate the polymerisation process. Monomer radicals add onto other monomer double bonds to produce a polymer chain radical which is then propagated by the addition of further monomers (Figure 7.1a). The inclusion of crosslinking monomers such as ethylene dimethacrylate (EDMA), containing two vinyl groups, allows the formation of links between growing polymer chains so that a network is formed (Figure 7.1b). Polymer chains are terminated by a reaction between two growing radicals to produce a non radical product (Figure 7.1c)(Munk, 1989).

p(HEMA) has a number of ECM like characteristics which make it suitable for consideration as a KPro material. The following study sought to investigate the effect of incorporating hydrophobic, negatively charged or positively charged co-monomers on cell adhesion to p(HEMA). A number of p(HEMA) based materials incorporating various amounts of phenoxyethyl methacrylate (PEM), MA or DEM were first generated using a free radical polymerisation technique. The structures of these monomers are given in Figure 7.2. The incorporation of charged groups into the polymers was analysed using a dye absorption assay. Polymer cytotoxicity and adhesion characteristics were analysed using an ATP assay and a calcein-AM based assay which assessed viable cell growth. A preliminary investigation of methods by which pores may be introduced into the polymers was also carried out.

Figure 7.1
The (a) initiation and propagation, (b) branching and (c) termination steps of the free radical polymerisation process.

(a)

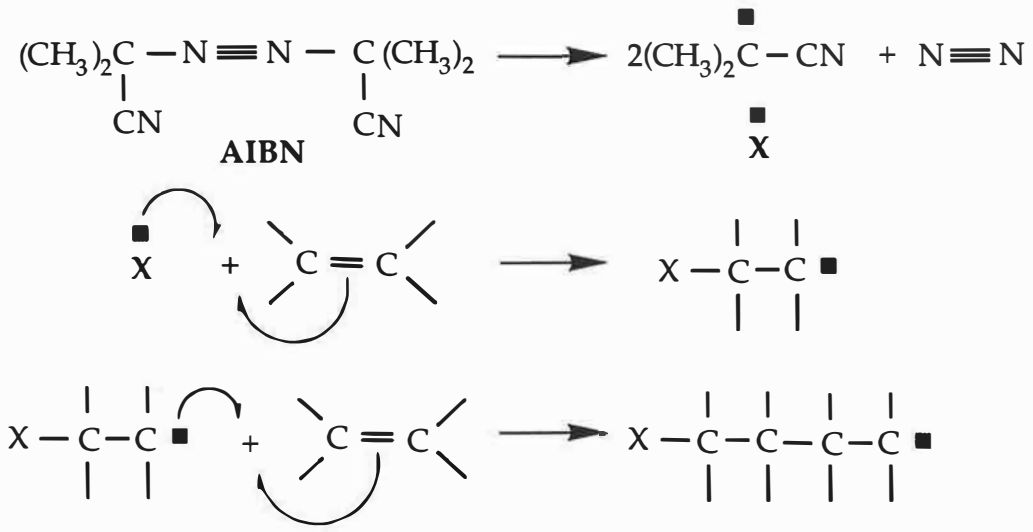

(b)

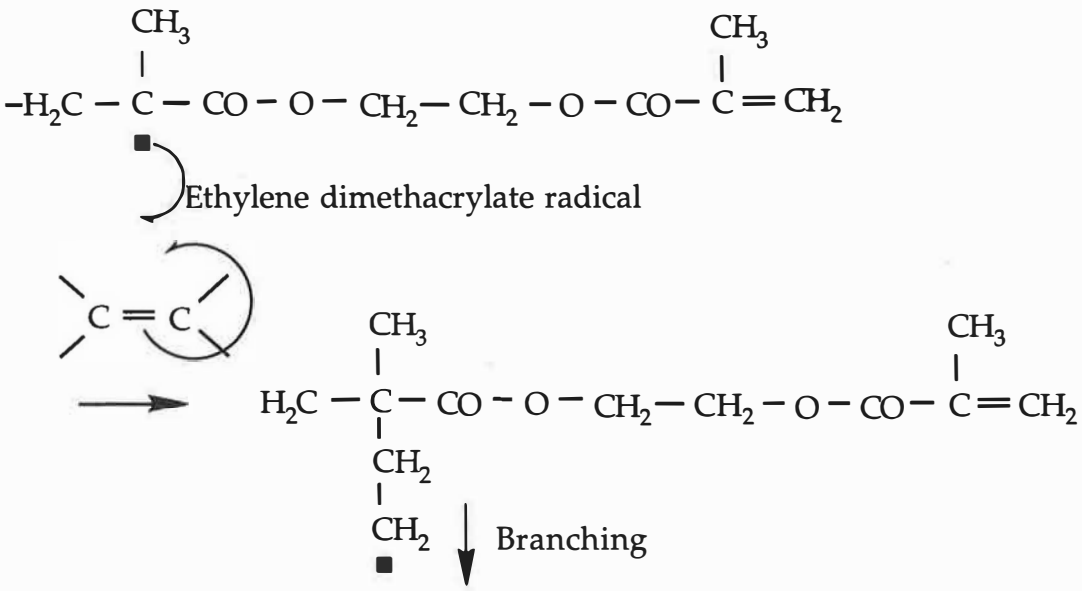

(c)

R represents possible substituent groups

Figure 7.2
The chemical structures of (a) hydroxyethyl methacrylate (HEMA), (b) methacrylic acid (MA), (c) 2-(dimethylamino)ethyl methacrylate (DEM) and (d) phenoxyethyl methacrylate (PEM).

(a)

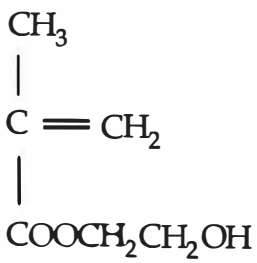

(b)

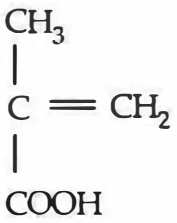

(c)

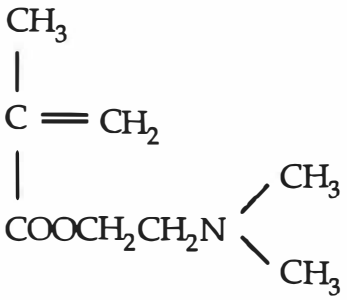

(d)

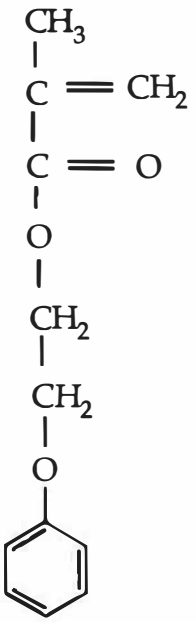

7.2 Materials & Equipment

7.2.1 Polymerisation

The initiator azo-iso-butyronitrile (AIBN) was supplied by Fisons Scientific Equipment, Bishop Meadow Road, Loughborough, Leicestershire, LE11 0RG, UK.

The crosslinker ethylene dimethacrylate (EDMA), sodium metabisulphite and the monomer 2-(dimethylamino)ethyl methacrylate (DEM) were supplied by Sigma-Aldrich Company Ltd, Fancy Rd, Poole, Dorset, BH12 4QH, UK.

The monomer phenoxyethyl methacrylate (PEM) was supplied by Polysciences Inc., Distributed by Park Scientific Ltd, 24 Low Farm Place, Moulton Park, Northampton, NN3 6HY, UK.

The monomer methacrylic acid (MA) was supplied by ACROS Organics, Bishop Meadow Road, Loughborough, Leicestershire, LE11 0RG, UK.

Ammonium persulphate were supplied by BIO-RAD Laboratories Ltd, Bio-Rad House, Maylands Avenue, Hemel Hempstead, Hertfordshire, HP2 7TD, UK.

7.2.2 Dye Absorption Assay

Amaranth, citric acid and potassium chloride were supplied by Sigma-Aldrich Company Ltd (address as above).

Methylene blue and sodium phosphate were supplied by MERCK Ltd, Hunter Boulevard, Magna Park, Lutterworth, Leicestershire, LE17 4XN, UK.

Titertek multiscan plus MK11 plate reader (type 314) supplied by Flow Laboratories Ltd., PO Box 17, Second Avenue, Industrial Estate Irvine, Ayrshire, Scotland, UK.

7.2.3 Viability/Cytotoxicity Assays

Calcein AM in DMSO (1M) and Ethidium homodimer-1 (2mM) in 1:4 DMSO/H_2O as part of a LIVE/DEAD viability/cytotoxicity kit were supplied by Molecular Probes, distributed by Cambridge Bio Science, 25 Signet Court, Newmarket Road, Cambridge, CB5 8LA, UK.

The ATP assay kit was supplied by Labtech International, Woodside, Easons Green, Uckfield, E. Sussex, TN22 5RE, UK. It included an ATP monitoring reagent containing luciferase and D-luciferin, an ATP standard and a 0.1 M TRIS acetate buffer, 2mM EDTA, pH 7.75 (TRIS-Ac buffer).

Amerlite luminometer supplied by Amersham International plc., Amersham Place, Little Chalfont, Buckinghamshire, HP7 9NA, UK.

7.2.4 Pore Formers

Dextran was supplied by Sigma-Aldrich Company Ltd (address as above).

7.3 Methods

7.3.1 The Polymerisation Process

Two 6 cm^2 square sheets of each polymer were made. The polymerisation chambers consisted of two outer glass plates separated by two sheets of polyethylene terathyalate (PET) and a central hollow, teflon perimeter clamped together with four large clips. One side of the PET sheets was coated with a hydrophobe and the moulds were constructed so that the hydrophobic side of the PET sheets was in contact with the polymer. The teflon spacer, placed between two sheets of PET, was hollowed centrally to provide a chamber for polymerisation and was cut diagonally in one corner so that a 25 gauge/ 1 inch syringe needle could be inserted for injection of the monomer solution. Gram amounts of each monomer were calculated by multiplying the Mol% required with the relevant molecular weight (Appendix 5). Amounts were scaled down by a factor of $5x10^{-4}$ to give appropriate volumes. The monomers were weighed out in the amounts given in Table 7.1, mixed and degassed

poiymer	HEMA (g)	MA (g)	DEM (g)	PEM (g)
p(HEMA)	6.5	-	-	-
0.5Mol% MA/99.5Mol% HEMA	6.47	0.022	-	-
1Mol% MA/99Mol% HEMA	6.44	0.043	-	-
1.5Mol% MA/98.5Mol% HEMA	6.4	0.065	-	-
2Mol% MA/98Mol% HEMA	6.37	0.086	-	-
20Mol% MA / 80Mol% HEMA	5.2	0.88	-	-
0.5Mol% DEM/99.5Mol% HEMA	6.47	-	0.039	-
0.5Mol% DEM/99.5Mol% HEMA	6.44	-	0.079	-
1.5Mol% DEM/ 98.5Mol% HEMA	6.4	-	0.118	-
2Mol% DEM/98Mol% HEMA	6.37	-	0.157	-
20Mol% DEM/ 80Mol% HEMA	5.2	-	1.57	-
15Mol% PEM/85Mol% HEMA	5.33	-	-	1.55
25Mol% PEM/75Mol% HEMA	4.88	-	-	2.58
10Mol%PEM/0.5Mol%DEM /89.5Mol%HEMA	5.82	-	0.039	1.03
10Mol%PEM/10Mol%DEM /80Mol%HEMA	5.2	-	0.79	1.03

Table 7.1 Polymer Formulations

by sonication for ten minutes. 0.0164 g (0.2 Mol%) of the initiator AIBN and 0.05 g (0.5 Mol%) of the cross linker EDMA were weighed out. The initiator was dissolved in the degassed monomer solution then mixed with the crosslinker. The solution was syringed into the polymerisation chambers using a 5 ml syringe and incubated at 60°C overnight. The polymers were removed from the chambers and placed in distilled water to remove unpolymerised monomer and crosslinker. Water was

changed frequently for the first twenty four hours and daily for a week. Polymers containing PEM were first soaked in ethanol for twenty four hours to remove excess PEM monomer then soaked in distilled water as for the other polymers

7.3.2 Dye Absorption Assay

100 ml of McIlvaine's phosphate/citrate buffer (0.5 M) was made up at pH 2.2, 4, 5 and 6 as shown in Table 7.2. Buffer at each pH was divided into two 50 ml bottles. 0.01% volume methylene blue and amaranth dye solutions were made up by adding 0.005 g of methylene blue to the first 50 ml of buffer solution and 0.005 g of amaranth to the second 50 ml of buffer solution at each pH. The dye absorption assay was carried out for MA containing polymers and then repeated for polymers containing DEM at varying concentrations. For each experiment triplicate discs of each of the 0.5 Mol%, 1 Mol%, 1.5 Mol%, 2 Mol% and 20 Mol% MA or DEM containing p(HEMA) polymers were prepared for testing with each of the four dye containing buffers at increasing pH. Control p(HEMA) discs were included in the absorption assay for the DEM containing polymers. Discs were placed in the wells of two ninety six well tissue culture plates. Amaranth containing buffers were added to the disc containing wells of the first plate and methylene blue containing buffers were added to the second. 200 µl of dye containing buffer was pipetted onto each of the discs so that triplicate discs of each polymer were tested at each buffer pH with both the amaranth and methylene blue containing buffers. The discs were left in the buffer solutions for two hours at room temperature. Dye containing buffer was removed from each of the wells and discs were washed with distilled water until all excess dye was removed. Absorbence readings were then taken on a plate reader at a wavelength of 540 nm.

pH at 25°C	Dibasic Sodium Phosphate (g/100 ml)	Citric Acid (g/100 ml)	Potassium Chloride (g/100 ml)
2.2	0.143	2.16	3.72
4	2.76	1.29	2.55
5	3.69	1.02	1.82
6	4.52	0.774	1.16

Table 7.2 McIlvaine's phosphate/citrate buffer recipe

7.3.3 Polymer Cytotoxicity and Cell Adhesion Characteristics

7.3.3.1 Viability/Cytotoxicity Assay

The first set of polymers tested for cytotoxicity using the fluorescent markers calcein AM and EthD-1 were p(HEMA) hydrogels incorporating 0.5 Mol%, 1 Mol%, 1.5 Mol%, 2 Mol% and 20 Mol% MA or DEM and p(HEMA) hydrogels incorporating 15 Mol% PEM. The second set of polymers tested for cytotoxicity included the initial p(HEMA) hydrogels incorporating 20 Mol% DEM and 15 Mol% PEM with the addition of p(HEMA) hydrogels incorporating 10 Mol% DEM/10 Mol% PEM and 0.5 Mol% DEM/10 Mol% PEM. 11 mm discs of each material were cut out and sterilised by washing with ethanol and then sterile water. Following continued bacterial growth on some of the discs subsequent materials were sterilised by autoclaving at 115°C for five minutes. For each experiment one disc of each material was placed in the wells of a twenty four well plate. A sterile, 13 mm glass coverslip was included as a positive control. Discs were incubated in 1 ml of PBS at 37°C in a 5% CO_2/air incubator for at least twenty four hours. EK1.BR keratocytes from 20 to 30 cpds were passaged as previously described in section 2.1.3. A pellet of cells was resuspended in media so that 1 ml of media contained $4x10^4$ cells. 1 ml of cell suspension was pipetted onto each polymer disc and plates were incubated for seventy two hours at 37°C.

Media was removed from the wells and 0.5 ml of calcein AM solution (0.5 mM) followed by 0.5 ml EthD-1 solution (0.5 μM) was added. Dilutions were made by adding 4 μl of 1 mg ml^{-1} calcein AM to 8 ml PBS and 4 μl of 2 μg ml^{-1} EthD-1 to 16 ml PBS. Discs covered in calcein AM and EthD-1 solution were left for ten minutes at room temperature then viewed under fluorescent microscope. Calcein AM positive and EthD-1 positive cells were counted in each of thirty fields for each material. The dyes fluoresced at a peak wavelength of 500 nm and 625 nm respectively. The calcein AM count indicated the number of live cells present on each material while the EthD-1 count indicated the number of dead cells present.

7.3.3.2 Reconstitution of ATP Assay Kit Reagents

10 ml of TRIS-Ac buffer was added to the ATP monitoring reagent powder and the solution was mixed gently. 1 ml aliquots of the solution were prepared and stored at -18°C for a maximum of two months. 10 ml of distilled water was added to the ATP standard powder and mixed gently to give a $1x10^{-5}$ M stock solution. 500 μl aliquots were prepared and stored at -18°C for a maximum of two months.

7.3.3.3 ATP Assay of Cell Dilutions

In order to confirm that ATP concentration and cell number are directly related an ATP assay using serially decreasing cell concentrations was carried out. EK1.BR keratocytes were passaged as previously described. Each cell concentration was prepared in quadruplicate. Cell suspensions containing 4($1x10^5$, $5x10^4$, $1x10^4$, $5x10^3$, $1x10^3$) cells were prepared in universal tubes so that each cell concentration was suspended in the same amount of media for centrifugation. Cell suspensions were centrifuged at 400 g for five minutes so that a pellet of cells formed at the base of the tube. Media was aspirated off and each cell pellet was resuspended in 300 μl of hypotonic lysis buffer (recipe given below). Each cell lysate suspension was transferred to a 1.5 ml eppendorf tube and placed in the freezer at -18°C overnight. Following thawing each tube of cell lysate was diluted 1:1 with 300 μl TRIS-Ac buffer. Aliquots of

ATP monitoring reagent and ATP standard were defrosted. 50 µl of ATP monitoring reagent was added to the wells of a ninety six well microtitre plate so that the assay could be carried out in triplicate for each cell concentration. An initial background reading for the monitoring reagent was taken using the luminometer. 150 µl of cell lysate was added to each of three wells for each cell concentration and a second reading was taken. The ATP standard underwent a 1:10 dilution with TRIS-Ac buffer. 50 µl of the ATP standard solution was added to each well and a third reading was taken. All plates and reagents were kept on ice throughout the experiment.

7.3.3.4 ATP Assay of Materials

The polymers to be tested were p(HEMA) hydrogels incorporating 0.5 Mol%, 1 Mol% and 1.5 Mol% MA, 0.5 Mol%, 1 Mol% and 20 Mol% DEM, 15 Mol% PEM, 10 Mol% DEM/10 Mol% PEM and 0.5 Mol% DEM/10 Mol% PEM. Six 11 mm discs of each material were cut out and initially sterilised by washing in ethanol followed by sterile water. As for the previous assay the method of sterilisation was changed to autoclaving for five minutes at 115°C following continued detection of bacterial growth after soaking in ethanol. The sterilised discs were placed in the wells of twenty four well tissue culture plates and each soaked in 1 ml PBS for at least twenty four hours. EK1.BR keratocytes were passaged as previously described and resuspended in media so that 1 ml of media contained $4x10^4$ cells. 1 ml of cell suspension was then pipetted onto each disc. Controls were set up by seeding $4x10^4$ cells directly onto the plastic base of each of six wells. Plates were incubated at 37°C for seventy two hours. Media was removed from the wells and discs were washed in PBS two times. The discs were moved to a second twenty four well plate and covered with 300 µl of sterile filtered hypotonic lysis buffer. The lysis buffer consisted of 5 ml of 0.1 M TRIS-acetate buffer (supplied with the ATP kit), 3.2 ml of a 0.1 M solution of EDTA and 16.8 ml of sterile water. Plates were placed in a freezer at -18°C overnight. Following defrost lysate solutions underwent a 1:1 dilution by the addition of 300 µl TRIS-Ac buffer to each well. Aliquots of ATP

monitoring reagent and ATP standard were defrosted. 50 µl of monitoring reagent was added to the wells of a ninety six well microlite plate so that lysate solution from each disc could be tested. Background readings given out by the monitoring reagent were first measured on the luminometer. 150 µl of diluted lysate solution covering each polymer disc was added to the wells containing monitoring reagent and a second luminescence reading was taken. The ATP standard underwent a 1:10 dilution with TRIS-Ac buffer. 50 µl was added to each of the wells containing lysate solution and monitoring reagent and a third luminescence reading was taken. All of the reagents and plates were kept on ice throughout the experiment.

7.3.4 Pore Formers

7.3.4.1 Ethanol and Water Based Porous Polymers

Porous p(HEMA) polymers were made containing 45, 56, 63 and 68% (v/v) ethanol. 0.0164 g of AIBN was dissolved in the appropriate amount of ethanol (10, 15, 20 and 25 ml of ethanol respectively). 11.7 g of HEMA and 1.98 g of EDMA were weighed out, mixed and sonicated for ten minutes. AIBN dissolved in ethanol was added and the solution was injected into the casting chambers and incubated as above. An 80 wt%, water based p(HEMA) gel was also prepared using a sodium metabisulphite/ ammonium persulphate initiator/accelerator system. 0.012 g of the initiator and accelerator was dissolved in 0.2 ml of distilled water each to give a total volume of 0.4 ml. 2 g of HEMA, 8 g of water and 0.05 g of EDMA were mixed and sonicated for fifteen minutes. 0.4 ml of the initiator/accelerator solution was added. The monomer solution was injected into two polymerisation chambers and incubated as described in section 7.3.1. Polymers were viewed using cryogenic scanning electron microscopy (cryo-SEM) with the assistance of technician Mr M. Helias.

7.3.4.2 Dextran Based Porous Polymers

A 15 Mol% PEM/ 85 Mol% HEMA monomer solution was made up as previously in section 7.3.1. Dextran was sieved and particles with a diameter of 70 µm were used as pore formers. Following sonication and

the addition of AIBN and EDMA 0.4 g of dextran was added to the monomer solution. The cloudy solution containing dextran particles was injected into a casting chamber and incubated as previously described. Following incubation the polymers were soaked in water to desolve some of the dextran incorporated into the polymers. The resulting polymers were viewed using cryo-SEM.

7.4 Results

7.4.1 MA, PEM and DEM containing p(HEMA) Polymers

HEMA polymerisation using an AIBN/EDMA initiator system produced a transparent, flexible material which was easily cut into discs and sterilised by autoclaving. Inclusion of MA and DEM monomers into the polymer formulation at low Mol%s resulted in the production of transparent materials of similar flexibility to the 100 Mol% HEMA polymer. At higher concentrations of MA and DEM the materials produced were tougher and were less easily cut into discs. Polymers containing PEM were also initially transparent. Soaking the materials in ethanol to remove excess PEM monomer caused the polymer to become very flexible. On transferal of the polymer into water the material became translucent and less flexible with time. While the transparency of the 15 Mol% PEM polymers returned after two days in water the resulting polymers were more brittle than the other polymers and were difficult to cut into discs with a borer. Initial studies using higher concentrations of PEM resulted in polymers which were very brittle and remained translucent. The use of benzyl methacrylate rather than PEM had no observable effect on polymer flexibility. Incorporation of PEM and DEM within one polymer produced materials of variable thickness. Polymers were often thinner at the centre. Short, broken lines were observed in patches across some of the polymers giving the appearance of shattering. The variable properties of the DEM/PEM mixed polymers suggests that the monomers were not evenly dispersed during the polymerisation process.

7.4.2 Dye Absorption Assay

7.4.2.1 DEM Containing p(HEMA) Hydrogels

An increase in absorption of the negatively charged dye amaranth was observed with increasing concentration of DEM within the polymers while amaranth absorption by p(HEMA) remained low (Figure 7.3). DEM has a high pKa of approximately 9.5 and would be protonated and available for amaranth binding at the buffer pHs used in this study. Absorption of the positively charged dye methylene blue by any of the DEM containing or control p(HEMA) polymers was low (Figure 7.4).

7.4.2.2 MA Containing p(HEMA) Hydrogels

At pH 6 MA incorporated within the p(HEMA) polymer is completely unprotonated and readily available to bind with the positively charged methylene blue dye. As expected, dye absorbence increased with increasing concentration of MA at pH 6 (Figure 7.5). At pHs around the pKa of MA low levels of absorption occurred since MA remains at least partially protonated and unable to bind to methylene blue. Low levels of amaranth absorption were observed for polymers at all concentrations of MA (Figure 7.6).

7.4.3 Polymer Cytotoxicity and Cell Adhesion Characteristics

7.4.3.1 Cell Viability/Cytotoxicity Assay

The number of viable cells adhering to the first set of test materials was low on all of the MA containing polymers and on the p(HEMA), 0.5 Mol% and 1 Mol% DEM containing polymers. Viable cell adhesion to the 1.5 Mol% and 2 Mol% DEM containing polymers was slightly higher. The polymers most conducive to cell growth were the 20 Mol% DEM and 15 Mol% PEM containing p(HEMA) polymers on which viable cell counts were 73% and 66% that of the controls respectively (Figure 7.7). Keratocytes growing on these discs exhibited normal spindle shaped fibroblast morphology while cells growing on the other materials tended to be rounded and clumped in places (Figure 7.8). 20 Mol% MA containing polymers expanded and were too acidic to support viable cell growth. The material was not included in any further assays.

Figure 7.3
Amaranth absorption by p(HEMA) gels incorporating increasing concentrations of 2-(dimethylamino)ethyl methacrylate. Results are expressed as the mean +/- SEM (n=3).

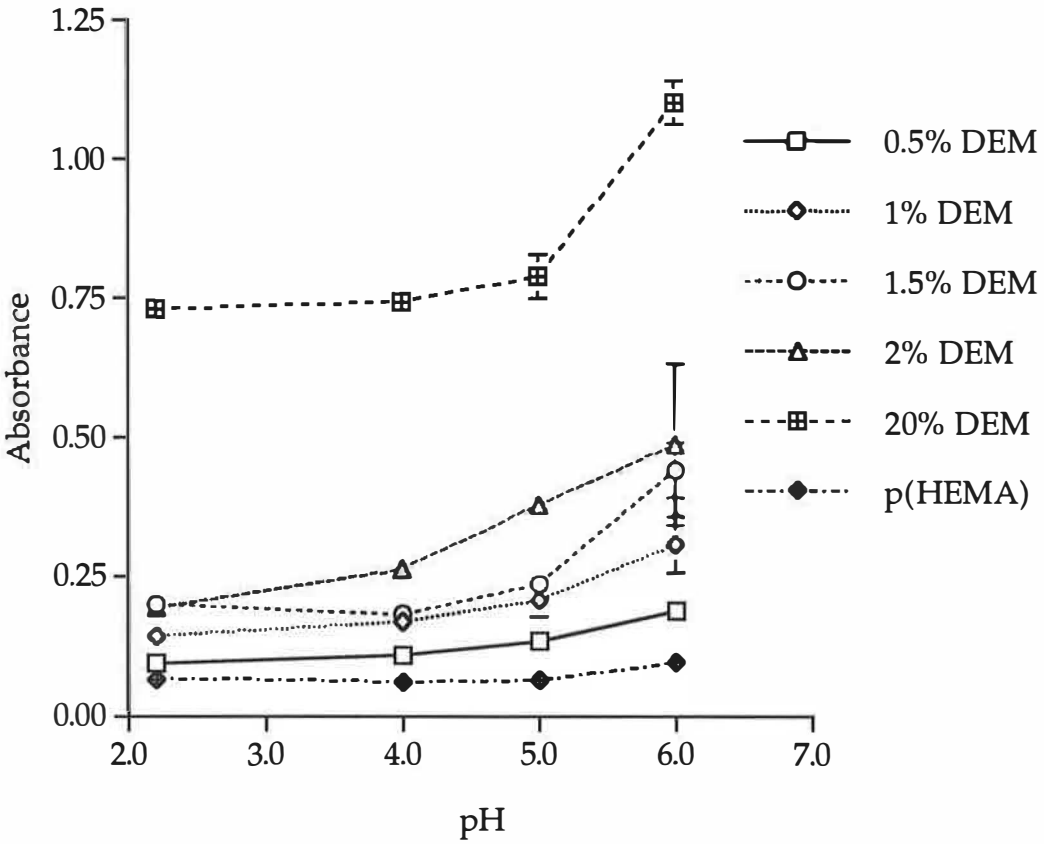

Figure 7.4
Methylene blue absorption by p(HEMA) gels incorporating increasing concentrations of 2-(dimethylamino)ethyl methacrylate. Results are expressed as the mean +/- SEM (n=3).

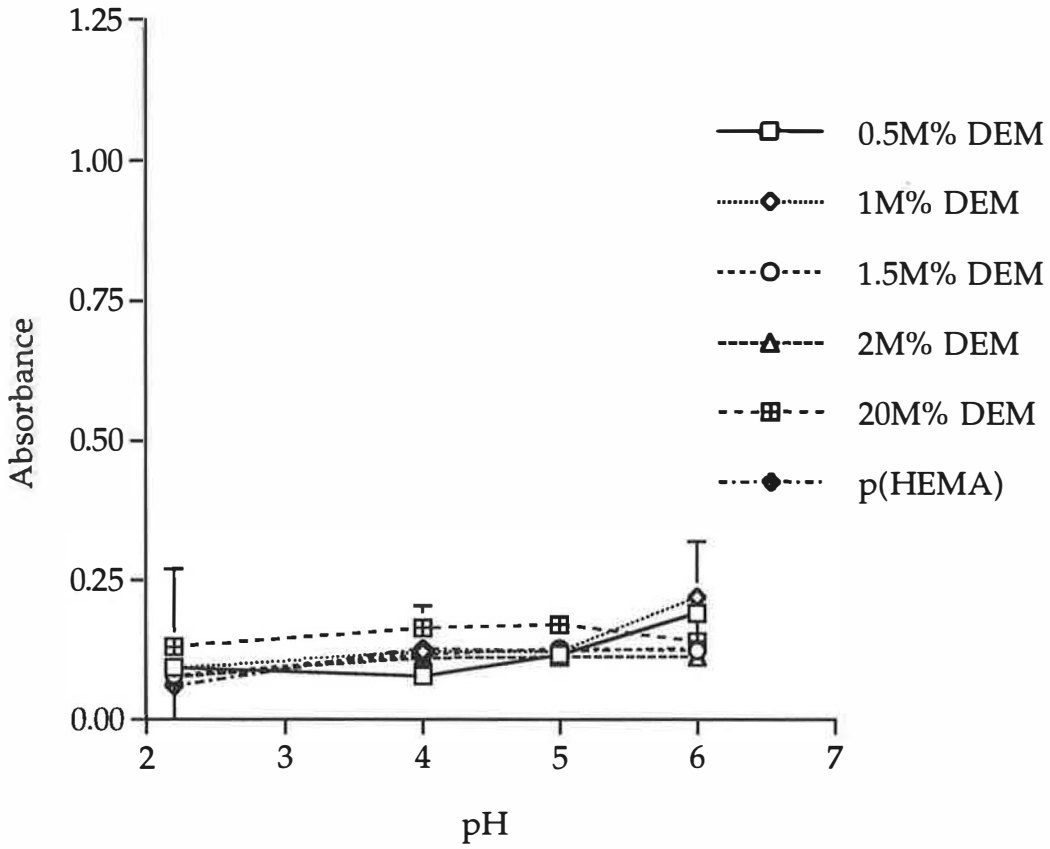

Figure 7.5
Methylene blue absorption by P(HEMA) gels incorporating increasing concentrations of methacrylic acid. Results are expressed as the mean +/- SEM (n=3).

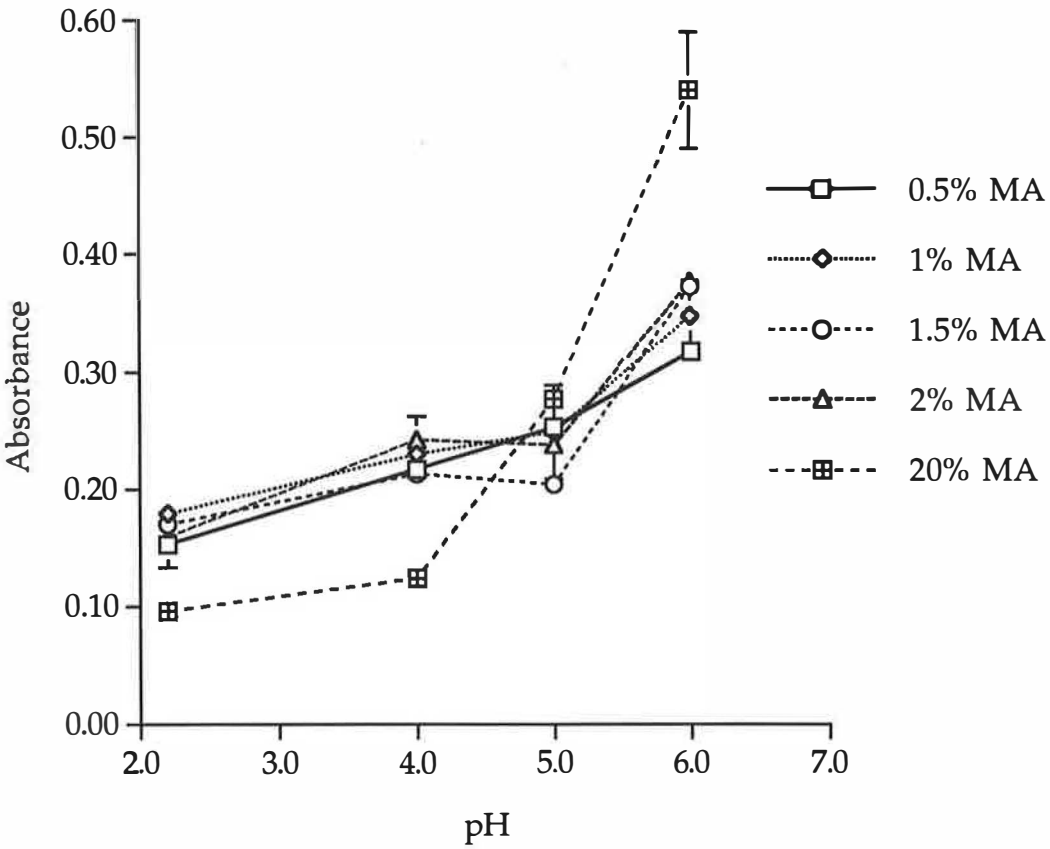

Figure 7.6
Amaranth absorption by P(HEMA) gels incorporating increasing concentrations of methacrylic acid. Results are expressed as the mean +/- SEM (n=3).

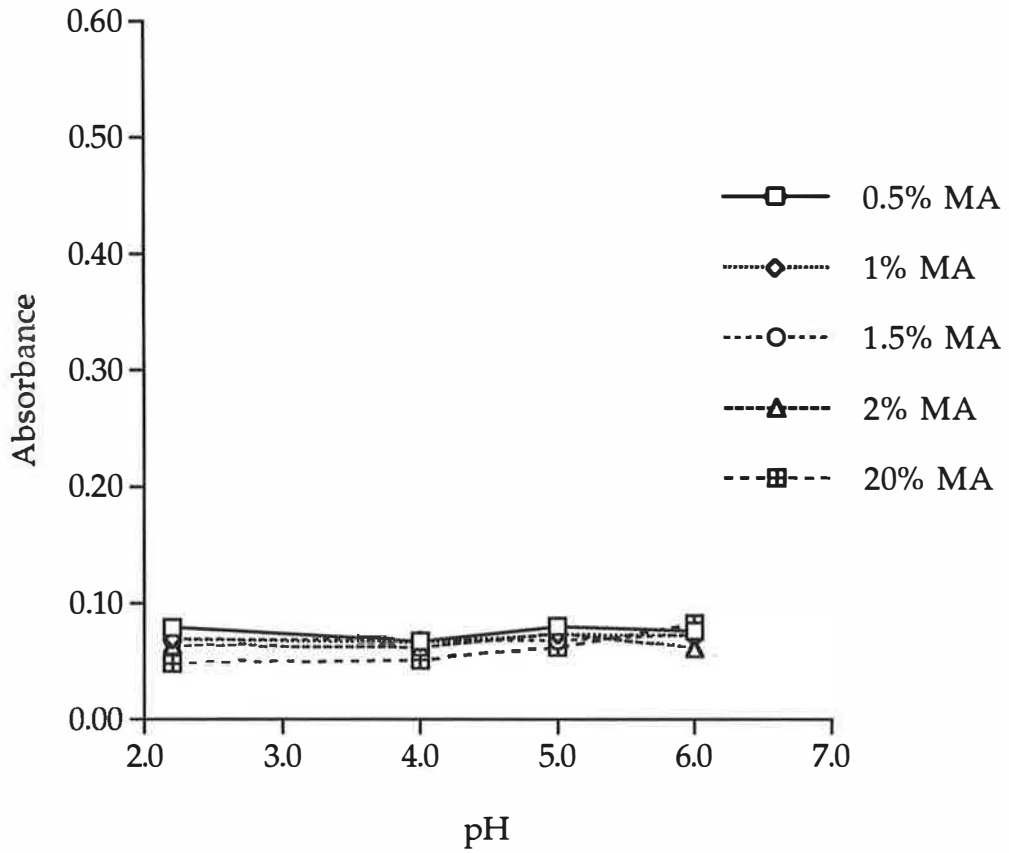

Figure 7.7
Viability/ Cytotoxicity Assay of p(HEMA) hydrogels incorporating negatively charged methacrylic acid, positively charged 2(dimethylamino)ethyl methacrylate and hydrophobic phenoxyethyl methacrylate copolymers at varying concentrations. Results are expressed as the mean +/- SEM (n=4).

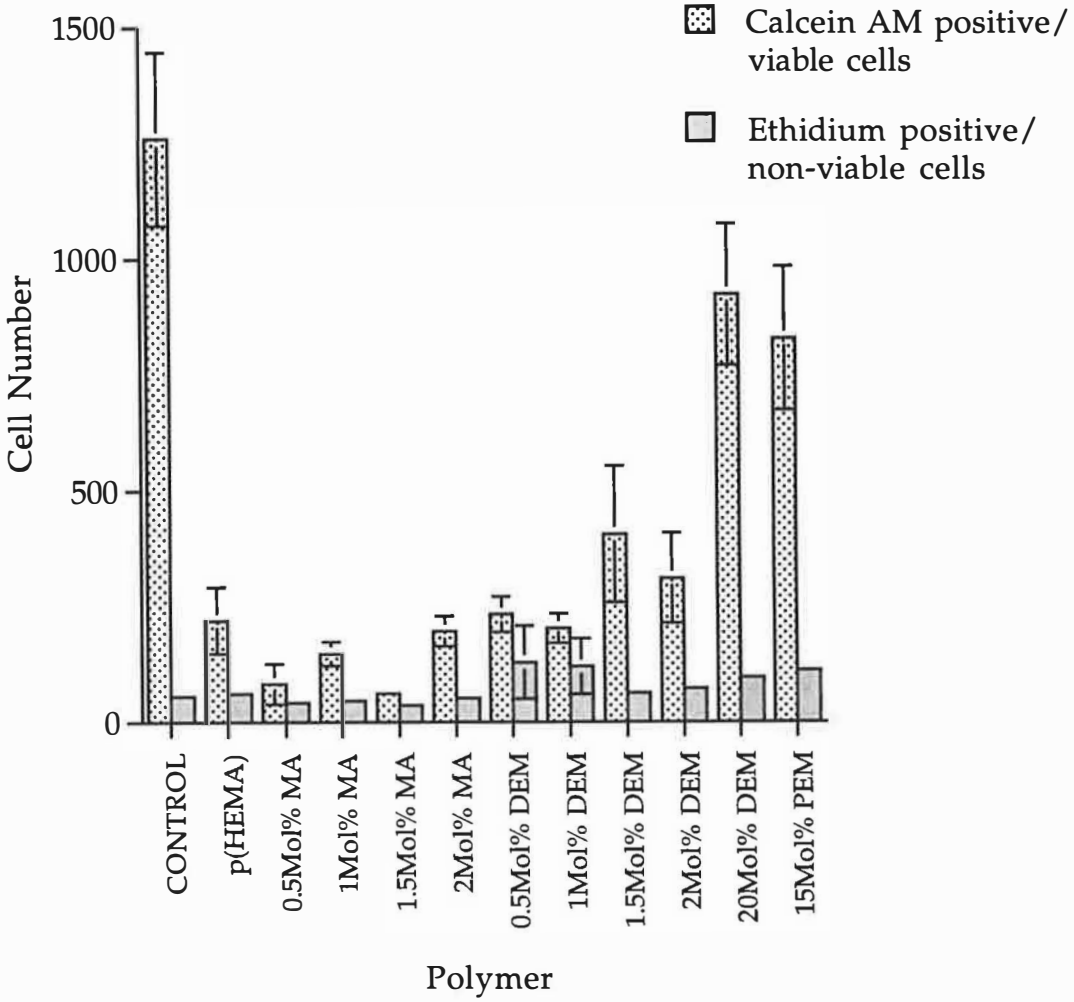

Figure 7.8
Calcein AM fluorescent staining depicting EK1.BR keratocyte adhesion to various methacrylic acid, 2-(dimethylamino)ethyl methacrylate and phenoxyethyl methacrylate containing p(HEMA) based hydrogels (x100 magnification)(images were captured in black and white on an Argus 50 image processor).

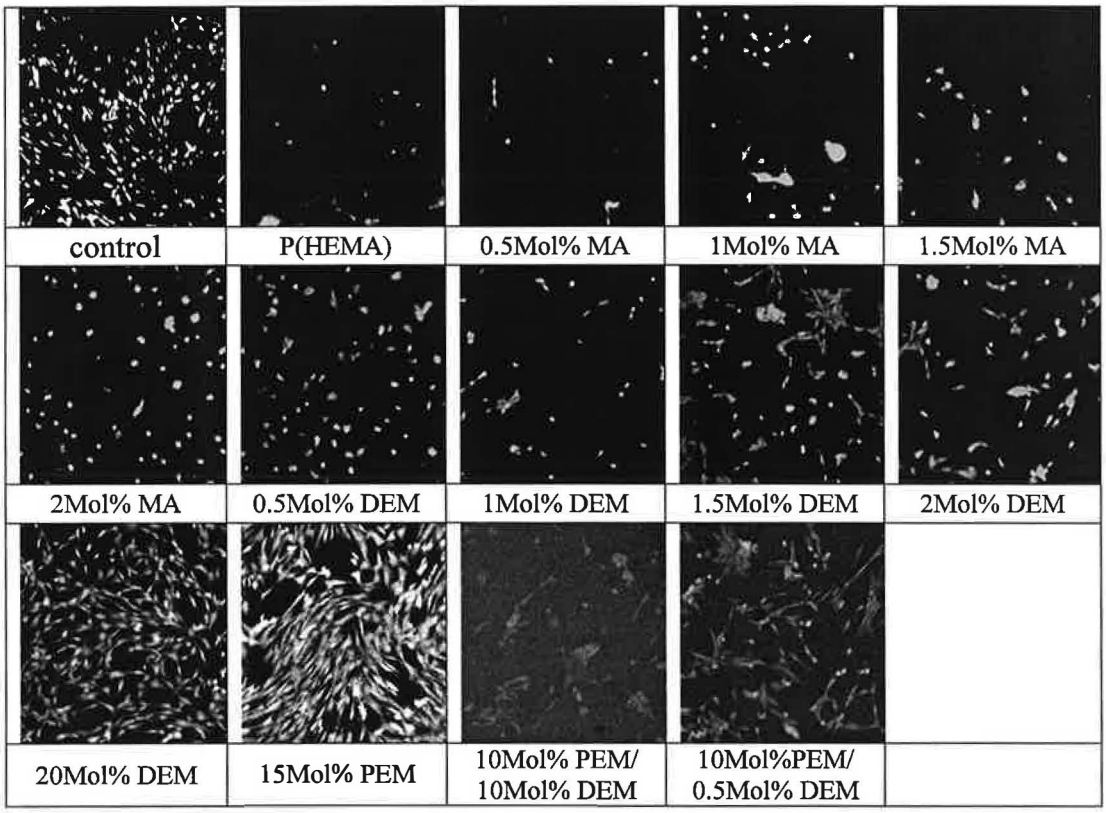

The second set of test materials included polymers mixing PEM and DEM in order to assess whether these materials have an additive effect on cell growth. It was also hoped that a combination polymer would possess improved physical properties since the 20 Mol% DEM polymer tended to swell and indicate alkalinity while the 15 Mol% PEM polymer tended to be brittle. Combining PEM and DEM within one polymer did not have the effect of each alone on cell growth. Swelling was reduced but the material still tended to be brittle. Viable cell counts were lower for the combination polymers than for the 20 Mol% DEM and 15 Mol% PEM containing polymers which were again similar to those observed for the controls (Figure 7.9). Results for cell adhesion to the combination polymers were variable as indicated by the large error bars in Figure 7.9. Some assays showed a large number of adherent cells with normal fibroblast-like morphology while other assays showed little cell growth onto the discs.

The number of non-viable cells adherent to the discs was low for all of the materials tested. The 0.5 and 1 Mol% DEM containing polymers were the only discs to show a slightly higher number of non-viable cells adherent to the material (Figure 7.7). In these cases remnants of the unpolymerised monomer or the ethanol initially used to sterilise the discs may have produced a cytotoxic effect.

7.4.3.2 ATP Assay

The ATP assay of serially decreasing cell concentrations showed that ATP content increased with increasing cell concentration making it possible to use the assay as a measure of cell adhesion to the various polymers. While ATP content appeared to be directly related to cell number at low cell concentrations it levelled off at cell concentrations higher than $5x10^4$ cells (Figure 7.10).

The ATP assay of materials revealed low levels of ATP and therefore cellular adhesion onto the surface of the p(HEMA), MA and 0.5 to 2 Mol% DEM containing polymers (Figure 7.11). The detection of ATP was high for the 15 Mol% PEM containing polymer discs. These results were

Figure 7.9
Viability/ Cytotoxicity Assay of p(HEMA) hydrogels incorporating positively charged 2(dimethylamino)ethyl methacrylate and hydrophobic phenoxyethyl methacrylate copolymers at varying concentrations. Results are expressed as the mean +/- SEM (n=4).

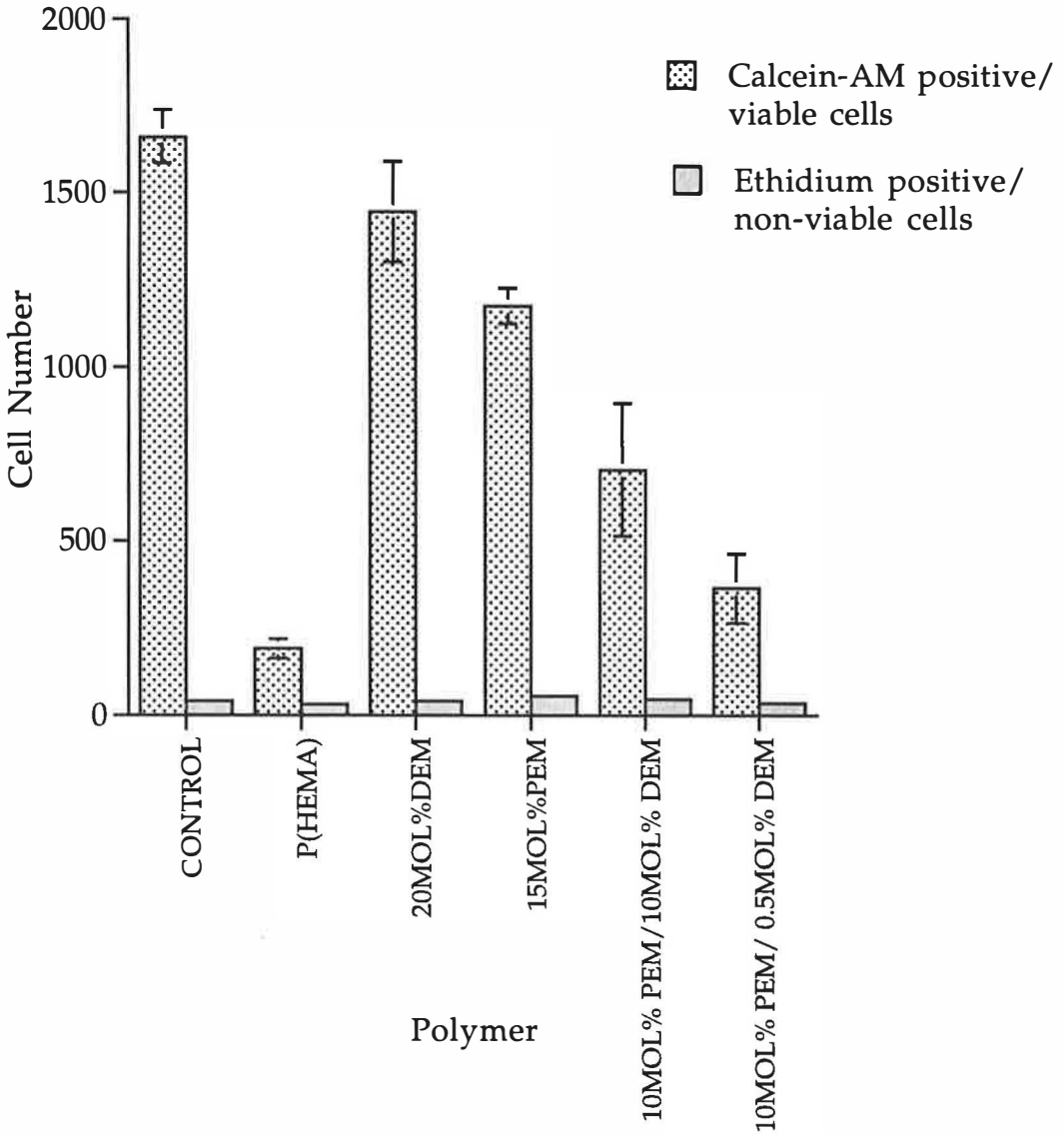

Figure 7.10
ATP assay of serially decreasing cell concentrations. Results are expressed on a log scale as the mean +/- SEM of 9 readings at each cell concentration. Triplicate readings of each cell concentration were taken in each of 3 separate experiments.

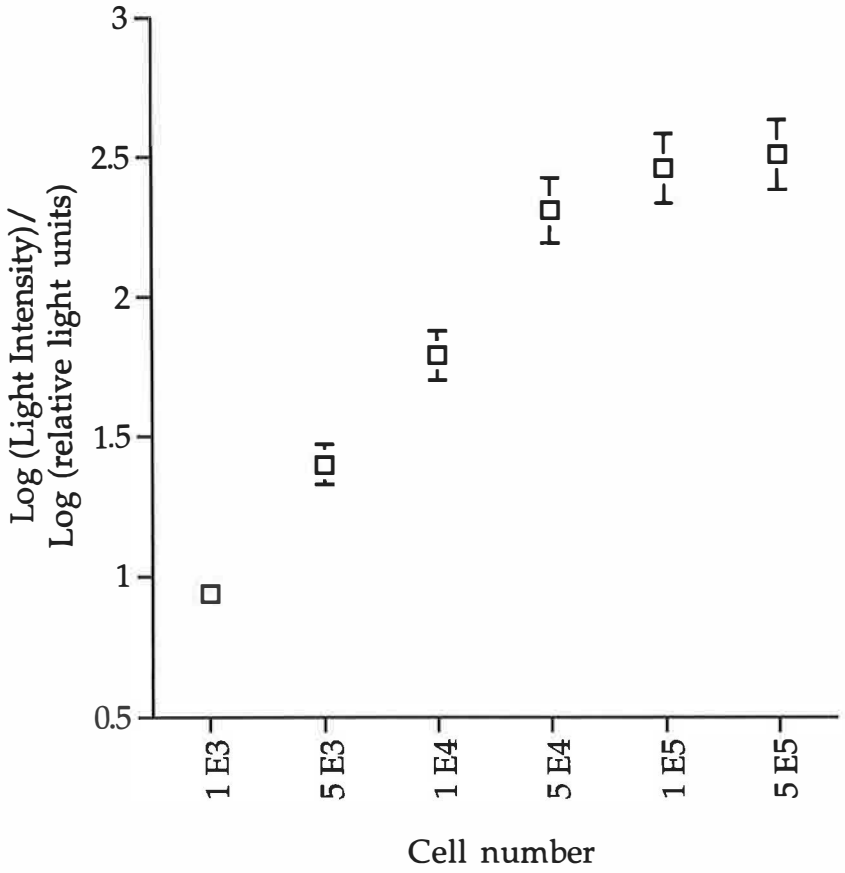

Figure 7.11
Use of a bioluminescence ATP assay as a measure of viable cell adhesion to various p(HEMA) based polymers. Results are expressed as the mean +/- SEM (n=6).

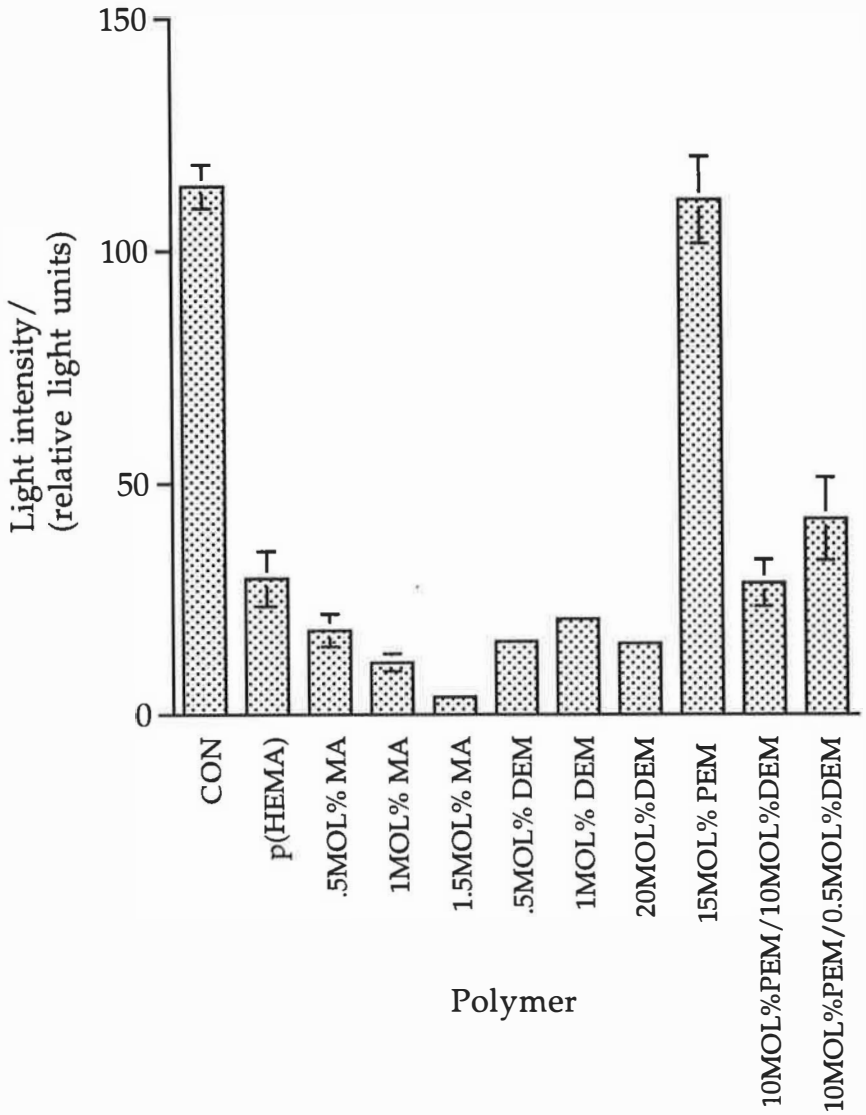

in agreement with the results of the viability/cytotoxicity assay. However, the detection of ATP lysed from cells adherent to the 20 Mol% DEM polymer was consistently low despite the observance under light microscope, of high numbers of adherent cells on the discs prior to the assay and the results of the viability/cytotoxicity assays.

The possibility that the ATP released following lysis of adherent cells was being absorbed by the material was tested. One disc of each material was placed at -18°C overnight with a known amount of the ATP standard in 400 µl TRIS-AC buffer covering each disc. On comparison to a control with no material present the DEM discs produced a lower light intensity reading indicating that the DEM containing discs were absorbing some of the ATP released on lysis of the cells so that it was unavailable for the assay.

7.4.4 Porous Polymers

Initial studies using varying concentrations of ethanol as a solvent resulted in less flexible polymers which were translucent above a concentration of 60% (v/v) ethanol. An 80 wt% water based p(HEMA) polymer using a hydrophilic, sodium metabisulphite/ammonium persulphate initiator system resulted in a translucent polymer which was extremely fragile. Pores formed in the water based polymer were larger than those formed using a similar volume of ethanol (Figure 7.12). Incorporation of 0.4 g of dextran into a 15 Mol% p(HEMA) polymer did not produce an even distribution of pores within the resulting polymer. On one side of the polymer some 'crater-like' structures, formed by dextran particles were observed under cryo-SEM (Figure 7.13). There was also some evidence that dextran particles were still present within the fabric of the polymer. The casting chambers were placed horizontally into the incubators and it is probable that the dextran within the monomer solution settled to the bottom prior to polymerisation producing pore like 'craters' in the bottom half of the resulting polymers only.

Figure 7.12
Cryo-SEM images comparing the structures of (a) 45% (v/v) ethanol (x15000) (b) 68% (v/v) ethanol (x15000) (c) 80 wt% water, porous p(HEMA) hydrogels (x5500) with that of (d) a 100% P(HEMA) hydrogel (x2000). Images were taken of a vertical section through each polymer.

(a)

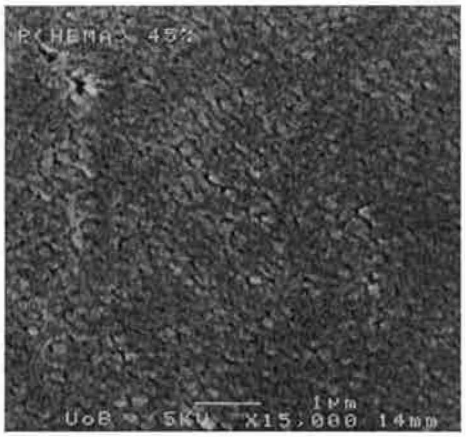

(b)

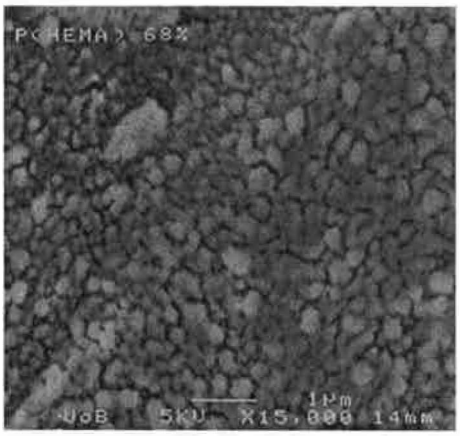

(c)

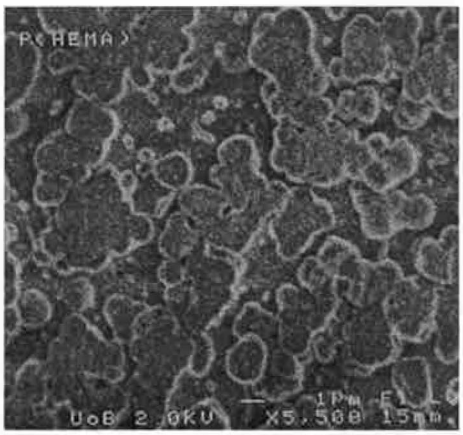

(d)

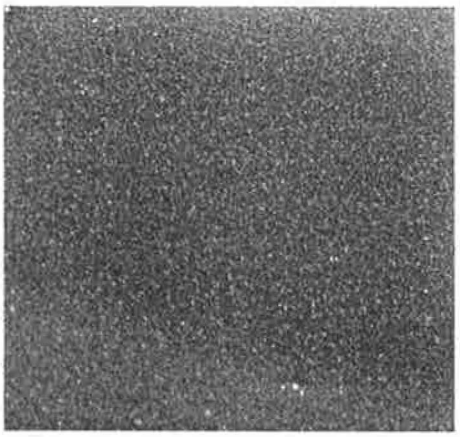

Figure 7.13
Cryo-SEM images depicting the effect of incorporating 0.4 g of dextran on the structure of a 15 Mol% PEM p(HEMA) polymer. Images were taken of a vertical section through each polymer.

(a) - dextran (x2000)

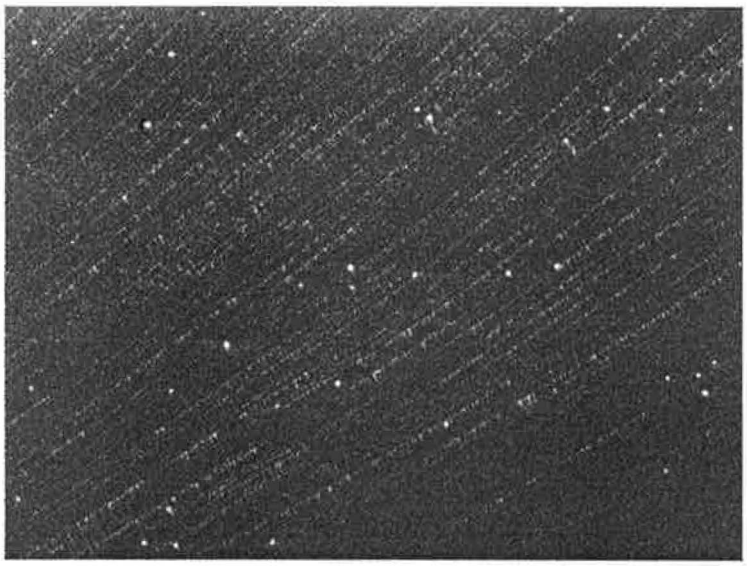

(b) + dextran (x9000)

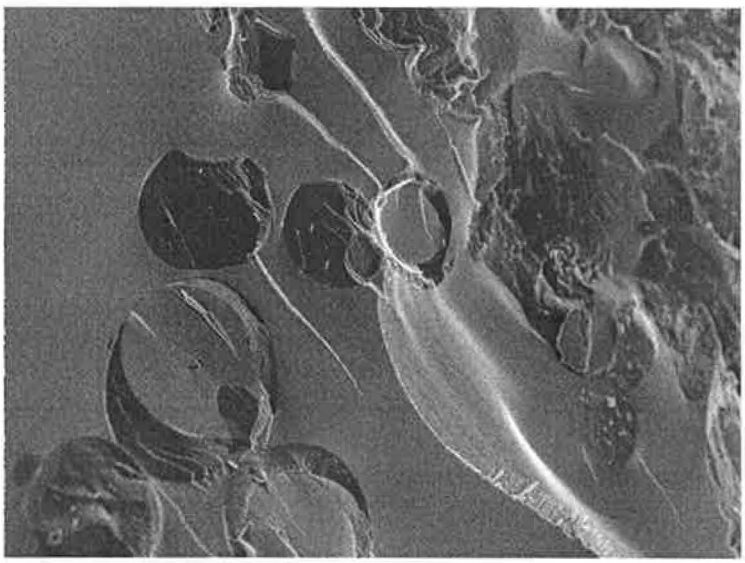

7.5 Discussion

7.5.1 Dye Absorption Assay

The dye absorption assays confirmed the incorporation of positively charged DEM and negatively charged MA within the p(HEMA) incorporation of MA or DEM within the p(HEMA) hydrogels produces a concentration and pH dependent effect on polymer surface charge characteristics.

7.5.2 Polymer Cytotoxicity and Adhesion Characteristics

7.5.2.1 Cell Cytotoxicity/Viability Assay

As previously observed cell adhesion and spreading onto the 100% p(HEMA) hydrogels was low (Peluso et al, 1997). Keratocytes tended to be sparse and rounded on the discs although some cell spreading occurred in patches. The incorporation of 20 Mol% DEM but not low concentrations of MA or DEM improved cell adhesion and spreading onto p(HEMA) based hydrogels. Results were in agreement with those of Smetana et al (1997) but not with those of Bergethon et al (1989) who found that both DEM and MA (0.1% vol) enhanced cell spreading. Since serum proteins tend to be negatively charged it is possible that protein absorption, which is required for cell adhesion, occurs more readily onto surfaces incorporating positive charge (Lee et al, 1997). The hydrophobic monomer PEM also appears to enhance cell adhesion and spreading onto p(HEMA) based hydrogels. Lydon et al (1985) suggest that moderation of p(HEMA) based hydrogel hydrophilicity by the incorporation of hydrophobic monomers enhances cell spreading and it may be that PEM alters the cell adhesion characteristics of p(HEMA) hydrogels in this way.

A slightly higher number of viable cells adhered to the 20 Mol% DEM p(HEMA) hydrogel discs than to the 15 Mol% PEM p(HEMA) discs (Figure 7.7 & 7.9). On the basis of their ability to support cell adhesion and growth both materials are potential KPro skirt materials. However, the 20 Mol% DEM discs tended to swell and the colour of the absorbed media suggested alkalinity. While the PEM containing discs tended to be brittle this may be reduced once pores are incorporated into the material.

The 15 Mol% PEM polymer may therefore be the better choice for further work towards a KPro skirt material. A polymer containing both PEM and DEM failed to improve the cell adhesion characteristics of either polymer and produced variable results (Figure 7.9). Inconsistencies during the polymerisation process may have caused the surface properties of the resulting polymers to vary so that some discs from the same material had a greater effect on cell adhesion that others.

7.5.2.2 ATP Assay

While the ATP assay gives some measure of the differences in cell adhesion to various polymers it was not found to be a sensitive or reliable assay and should be used in this context only in conjunction with the results of other assays. The potential for ATP absorption by the materials may produce errors. Also the light intensity readings vary considerably within a short amount of time making comparison of results both within and between assays difficult and making it necessary to analyse all materials for comparison in one assay. Variability is probably produced by the decay in activity of both the monitoring reagent and the lysed ATP which begins immediately following thawing.

Variability in readings with time also makes it impossible to accurately calculate the number of cells adherent to each material from a standard curve of cell concentration against light intensity. It is difficult to reproduce the same time frame for each part of the assay with enough accuracy to ensure that light intensity readings reflect only cell concentration. From the results of cell concentration against light intensity it is only possible to confirm that an increase in light intensity and thus ATP concentration indicates a greater number of cells adhering to the materials. The low sensitivity of the assay prevents accurate estimation of cell numbers. From the results of the ATP assay it is possible to confirm that the incorporation of PEM into a p(HEMA) hydrogel improves the ability of the material to maintain viable keratocyte growth. Although it is probable that the incorporation of 20 Mol% DEM also enhances p(HEMA) cell adhesion characteristics the absorption of ATP by the DEM containing polymers made it impossible

to analyse this probability using the ATP assay.

7.5.3 Pore Formers

The results of the cytotoxicity and adhesion studies suggest that a p(HEMA) hydrogel incorporating 20 Mol% DEM or PEM may be suitable for use as a KPro skirt material. The 15 Mol% PEM p(HEMA) polymer formulation was used in the dextran based pore forming studies while initial porous hydrogels, incorporating ethanol and water, were made completely of HEMA. Previous studies have suggested that an opening pore diameter of 10 μm is required for fibroblast migration into a p(HEMA) hydrogel (Chirila et al, 1993). Only the water based p(HEMA) hydrogel in this study had a structure which suggested the presence of pores of this size. However, the fragility of the polymer makes it unsuitable for use. Dextran particles which dissolved out while the polymers were being washed in water appeared to leave holes in the structure of the polymer. However, no continuous porous structure was apparent throughout the fabric of the polymer. Methods which maintain the even distribution of dextran during polymerisation may lead to the formation of a more continuous porous structure. Further development of techniques which introduce a porous infrastructure, large enough for cell invasion, but which allow adequate mechanical strength is necessary to establish a KPro skirt material which is suitable for implantation within the cornea.

Chapter 8

General Discussion

8.1 Requirements for a Successful Keratoprosthesis

The inability of some individuals with conditions resulting in corneal opacity to maintain a donor cornea and the shortage of donors in some areas necessitate the development of KPros with properties conducive to long-term retention within the eye. The high complication and extrusion rates of current designs are primarily related to the use of materials which are not compatible with the cornea and thus fail to induce an adequate repair response followed by integration of the KPro within the cornea and a return to relative quiescence.

Numerous properties which may enhance the long-term success of KPro designs have previously been highlighted (Hicks et al, 1997[a]). Materials should maintain a continuous epithelial sheet anteriorly but limit cell adhesion and retroprosthetic membrane growth posteriorly. Materials at the periphery of the KPro should limit avenues for cellular downgrowth and infection by encouraging rapid keratocyte migration into a porous interior. Porosity additionally allows nutrient through-flow and maintenance of hydration anterior to the KPro. Materials should be of adequate strength but should maintain flexibility so that mechanical friction and tissue necrosis are avoided. Adequate joins between the periphery and centre of the KPro should also limit epithelial downgrowth and infection. The protective function of the cornea against uv damage may be maintained by the incorporation of a ultraviolet light absorber. These properties only benefit the long-term retention of a KPro within the eye if the host cornea is capable of an adequate repair response to KPro insertion. The development of a successful KPro should therefore also consider the process of corneal wound repair, underlying changes which may hinder KPro integration and methods to accommodate such changes.

8.2 The Potential Effects of Ageing and Keratocyte Senescence on Corneal Wound Repair and KPro Integration

Age and the associated accumulation of senescent cells may produce changes in corneal wound repair and affect the corneal response to KPro implantation. A number of structural changes have been identified in

the cornea with age but little is known about changes in the process of corneal wound repair and the effects of senescence on corneal function. Corneal wound healing is a coordinated response to tissue damage which may be disrupted by the observed breakdown of fibroblast interactions with regulatory factors and the ECM following fibroblast senescence.

8.2.1 Corneal Wound Healing

The cornea's response to wounding is specifically designed for rapid restructuring of the corneal matrix and a return to visual acuity. The cornea is structurally designed to protect the eye and carries out the majority of light refraction required for focal imaging on the retina (Rawe et al, 1994). Collagen fibrillar spacing and hydration predominantly mediate the light refractive capability of the cornea (Svoboda et al, 1998). Restoration of visual acuity following corneal injury thus depends on restoration of corneal structure which in turn depends on the coordinated involvement of numerous regulatory factors to control the temporal activation of reparative pathways. Inflammatory cells are recruited into the area of tissue damage and secrete cytokines which activate resident corneal epithelial cells and keratocytes. Epithelial cells migrate across a FN/fibrin mesh to close the wound and anterior keratocyte apoptosis occurs followed by posterior keratocyte migration into the wound (Wilson, 1997; Wilson et al, 1996). Activated keratocytes remove debris, contract the wound and lay down a primary collagen matrix which is remodelled over time (Tuft et al, 1993). The inflammation, granulation tissue formation, wound contraction, scar formation and scar resolution stages of corneal wound repair are each mediated by the coordinated presence of specific activating and inhibitory factors secreted by inflammatory and resident cells.

Keratocytes are primarily responsible for the remodelling and resolution stages. They secrete proteases such as the MMPs in association with the TIMPS and structural proteins by autocrine, paracrine and exocrine mediated feedback pathways. Secretion occurs in association with corneal epithelial cell and ECM interactions so that excessive tissue

breakdown or deposition is prevented and a return to structural integrity is achieved. MMP activity unchecked by the balance of TIMPs may result in excessive tissue degradation as occurs in corneal ulceration and other inflammatory conditions. Excessive tissue deposition as occurs when scarring fails to be resolved may result from excessive TGF-β synthesis unchecked by the activity of growth factors with opposing effects on keratocyte secretion (O'Kane & Ferguson, 1997). The importance of a coordinated response to corneal wounding is apparent and is required following KPro implantation for integration within the cornea.

8.2.2 Senescence and Corneal Wound Healing

Senescent fibroblast activity is characterised by a lack of coordination in response to wounding and by an increase in matrix degradation (Sottile et al, 1987). The secretion of novel and defective proteins occurs (Cristofalo & Pignolo, 1993). The MMPs collagenase and stromelysin are constitutively overexpressed irrespective of serum conditions while the expression of TIMP-1 decreases (Millis et al, 1992; Millis et al, 1989; Sottile et al, 1988). The synthesis of the PGs and collagen is reduced (Takeda et al, 1992). The structure of FN and it's ability to mediate cell adhesion is altered (Chandrasekhar et al, 1983). Senescent fibroblasts are unable to proliferate in response to mitogenic stimulation and migration is slower (Wang, 1985; Kondo & Yonezawa, 1992). Some changes in the fibroblast's response to wounding are thought to be due to alterations in the signal transduction mechanisms which mediate signals following growth factor binding (Macieira-Coelho, 1983; Cristofalo & Pignolo, 1996; De Tata et al, 1993). The actin cytoskeleton, which mediates cell migration and the activation of some transcription factors, takes on a more rigid structure which may alter its ability to function normally (Wang & Gundersen, 1984). While the accumulation of senescent fibroblasts with altered repair characteristics in addition to a decline in rates of wound closure has been observed in the dermis with age the presence of senescent keratocytes within the cornea and their effect on wound healing has not previously been investigated (Dimri et al, 1995). A fall in the number of proliferating keratocytes, in keratocyte migration, in the secretion of structural proteins, changes in the structure of

proteins which mediate keratocyte adhesion and migration and an increase in degradative protease activity may limit the rate at which KPro integration occurs. However, since the phenotypic changes which accompany senescence show tissue specific variation it is necessary to directly assess the changes in senescent keratocyte phenotype rather than extrapolate the results of previous studies using other fibroblast types (Faragher et al, 1997).

A number of avenues exist by which keratocyte senescence may occur within the cornea. Keratocyte turnover in the corneal stroma has been estimated to occur every two to three years (Nishida, 1997). Also levels of DNA synthesis, indicative of keratocyte division across a twenty four hour period, have been detected in the stroma of embryonic, organ cultured eye globes (Hyldahl, 1986). Such evidence suggests that senescent keratocytes accumulate within the cornea following an increasing number of cell divisions throughout life. Keratocyte senescence may also occur as a by-product of cell cycle activation following initiation of a repair response or in response to DNA damage. Epithelial debridement has been shown to induce anterior keratocyte apoptosis and increases the probability of senescence by rapid induction of cell turnover during keratocyte repopulation of the stroma (Wilson et al, 1996). The induction of activated H-ras was recently shown to induce early senescence in dividing fibroblasts and suggests that corneal senescence may also result from mutational damage to cell DNA (Serrano et al, 1997).

In continuously dividing tissues the number of senescent fibroblasts tends to increase in an age related manner. In the cornea, where keratocytes tend to remain quiescent, the probability that an individual keratocyte will exit the cell cycle permanently and become senescent may remain relatively low unless numerous corneal insults occur. The need for continual tissue repair then requires rapid turnover of activated keratocytes and raises the probability of senescence within the keratocyte population. It is possible that within the cornea the presence of senescent keratocytes is related to the number of corneal insults

encountered throughout life rather than primarily to chronological age. In the corneae of elderly individuals the number of senescent keratocytes, with the potential to disrupt wound repair, would then be expected to vary considerably depending on the history of corneal damage. Individuals requiring KPros would be expected to undergo a sustained inflammatory response with heightened keratocyte turnover and the probability of increased keratocyte senescence. If this is the case the deleterious effects of senescent on corneal wound repair would not only be a consideration for the elderly but for all individuals requiring KPros. The universal impact of keratocyte senescence on KPro success would then demand its prioritisation in studies considering corneal wound healing and methods to enhance KPro biointegration.

8.3 Investigation of Changes in the Senescent Keratocyte Repair Response in Relation to KPro Biointegration

While previous literature highlights the properties required for KPro retention a suitable material has yet to be developed. Also the role which ageing and senescence play in corneal wound healing and KPro integration are unknown. Since the effects of senescence on keratocyte activity are poorly understood and may have an important impact on the successful integration of KPros within the cornea the present study considered aspects of the keratocyte repair response which may be affected by senescence. Materials used for the peripheral skirt of a KPro should ideally limit inflammation and enhance the keratocyte's response to wounding by encouraging the migration of host keratocytes into the fabric of the material to anchor it within the cornea. The present study also assessed potential KPro skirt materials by a preliminary investigation of their ability to enhance cell adhesion and spreading. Since keratocyte colonisation and maintenance of the anterior cornea requires the incorporation of pores within the KPro skirt, methods of pore formation were also considered.

8.3.1 Use of a Collagen Gel Matrix to Investigate Keratocyte Migration

The keratocyte response to wounding is multifaceted. Initial migration towards the area of tissue damage occurs in response to cytokines,

collagen fragments and other ECM components such as FN and HA. Activated keratocytes contract the wound and remodel damaged tissue. Collagen, FN, proteases, additional cytokines and structural proteins are secreted. Collagenase, the gelatinases and other proteases breakdown damaged collagen matrix and remodel the preliminary secreted matrix into a more ordered structure. These responses all occur in conjunction with ECM signalling so that accurate assessment of keratocyte responses and changes in responsiveness with senescence may be limited by the experimental environment. Previously, differences in fibroblast migratory response to FN fragments and TGF-β have been observed to depend on the experimental system used (Postlethwaite et al, 1991; Schor et al, 1996; Andresen et al, 1997; Schultz et al, 1992). The present study used a collagen matrix rather than a monolayer assay to assess keratocyte migration in an attempt to duplicate the environment in which normal keratocyte activity occurs. While a collagen matrix does not contain the same balance of PGs, FN, collagens and other components found in the ECM the environment is conducive to normal keratocyte responses. In a monolayer assay fibroblasts continue to proliferate until contact inhibition occurs while in a matrix fibroblasts exhibit similar proliferative constraints as those seen in the ECM. It was hoped that keratocyte migratory responses would also be reflective of *in vivo* behaviour.

8.3.2 Use of a Keratocyte Cell Strain to Investigate Senescence and Corneal Wound Healing

The current study used an embryonic keratocyte cell strain EK1.BR to investigate the keratocyte repair response. The effects of keratocyte ageing and an increase in senescent keratocyte activity were assessed by using EK1.BR keratocytes at the end of their proliferative lifespan in culture. Results were then used to make inferences about the effects of keratocyte senescence and corneal ageing on wound repair capacity. Since these studies assume that late passage embryonic keratocytes mirror the activity of keratocytes derived from elderly donors the migratory response was also assessed using an adult keratocyte cell strain. Although inferences can be made, it was not possible, within the

confines of the present study, to directly confirm that the accumulation of senescent keratocytes with detrimental effects on the repair response occurs to any significant extent within the ageing cornea. However, the occurrence of keratocyte turnover within the cornea indicates the accumulation of senescent keratocytes throughout life. Comparison of the shortened proliferative lifespan of the adult keratocyte cultures with that of the EK1.BR cultures in the present study also indicates keratocyte turnover and an increase in the number of senescent keratocytes within the cornea with age.

8.3.3 EK1.BR Keratocyte Migration

EK1.BR migration into a collagen matrix was initially assessed in the presence of serum and indicated that keratocyte senescence slows the migratory response. Previous studies have suggested that the decline in fibroblast migration associated with senescence is due to a decline in responsiveness to cytokine stimulation and is related to changes in cell structure, cellular pathways mediating migration and cell association with the ECM (Macieira-Coelho, 1983). A second study considered changes in keratocyte responsiveness to cytokine stimulation. Changes in migratory responsiveness to EGF were assessed under low serum conditions and indicated for the first time that the keratocyte migratory response to EGF is specifically reduced following senescence. Since FN mediates keratocyte adhesion and migration the effect of FN and the gelatin binding domain of FN on keratocyte migration were assessed. In contrast to previous studies investigating fibroblast responsiveness to FN and its domains, FN and GBD had no effect on keratocyte migration (Postlethwaite et al, 1991; Schor et al, 1996). These results may reflect a difference in tissue type response to exogenous FN addition or the ineffectiveness of the FN and GBD glycoprotein sources used. Since HA is also active during corneal wound healing its effect on keratocyte migration was also considered under low serum conditions (Fitzsimmons et al, 1992; Fagerholm et al, 1992). Again no effect on keratocyte migration was observed. The lack of keratocyte response may also be related to the source of HA used and to differences in EK1.BR responsiveness to exogenous HA addition.

8.3.4 Comparison of Adult and Embryonic Keratocyte Migration

In order to justify the use of late passage EK1.BR keratocyte cultures to predict changes in the activity of keratocytes within the aged cornea the migratory response of keratocytes derived from an elderly donor to EGF was also assessed. Analysis of adult keratocyte proliferative capacity indicated a rapid reduction in the percentage of proliferating adult keratocytes, as observed for the late passage EK1.BR keratocytes, until the cell culture effectively reached senescence at 16 cpds. EK1.BR keratocyte cultures passed through approximately 43 cpds prior to reaching senescence suggesting that the primary adult keratocyte cultures had passed through more divisions within the cornea and therefore had fewer cell cycles to go through in culture prior to senescence. Previously, it has been indicated that keratocytes divide within the cornea on average every two to three years (Nishida et al, 1997). The results of the present study suggest indirectly that keratocyte turnover and the accumulation of senescent keratocytes occurs within the cornea.

While more adult keratocytes migrated into the collagen gels in the presence and absence of EGF, addition of the growth factor had little additional effect on adult keratocyte migration. Although the number of adult keratocytes migrating into the collagen matrix does not indicate a decline in migratory ability with age, the results suggest that a reduction in migratory response to EGF occurs. Other variables may have influenced the heightened migration of the adult keratocytes. However, based on these results it can be concluded that the behaviour of late passage EK1.BR keratocytes does not exactly mirror the effects of ageing on keratocyte responses within the cornea but does give a general indication of the changes which occur with age. Some variation is to be expected since the constraints on the keratocyte within the cornea throughout life are different to those experienced by the keratocyte over a much shorter proliferative lifespan in culture. Additionally, previous investigations considering the differences in regulation of embryonic and adult fibroblast activity suggest that embryonic keratocytes may be influenced by different factors to those governing the behaviour of adult keratocytes (Cullen et al, 1997). Comparison of postnatal keratocyte

activity with that of the embryonic keratocytes may clarify this issue since differences in the type of factors regulating the migratory response add an additional variable which may complicate the interpretation of results.

8.3.5 EK1.BR Keratocyte Wound Contraction

The ability of EK1.BR keratocyte cultures to contract a corneal wound was also investigated using a collagen gel matrix. Keratocytes were able to contract a collagen matrix down to a sixth of its original height in a cell concentration dependent manner which did not alter at late passage. An increase in keratocyte senescence does not appear to alter the contractile ability of keratocyte cultures at the collagen gel concentration used in the present study. The results of the migration study suggest that contraction is not primarily a locomotion based event since a decline in keratocyte ability to contract a collagen matrix would be expected in concurrence with the observed decline in migratory capacity.

8.3.6 EK1.BR Gelatinase Secretion

MMP activity is central to the keratocyte's role in matrix remodelling. In the cornea the gelatinases MMP-2 and MMP-9 and collagenase are secreted in response to wounding. The constitutive secretion of MMP-2 by keratocytes is upregulated following wounding for involvement in long-term remodelling of the primary matrix. While upregulation of the MMPs collagenase and stromelysin has been detected in senescent fibroblasts the effect of keratocyte senescence on gelatinase secretion has not been investigated (Millis et al, 1992). Zymography was used to detect gelatinase activity and indicated that EK1.BR keratocytes secrete MMP-2 but not MMP-9 in detectable quantities in culture. In late passage cultures MMP-2 activity significantly decreased so that early passage keratocyte gelatinase activity was 130.5% +/- 15.5% (mean +/- SEM, n=8) that of late passage keratocyte gelatinase activity (Appendix 4.2). However, when normalised to cell number, gelatinase activity was found to increase in the protein samples extracted from late passage cell cultures from 1.1 +/- 0.12 uA to 1.8 +/- 0.15 uA per 10^6 cells (mean +/- SEM, n=11) (Appendix 4.3). The real impact of this increase in

remodelling capacity on corneal wound healing is unknown. However, additional changes in the activity of the other MMPs involved in corneal remodelling may produce a cumulative hindrance to corneal repair.

8.4 Investigation of Polymers for Use as KPro Skirt Materials

Following an investigation of changes in the keratocyte repair response to KPro implantation with increasing keratocyte senescence, a preliminary investigation of polymers suitable for use as KPro skirt materials was carried out. Polymers investigated for use as KPro skirt materials with characteristics conducive to keratocyte adhesion were p(HEMA) based. Although p(HEMA) has previously exhibited biocompatability with ocular tissues its ability to support cell adhesion and growth is poor (Peluso et al, 1997; Bergethon et al, 1989). The co-monomers MA, PEM and DEM were incorporated in varying amounts in an attempt to moderate p(HEMA) hydrophilicity and enhance cell adhesion. Assessment of viable keratocyte adhesion to the resulting polymers indicated that p(HEMA) polymers incorporating 20 Mol% DEM or 15 Mol% PEM were most conducive to cell adhesion and would form suitable KPro skirt materials in this respect. Pore formation within the polymers using the pore former dextran had limited success. The even distribution of dextran across the polymer and the formation of pores of a suitable size with channels throughout the polymer was difficult to achieve. Further development of this pore forming technique and other methods by which channels for keratocyte migration may be introduced into the structure of the polymer is required.

8.5 Conclusions and Further Work

Investigation of the migratory, contractile and secretory responses of EK1.BR keratocytes and changes occurring with senescence in culture suggest that a decline in wound healing capacity occurs. The migratory response of the keratocytes was generally reduced and a specific reduction in migratory responsiveness to EGF was observed. While keratocyte contractile ability appeared unchanged an increase in the activity of MMP-2 secreted by late passage keratocyte cultures occurred. Since the effects of senescence and corneal ageing on corneal wound

repair were assessed by comparison of early and late passage cultured embryonic keratocyte responses inferences can only be cautiously made. However, comparison of elderly donor and EK1.BR proliferative capacity suggests that some accumulation of senescent keratocytes occurs within the ageing cornea. The changes in keratocyte migration and secretory capacity observed in the present study may explain in part the decline in corneal wound healing observed in aged corneae and suggest that keratocyte senescence does have an impact on corneal functioning and specifically on corneal repair. In addition changes in the ability of the senescent keratocyte to respond to wounding will limit the rate of keratocyte colonisation of implanted KPros with effect at least on elderly patients but with the potential to affect all individuals requiring KPros. Comparison of corneae over a wide age range and corneae of similar ages which have undergone numerous or limited corneal insults throughout life is required to assess this possibility. The development of methods which directly demonstrate the presence of senescent keratocytes within the cornea and investigation of the molecular mechanisms by which keratocyte senescence results in the observed changes in migration, EGF responsiveness and MMP-2 secretion are an additional focus for further research.

p(HEMA) hydrogels incorporating 15 Mol% PEM and 20 Mol% DEM have been identified as potential KPro skirt materials by their ability to support keratocyte adhesion and spreading. In addition to the inclusion of pores further investigation may also consider the incorporation of other factors which enhance the corneal wound healing response. The incorporation of controlled release cytokines within the KPro design to assist in the reduction of inflammatory complications following implantation is already under consideration (Trinkaus-Randall & Nugent, 1998). FN and the growth factor EGF have previously been shown to enhance epithelial wound healing and EGF to specifically enhance stromal wound repair and wound tensile strength (Woost et al, 1985). Also the application of EGF, FN, aprotonin and an MMP inhibitor specifically blocked ulcerative inflammation following alkali burn related corneal injury (Schultz et al, 1992). Such results indicate that the

combined incorporation of factors associated with the repair response may help to limit inflammation and enhance KPro biointegration. In the present study, while senescence was found to be detrimental to the keratocyte migratory response to EGF and thus to corneal wound healing some response still occurred. This limited response may be exaggerated following KPro implantation either by incorporating an EGF release system within the design or by topical application. Numerous other factors with positive effects on corneal wound healing may also be considered to accommodate the changes in senescent keratocyte activity. However, the balance of regulatory factors required for a controlled response to wounding and thus for KPro incorporation within the cornea require careful investigation of methods to enhance corneal wound healing. Disruption of the balanced expression of regulatory factors, leading to excessive scarring or tissue breakdown, will enhance the complications common to KPro implantation and may lead to extrusion rather than to any beneficial effect.

In summary, keratocyte senescence appears to reduce the capacity of the keratocyte to respond to corneal wounding. Changes in the responsiveness of late passage keratocyte cultures appear to reflect, to some extent, the changes which occur in keratocyte responsiveness with age. Since the integration of KPro materials within the cornea is dependent on an adequate response to wounding, keratocyte senescence may provide an additional complication to KPro success. A polymer for use as a KPro skirt material has been identified which will enhance keratocyte adhesion and spreading. Further investigation of factors which may be incorporated into the design to enhance the keratocyte response to wounding will also help to accommodate the reduced capacity of senescent keratocytes to respond to wounding and the success of KPros within the ageing cornea.

Appendix 1

Buffer Recipes

1.1. For Cytochemical assays

a. Cacodylate buffer, pH 5.6

Make up a 0.2M solution of sodium cacodylate by dissolving 42.8 g of $Na(CH_3)_2AsO_2.3H_2O$ in 1000 ml of distilled water. Add 50 mls of this solution to 39.2 ml of 0.2M HCl and adjust the volume to 200 ml with distilled water.

b. Phosphate buffer, pH 7.4

Make up a 0.2M solution of monobasic sodium phosphate (27.8 g in 1000 mls of water).

Make up a 0.2M solution of dibasic sodium phosphate (71.7 g of $Na_2HPO_4.12H_2O$ in 1000 ml of water).

Add 19 ml of the monobasic solution to 81 ml of the dibasic solution and make the total volume up to 200 ml with distilled water.

1.2. For protein precipitation and sample preparation.

0.05M Tris HCl buffer pH 7.4 with 1% SDS and 10% glyerol.

0.05M Tris (MW=121) - 6.1 g/l

Mix 0.6 g Tris in 60ml water. Add SDS (1 g/100 ml) and glycerol (10 ml/100 ml). Add 1N HCl until pH 7.4 is reached. Adjust volume to 100 ml.

1.3. For SDS-PAGE

a. 10x Tris-glycine running buffer.

Add 72.1 g of glycine (MW=75) and 15.1 g of Tris to 500 ml water. Prior to use dilute 10x and add SDS (0.1% final concentration).

b. 1M Tris-HCl

1M Tris (MW=121)- 121 g/l

pH 8.8 - 12 g Tris in 80 ml water. Add 1N HCl until pH 8.8 is reached. Adjust volume to 100 ml.

pH 6.8 - 12 g Tris in 60 ml water. Add 1N HCl until pH 6.8 is reached.

Adjust volume to 100 ml.

1.4. For development of zymograms.

0.05M Tris-HCl pH 7.4 with 0.05M $CaCl_2$ added.

Add 0.6 g Tris to 60 ml water. Add 0.56 g of $CaCl_2$. Adjust pH to 7.4 using HCl. Make up to 100 ml.

0.05M $CaCl_2$ (FW=111) - 5.55 g/l

Appendix 2

DAPI Counts

2.1. DAPI counts for EK1.BR keratocyte migration data

Values indicate the total number of keratocytes counted in 3 fields across the surface of each gel.

CPD	Gel 1	Gel 2	Gel 3	Gel 4	Gel 5	Gel 6	MEAN
8.6	486	452	387	467	382	480	442
14.5	540	578	704	557	633	576	598
16.2	596	494	501	487	384	474	489
37.4	476	583	547	480	544	512	524
40.8	413	411	488	480	448	521	460
41.3	455	517	403	625	510	544	510

2.2 DAPI counts for EK1.BR migration in response to EGF data.

Values indicate the total number of keratocytes counted in 6 fields across each gel.

CPD	EGF1	EGF2	EGF3	MEAN	CON1	CON2	CON3	MEAN
10.2	667	681	679	675	630	509	570	570
10.2	695	759	712	722	650	693	632	661
11.9	886	898	898	893	1010	855	714	860
12.1	752	705	747	735	801	727	802	777
38.2	694	683	592	659	644	678	568	630
39	742	793	684	740	714	642	603	653
39.9	834	741	785	787	675	692	859	742
40.8	898	729	895	841	794	866	1014	891

2.3 DAPI counts for adult keratocyte migration in response to EGF data

Values indicate the total number of keratocytes counted in 6 fields across each gel.

CPD	EGF1	EGF2	EGF3	MEAN	CON1	CON2	CON3	MEAN
4.4	538	589	549	559	536	517	486	513
5.1	717	681	626	675	642	682	633	652
5.5	516	520	574	537	550	459	544	501
12.8	506	560	671	579	508	515	591	535
13.5	484	565	676	575	494	533	516	514
14.1	496	491	616	534	532	452	530	508
14.7	519	512	525	519	529	492	375	465

Appendix 3

Total protein concentration data

sample CPD	protein conc. range (μg/ml)	mean protein conc. (μg/ml)	no. of cells on passage	mean protein conc. per 10^6 cells
14.12	318, 382	350	$4x10^6$	87.5
16.05	236, 216, 225	225	$4x10^6$	56.25
17.97	368, 304, 324	331.6	$2.7x10^6$	122.8
17.61	215.8, 226.7, 239.2	227.2	$3.1x10^6$	73.3
44.12	202.5, 251.6	227.1	$1.63x10^6$	139.3
44.8	323, 247	285	$1.73x10^6$	164.7
46.3	300, 232, 294	275.3	$1.64x10^6$	167.9
46.2	338.3, 318.3	328.3	$1.2x10^6$	273.6
46.27	268.3, 284.2	276.25	$1.74x10^6$	158.8

Appendix 4

4.1. Zymogram 100 μg ml^{-1} protein bands expressed as a percentage of the total density of both bands.

cpd	late passage %	early passage %
46.3 v 14.12	33.5	66.5
44.12 v 14.12	48.6	51.4
44.8 v 16.05	50.9	49.1
46.3 v 17.97	58.3	41.7
46.2 v 17.61	36.4	63.6
46.27 v 17.61	43.2	56.8
46.27 v 17.61	38.3	61.7
46.3 v 16.05	48.7	51.3

4.2. Early passage (EP) gelatinase activity as a percentage of late passage (LP) gelatinase activity using IDV values from densitometric analysis of the zymograms (IDV= sum of all pixel values after background correction).

cpd	Early Passage IDV	Late Passage IDV	EP IDV/LP IDV x 100
46.3 v 14.12	160839	81144	198.2
44.12 v 14.12	182280	172050	105.9
44.8 v 16.05	38766	40257	96.3
46.3 v 17.97	9100	12740	71
46.2 v 17.61	148176	84672	175
46.27 v 17.61	93150	70725	131.7
46.27 v 17.61	115440	71760	160.8
46.3 v 16.05	28500	27075	105.2

mean=130.5%, SD=43.8, SEM=15.5

4.3 Units of gelatinase activity (uA) for each protein sample obtained from early and late passage EK1.BR cell cultures.

cpd	protein concentration µg/ml	uA*
14.12	318, 382	1.03, 1.24
16.05	236, 216, 225	.77, .70, .73
17.97	368, 304, 324	1.77, 1.46, 1.56
17.61	215.8, 226.7, 239.2	.91, .95, 1
44.12	202.5, 251.6	1.24, 1.54
44.8	323, 247	187, 1.43
46.3	300, 232, 294	1.83, 1.42, 1.79
46.2	338.3, 318.3	2.82, 2.65
46.27	268.3, 284.2	1.54, 1.63

Mean EP uA=1.1, SD=0.36, SEM=0.12
Mean LP uA=1.8, SD=0.5, SEM=0.15

*uA calculated as (protein concentration x 1.3/100) divided by the number of 10^6 keratocytes counted on passage of early passage cell cultures and as (protein concentration x 1/100) divided by the number of 10^6 keratocytes counted on passage of late passage cell cultures given in appendix 3.

Appendix 5

Monomer Molecular Weights

Monomer	Molecular Weight
Hydroxyethyl methacrylate (HEMA)	130
Phenoxyethyl methacrylate (PEM)	206.2
2-(Dimethylamino)ethyl methacrylate (DEM)	157.22
Methacrylic Acid (MA)	86.09

References

Albert, D. M. and F. A. Jakobiec. 1994. Principles and Practice of Ophthalmology. W.B. Saunders Company, London.

Albini, A., B. Pontz, M. Pulz, G. Allavena, H. Mensing, and P. Muller. 1988. Decline of fibroblast chemotaxis with age of donor and cell passage number. Collagen Rel. Res. 1:23-37.

Alcorta, D., Y. Xiong, D. Phelps, G. Hannon, D. Beach, and J. Barrett. 1996. Involvement of the cyclin-dependent kinase inhibitor p16 (INK4a) in replicative senescence of normal human fibroblasts. Proc. Natl. Acad. Sci. USA. 93:12742-13747.

al-Khateeb, T., P.Stephens, J. Shepherd, and D. Thomas. 1997. An investigation of preferential fibroblast wound repopulation using a novel *in vitro* wound model. J. Periodontol. 68:1063-1069.

Allsopp, R. A. and C. B. Harley. 1995. Evidence for a critical telomere length in senescent human fibroblasts. Exp. Cell Res. 219:130-136.

Altankov, G. and T. Groth. 1994. Reorganization of substratum-bound fibronectin on hydrophilic and hydrophobic materials is related to biocombatibility. J. Mat. Sci.: Mat. in Med. 5:732-737.

Alvarado, J., C. Murphy, and R. Juster. 1983. Age-related changes in the basement membrane of the human corneal epithelium. Invest. Ophthalmol. Vis. Sci. 24:1015-1028.

Andresen, J., T. Ledet, and N. Ehlers. 1997. Keratocyte migration and peptide growth factors: the effect of PDGF, bFGF, EGF, IGF-I, aFGF and TGF-β on human keratocyte migration in a collagen gel. Curr. Eye Res. 16:605-613.

Asari, A., S. Miyauchi, T. Takahashi, K. Kohno, and Y. Uchiyama. 1992. Localization of hyaluronic acid, chondroitin sulphate, and CD44 in rabbit cornea. Arch. Histol. Cytol. 55 (5):503-510.

Ashcroft, G. S., M. A. Boran, and M. W. Ferguson. 1995. The effects of aging on cutaneous wound healing in mammals. J. Anat. 187:1-26.

Azar, D. T., T. W. Hahn, S. Jain, Y. C. Yeh, and W. G. Stetler-Stevenson. 1996. Matrix metalloproteinases are expressed during wound healing after excimer laser keratectomy. Cornea. 15:18-24.

Bailey, A. 1987. Structure, function and ageing of the collagens of the eye. Eye. 1:175-183.

Baker, H. and C. P. Blair. 1968. Cell replacement in the human stratum corneum in old age. Br. J. Derm. 80:367-372.

Barnham, J. J. and M. J. Roper-Hall. 1983. Keratoprosthesis: a long-term review. Br. J. Ophthalmol. 67:468-474.

Begovac, P., Y. Shi, D. Mansfield, and B. Shur. 1994. Evidence that cell surface beta1,4-galactosyltransferase spontaneously galactosylates an underlying laminin substrate during fibroblast migration. J. Biol. Chem. 269 (50):31793-31799.

Bell, E., B. Ivarsson, and C. Merrill. 1979. Production of a tissue-like structure by contraction of collagen lattices by human fibroblasts of different proliferative potential in vitro. Proc. Natl. Acad. Sci. USA. 76 (3):1274-1278.

Bergethon, P., V. Trinkaus-Randell, and C. Franzblau. 1989. Modified hydroxyethylmethacrylate hydrogels as a modelling tool for the study of cell-substratum interactions. J. Cell Sci. 92:111-121.

Berman, M. 1994. Regulation of corneal fibroblast MMP-1 secretion by cytochalasins. Cornea. 31 (1):51-57.

Birk, D. E., J. M. Fitch, J. P. Babiarz, K. J. Doane, and T. F. Linsenmayer. 1990. Collagen fibrillogenesis in vitro: interaction of types I and V collagen regulates fibril diameter. J. Cell Sci. 95:649-657.

Birkedal-Hansen, H. 1995. Proteolytic remodeling of extracellular matrix. Current Opinion in Cell Biology. 7:728-735.

Birkedal-Hansen, H., W. Moore, M. Bodden, L. Windsor, B. Birkedal-Hansen, A. DeCarlo, and J. Engler. 1993. Matrix Metalloproteinases: a review. Critical Reviews in Oral Biology and Medicine. 4 (2):197-250.

Bodnar, A., M. Ouellette, M. Frolkis, S. Holt, C. Chiu, G. Morin, C. Harley, J. Shay, S. Lichtsteiner, and W. Wright. 1998. Extension of life-span by introduction of telomerase into normal human cells. Science. 270:349-352.

Bond, J., J. Blaydes, J. Rowson, M. Haughton, J. Smith, D. Wynford-Thomas, and F. Wyllie. 1995. Mutant p53 rescues human diploid cells from senescence without inhibiting the induction of SDI1/WAF1. Cancer Research. 55:2404-2409.

Bond, J., M. Haughton, J. Blaydes, V. Gire, D. Wynford-Thomas, and F. Wyllie. 1996. Evidence that transcriptional activation by p53 plays a direct role in the induction of cellular senescence. Oncogene. 13:2097-2104.

Bosmann, H., R. Gutheil, and K. Case. 1976. Loss of a critical neutral protease in ageing WI-38 cells. Nature. 261:499-501.

Bowen, I., S. Bowen, and A. Jones. 1998. Mitosis and apoptosis. Matters of life and death. Chapman & Hall. London.

Bradford, M. 1976. A rapid and sensitive method for the quantification of microgram quantities of protein utilizing the principle of protein-dye binding. Anal. Biochem. 72:248-254.

Brenner, A., M. Stampfer, and C. Aldaz. 1998. Increased p16 expression with senescence arrest in human mammary epithelial cells and extended growth capacity with p16 inactivation. Oncogene. 17:199-205.

Broberg, A. and J. Heino. 1996. Integrin alpha2beta1-dependent contraction of floating collagen gels and induction of collagenase are inhibited by tyrosine kinase inhibitors. Exp. Cell Res. 228:29-35.

Brown, D., M. Chwa, M. Escobar, and M. Kenney. 1991. Characterization of the major matrix degrading metalloproteinases of human corneal stroma. Evidence for an enzyme /inhibitor complex. Exp. Eye Res. 52:5-16.

Brown, J., W. Wei, and J. Sedivy. 1997. Bybass of senescence after disruption of p21 CIP1/WAF1 gene in normal diploid human fibroblasts. Science. 277:831-833.

Brown, S. and C. Weller. 1970. Cell origin of collagenase in normal and wounded corneas. Arch. Ophthalmol. 83:74-77.

Bruce, S. and S. Deamond. 1991. Longitudinal study of in vivo wound repair and in vitro cellular senescence of dermal fibroblasts. Experimental Gerontology. 26:17-27.

Bruin, P., E. Meeuwsen, M. van Andel, J. Worst, and A. Pennings. 1993. Autoclavable highly cross-linked polyurethane networks in ophthalmology. Biomaterials. 14 (14):1089-1097.

Buckley-Sturrock, A., S. W. Woodward, R. M. Senior, G. L. Griffin, M. Klagsbrun, and J. M. Davidson. 1989. Differential stimulation of collagenase and chemotactic activity in fibroblasts derived from rat wound repair tissue and skin by growth factors. J. Cell. Physiol. 138:70-78.

Cameron, J. 1997. Corneal reaction to injury. In Cornea- Fundamentals of Cornea and External Disease. Volume I. Krachmer, Mannis, and Holland, editors. Mosby- Year Book Inc., St. Louis. 163-182.

Campisi, J. 1997. The biology of replicative senescence. European Journal of Cancer. 33(5):703-709.

Cardona, H. 1962. Keratoprosthesis. Am J. Ophthalmol. 54:284-294.

Cardona, H. 1991. The cardona experience: 40 years experience. Refractive and Corneal Surgery. 7:468-471.

Cardona, H. 1969. Mushroom transcorneal keratoprosthesis. Am J. Ophthalmol. 68 (4):604-612.

Carver, W., I. Molano, T. Reaves, T. Borg, and L. Terracio. 1995. Role of the alpha1beta1 integrin complex in collagen gel contraction in vitro by fibroblasts. J. Cell. Physiol. 165:425-437.

Castroviejo, R., H. Cardona, and G. DeVoe. 1969. Present studies of prosthokeratoplasty. Am J. Ophthalmol. 68 (4):613-625.

Chandrasekhar, S., J. A. Sorrentino, and A. J. T. Millis. 1983. Interaction of fibronectin with collagen: age-specific defect in the biological activity of human fibroblast fibronectin. Proc. Natl. Acad. Sci. USA. 80:4747-4751.

Chang, P., S. Lee, and G. Hsiue. 1998. Heterobifunctional membranes by plasma induced graft polymerization as an artificial organ for penetration keratoprosthesis. J. Biomed. Mater. Res. 39:380-389.

Chatterjee, A., J. Freeman, and H. Busch. 1987. Identification and partial characterization of a Mr 40,000 nucleolar antigen associated with cell proliferation. Cancer Research. 47:1123-1129.

Chellappan, S., S. Hiebert, M. Mudryj, J. Horowitz, and J. Nevins. 1991. The E2F transcription factor is a cellular target for the RB protein. Cell. 65:1053-1061.

Chen, J., M. Grant, A. Schor, and S. Schor. 1989. Differences between adult and foetal fibroblasts in the regulation of hyaluronate synthesis: correlation with migratory activity. J. Cell Sci. 94:577-584.

Chirila, T. 1997. Artificial cornea with a porous polymeric skirt. TRIP. 5 (11):346-348.

Chirila, T., I. Constable, G. Crawford, S. Vijayasekaran, D. Thompson, Y. Chen, and W. Fletcher. 1993. Poly(2-hydroxyethyl methacrylate) sponges as implant materials: in vivo and in vitro evaluation of cellular invasion. Biomaterials. 14 (1):26-38.

Chiou, A., G. Florakis, and M. Kazim. 1998. Management of conjunctival cicatrizing diseases and severe ocular surface dysfunction. Surv. Ophthalmol. 43:19-46.

Chirila, T., D. Yu, Y. Chen, and G. Crawford. 1995. Enhancement of mechanical strength of poly(2-hydroxyethyl methacrylate) sponges. J. Biomed. Mater. Res. 29:1029-1032.

Chirila, T. V. 1994. Modern artificial corneas: the use of porous polymers. TRIP. 2 (9):296-300.

Chirila, T. V., D. E. Thompson-Wallis, G. J. Crawford, I. J. Constable, and S. Vijayasekaran. 1996. Production of neocollagen by cells invading hydrogel sponges implanted in the rabbit cornea. Graefe's Arch. Clin. Exp. Ophthalmol. 234:193-198.

Chiu, C. and C. Harley. 1997. Replicative senescence and cell immortality: the role of telomeres and telomerase. P. S. E. B. M. 214:99-106.

Cintron, C., L. Hassinger, C. Kublin, and D. Cannon. 1978. Biochemical and ultrastructural changes in collagen during corneal wound healing. Journal of Ultrastructure Research. 65:13-22.

Civerchia-Perez, L., B. Faris, G. LaPointe, J. Beldekas, H. Leibowitz, and C. Franzblau. 1980. Use of collagen-hydroxyethylmethacrylate hydrogels for cell growth. Proc. Natl. Acad. Sci. USA. 77 (4):2064-2068.

Clayton, A., T. Chirila, and P. Dalton. 1997[a]. Hydrophilic sponges based on 2-hydroxyethyl methacrylate. III. Effect of incorporating a hydrophilic crosslinking agent on the equilibrium water content and pore structure. Polymer International. 42:45-56.

Clayton, A., T. Chirila, and X. Lou. 1997[b]. Hyrophilic sponges based on 2-hydroxyethyl methacrylate. V. effect of crosslinking agent reactivity on mechanical properties. Polymer International. 44:201-207.

Coupland, S., P. Penfold, and F. Billson. 1993. Histochemical survey of the anterior segment of the normal human foetal and adult eye. Graefe's Arch. Clin. Exp. Ophthalmol. 231:533-540.

Coupland, S., F. Billson, and F. Hoffmann. 1994[a]. Hydrolase participation in allograft rejection in rat penetrating keratoplasty. Graefe's Arch. Clin. Exp. Ophthalmol. 232:614-621.

Coupland, S., P. Penfold, and F. Billson. 1994[b]. Hydrolases of anterior segment tissues in the normal human, pig and rat eye: a comparative study. Graefe's Arch. Clin. Exp. Ophthalmol. 232:182-191.

Courvalin, J., G. Segil, G. Blobel, and H. Worman. 1992. The lamin B receptor of the inner nuclear membrane undergoes mitosis-specific phosphorylation and is a substrate for p34[cdc2]-type protein kinase. J. Biol. Chem. 267(27): 19035-19038.

Crawford, G., T. Chirila, S. Vijayasekaran, P. Dalton, and I. Constable. 1996. Preliminary evaluation of a hydrogel core-and -skirt keratoprosthesis in the rabbit cornea. Journal of Refractive Surgery. 12:525-529.

Crawford, G., I. Constable, T. Chirila, S. Vijayasekaran, and D. Thompson. 1993. Tissue interaction with hydrogel sponges implanted in the rabbit cornea. Cornea. 12 (4):348-357.

Cristofalo, V. J. and R. J. Pignolo. 1993. Replicative senescence of human fibroblast-like cells in culture. Physiology Reviews. 73 (3):617-638.

Cristofalo, V. and R. Pignolo. 1996. Molecular markers of senescence in fibroblast-like cultures. Experimental Gerontology. 31 (1/2):111-123.

Cristofalo, V. and M. Tresini. 1998. Defects in signal transduction during replicative senescence of diploid human fibroblasts in vitro. Aging Clin. Exp. Res. 10 (2):151-152.

Cullen, B., D. Silcock, L. Brown, A. Gosiewska, and J. Geesin. 1997. The differential regulation and secretion of proteinases from fetal and neonatal fibroblasts by growth factors. Int. J. Biochem. Cell Biol. 29 (1):241-250.

Davison, H. 1991. Physiology of the Eye. MacMillan Academic and Professional Ltd., London.

Davison, P. and E. Galbavy. 1986. Connective tissue remodeling in corneal and scleral wounds. Invest. Ophthalmol. Vis. Sci. 27 (10):1478-1484.

Daxer, A., K. Misof, B. Grabner, A. Ettl, and P. Fratzl. 1998. Collagen fibrils in the human corneal stroma: structure and aging. Invest. Ophthalmol. Vis. Sci. 39 (3):644-648.

De Tata, V., A. Ptasznik, and V. Cristofalo. 1993. Effect of the tumor promoter phorbol 12-myristate 13-acetate (PMA) on proliferation of young and senescent WI-38 human diploid fibroblasts. Exp. Cell Res. 205:261-269.

Desmouliere, A. 1995. Factors influencing myofibroblast differentiation during wound healing and fibrosis. Cell Biology International. 19 (5):471-476.

Dice, F. 1993. Cellular and molecular mechanisms of aging. Physiological Reviews. 73 (1):149-159.

Dimri, G. P., E. Hara, and J. Campisi. 1994. Regulation of two E2F-related genes in presenescent and senescent human fibroblasts. J Biol. Chem. 269 (23):16180-16186.

Dimri, G., X. Lee, G. Basile, M. Acosta, G. Scott, C. Roskelley, E. Medrano, M. Linskens, I. Rubelj, O. Pereira-Smith, M. Peacocke, and J. Campisi. 1995. A biomarker that identifies senescent human cells in culture and in aging skin in vivo. Proc. Natl. Acad. Sci. USA. 92:9363-9367.

Dimri, G. P., A. Testori, M. Acosta, and J. Campisi. 1996. Replicative senescence, aging and growth-regulatory transcription factors. Biological Signals. 5:154-162.

Ding, M. and N. Burstein. 1988. Review: Fibronectin in corneal wound healing. Journal of Ocular Pharmacology. 4 (1):75-91.

Dohlman, C. H. and M. G. Doane. 1994. Some factors influencing outcome after keratoprosthesis surgery. Cornea. 13 (3):214-218.

Dohlman, C. and H. Terada. 1998. Keratoprosthesis in pemphigoid and Stevens-Johnson syndrome. Advances in Experimental Medicine and Biology. 438:1021-1025.

Doughty, M. 1994. The cornea and corneal endothelium in the aged rabbit. Optometry and Vision Science. 71 (12):809-818.

Drescher-Lincoln, C. K. and J. R. Smith. 1983. Inhibition of DNA synthesis in proliferating human diploid fibroblasts by fusion with senescent cytoplasts. Exp. Cell Res. 144:455-462.

Dropcova, S., S. Denyer, A. Lloyd, P. Gard, G. Hanlon, S. Mikhalovsky, S. Sandeman, C. Olliff, and R. Faragher. 1999. A standard strain of human ocular keratocytes. Ophthalmic Res. 31:33-41.

Drubaix, I., J. M. Legeais, N. Malek-Chehire, M. Savoldelli, M. Menasche, L. Robert, G. Renard, and Y. Pouliquen. 1996. Collagen synthesized in fluorocarbon polymer implant in the rabbit cornea. Exp. Eye Res. 62:367-376.

Drubaix, I., J. M. Legeais, L. Robert, and G. Renard. 1997. Corneal hyaluronan content during post-ablation healing: evidence for a transient depth-dependent contralateral effect. Exp. Eye Res. 64:301-304.

Drubaix, I., J. Legeais, F. Mounier, B. Briat, L. Robert, and G. Renard. 1998. Quantification and localization of hyaluronan in a PTFE polymer implanted in the corneal stroma. J. Biomed. Mater. Res. 40:442-448.

Dulic, V., L. Drullinger, E. Lees, S. Reed, and G. Stein. 1993. Altered regulation of G_1 cyclins in senescent human diploid fibroblasts: Accumulation of inactive cyclin E-Cdk2 and cyclin D1-Cdk2 complexes. Proc. Natl. Acad. Sci. USA. 90:11034-11038.

Drummond, A. H. 1996. Matrix metalloproteases and disease. FASEB. 10 (6):754.(Abstr.)

Dutt, S., R. Steinert, M. Raizman, and C. Puliafito. 1994. One-year results of eximer laser photorefractive keratectomy for low to moderate myopia. Arch. Ophthalmol. 112:1427-1436.

Edwards, D., K. Leco, P. Beaudry, P. Atadja, C. Veillette, and K. Riabowol. 1996. Differential effect of transforming growth factor-beta1 on the expression of matrix metalloproteinases and tissue inhibitors of metalloproteinases in young and old human fibroblasts. Experimental Gerontology. 31 (1/2):207-223.

Ehrlich, H. and J. Rajaratnam. 1990. Cell locomotion forces versus cell contraction forces for collagen lattice contraction: an in vitro model of wound contraction. Tissue and Cell. 22 (4):407-417.

Ejim, O. S., G. W. Blunn, and R. A. Brown. 1993. Production of artificial-orientated mats and strands from plasma fibronectin: a morphological study. Biomaterials. 14(10):743-748.

El-Deiry, W., T. Tokino, V. Velculescu, D. Levy, R. Parsons, J. Trent, D. Lin, W. Mercer, K. Kinsler, and B. Vogelstein. 1993. WAF1, a potential mediator of p53 tumor suppression. Cell. 75:817-825.

Eleftheriou, C. S., N. B. Trakas, and S. J. Tzartos. 1991. Cellular ageing related proteins secreted by human fibroblasts. Mutation Research. 256:127-138.

Ellis, I., A. M. Grey, A. M. Schor, and S. L. Schor. 1992. Antagonistic effects of TGF-beta1 and MSF on fibroblast migration and hyaluronic acid synthesis. J. Cell Sci. 102:447-456.

Ellis, I., J. Banyard, and S. Schor. 1997. Differential response of fetal and adult fibroblasts to cytokines: cell migration and hyaluronan synthesis. Development. 124:1593-1600.

Elsdale, T. and J. Bard. 1972. Collagen substrata for studies on cell behaviour. J. Cell Biol. 54:626-637.

Fagerholm, P., T. Fitzsimmons, A. Harfstrand, and M. Schenholm. 1992. Reactive formation of hyaluronic acid in the rabbit corneal alkali burn. Acta. Ophthalmologica. 70 (202):67-72.

Faragher, R. G., I. R. Kill, J. A. Hunter, F. M. Pope, C. Tannock, and S. Shall. 1993. Proc. Natl. Acad. Sci. USA. 90:12030-12034.

Faragher, R., B. Mulholland, S. Tuft, S. Sandeman, and P. Khaw. 1997. Aging and the cornea. Br. J. Ophthalmol. 81 (10):814-817.

Fini, M. E. and M. T. Girard. 1990[a]. Expression of collagenolytic/gelatinolytic metalloproteinases by normal cornea. Invest. Ophthalmol. Vis. Sci. 31:1779-1788.

Fini, M. E. and M. T. Girard. 1990[b]. The pattern of metalloproteinase expression by corneal fibroblasts is altered by passage in cell culture. J. Cell Sci. 97:373-383.

Fini, M. E., M. T. Girard, and M. Matsubara. 1992[a]. Collagenolytic/Gelatinolytic enzymes in corneal wound healing. Acta. Ophthalmologica Suppl. 202:26-33.

Fini, M. E., Y. J. T. Yue, and J. Sugar. 1992[b]. Collagenolytic/gelatinolytic metalloproteinaases in normal and keratoconus corneas. Curr. Eye Res. 11:849-862.

Finkel, E. 1996. Telomerase highlights senescence as a factor in cancer. The Lancet. 347:529.

Fitch, J., D. Birk, C. Linsenmayer, and T. Linsenmayer. 1990. The spatial organization of descemet's membrane-associated type IV collagen in the avian cornea. J. Cell Biol. 110:1457-1468.

Fitton, J., B. Ziegalaar, C. Hicks, A. Clayton, G. Crawford, I. Constable, and T. Chirila. 1998. Assessment of anticollagenase treatments after insertion of a keratoprosthetic material in the rabbit cornea. Cornea. 17 (1):108-114.

Fitzsimmons, T., P. Fagerholm, A. Harfstrand, and M. Schenholm. 1992. Hyaluronic acid in the rabbit cornea after eximer laser superficial keratectomy. Invest. Ophthalmol. Vis. Sci. 33 (11):3011-3016.

Fukami, J., K. Anno, K. Ueda, T. Takahashi, and T. Ide. 1995. Enhanced expression of cyclin D1 in senescent human fibroblasts. Mechanisms of Ageing and Development. 81:139-157.

Funderburgh, J. and J. Chandler. 1989. Proteoglycans of rabbit corneas wih nonperforating wounds. Invest. Ophthalmol. Vis. Sci. 30 (3):435-442.

Fundingsland, B. R. and K. A. Buzard. 1996. Non-invasive assessment of corneal wound healing. Invest. Ophthalmol. Vis. Sci. 37 (3):S320.

Garkavtsev, I., C. Hull, and K. Riabowol. 1998. Molecular aspects of the relationship between cancer and aging: tumor suppressor activity during cellular senescence. Experimental Gerontology. 33 (1/2):81-94.

Gerdes, J., U. Schwab, H. Lemke, and H. Stein. 1983. Production of a mouse monoclonal antibody reactive with a human nuclear antigen associated with cell proliferation. Int. J. Cancer. 31:13-20.

Gibson, I. and R. Anderson. 1977. Actin filaments in normal and migrating corneal epithelial cells. Invest. Ophthalmol. Vis. Sci. 16 (2):161-166.

Gibson, J., S. Milam, and R. Klebe. 1989. Late passage cells display an increase in contractile behaviour. Mechanisms of Ageing and Development. 48:101-110.

Gibson, I. K., H. Watanabe, and J. D. Zieske. 1993. Corneal wound healing and fibronectin. International Ophthalmology. 33 (4):149-163.

Gipson, I., S. Spurr-Michaud, and A. Tisdale. 1987. Anchoring fibrils form a complex network in human and rabbit cornea. Invest. Ophthalmol. Vis. Sci. 28:212-220.

Girard, L. J. 1983. Keratoprosthesis. Cornea. 2:207-224.

Girard, M., M. Matsubara, and M. Fini. 1991. Transforming growth factor-beta and interleukin-1 modulate metalloproteinase expression by corneal stromal cells. Invest. Ophthalmol. Vis. Sci. 32:2441-2454.

Gire, V. and D. Wynford-Thomas. 1998. Reinitiation of DNA synthesis and cell division in senescent human fibroblasts by microinjection of anti-p53 antibodies. Molecular and Cellular Biology. 18 (3):1611-1621.

Goa, K. and P. Benfield. 1994. Hyaluronic acid. Drugs. 47 (3):536-566.

Gomez, D., D. Alonso, H. Yoshiji, and U. Thorgeirsson. 1997. Tissue inhibitors of metalloproteinases: structure, regulation and biological functions. European Journal of Cell Biology. 74:111-122.

Gordon, J., E. Bauer, and A. Eisen. 1980. Collagenase in human cornea. Arch. Ophthalmol. 98:341-345.

Grana, X. and P. Reddy. 1995. Cell cycle control in mammalian cells: role of cyclins, cyclin dependent kinases (CDKs), growth suppressor genes and cyclin-dependent kinase inhibitors (CKIs). Oncogene. 11:211-219.

Gray, R. D. and C. A. Paterson. 1994. Application of peptide-Based matrix metalloproteinase inhibitors in corneal ulceration. Annals New York Academy of Sciences. 732:206-216.

Green, K. 1991. Corneal endothelial structure and function under normal and toxic conditions. Cell Biology Reviews. 25 (3):169-207.

Greider, C. W. 1990. Telomeres, telomerase and senescence. Bioessays. 12 (8):363-369.

Greiling, D. and R. Clark. 1997. Fibronectin provides a conduit for fibroblast transmigration from collagenous stroma into fibrin clot provisional matrix. J. Cell Sci. 110:861-870.

Grey, A., A. Schor, G. Rushton, I. Ellis, and S. Schor. 1989. Purification of the migration stimulating factor produced by fetal and breast cancer patient fibroblasts. Proc. Natl. Acad. Sci. USA. 86:2438-2442.

Grigoriev, V., R. Thweatt, E. Moerman, and S. Goldstein. 1996. Expression of senescence-induced protein WS3-10 in vivo and in vitro. Experimental Gerontology. 31 (1/2):145-157.

Grove, G. 1982. Age-related differences in healing of superficial skin wounds in humans. Arch Dermatol Res. 272:381-385.

Guidry, C. and F. Grinnell. 1985. Studies on the mechanism of hydrated collagen gel reorganization by human skin fibroblasts. J. Cell Sci. 79:67-81.

Hanna, C., D. Bicknell, and J. O'Brien. 1961. Cell turnover in the adult human eye. Archives of Ophthalmology. 65:111-114.

Harris, A., D. Stopak, and P. Wild. 1981. Fibroblast traction as a mechanism for collagen morphogenesis. Nature. 290:249-251.

Hassell, J., C. Cintron, C. Kublin, and D. Newsome. 1983. Proteoglycan changes during restoration of transparency in corneal scars. Archiv. Biochem. Biophys. 222:362-369.

Hassell, J., P. Schrecengost, J. Rada, N. SundarRaj, G. Sossi, and R. Thoft. 1992. Biosynthesis of stromal matrix proteoglycans and basement membrane components by human corneal fibroblasts. Invest. Ophthalmol. Vis. Sci. 33 (3):547-557.

Hayflick, L. and P. Moorhead. 1961. The serial cultivation of human diploid cell strains. Exp. Cell Res. 25:585-621.

Hayflick, L. 1965. The limited *in vitro* lifetime of human diploid cell strains. Exp. Cell Res. 37:614-636.

Heidebrecht, H. J., F. Buck, K. Haas, H. H. Wacker, and R. Parwaresch. 1996. Monoclonal antibodies Ki-S3 and Ki-S5 yield new data on the 'Ki-67' proteins. Cell Prolif. 29:413-425.

Helena, M., F. Baerveldt, W-J. Kim, and S. Wilson. 1998. Keratocyte apoptosis after corneal surgery. Invest. Ophthalmol. Vis. Sci. 39:276-283.

Hensler, P. J., L. A. Annab, J. C. Barrett, and O. M. Pereira-Smith. 1994. A gene involved in control of human cellular senescence on human chromosome 1q. Molecular and Cellular Biology. 14 (4):2291-2297.

Hensler, P. J. and O. M. Pereira-Smith. 1995. Human replicative senescence a molecular study. American Journal of Pathology. 147 (1):1-8.

Hicks, C., T. Chirila, P. Dalton, A. Clayton, S. Vijayasekaran, G. Crawford, and I. Constable. 1996. Keratoprosthesis: preliminary results of an artificial corneal button as a full-thickness implant in the rabbit model. Australian and New Zealand Journal of Ophthalmology. 24 (3):297-303.

Hicks, C., H. Fitton, T. Chirila, G. Crawford, and I. Constable. 1997[a]. Keratoprostheses: advancing toward a true artificial cornea. Surv. Ophthalmol. 42:175-189.

Hicks, C., X. Lou, S. Platten, A. Clayton, S. Vijayasekaran, H. Fitton, T. Chirila, G. Crawford, and I. Constable. 1997[b]. Keratoprosthesis results in animals: an update. Australian and New Zealand Journal of Ophthalmology. 25 (Suppl. 1):S50-S52.

Hicks, C., T. Chirila, A. Clayton, J. Fitton, S. Vijayasekaran, P. Dalton, X. Lou, S. Platten, B. Ziegelaar, Y. Hong, G. Crawford, and I. Constable. 1998. Clinical results of implantation of the chirila keratoprosthesis in rabbits. Br. J. Ophthalmol. 82 (1):18-25.

Holt, D., S. Kirk, M. Regan, M. Hurson, W. Lindblad, and A. Barbul. 1992. Effect of age on wound healing in healthy human beings. Surgery. 112:293-298.

Hoppenreijs, V., E. Pels, G. Vrensen, and W. Treffers. 1994. Effects of platelet-derived growth factor on endothelial wound healing of human corneas. Invest. Ophthalmol. Vis. Sci. 35:150-161.

Hoppenreijs, V., E. Pels, F. Vrensen, and F. Treffers. 1996. Corneal endothelium and growth factors. Surv. Ophthalmol. 41:155-164.

Horikawa, I., M. Oshimura, and J. Barrett. 1998. Repression of the telomerase catalytic subunit by a gene on human chromosome 3 that induces cellular senescence. Mol. Carcinog. 22:65-72.

Hyldahl, L. 1986. Control of cell proliferation in the human embryonic cornea: an autoradiographic analysis of the effect of growth factors on DNA synthesis in endothelial and stromal cells in organ culture and after explantation in vitro. J. Cell Sci. 83:1-21.

Hyman, L. 1987. Epidemiology of eye disease in the elderly. Eye. 1:330-341.

Hynes, R. 1981. Relationships between fibronectin and the cytoskeleton. Cell Surf. Rev. 7:97-136.

Hynes, R. and K. Yamada. 1982. Fibronectins: multifunctional modular glycoproteins. J. Cell Biol. 95:369-377.

Iatropoulos, M. and G. Williams. 1996. Proliferation markers. Exp. Toxic. Pathol. 48:175-181.

Inoue, M. and C. Katakami. 1993. The effect of hyaluronic acid on corneal epithelial cell proliferation. Invest. Ophthalmol. Vis. Sci. 34 (7):2313-2315.

Jacob-LaBarre, J. and D. Caldwell. 1990. Development of a new type of artificial cornea for treatment of endstage corneal diseases. In Progress in Biomedical Polymers. C. Gebelein and R. Dunn, editors. Plenum Press., New York. 27-39.

Jester, J., W. Petroll, P. Barry, and D. Cavanagh. 1995. Expression of alpha-smooth muscle (alpha-SM) actin during corneal stromal wound healing. Invest. Ophthalmol. Vis. Sci. 36 (5):809-819.

Jester, J., P. Barry-Lane, W. Petroll, D. Olsen, and H. Cavanagh. 1997. Inhibition of corneal fibrosis by topical application of blocking antibodies to TGFbeta in the rabbit. Cornea. 16 (2):177-187.

Jeyanthi, R. and P. Rao. 1990. In vivo biocompatibility of collagen-poly(hydroxyethyl methacrylate) hydrogels. Biomaterials. 11:238-243.

Johnson-Muller, B. and J. Gross. 1978. Regulation of corneal collagenase production: epithelial-stromal cell interactions. Proc. Natl. Acad. Sci. USA. 75 (9):4417-4421.

Kao, W., C. Kao, A. Kaufman, K. Kombrinck, K. Converse, W. Good, T. Bugge, and J. Degen. 1998. Healing of corneal epithelial defects in plasminogen-and fibrinogen-deficient mice. Invest. Ophthalmol. Vis. Sci. 39:502-508.

Kenyon, K. 1979. Recurrent corneal erosion: pathogenesis and therapy. Int. Ophthalmol. Clin. 19:169-195.

Kill, I., R. Faragher, K. Lawrence, and S. Shall. 1994. The expression of proliferation-dependent antigens during the lifespan of normal and progeroid human fibroblasts in culture. J. Cell Sci. 107:571-579.

Kill, I. 1996. Localisation of the Ki-67 antigen within the nucleolus. Evidence for a fibrillarin-deficient region of the dense fibrillar component. J. Cell Sci. 109:1253-1263.

King, S., W. Hickerson, K. Proctor, and M. Newsome. 1991. Beneficial actions of exogenous hyaluronic acid on wound healing. Surgery. 109:76-84.

Kipling, D. and R. Faragher. 1997. Progeroid syndromes: probing the molecular basis of aging? J. Clin. Pathol: Mol. Pathol. 50:234-241.

Kirkham, S. and M. Dangle. 1991. The keratoprosthesis: improved biocompatability through design and surface modification. Ophthalmic Surgery. 22 (8):455-461.

Koli, K. and J. Keski-Oja. 1992. Cellular senescence. Ann. Med. 24 (5):313-318.

Komai, Y. and T. Ushiki. 1991. The three-dimensional organization of collagen fibrils in the human cornea and sclera. Invest. Ophthalmol. Vis. Sci. 32 (8):2244-2258.

Kondo, H., R. Matsuda, and Y. Yonezawa. 1992. Platelet-derived growth factor in combination with collagen promotes the migration of human skin fibroblasts into a denuded area of a cell monolayer. Exp. Cell Res. 202:45-51.

Kondo, H. and Y. Yonezawa. 1992. Changes in the migratory ability of human lung and skin fibroblasts during in vitro aging and in vivo cellular senescence. Mechanisms of Ageing and Development. 63:223-233.

Kondo, H., R. Matsuda, and Y. Yonezawa. 1993. Autonomous migration of human fetal skin fibroblasts into a denuded area in a cell monolayer is mediated by basic fibroblast growth factor and collagen. In Vitro Cell Dev. Biol. 29A:929-935.

Kondo, H. and Y. Yonezawa. 1995. Fetal-adult phenotype transition, in terms of the serum dependency and growth factor requirements, of human skin fibroblast migration. Exp. Cell Res. 220:501-504.

Kono, T., T. Tanii, M. Furukawa, N. Mizuno, I. Kitajima, M. Ishii, and T. Hamada. 1990. Correlation between ageing and collagen gel contractility of human fibroblasts. Acta. Derm. Venereol. (Stockh). 70:241-244.

Koochekpour, S., G. Pilkington, and A. Merzak. 1995. Hyaluronic acid/CD44H interaction induces cell detachment and stimulates migration and invasion of human glioma cells in vitro. Int. J. Cancer. 63:450-454.

Kremer, M., E. Pothmann, T. Rossler, J. Baker, A. Yee, H. Blanch, and J. Prausnitz. 1994. Pore-size distributions of cationic polyacrylamide hydrogels varying in initial monomer concentration and cross-linker/monomer ratio. Macromolecules. 27:2965-2973.

Krieg, T. 1995. Collagen in the healing wound. Wounds. 7 Suppl A (5):5A-12A.

Kumazaki, T., R. S. Robertorye, S. C. Robertorye, and J. R. Smith. 1991. Fibronectin expression increases during in vitro cellular senescence: correlation with increased cell area. Exp. Cell Res. 195:13-19.

Kurosaka, H., D. Kurosaka, K. Kato, Y. Mashima, and Y. Tanaka. 1998. Transforming growth factor-beta1 promotes contraction of collagen gel by bovine corneal fibroblasts through differentiation of myofibroblasts. Invest. Ophthalmol. Vis. Sci. 39 (5):699-704.

Latkany, R., A. Tsuk, M. Sheu, I. Loh, and V. Trinkaus-Randall. 1997. Plasma surface modification of artificial corneas for optimal epithelialization. J. Biomed. Mater. Res. 36:29-37.

Lauffenburger, D. and A. Horwitz. 1996. Cell migration: a physically integrated molecular process. Cell. 84:359-369.

Laurent, T. and R. Fraser. 1992. Hyaluronan. FASEB J. 6:2397-2404.

Lecka-Czernik, B., E. Moerman, R. Jones, and S. Goldstein. 1996. Identification of gene sequences overexpressed in senescent and werner syndrome human fibroblasts. Experimental Gerontology. 31 (1/2):159-174.

Lee, J., G. Khang, and H. Lee. 1997. Interaction of cells on chargeable functional group gradient surfaces. Biomaterials. 18 (4):351-358.

Lee, S. D., G. H. Hsiue, C. Y. Kao, and P. Chang. 1996. Artificial cornea: surface modification of silicone rubber membrane by graft polymerization of pHEMA via glow discharge. Biomaterials. 17:587-595.

Legeais, J. M., C. Rossi, G. Renard, M. Salvoldelli, F. D'Hermies, and Y. J. Pouliquen. 1992. A new fluorocarbon for keratoprosthesis. Cornea. 11:538-545.

Legeais, J. M., G. Renard, J. M. Parel, O. Serdarevic, M. Mei-Mui, and Y. Pouliquen. 1994. Expanded fluorocarbon for keratoprosthesis cellular ingrowth and transparency. Exp. Eye Res. 58:41-52.

Legeais, J., G. Renard, J. Parel, M. Savoldelli, and Y. Pouliquen. 1995. Keratoprosthesis with biocolonizable microporous fluorocarbon haptic. Arch Ophthalmol. 113:757-763.

Legeais, J. and G. Renard. 1998. A second generation of artificial cornea (Biokpro II). Biomaterials. 19:1517-1522.

Leon, C. and J. Barraquer. 1997. Coralline hydroxyapatite keratoprosthesis in rabbits. Journal of Refractive Surgery. 13 (1):74-78.

Levy, S., J. Moss, H. Sawanda, P. Dopping-Hepenstal, and A. McCartney. 1996. The composition of wide-spaced collagen in normal and diseased Descemet's membrane. Curr. Eye. Res. 15:45-52.

Linnola, R. J., R. Happonein, O. H. Andersson, E. Vedel, A. U. Yli-Urpo, U. Krause, and L. Laatikainen. 1996. Titanium and bioactive glass-ceramic coated titanium as materials for keratoprosthesis. Exp. Eye Res. 63:471-478.

Linskens, M. H., J. Feng, W. H. Andrews, B. E. Enlow, S. M. Saati, L. A. Tonkin, W. D. Funk, and B. Villeponteau. 1995. Catologing altered gene expression in young and senescent cells using enhanced differential display. Nucleic Acids Research. 23 (16):3244-3251.

Littlefield, J. W. 1996. Escape from senescence in human keratinocyte cultures. Experimental Gerontology. 31 (1/2):29-32.

Liu, S., R. Thweatt, C. K. Lumpkin, and S. Goldstein. 1994. Suppression of calcium-dependent membrane currents in human fibroblasts by replicative senescence and forced expression of a gene sequence encoding a putative calcium-binding protein. Proc. Natl. Acad. Sci, USA. 91:2186-2190.

Liu, Y., M. Gorospe, G. Kokkonen, M. Boluyt, A. Younes, Y. Mock, X. Wang, G. Roth, and N. Holbrook. 1998. Impairments in both p70 S6 kinase and extracellular signal-regulated kinase signaling pathways contribute to the decline in proliferative capacity of aged hepatocytes. Exp. Cell Res. 240:40-48.

Lucibello, F., A. Sewing, S. Brusselbach, C. Burger, and R. Muller. 1993. Deregulation of cyclins D1 and E and suppression of cdk2 and cdk4 in senescent human fibroblasts. J. Cell Sci. 105:123-133.

Lydon, M., T. Minnett, and B. Tighe. 1985. Cellular interactions with synthetic polymer surfaces in culture. Biomaterials. 6:396-402.

Macieira-Coelho, A. 1983. Changes in membrane properties associated with cellular aging. International Review of Cytology. 83:183-212.

Maldonado, B. and L. Furcht. 1995. Epidermal growth factor stimulates integrin-mediated cell migration of cultured human corneal epithelial cells on fibronectin and arginine-glycine-aspartic acid peptide. Invest. Ophthalmol. Vis. Sci. 36(10):2120-2126.

Malik, N., S. Moss, N. Ahmed, A. Furth, R. Wall, and K. Meek. 1992. Ageing of the human corneal stroma: structural and biochemical changes. Biochimica et Biophysica Acta. 1138:222-228.

Marchi, V., R. Ricci, I. Pecorella, A. Ciardi, and U. Tondo. 1994. Osteo-Odonto-Keratoprosthesis. Cornea. 13 (2):125-130.

Marshall, G., A. Konstas, and W. Lee. 1991a. Immunogold fine structural localization of extracellular matrix components in aged human cornea. I. Types I-IV collagen and laminin. Graefe's Arch. Clin. Exp. Ophthalmol. 229:157-163.

Marshall, G., A. Konstas, and W. Lee. 1991b. Immunogold fine structural localisation of extracellular matrix components in aged human cornea. II. Collagen types V and VI. Graefe's Arch. Clin. Exp. Ophthalmol. 229:164-171.

Marshall, G. E., A. G. P. Konstas, and W. R. Lee. 1993. Collagens in ocular tissues. Br. J. Ophthalmol. 77:515-524.

Martin, G. R., D. B. Danner, and N. J. Holbrook. 1993. Aging- causes and defenses. Annu. Rev. Med. 44:419-429.

Marx, J. 1994. Chromosome ends catch fire. Science. 265:1656-1658.

Matrisian, L. 1990. Metalloproteinases and their inhibitors in matrix remodelling. TIG. 6(4):121-125.

Matrisian, L. M. 1994. Matrix metalloproteinase gene expression. Annals New York Academy of Sciences. 732:42-49.

Matsubura, M., J. Zieske, and E. Fini. 1991. Mechanism of basement membrane dissolution proceding corneal ulceration. Invest. Ophthalmol. Vis. Sci. 32:3221-3237.

Maurice, D. 1987. The biology of wound healing in the corneal stroma. Cornea. 6 (3):162-168.

McConnell, B., M. Starborg, S. Brookes, and G. Peters. 1998. Inhibitors of cyclin-dependent kinases induce features of replicative senescence in early passage human diploid fibroblasts. Current Biology. 8:351-354.

McCormick, A. and J. Campisi. 1991. Cellular aging and senescence. Current Opinion in Cell Biology. 3:230-234.

Mensing, H., B. Pontz, P. Muller, and V. Gauss-Muller. 1983. A study of fibroblast chemotaxis using fibronectin and conditioned medium as chemoattractants. European Journal of Cell Biology. 29:268-273.

Millis, A., J. Sottile, M. Hoyle, D. Mann, and V. Diemer. 1989. Collagenase production by early and late passage cultures of human fibroblasts. Experimental Gerontology. 24:559-575.

Millis, A. T., M. Hoyle, H. M. McCue, and H. Martini. 1992. Differential expression of metalloproteinase and tissue inhibitor of metalloproteinase genes in aged human fibroblasts. Exp. Cell Res. 201:373-379.

Milo, G. and R. Hart. 1976. Age-related alterations in plasma membrane glycoprotein content and scheduled or unscheduled DNA synthesis. Archiv. Biochem. Biophys. 176:324-333.

Mitchison, T. and L. Cramer. 1996. Actin-based cell motility and cell locomotion. Cell. 84:371-379.

Molander, N., U. Lindquist, U. Stenevi, A. von Malmborg, and B. Ehinger. 1993. Influence of radial keratotomy on endogenous hyaluronan in cornea and aqueous humour. Refractive and Corneal Surgery. 9:358-365.

Moller-Pederson, T., T. Ledet, and N. Ehlers. 1994. The keratocyte density of human donor corneas. Curr. Eye Res. 13:163-169.

Moller-Pederson, T. 1997. A comparative study of human corneal keratocyte and endothelial cell density during aging. Cornea. 16(3):333-338.

Moller-Pedersen, T., H. Li, W. Petroll, H. Cavanagh, and J. Jester. 1998. Confocal microscopic characterization of wound repair after photorefractive keratectomy. Invest. Ophthalmol. Vis. Sci. 39 (3):487-501.

Monti, D., E. Grassilli, L. Troioano, A. Cossarizza, S. Salvioli, D. Barbieri, C. Agnesini, S. Bettussi, M. C. Ingletti, A. Corti, and C. Franceschi. 1992. Senescence, immortalization, and apoptosis. Annals New York Academy of Sciences. 673:70-82.

Mooradian, D., J. McCarthy, J. Cameron, A. Skubitz, and L. Furcht. 1992. Rabbit corneal epithelial cells adhere to two distinct heparin-binding synthetic peptides derived from fibronectin. Invest. Ophthalmol. Vis. Sci. 33 (11):3034-3040.

Morgan, D. 1995. Principles of CDK regulation. Nature. 374:131-135.

Moulin, V., G. Castilloux, F. Auger, D. Garrel, M. O'Connor-McCourt, and L. Germain. 1998. Modulated response to cytokines of human wound healing myofibroblats compared to dermal fibroblasts. Exp. Cell Res. 238:283-293.

Munk, P. 1989. Introduction to Macromolecular Science. John Wiley & Sons. New York.

Murphy, G., S. Atkinson, R. Ward, J. Gavrilovic, and J. J. Reynolds. 1992. The role of plasminogen activators in the regulation of connective tissue metalloproteinases. Annals New York Academy of Sciences. 667:1-12.

Murphy, G. and A. Docherty. 1992. The matrix metalloproteinases and their inhibitors. American Journal of Respiratory Cell and Molecular Biology. 7:120-125.

Murphy, G. 1995. Matrix metalloproteinases and their inhibitors. Acta Orthopaedica Scandinavia. 66:55-60.

Mutsaers, S., J. Bishop, G. McGrouther, and G. Laurent. 1997. Mechanisms of tissue repair: from wound healing to fibrosis. Int. J. Biochem. Cell Biol. 29(1):5-17.

Nakagawa, S., T. Nishida, and R. Manabe. 1985. Actin organization in migrating corneal epithelium of rabbits in situ. Exp. Eye Res. 41:334-343.

Nakagawa, S., P. Pawelek, and F. Grinnell. 1989. Extracellular matrix organization modulates fibroblast growth and growth factor responsiveness. Exp. Cell Res. 182:572-582.

Nakamura, M., M. Hikida, and T. Nakano. 1992. Concentration and molecular wieght dependency of rabbit corneal epithelial wound healing on hyaluronan. Curr. Eye Res. 11 (10):981-986.

Nakamura, M., M. Kobayashi, K. Hirano, K. Kobayashi, T. Hoshino, and S. Awaya. 1994[a]. Glycosaminoglycan and collagen fibrillar interactions in the mouse corneal stroma. Matrix Biology. 14:283-286.

Nakamura, M., T. Nishida, M. Hikida, and T. Otori. 1994[b]. Combined effects of hyaluronan and fibronectin on corneal epithelial wound closure of rabbit in vivo. Curr. Eye Res. 13:385-388.

Nakazawa, K., A. Morita, H. Nakano, C. Mano, and N. Tozawa. 1996. Keratan sulphate synthesis by corneal stromal cells within three-dimensional collagen gel cultures. J. Biochem. 120:117-125.

Newsome, D., J. Gross, and J. Hassell. 1982. Human corneal stroma contains three distinct collagens. Invest. Ophthalmol. Vis. Sci. 22:376-381.

Nimni, M. 1997. Polypeptide growth factors: targeted delivery systems. Biomaterials. 18:1201-1225.

Ning, Y., J. Shay, M. Lovell, L. Taylor, D. Ledbetter, and O. Pereira-Smith. 1991. Tumor suppression by chromosome 11 is not due to cellular senescence. Exp. Cell Res. 192:220-226.

Nishida, T., S. Nakagawa, C. Nishibayashi, H. Tanaka, and R. Manabe. 1984. Fibronectin enhancement of corneal epithelial wound healing of rabbits in vivo. Arch. Ophthalmol. 102:455-456.

Nishida, T. 1992. Extracellular matrix and growth factors in corneal wound healing. Current Opinion in Ophthalmology. 4 (4):4-13.

Nishida, T., J. Nakamura, J. Murakami, H. Mishima, and T. Otori. 1992. Epidermal growth factor stimulates corneal epithelial cell attachment to fibronectin through a fibronectin receptor system. Invest. Ophthalmol. Vis. Sci. 33 (8):2464-2469.

Nishida, T. 1997. Cornea. In Cornea- Fundamentals of Cornea and External Disease. Volume I. Krachmer, Mannis, and Holland, editors. Mosby- Year Book Inc., St. Louis. 3-27.

Noda, A., S. Ning, S. Venable, O. Pereira-Smith, and J. Smith. 1994. Cloning of senescent cell-derived inhibitors of DNA synthesis using an expression screen. Exp. Cell Res. 211:90-98.

Norsgaard, H., B. F. Clark, and S. I. Rattan. 1996. Distinction between differentiation and senescence and the absence of increased apoptosis in human keratinocytes undergoing cellular aging in vitro. Experimental Gerontology. 31 (5):563-570.

Ocalan, M., S. Goodman, U. Kuhl, S. Hauschka, and K. von der Mark. 1988. Laminin alters cell shape and stimulates motility and proliferation of murine skeletal myoblasts. Developmental Biology. 125:158-167.

Ogata, T., D. Ayusawa, M. Namba, E. Takahashi, M. Oshimura, and M. Oishi. 1993. Chromosome 7 suppresses indefinite division of nontumorigenic immortalized human fibroblast cell lines KMST-6 and SUSM-1. Molecular and Cellular Biology. 13 (10): 6036-6043.

Ohashi, Y., S. Nakagawa, T. Nishida, T. Suda, K. Watanabe, and R. Manabe. 1983. Appearance of fibronectin in rabbit cornea after thermal burns. Jpn. J. Ophthalmol. 27:547-555.

Okamato, A., D. Demetrick, E. Spillare, K. Hagiwara, S. Hussain, W. Bennett, K. Forrester, B. Gerwin, M. Serrano, D. Beach, and C. Harris. 1994. Mutations and altered expression of p16INK4 in human cancer. Proc. Natl. Acad. Sci. USA. 91:11045-11049.

O'Kane, S. and M. Ferguson. 1997. Transforming growth factor βs and wound healing. Int. J. Biochem. Cell Biol. 29 (1):63-78.

Olsen, T. 1982. Light scattering from the human cornea. Invest. Ophthalmol. Vis. Sci. 23:81-86.

Oshimara, M. and J. Barrett. 1997. Multiple pathways to cellular senescence: role of telomerase repressors. European Journal of Cancer. 33 (5):710-715.

Otori, T. 1967. Electrolyte content of the rabbit corneal stroma. Exp. Eye Res. 6:356-367.

Pahlitzsch, T. and P. Sinha. 1985. The alkali burned cornea: electron microscopical, enzyme histochemical, and biochemical observations. Graefe's Arch. Clin. Exp. Ophthalmol. 223:278-286.

Pakker, A., R. Rofougaran, K. Lu, W. Wee, A. Isfahani, and P. McDonnell. 1998. Effects of gamma-interferon on keratocyte-induced collagen gel contraction and keratocyte proliferation. Journal of Refractive Surgery. 14:152-155.

Pancholi, S., S. Tullo, A. Khaliq, D. Foreman, and M. Boulton. 1998. The effects of growth factors and conditioned media on the proliferation of human corneal epithelial cells and keratocytes. Graefe's Arch. Clin. Exp. Ophthalmol. 236:1-8.

Paul, R., J. Tarlton, P. Purslow, T. Sims, P. Watkins, F. Marshall, M. Ferguson, and A. Bailey. 1997. Biomechanical and biochemical study of a standardized wound healing model. Int. J. Biochem. Cell Biol. 29 (1):211-220.

Paulsson, Y., M. Bywater, C. Heldin, and B. Westermark. 1987. Effects of epidermal growth factor and platelet-derived growth factor on c-fos and c-myc mRNA levels in normal human fibroblasts. Exp. Cell Res. 171:186-194.

Peacocke, M. and J. Campisi. 1991. Cellular senescence: a reflection of normal growth control, differentiation, or aging? J. Cell. Biochem. 45:147-155.

Peluso, G., O. Petillo, J. Anderson, L. Ambrosio, L. Nicolais, M. Melone, F. Eschbach, and S. Huang. 1997. The differential effects of poly(2-hydroxyethyl methacrylate) and poly(2-hydroxyethyl methacrylate)/poly(caprolactone) polymers on cell proliferation and collagen synthesis by human lung fibroblasts. J. Biomed. Mater. Res. 34:327-336.

Pereira-Smith, O. M. and J. R. Smith. 1988. Genetic analysis of indefinite division in human cells: identification of four complementation groups. Proc. Natl. Acad. Sci. USA. 85:6042-6046.

Peters, D. and D. Mosher. 1987. Localisation of cell surface sites involved in fibronectin fibrillogenesis. J. Cell Biol. 104:121-130.

Pettit, D., T. Horbett, A. Hoffman, and Y. Chan. 1990. Quantitation of rabbit corneal epithelial cell outgrowth on polymeric substrates *in vitro*. Invest. Ophthalmol. Vis. Sci. 31:2269-2277.

Phillips, P., E. Kuhnle, and V. Cristofalo. 1983. [125]EGF binding ability is stable throughout the replicative life-span of WI-38 cells. J Cell Physiol. 114:311-316.

Pignolo, R., M. Rotenberg, and V. Cristofalo. 1994. Alterations in contact and density-dependent arrest state in senescent WI-38 cells. In Vitro Cell. Dev. Biol. 30A:471-476.

Pignolo, R., B. Martin, J. Horton, A. Kalbach, and V. Cristofalo. 1998[a]. The pathway of cell senescence: WI-38 cells arrest in late G1 and are unable to traverse the cell cycle from a true G0 state. Experimental Gerontology. 33 (1/2):67-80.

Pignolo, R., M. Rotenberg, J. Horton, and V. Cristofalo. 1998[b]. Senescent WI-38 fibroblasts overexpress LPC-1, a putative transmembrane shock protein. Exp. Cell Res. 240:305-311.

Pintucci, S., F. Pintucci, M. Cecconi, and S. Caiazza. 1995. New dacron tissue colonisible keratoprosthesis: clinical experience. Br. J. Ophthalmol. 79:825-829.

Postlethwaite, A., J. Seyer, and A. Kang. 1978. Chemotactic attraction of human fibroblasts to type I, II, and III collagens and collagen-derived peptides. Proc. Natl. Acad. Sci. USA 75 (2):871-875.

Postlethwaite, A., J. Keski-Oja, G. Balian, and A. Kang. 1981. Induction of fibroblast chemotaxis by fibronectin. J. Exp. Med. 153:494-499.

Rao, K. M. K. and H. J. Cohen. 1990. The role of the cytoskeleton in aging. Experimental Gerontology. 24:7-22.

Rawe, I., S. Tuft, and K. Meek. 1992. Proteoglycan and collagen morphology in superficially scarred rabbit cornea. Histochemical Journal. 24:311-318.

Rawe, I., K. Meek, D. Leonard, T. Takahashi, and C. Cintron. 1994. Structure of corneal scar tissue: an x-ray diffraction study. Biophys. J. 67:1743-1748.

Reed, M., R. Vernon, I. Abrass, and H. Sage. 1994. TGF-beta induces the expression of type I collagen and SPARC, and enhances contraction of collagen gels, by fibroblasts from young and aged donors. J Cell Physiol. 158:169-179.

Renard, G., B. Cetinel, J. Legeais, M. Savoldelli, and J. Durand. 1996. Incorporation of a fluorocarbon polymer implanted at the posterior surface of the rabbit cornea. Journal of Biomedical Materials Research. 31:193-199.

Ricci, R., I. Pecorella, A. Ciardi, C. Rocca, U. Tondo, and V. Marchi. 1992. Strampelli's osteo-odonto-keratoprosthesis. Clinical and histological long-term features of three prostheses. Br. J. Ophthalmol. 76:232-234.

Riikonen, T., L. Koivisto, P. Vihinen, and J. Heino. 1995. Transforming growth factor-beta regulates collagen gel contraction by increasing alpha2beta1 integrin expression in osteogenic cells. J. Biol. Chem. 270 (1):376-382.

Robetorye, R., M. Nakanishi, S. Venable, O. Pereira-Smith, and J. Smith. 1996. Regulation of p21 and expression of other cyclin-dependent kinase inhibitors in senescent human cells. Molecular and Cellular Differentiation. 4(1):113-126.

Rose, D., G. McCabe, J. Feramisco, and M. Adler. 1992. Expression of c-fos and AP-1 activity in senescent human fibroblasts is not sufficient for DNA synthesis. J. Cell Biol. 119 (6):1405-1411.

Roy, P., W. Petroll, H. Cavanagh, C. Chuong, and J. Jester. 1997. An in vitro force measurement assay to study the early mechanical interaction between corneal fibroblasts and collagen matrix. Exp. Cell Res. 232:106-117.

Ruoslahti, E. 1989. Proteoglycans in cell regulation. J. Biol. Chem. 15:13369-13372.

Rouslahti, E. 1991. Integrins. J. Clin. Invest. 87:1-5.

Saika, S., O. Yamanaka, N. Hashizume, S. Kobata, Y. Okada, K. Uenoyama, and A. Ooshima. 1993. Cis-Hydroxyproline inhibits adhesion, migration and proliferation of cultured rabbit keratocytes. Ophthalmic Res. 25:363-370.

Saika, S., A. Ooshima, K. Shima, S. Tanaka, and Y. Ohnishi. 1996. Collagen types in healing alkali-burned corneal stroma in rabbits. Jpn. J. Ophthalmol. 40:303-309.

Saltzman, W. M., P. Parsons-Wingerter, K. W. Leong, and S. Lin. 1991. Fibroblast and hepatocyte behaviour on synthetic polymer surfaces. Journal of Biomedical Materials Research. 25:741-759.

Sandeman, S., R. Faragher, M. Allen, and A. Lloyd. 1998. Keratocyte invasion into collagen gels declines with in vitro age. Invest. Ophthalmol. Vis. Sci. 39 (4):S756.(Abstr.)

Sarber, R., B. Hull, C. Merrill, T. Soranno, and E. Bell. 1981. Regulation of proliferation of fibroblasts of low and high population doubling levels grown in collagen lattices. Mechanisms of Ageing and Development. 17:107-117.

Sasaki, M., T. Honda, H. Yamada, N. Wake, J. K. Barrett, and M. Oshimura. 1994. Evidence for multiple pathways to cellular senescence. Cancer Research. 54:6090-6093.

Sawada, H., H. Konomi, and K. Hirosawa. 1990. Characterization of the collagen in the hexagonal lattice of descemet's membrane: its relation to type VIII collagen. J. Cell Biol. 110:219-227.

Sawhney, N. and P. Hall. 1992. Ki67-structure, function, and new antibodies. Journal of Pathology. 168:161-162.

Schaffer, C. and L. Nanney. 1996. Cell Biology of Wound Healing. International Review of Cytology. 169:151-181.

Schneider, E. L. and Y. Mitsui. 1976. The relationship between in vitro cellular aging and in vivo human age. Proc. Natl. Acad. Sci. USA. 73 (10):3584-3588.

Schor, S. 1980. Cell proliferation and migration on collagen substrata in vitro. J. Cell Sci. 41:159-175.

Schor, S. L., A. M. Schor, G. Rushton, and L. Smith. 1985. Adult, foetal and transformed fibroblasts display different migratory phenotypes on collagen gels: evidence for isoformic transition during foetal development. J. Cell Sci. 73:221-234.

Schor, S. L., A. M. Schor, M. Grey, and G. Rushton. 1988. Foetal and cancer patient fibroblasts produce an autocrine migration-stimulating factor not made by normal adult cells. J. Cell Sci. 90:391-399.

Schor, S. 1994. Cytokine control of cell motility: modulation and mediation by the extracellular matrix. Progress in Growth Factor Research. 5:223-248.

Schor, S. L., I. Ellis, E. C. Dolman, J. Banyard, M. J. Humphries, D. F. Mosher, A. M. Grey, A. P. Mould, J. Sorttile, and A. M. Schor. 1996. Substratum-dependent stimulation of fibroblast migration by the gelatin-binding domain of fibronectin. J. Cell Sci. 109:2581-2590.

Schreier, T., E. Degen, and W. Baschong. 1993. Fibroblast migration and proliferation during in vitro wound healing. Res. Exp. Med. 193:195-205.

Schultz, G., N. Chegini, M. Grant, P. Khaw, and S. MacKay. 1992. Effects of growth factors on corneal wound healing. Acta. Ophthalmologica. 70 (S202):60-66.

Schultz, G., P. Khaw, K. Oxford, S. Macauley, G. Van Setten, and N. Chegini. 1994. Growth factors and ocular wound healing. Eye. 8:184-187.

Schultz, G. 1997. Modulation of Corneal Wound Healing. In Cornea-Fundamentals of Cornea and External Disease. Volume I. Krachmer, Mannis, and Holland, editors. Mosby- Year Book Inc., St. Louis. 183-198.

Scott, J., C. Orford, and E. Hughes. 1981. Proteoglycan-collagen arrangements in developing rat tail tendon. Biochem. J. 195:573-581.

Sell, D. and V. Monnier. 1989. Isolation, purification and partial characterization of novel fluorophores from aging human insoluble collagen-rich tissue. Connective Tissue Research. 19:77-92.

Serrano, M. 1997. The tumor suppressor protein p16INK4a. Exp. Cell Res. 237:7-13.

Serrano, M., A. Lin, M. McCurrach, D. Beach, and S. Lowe. 1997. Oncogenic ras provokes premature cell senescence associated with accumulation of p53 and p16INK4a. Cell. 88:593-602.

Seshadri, T. and J. Campisi. 1990. Repression of c-fos transcription and an altered genetic program in senescent human fibroblasts. Science. 247:205-209.

Sherrard, E., P. Novakovic, and L. Speedwell. 1987. Age-related changes of the corneal endothelium and stroma as seen in vivo by specular microscopy. Eye. 1:197-203.

Sherwood, S. W., D. Rush, J. L. Ellsworth, and R. T. Schimke. 1988. Defining cellular senescence in IMR-90 cells: a flow cytometric analysis. Proc. Natl. Acad. Sci. USA. 85:9086-9090.

Shimizu, M., K. Minakuchi, S. Kaji, and J. Koga. 1997. Chondrocyte migration to fibronectin, type I collagen and type II collagen. Cell Structure and Function. 22:309-315.

Sintzel, M., S. Bernatchez, C. Tabatabay, and R. Gurny. 1996. Biomaterials in ophthalmic drug delivery. Eur. J. Pharm. Biopharm. 42 (6):358-374.

Smetana, K., J. Lukas, V. Paleckova, J. Bartunkova, F. T. Liu, J. Vacik, and H. Gabius. 997. Effect of chemical structure of hydrogels on the adhesion and phenotypic characteristics of human monocytes such as expression of galectins and other carbohydrate-binding sites. Biomaterials. 18 (14):1009-1014.

Smith, J. R. and L. Hayflick. 1974. Variation in the life-span of clones derived from human diploid cell strains. J. Cell Biol. 62:48-53.

Smith, J. R. and D. W. Lincoln. 1984. Aging of cells in culture. International Review of Cytology. 89:151-177.

Smith, J. R. and O. M. Pereira-Smith. 1996. Replicative senescence: implications for in vivo aging and tumor suppression. Science. 273:63-67.

Smith, V. A. and D. L. Easty. 1995. Corneal gelatinase A: characterisation and activation. Vision Research. 35(55):S314.

Smith, V. A., B. Hoh, M. Littleton, and D. Easty. 1995. Over-expression of a gelatinase A activity in keratoconus. Eye. 9:429-433.

Sotozono, C., S. Kinoshita, M. Kita, and J. Imanishi. 1994. Paracrine role of keratocyte growth factor in rabbit corneal epithelial cell growth. Exp. Eye Res. 59:385-392.

Sottile, J., M. Hoyle, and A. J. Millis. 1987. Enhanced synthesis of a Mr =55,000 dalton peptide by senescent human fibroblasts. J Cell Physiol. 131:210-217.

Sottile, J., M. Hoyle, and A. Millis. 1988. Differential response of early and late passage fibroblasts to collagenase stimulatory factor in conditioned media. Collagen Rel. Res. 8:361-374.

Steele, J., G. Johnson, H. Griesser, and P. Underwood. 1997. Mechanism of initial attachment of corneal epithelial cells to polymeric surfaces. Biomaterials. 18:1541-1551.

Stein, G. H. and V. Dulic. 1995. Origins of G1 arrest in senescent human fibroblasts. Bioassays. 17 (6):537-543.

Stephens, P., P. Genever, E. Wood, and M. Raxworthy. 1997. Integrin receptor involvement in actin cable formation in an in vitro model of events associated with wound contraction. Int. J. Biochem. Cell Biol. 29 (1):121-128.

Stone, W. and E. Herbert. 1953. Experimental study of plastic material as replacement for the cornea. Am J. Ophthalmol. 36:168-173.

Svoboda, K., H. Gong, and V. Trinkaus-Randall. 1998. Collagen expression and orientation in ocular tissues. Prog. Polym. Sci. 23:329-374.

Szerenyi, K., X. Wang, K. Gabrielian, and P. McDonnell. 1994. Keratocyte loss and repopulation of anterior corneal stroma after de-epithelialization. Arch. Ophthalmol. 112:973-976.

Takeda, K., A. Gosiewska, and B. Peterkofsky. 1992. Similar, but not identical, modulation of expression of extracellular matrix components during in vitro and in vivo aging of human skin fibroblasts. J Cell Physiol. 153:450-459.

Tang, Z., Z. Zhang, Y. Zheng, M. Corbley, and T. Tong. 1994. Cell aging of human diploid fibroblasts is associated with changes in responsiveness to epidermal growth factor and changes in HER-2 expression. Mechanisms of Ageing and Development. 73:57-67.

Trinkaus-Randall, V., J. Capecchi, A. Newton, A. Vadasz, H. Leibowitz, and C. Franzblau. 1988. Development of a biopolymeric keratoprosthetic material. Invest. Ophthalmol. Vis. Sci. 29 (3):393-400.

Trinkaus-Randall, V., R. Bansatt, J. Capecchi, H. M. Leibowitz, and C. Fransblau. 1991. In vivo fibroplasia of a porous polymer in the cornea. Invest. Ophthalmol. Vis. Sci. 32 (13):3245-3251.

Trinkaus-Randall, V., M. Tong, P. Thomas, and A. Cornell-Bell. 1993. Confocal imaging of the alpha6 and beta4 integrin subunits in the human cornea with aging. Invest. Ophthalmol. Vis. Sci. 34 (11):3103-3109.

Trinkaus-Randall, V., R. Banwatt, X. Wu, H. Leibowitz, and C. Franzblau. 1994. Effect of pretreating porous webs on stromal fibroplasia in vivo. Journal of Biomedical Materials Research. 28:195-202.

Trinkaus-Randall, V., X. Wu, R. Tablante, and A. Tsuk. 1997. Implantation of a synthetic cornea: design, development and biological response. Artificial Organs. 21 (11):1185-1191.

Trinkaus-Randall, V. and M. Nugent. 1998. Biological response to a synthetic cornea. Journal of Controlled Release. 53:205-214.

Tsuk, A., V. Trinkaus-Randall, and H. Leibowitz. 1997. Advances in polyvinyl alcohol hydrogel keratoprostheses: protection against ultraviolet light and fabrication by a molding process. J. Biomed. Mater. Res. 34:299-304.

Tuft, S., R. Zabel, and J. Marshall. 1989. Corneal repair following keratectomy. Invest. Ophthalmol. Vis. Sci. 30 (8):1769-1777.

Tuft, S., D. Gartry, I. Rawe, and K. Meek. 1993. Photorefractive keratectomy: implications of corneal wound healing. Br. J. Ophthalmol. 77:243-247.

Turley, E. 1992. Hyaluronan and cell locomotion. Cancer and Metastasis Reviews. 11:21-30.

Vazori, H. and S. Benchimol. 1996. From telomere loss to p53 induction and activation of a DNA-damage pathway at senescence: the telomere loss/ DNA damage model of cell aging. Experimental Gerontology. 31 (1/2):295-301.

Venable, M., G. Blobe, and L. Obeid. 1994. Identification of a defect in the phospholipase D/Diacylglycerol pathway in cellular senescence. J. Biol. Chem. 269(42):26040-26044.

Verheijen, R., H. Kuijpers, R. Schlingemann, A. Boehmer, R. van Driel, G. Brakenhoff, and F. Ramaekers. 1989. Ki67 detects a nuclear matrix-associated proliferation-related antigen I. intracellular localization during interphase. J. Cell Sci. 92:123-130.

Vijayasekaran, S., C. Hicks, T. Chirila, H. Fitton, A. Clayton, X. Lou, S. Platten, G. Crawford, and I. Constable. 1997. Histological evaluation during dealing of hydrogel core-and skirt keratoprostheses in the rabbit eye. Cornea. 16 (3):352-359.

Vojta, P. J. and J. C. Barrett. 1995. Genetic analysis of cellular senescence. Biochimica et Biophysica Acta. 1242:29-41.

Walther, D., G. Sin, H. Blanch, and J. Prausnitz. 1994. Pore-size distributions of cationic polyacrylamide hydrogels of different compositions maintained at the same swelling capacity. J. Macromol. Sci. -Phys. B33 (3&4):267-286.

Wang, E. and D. Gundersen. 1984. Increased organization of cytoskeleton accompanying the aging of human fibroblasts in vitro. Exp. Cell Res. 154:191-202.

Wang, E. 1985. Are cross-bridging structures involved in the bundle formation of intermediate filaments and the decrease in locomotion that accompany cell aging. J. Cell Biol. 100:1466-1473.

Wang, E. and G. Tomaszewski. 1991. Granular presence of terminin is the marker to distinguish between the senescent and quiescent states. J. Cell Physiol. 147:514-522.

Watt, F. M. 1994. Studies with cultured human epidermal keratinocytes: potential relevance to corneal wound healing. Eye. 8 (2):161-162.

Weinberg, R. 1995. The retinoblastoma protein and cell cycle control. Cell. 81:323-330.

West, M. D., O. M. Pereira-Smith, and J. R. Smith. 1989. Replicative senescence of human skin fibroblasts correlates with a loss of regulation and overexpression of collagenase activity. Exp. Cell Res. 184:138-147.

West, M. D., J. W. Shay, W. E. Wright, and M. H. Linskens. 1996. Altered expression of plasminogen activator and plasminogen activator inhibitor during cellular senescence. Experimental Gerontology. 31:175-193.

West, D., S. Shaw, P. Lorenz, N. Adzick, and M. Longaker. 1997. Fibrotic healing of adult and late gestation fetal wounds correlates with increased hyaluronidase activity and removal of hyaluronan. Int. J. Biochem. Cell Biol. 29 (1):201-210.

West-Mays, J. A., P. M. Sadow, T. W. Tobin, K. J. Strissel, C. Cintron, and M. E. Fini. 1997. Repair phenotype in corneal fibroblasts is controlled by an interleukin-1alpha autocrine feedback loop. Invest. Ophthalmol. Vis. Sci. 38 (7):1367-1379.

Wichterle, O. and D. Lim. 1960. Hydrophilic gels for biological use. Nature. 185:117-118.

Wigham, C. and S. Hodson. 1987. Physiological changes in the cornea of the ageing eye. Eye. 1:190-196.

Wilson, S., Y. G. He, and S. Lloyd. 1992. EGF, EGF receptor, basic FGF, TGF beta-1, and IL-1 alpha mRNA in human corneal epithelial cells and stromal fibroblasts. Invest. Ophthalmol. Vis. Sci. 33 (5):1756-1765.

Wilson, S., J. Walker, E. Chwang, and Y. G. He. 1993. Hepatocyte growth factor, keratinocyte growth factor, their receptors, fibroblast growth factor receptor-2, the cells of the cornea. Invest. Ophthalmol. Vis. Sci. 34 (8):2544-2561.

Wilson, S., G. Schultz, N. Chegini, J. Weng, and Y. He. 1994[a]. Epidermal growth factor, transforming growth factor alpha, transforming growth factor beta, acidic fibroblast growth factor, basic fibroblast growth factor, and interleukin-1 proteins in the cornea. Exp. Eye Res. 59:63-72.

Wilson, S., Y. He, J. Weng, J. Zieske, J. Jester, and G. Schultz. 1994[b]. Effect of epidermal growth factor, hepatocyte growth factor, and keratocyte growth factor on proliferation, motility and differentiation of human corneal epithelial cells. Exp. Eye Res. 59:665-678.

Wilson, S. W., Y. G. He, J. Weng, Q. Li, A. W. McDowall, M. Vital, and E. L. Chwang. 1996. Epithelial injury induces keratocyte apoptosis: hypothesized role for the interleukin-1 system in the modulation of corneal tissue organisation and wound healing. Exp. Eye Res. 62:325-337.

Wilson, S. E. 1997. Molecular cell biology for the refractive corneal surgeon: programmed cell death and wound healing. Journal of Refractive Surgery. 13:171-175.

Woessner, J. F. 1991. Matrix metalloproteinases and their inhibitors in connective tissue remodelling. FASEB. 5:2145-2154.

Woessner, J. 1994. The family of matrix metalloproteinases. Annals New York Academy of Sciences. 732:11-21.

Wojciak-Stothard, B., M. Denyer, M. Mishra, and R. A. Brown. 1997. Adhesion, orientation, and movement of cells cultured on ultrathin fibronectin fibers. In Vitro Cell. Dev. Biol. 33(2):110-117.

Wojtowicz-Praga, S., R. Dickson, and M. Hawkins. 1997. Matrix metalloproteinase inhibitors. Investigational New Drugs. 15:61-75.

Wong, H. and K. Riabowol. 1996. Differential CDK-inhibitor gene expression in aging human diploid fibroblasts. Experimental Gerontology. 31 (1/2):311-325.

Woost, P., J. Brightwell, R. Eiferman, and G. Schultz. 1985. Effect of growth factors with dexamethasone on healing of rabbit corneal stromal incisions. Exp. Eye Res. 40:47-60.

Worthington, C. 1984. The structure of the cornea. Quarterly Review of Biophysics. 17 (4):423-451.

Wright, W. and J. Shay. 1992. Telomere positional effects and the regulation of cellular senescence. Trends in Genetics. 8 (6):193-197.

Wu, X. Y., A. Tsuk, H. M. Leibowitz, and V. Trinkaus-Randall. 1996. Comparison of three different porous materials intended for use in a keratoprosthesis. Invest. Ophthalmol. Vis. Sci. 17 (3):S316.

Wu, X., A. Tsuk, H. Leibowitz, and V. TrinkausRandall. 1998. In vivo comparison of three different porous materials intended for use in a keratoprosthesis. Br. J. Ophthalmol. 82 (5):569-576.

Wynford-Thomas, D. 1996. Telomeres, p53 and cellular senescence. Oncology Research. 10/11:387-398.

Wynford-Thomas, D. and D. Kipling. 1997. Cancer and the knockout mouse. Nature. 389:551-553.

Xu, H., Y. Zhou, W. Ji, G. Perng, R. Kruzelock, C. Kong, R. Bast, G. Mills, J. Li, and S. Hu. 1997. Reexpression of the retinoblastoma protein in tumor cells induces senescence and telomerase inhibition. Oncogene. 15:2589-2596.

Yamato, M., K. Yamamoto, and T. Hayashi. 1992. Decrease in cellular potential of collagen gel contraction due to in vitro cellular aging: a new aging index of fibroblasts with high sensitivity. Connective Tissue. 24:157-162.

Yamato, M., E. Adachi, K. Yamamoto, and T. Hayashi. 1995. Condensation of collagen fibrils to the direct vicinity of fibroblasts as a cause of gel contraction. J. Biochem. 117:940-946.

Ye, H. and D. Azar. 1998. Expression of Gelatinases A and B, and TIMPs 1 and 2 during corneal wound healing. Invest. Ophthalmol. Vis. Sci. 39 (6):913-921.

Yokoi, N, A. Komuro, K. Nishida & S. Kinoshita. 1997. Effectiveness of hyaluronan on corneal epithelial barrier function in dry eye. Br. J. Ophthalmol. 81:533-536.

Yong, V., C. Krekoski, P. Forsyth, R. Bell, and D. Edwards. 1998. Matrix metalloproteinases and diseases of the CNS. TINS. 21 (2):75-80.

Yu, F., J. Guo, and Q. Zhang. 1998. Expression and distribution of adhesion molecule CD44 in healing corneal epithelia. Invest. Ophthalmol. Vis. Sci. 39 (5):710-717.

Zask, A., J. Levin, L. Killar, and J. Skotnicki. 1996. Inhibition of matrix metalloproteinases: structure based design. Current Pharmaceutical Design. 2:624-661.

Zavala, E., S. Nayak, J. Deg, and P. Binder. 1984. Keratocyte attachment to hydrogel materials. Curr. Eye Res. 3 (10):1253-1263.

Zeng, G. and A. J. Millis. 1994. Expression of 72-kDa gelatinase and TIMP-2 in early and late passage human fibroblasts. Exp. Cell Res. 213:148-155.

Zeng, G., H. McCue, L. Mastrangelo, and A. Millis. 1996. Endogenous TGF-beta activity is modified during cellular aging: effects on metalloproteinase and TIMP-1 expression. Exp. Cell Res. 228:271-276.

Zent, R., M. Ailenberg, and M. Silverman. 1998. Tyrosine kinase cell signaling pathways of rat mesangial cells in 3-dimensional cultures: response to fetal bovine serum and platelet-derived growth factor-BB. Exp. Cell Res. 240:134-143.

Zhang, Y. and R. Akhtar. 1997. Epidermal growth factor stimulation of phosphatidylinositol 3-kinase during wound closure in rabbit corneal epithelial cells. Invest. Ophthalmol. Vis. Sci. 38 (6):1139-1148.

Zimmermann, D., B. Trueb, K. Winterhalter, R. Witmer, and R. Fischer. 1986. Type VI collagen is a major component of the human cornea. FEBS. 197 (1/2):55-58.

Bibliography

Image not available due to copyright restrictions

Image not available due to copyright restrictions

Image not available due to copyright restrictions

Image not available due to copyright restrictions

Image not available due to copyright restrictions

Image not available due to copyright restrictions

Image not available due to copyright restrictions

Image not available due to copyright restrictions

Image not available due to copyright restrictions

Image not available due to copyright restrictions

Image not available due to copyright restrictions

Image not available due to copyright restrictions

Image not available due to copyright restrictions